

Insights into the Activation Mechanism of PopA, a cyclic di-GMP Effector Protein Involved in Cell Cycle and Development of *Caulobacter Crescentus*

Inauguraldissertation

zur
Erlangung der Würde eines Doktors der Philosophie
vorgelegt der
Philosophisch-Naturwissenschaftlichen Fakultät
der Universität Basel

von

Annina Larissa Schalch-Moser
aus Seedorf (BE), Schweiz

Basel, 2012

Original document stored on the publication server of the University of Basel edoc.unibas.ch



This work is licenced under the agreement „Attribution Non-Commercial No Derivatives – 2.5 Switzerland“. The complete text may be viewed here:

creativecommons.org/licenses/by-nc-nd/2.5/ch/deed.en

Genehmigt von der Philosophisch-Naturwissenschaftlichen Fakultät auf Antrag von:

- Prof. Dr. Urs Jenal
- Prof. Dr. Hans-Martin Fischer

Basel, 13. Dezember 2011

Dekan Prof. Dr. Martin Spiess



Attribution-Noncommercial-No Derivative Works 2.5 Switzerland

You are free:



To Share – to copy, distribute and transmit the work

Under the following conditions:



Attribution. You must attribute the work in the manner specified by the author or licensor (but not in any way that suggests that they endorse you or your use of the work).



Noncommercial. You may not use this work for commercial purposes.



No Derivative Works. You may not alter, transform, or build upon this work.

- For any reuse or distribution, you must make clear to others the license terms of this work. The best way to do this is with a link to this web page.
 - Any of the above conditions can be waived if you get permission from the copyright holder.
 - Nothing in this license impairs or restricts the author's moral rights.

Your fair dealing and other rights are in no way affected by the above.

This is a human-readable summary of the Legal Code (the full license) available in German:
<http://creativecommons.org/licenses/by-nc-nd/2.5/ch/legalcode.de>

Disclaimer:

The Commons Deed is not a license. It is simply a handy reference for understanding the Legal Code (the full license) — it is a human-readable expression of some of its key terms. Think of it as the user-friendly interface to the Legal Code beneath. This Deed itself has no legal value, and its contents do not appear in the actual license. Creative Commons is not a law firm and does not provide legal services. Distributing of, displaying of, or linking to this Commons Deed does not create an attorney-client relationship.

Summary

In *Caulobacter crescentus*, a complex network integrating cyclic di-GMP and Phosphorylation-dependent signals controls the proteolysis of key regulatory proteins to drive cell cycle and polar morphogenesis. The c-di-GMP input is processed by the effector protein PopA. Upon binding of c-di-GMP, PopA is sequestered to the old cell pole where it recruits the replication and cell division inhibitors CtrA and KidO and mediates their destruction by the polar ClpXP protease prior to entry into S-phase. In addition to its role at the stalked cell pole, PopA localizes to the opposite cell pole in dependence of the general topology factor PodJ where it exerts a yet unknown function.

Here we address the activation and polar sequestration mechanism of PopA guided by an existing activation model for the highly homologous c-di-GMP signaling protein PleD. PopA and PleD do not only share an identical domain organization (Rec1-Rec2-GGDEF), but also show similar spatio-temporal behavior during the cell cycle. While PleD is activated and targeted to the old cell pole via phosphorylation-induced dimerization, we show that PopA stalked pole function is phosphorylation-independent and requires c-di-GMP binding as a primary input signal for activation and polar localization. c-di-GMP binds to conserved primary and secondary I-sites within the PopA GGDEF domain and we show that intact binding sites are required for PopA positioning and function. This suggests that c-di-GMP-dependent crosslinking of adjacent GGDEF domains contributes to the localization of an active PopA dimer to the cell pole. Consistent with this, we demonstrate that the GGDEF domain encodes the polar localization signal(s), while the N-terminal receiver domains serve as interaction platform for downstream components that are actively recruited by PopA.

Among these downstream factors is RcdA, a small mediator protein that interacts with the first PopA receiver domain and helps to recruit and degrade CtrA and KidO. In a screen for additional components of the PopA pathway we identify two novel proteins that directly interact with PopA, CC1462 and CC2616. CC1462 is a ClpXP substrate that requires PopA for polar positioning and subsequent degradation during swarmer-to-stalked cell transition. Although located in a flagellar gene cluster, deletion of CC1462 did not affect flagellar assembly and function. Its cellular role as well as the significance of its cell cycle-dependent degradation requires further studies. CC2616, the second PopA interaction partner, is not proteolytically processed and thus belongs to another class of PopA-dependent substrates. CC2616 is annotated as guanine deaminase, which is predicted to catalyze the conversion from guanine to xanthine thereby irreversibly removing

guanine based nucleotides from a cellular pool. A *CC2616* deletion leads to increased attachment and decreased motility, a phenocopy of strains with elevated c-di-GMP levels. It is not clear whether *CC2616* indeed has deaminase activity or whether it has adopted a novel function.

Taken together, this work provides insight into the activation mechanism of a c-di-GMP effector protein. We propose that PopA has evolved through gene duplication from its ancestor, the catalytic PleD response regulator but has lost catalytic activity of the diguanylate cyclase domain. Moreover, PopA has adopted an inverse intra-molecular information transfer originating through c-di-GMP binding at the C-terminal GGDEF domain, which in turn activates the N-terminal receiver stem to serve as platform for downstream partner recruitment.

Index

1	Introduction	1
1.1	Second messenger based signaling systems in prokaryotes	1
1.2	Synthesis and Degradation of cyclic di-GMP	2
1.3	Abundance of GGDEF, EAL and HD-GYP domains	4
1.4	Regulation of c-di-GMP metabolizing proteins	5
1.5	c-di-GMP sensing molecules	6
1.6	c-di-GMP controls cell motility, biofilm formation and virulence.....	8
1.7	Other phenotypes influenced by c-di-GMP	12
1.8	c-di-GMP signaling molecules are involved in <i>C. crescentus</i> cell cycle and development.....	14
1.9	<i>C. crescentus</i> cell cycle control	19
1.10	PopA, a c-di-GMP effector protein involved in both, cell cycle control and development.....	25
2	Aim of the thesis	28
3	Results	29
3.1	Unraveling the Polar Sequestration Mechanism of PopA, a c-di-GMP Effector Protein Involved in <i>C. crescentus</i> Cell Cycle Control.....	29
3.2	Identifying New Interaction Partners of PopA, a di-GMP Effector Protein Involved in Cell Cycle Control and Development of <i>Caulobacter Crescentus</i>	119
4	Outlook.....	197
5	Bibliography.....	201
6	Acknowledgements.....	215
7	Curriculum Vitae	216

1 Introduction

1.1 Second messenger based signaling systems in prokaryotes

Second messenger based signaling pathways are used throughout the kingdoms to rapidly respond to changing extracellular and intracellular environments. These second messengers are small and freely diffusible molecules that can allosterically regulate specific effectors which mediate appropriate cellular responses on the levels of protein, DNA or RNA^{1,2}. While in eukaryotic cells many different second messenger molecules such as cyclic AMP (cAMP), certain ions and phospholipids are known, only two second messengers have been reported to be involved in signal transduction of bacterial cells. These include the well studied cAMP which controls processes such as utilization of alternative sugars, motility and virulence³⁻⁷ and the linear molecule guanosine tetra/pentaphosphate ((p)ppGpp) which is also known as bacterial alarmone⁸. However, the past years have revealed that bacteria make use of several different second messengers systems similar to their eukaryotic counterparts (Fig. 1). Among these newly emerged second messengers are cyclic di-AMP (c-di-AMP) which plays a crucial role for viability in *Listeria monocytogenes*⁹ and has been reported to be involved in DNA damage-dependent cell cycle control in *Bacillus subtilis*^{10,11}, as well as the guanylate based nucleotide cyclic GMP (cGMP) which is involved in the regulation of cyst formation^{12,13}. Moreover, cyclic di-GMP (c-di-GMP), a second messenger present in the majority of bacterial species¹⁴, but absent in eukaryotic and archaeal cells has been identified. Since then, a growing number of studies linked the function of c-di-GMP to diverse physiological processes such as motile-sessile transition, virulence, cell cycle and cell differentiation^{2,15}.

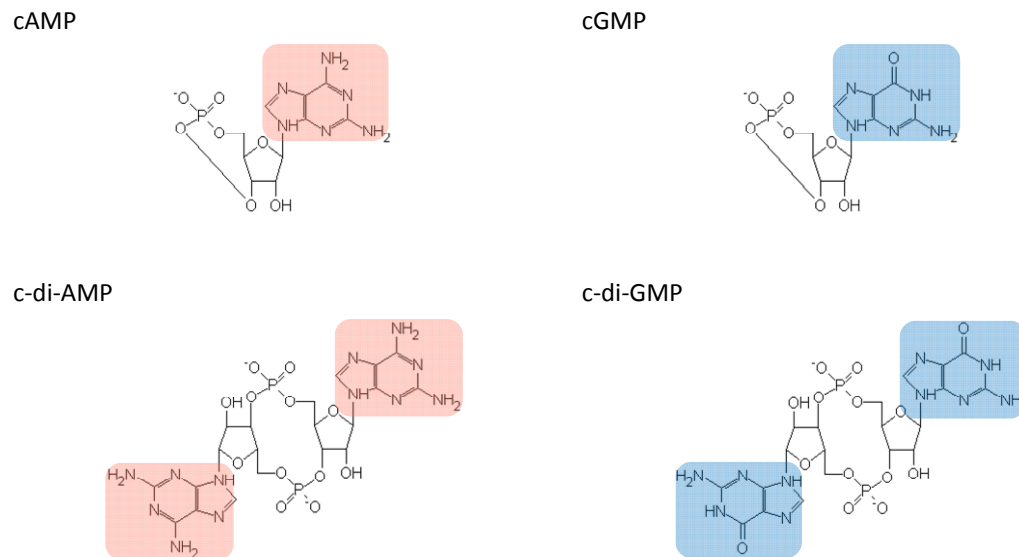


Figure 1: Chemical structures of the major cyclic mono- and dinucleotides in prokaryotes. The adenine of the cAMP and c-di-AMP is highlighted in red, whereas the guanine of cGMP and c-di-GMP is shown blue.

1.2 Synthesis and Degradation of cyclic di-GMP

Bis-(3'-5')-cyclic dimeric guanosine monophosphate (c-di-GMP) was first discovered as allosteric activator of cellulose synthase in *Gluconacetobacter xylinum* almost 30 years ago¹⁶. In the following years, two classes of enzymes controlling c-di-GMP turnover could be identified; the diguanylate cyclases (DGC) and the phosphodiesterases (PDE)¹⁷ (Fig. 2).

Diguanylate cyclases are characterized by the presence of a GGDEF domain which is named after its conserved amino acid motif. It catalyses the condensation of two GTP molecules into one molecule of c-di-GMP¹⁸⁻²¹ by a similar catalytic mechanism reported for the structurally related adenylate cyclases²⁰⁻²². The GGDEF motif is part of the active site (A-site), where all amino acids besides the tryptophan are involved in substrate binding and catalysis²⁰. Consequently, almost every mutation in this site abolishes enzymatic activity as it was shown for the DGCs PleD and WspR from *Caulobacter crescentus* and *Pseudomonas aeruginosa*^{18,23}. Moreover, many DGCs are subject to allosteric feedback regulation to avoid excessive GTP consumption and c-di-GMP accumulation². High affinity c-di-GMP binding to the conserved amino acid motif RxxD which is located five amino acids upstream of the A-site is responsible for this non-competitive inhibition of cyclase activity^{21,24}. Because of its function, it is also termed inhibitory site (I-site).

The enzymatic activity of phosphodiesterases relies on two unrelated protein families with conserved EAL or HD-GYP domains. EAL domain proteins require Mg^{2+} or Mn^{2+} to hydrolyze c-di-GMP into the linear molecule 5'-pGpG²⁴⁻²⁶ which is thought

to be further degraded into GMP by unspecific cellular phosphodiesterases^{25,27}. Crystal structures solved in *Bacillus subtilis*, *Klebsiella pneumoniae* and *P. aeruginosa* proposed a general Lewis base-assisted catalytic mechanism, although it is not yet clear if one or two divalent cations are involved²⁸⁻³⁰. The second protein family of HD-GYP domain proteins is less common and belongs to the metal-dependent phosphohydrolases which are able to degrade c-di-GMP to GMP directly³¹. Recently, the structure of an HD-GYP domain protein from the predatory bacterium *Bdellovibrio bacteriovorus* was solved. Its active site consists of binuclear metal center which was found in complex with phosphate. Because the active site and the overall fold differs from EAL domain proteins, a different mode of activity regulation and catalysis is proposed³².

GGDEF, EAL and HD-GYP domains can occur separately, but analysis of prokaryotic genomes revealed the existence of many composite proteins harboring two opposing enzyme activities in one polypeptide³³. However, these proteins usually have either DGC or PDE activity^{26,34-37}. In many cases they display one degenerate domain, often a slightly altered GGDEF domain³³, which retains substrate binding capability and allosterically modulates the activity of the conserved other domain. Such a mode of regulation was observed for PdeA in *C. crescentus* which regulates pole morphogenesis^{33,34}. Some composite proteins such as ScrC in *Vibrio parahaemolyticus* can also switch their activity in dependence of specific accessory factors that link cell density with c-di-GMP signalling^{38,39}. However, only a few examples of true bifunctional composite proteins are known so far^{38,40,41}.

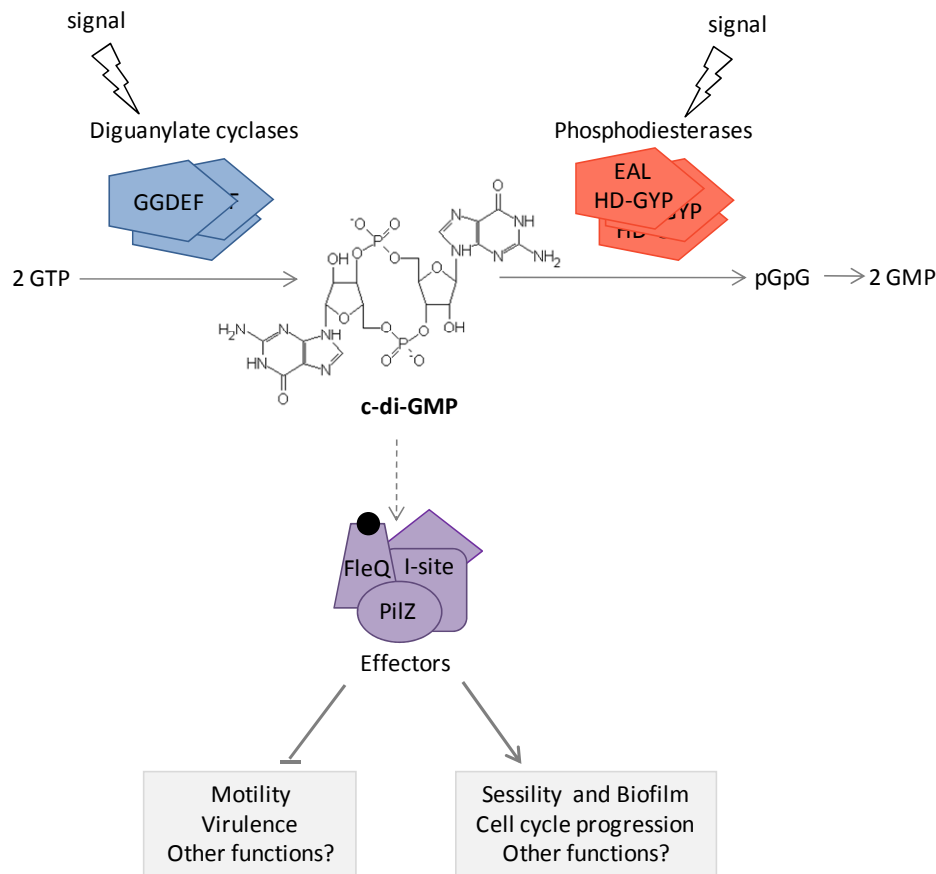


Figure 2: Components of c-di-GMP signaling pathways. Cellular c-di-GMP levels are adjusted by diguanylate cyclases harboring a catalytic GGDEF domain (blue) and phosphodiesterases carrying either catalytic EAL or HD-GYP domains (red). These enzymes respond to a variety of different signals sensed by their N-terminal sensory domains. Diverse c-di-GMP binding molecules, so called effectors, translate cellular c-di-GMP levels into a physiological response. Low levels of c-di-GMP promote a motile, virulent lifestyle, whereas high levels of c-di-GMP are generally associated with sessility and biofilm formation. In *C. crescentus* the localized action of c-di-GMP regulates cell cycle progression. pGp, 5'-phosphoguanylyl-(3'-5')-guanosine. Adapted from⁴².

1.3 GGDEF, EAL and HD-GYP domain proteins are highly abundant in prokaryotic genomes

Interestingly, the number of genes encoding for proteins with GGDEF, EAL and HD-GYP domains varies widely between different species. While GGDEF and/or EAL domain containing proteins are widespread in eubacteria, they are completely absent in eukaryotes and archaea. In the bacterial kingdom the average number of these proteins is highest in proteobacteria and lowest in gram positive bacteria¹⁴. The majority of bacterial chromosomes encodes an intermediate number, for example *E. coli* with 29 GGDEF/EAL domain containing proteins or *C. crescentus* with its four GGDEF, three EAL and seven GGDEF-EAL composite proteins. However, a few organisms like *Helicobacter pylori* or *Haemophilus influenza* contain none of these

domains, whereas various *Vibrio* species have over hundred of these proteins. This high abundance and variability of c-di-GMP signaling proteins within single bacterial species raises the question how such highly redundant systems can be regulated.

1.4 c-di-GMP metabolizing proteins are tightly regulated

The majorities of GGDEF and EAL domains do not stand alone, but are linked to diverse N-terminal sensory and regulatory domains such as PAS, HAMP, GAF and REC domains. These domains are involved in sensing oxygen, redox potential, light, nutrients, osmolarity and many other signals^{14,33,43} and activate their c-di-GMP metabolizing domains in response to specific external or internal signals. This posttranslational control of activity contributes to achieve signal specificity in these complex c-di-GMP signaling systems. However, several additional mechanisms contribute to avoid crosstalk between different c-di-GMP signaling modules. These separate the c-di-GMP pool in time and/or space.

In a temporal regulation different DGCs and PDEs would be active during different time windows or in different environmental conditions. This can be achieved by different gene expression and regulated proteolysis. An example for transcriptional regulation has been reported in *E. coli*, where only a few GGDEF and EAL protein are expressed during exponential growth, whereas others such as those for curli and fimbriae synthesis are under the control of σ^5 and therefore induced upon entry in the stationary phase^{44,45}. In *Yersinia pestis* the DGC HmsT is involved in biofilm formation which is crucial to colonize the flea. However, when cells are shifted to higher temperatures, which corresponds to a transmission from flea to mammalian host, this biofilm has to be dissolved and consequently, HmsT has to be proteolytically removed to allow acute infection of the host⁴⁶.

Spatial sequestration would require that different DGCs and PDEs operate in physically separated entities resulting in local c-di-GMP pools with separate regulatory outputs². Several examples for subcellular localization and activation of DGCs and PDEs have been described in *C. crescentus*. Two antagonistic and interacting enzymes, the PDE PdeA and the DGC DgcB, localize to the cell pole and keep c-di-GMP concentrations low in the motile cell type. During motile-to-sessile transition, PdeA is proteolytically degraded and the unopposed activity of DgcB, together with PleD activity, a second polar localized DGC, lead to a localized burst of c-di-GMP that drives pole morphogenesis in *C. crescentus*⁴⁷.

Based on the finding that small molecules like c-di-GMP rapidly diffuse in the cytoplasm, another mechanism assuming a global c-di-GMP pool was proposed. Specificity would be achieved by effectors that bind c-di-GMP with different affinities and would mediate various processes as a function of the cellular c-di-GMP concentration⁴³.

To summarize, many different mechanisms contribute to the activity control of DGCs and PDEs and the two controversial discussed assumptions of local and global c-di-GMP pools are probably not mutually exclusive.

1.5 c-di-GMP effector molecules mediate cellular functions

Signal transduction via second messengers requires receptor molecules that bind and translate cellular concentrations of the second messenger into a specific physiological response (Figure 2). So far, a few classes of such c-di-GMP binding molecules acting on the transcriptional, translational and post-translational levels have been identified so far (Figure 3).

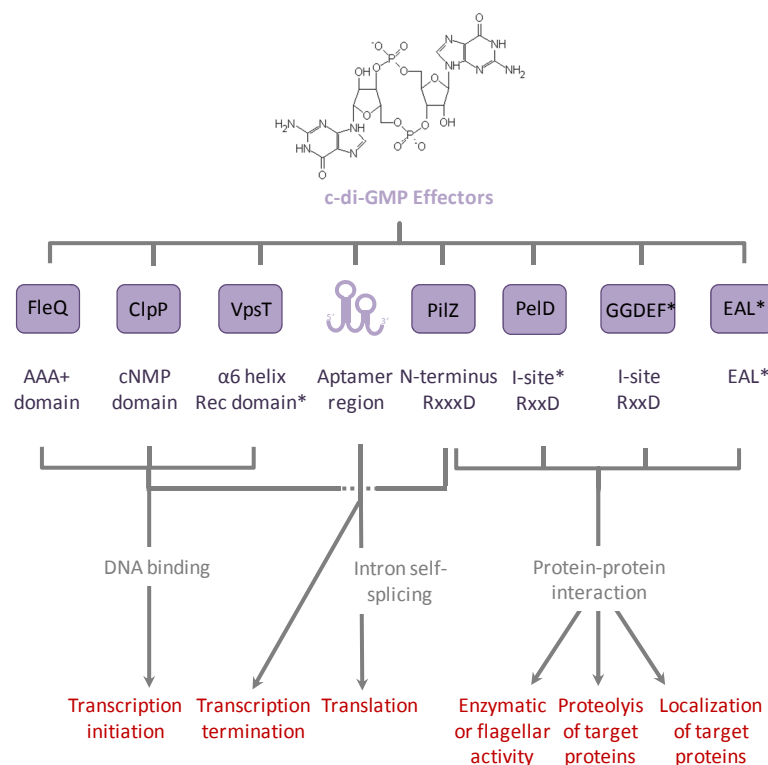


Figure 3: Diversity of c-di-GMP effectors. Transcription is affected by several types of transcriptional regulators which upon binding of c-di-GMP alter the affinity for target gene promoters. In c-di-GMP-dependent riboswitches c-di-GMP binds to a complex tertiary structure called aptamer and regulates transcription termination or translation initiation. PilZ, degenerate GGDEF and EAL domain containing proteins regulate enzymatic or flagellar activities, proteolysis and localization by direct interaction with their target proteins. PilZ domain transcriptional regulators can also affect transcription initiation. The different effector molecule types are shown in violet, GGDEF* and EAL* indicate degenerate domains. Below the proposed binding domains/sites are shown, Rec domain* and I-site* indicate unusual receiver domain and I-site. Adapted from⁴⁸.

Among these, the PilZ domain proteins are the best studied class. They were identified in *P. aeruginosa* where their function is linked to the production of exopolysaccharides⁴⁹. Other PilZ domains have been implicated in motility control like YcgR in *Salmonella enterica* and *E. coli* or DgrA in *C. crescentus*⁵⁰⁻⁵². The structures of PlzD, a PilZ domain protein from *Vibrio cholerae* and PA4608 from *P. aeruginosa* showed that c-di-GMP binds as intercalated dimer⁵³ to the β -barrel surface and to a conserved flexible N-terminal RxxxR motif of the PilZ domain. Binding leads to a conformational rearrangement and allows high affinity binding with a K_D ranging from 50 nM – 1 μ M^{50,52,54,55}.

Another group of c-di-GMP effectors consists of GGDEF and EAL domains which lost their enzymatic activity, but retained their ability to bind c-di-GMP into an allosteric binding site (I-site) or into the EAL site, respectively. Examples for proteins having degenerate c-di-GMP binding domains include the PleD paralog PopA from *C. crescentus*⁵⁶ and FimX from *P. aeruginosa*^{57,58}. PopA binds c-di-GMP into its degenerate GGDEF domain with a K_D of approximately 2 μ M⁵⁶ and is involved in cell cycle control, while FimX binds c-di-GMP via its catalytically inactive EAL site to regulate twitching motility in *P. aeruginosa*⁵⁷. Similar c-di-GMP binding into a degenerate EAL domain is reported for LapD, a protein involved in surface attachment of *P. fluorescens*^{59,60}.

Other recently found c-di-GMP effectors are transcriptional regulators, such as FleQ from *P. aeruginosa* and Clp from *Xanthomonas campestris*. FleQ was discovered as a transcriptional master regulator whose affinity for exopolysaccharide genes is regulated by c-di-GMP⁶¹. Interestingly, c-di-GMP was shown to bind to the AAA+ ATPase domain suggesting that c-di-GMP might interfere with the ATP dependent oligomerization of FleQ⁴². Similarly, in Clp, an unusual CRP family member, DNA binding is allosterically inhibited by c-di-GMP^{62,63}. Yet another transcriptional regulator functioning as c-di-GMP effector protein was identified in *V. cholera*. VpsT regulates the expression of *vps* exopolysaccharide genes and is composed of a C-terminal receiver domain fused to a DNA binding output domain. Binding of a c-di-GMP dimer within an additional C-terminal α -helix in its receiver domain, leads to a c-di-GMP dependent crosslinking of two adjacent VpsT molecules. This dimerization activates VpsT^{64,65}.

In addition, it was observed that c-di-GMP can bind to specialized RNA domains, which are present in the 5' untranslated region of some mRNAs and regulate their translation⁶⁶⁻⁶⁸. Such a so called riboswitch has been recently shown to regulate alternative splicing of a group I splicing ribozyme in *Clostridium difficile*. Depending on the presence of c-di-GMP and GTP these ribozymes use alternative splicing sites and make the ribosome binding site of a virulence gene accessible for translation

initiation factors⁶⁹. While a few bacteria extensively use riboswitches, they are absent in the majority of bacterial species².

It is very likely that additional effectors will be discovered in the future as the described effectors cannot account for all the cellular functions that are regulated by c-di-GMP.

1.6 c-di-GMP controls motility, biofilm formation and virulence

In the recent years growing evidence linked the action of c-di-GMP signaling molecules with the transition between motile and sessile bacterial lifestyles. Many studies have reported that low c-di-GMP concentrations correlate with motility, whereas elevated levels of c-di-GMP generally promote a sessile, biofilm associated lifestyle^{2,15,70}. Moreover, high levels of c-di-GMP were shown to suppress virulence phenotypes during acute infections, whereas low c-di-GMP concentrations promote persistence and the establishment of chronic infections. Therefore c-di-GMP is also considered to mediate the transition between acute and chronic infections⁷⁰⁻⁷².

1.6.1 c-di-GMP controls cell motility

Many mechanisms have evolved in prokaryotes to move across surfaces, these include swimming, swarming, twitching and gliding. Whereas twitching and some forms of gliding have been shown to require type IV pili^{73,74}, swimming and swarming are dependent on flagella. In contrast to swimming, swarming is powered by multiple flagella and bacteria that swarm can also swim. The majority of bacteria have one kind of flagella for both, swimming and swarming, some others like *V. parahaemolyticus* have distinct flagella for the two modes of motility^{74,75}. In the past years a growing number of studies have linked the action of c-di-GMP with these types of cell motility^{2,43,76}.

It has been reported that c-di-GMP can interfere with flagellar function at different levels: A transcriptional control was described for *V. cholerae*, where c-di-GMP binding to the transcriptional master regulator VpsT was shown to downregulate flagellar genes and induce genes required for polysaccharide biosynthesis and biofilm^{64,65}. An example for posttranslational control of motility was reported in *C. crescentus* where the c-di-GMP effector protein TipF (Y. Cohen, unpublished) interferes with correct flagellum assembly by an unknown mechanism⁷⁷. Moreover, c-di-GMP can also affect flagellar motor function after completion of the flagellum assembly. An example for such a functional interference was observed in *E. coli* where c-di-GMP controls swimming velocity. The PilZ domain protein YcgR binds c-di-GMP and modulates flagellar function by interacting with stator complexes of the flagellum. These complexes consist of the motor proteins

MotA and the stator proteins MotB in the stoichiometry of four MotA to two MotB proteins. They function as individual stator units which surround the flagellar basal body and conduct the passage of protons to power flagellar rotation⁷⁸. c-di-GMP loaded YcgR directly interacts with MotA and limits the number of individual stator complexes which can be assembled. Successive occupation of stator complexes with c-di-GMP bound YcgR leads to a gradual reduction of proton influx and torque generation and finally to decreased swimming velocity⁵¹ (Fig. 4). A similar mechanism was proposed for *Salmonella*, however in contrast to *E. coli*, c-di-GMP loaded YcgR was shown to interact with the switch units FliG leading to an altered interface between FliG and MotA, which together generate torque⁷⁹. In *C. crescentus*, paralysis of the flagellum is mediated by the PilZ effector protein DgrA. It is proposed that upon binding of c-di-GMP, DgrA represses FliF, which is required for flagellar rotation by a yet unknown mechanism⁵².

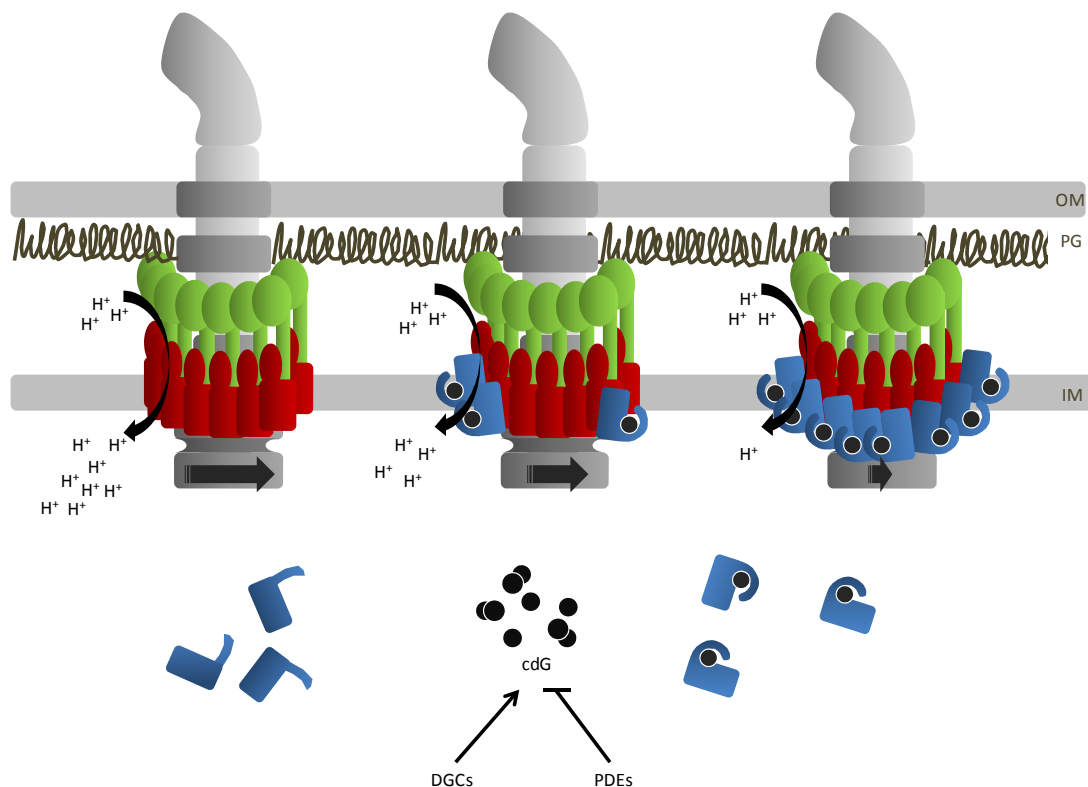


Figure 4: Model for c-di-GMP mediated adjustment of swimming velocity. Flagellar hook basal bodies (grey) and surrounding stator units (red: MotA, green: MotB) are shown. Several DGCs and PDEs balance cellular c-di-GMP levels (black circles). Upon c-di-GMP binding, the PilZ domain protein YcgR (blue) interacts with MotA and limits the number of individual stator complexes which can be assembled. Successive occupation of MotA with c-di-GMP loaded YcgR in response to increasing c-di-GMP levels blocks stator complexes and leads to a stepwise decrease of torque production (black arrows) which is associated with decreased proton (H⁺) influx and decreased swimming speed. OM, outer membrane; IM, inner membrane; PG, peptidoglycan. Adapted from⁵¹.

c-di-GMP is also involved in the regulation of twitching motility. In *P. aeruginosa* the GGDEF/EAL composite protein FimX was found in a transposon screen for reduced twitching motility³⁷. FimX is a GGDEF/EAL composite protein that lacks DGC and PDE activity, but retained the ability to bind c-di-GMP into its degenerate EAL site. It localizes to the cell pole where it is required for the assembly of type IV pili^{36,58} which through a cycle of assembly, attachment and retraction mediate twitching motility⁸⁰. However, it is not yet clear how c-di-GMP binding to FimX finally promotes the assembly of type IV pili.

1.6.2 c-di-GMP controls biofilm formation

Aggregation in biofilms is one of the most successful microbial lifestyles in nature and has been associated with persistence in hostile environments⁸¹. Biofilms are highly structured multicellular communities that adhere to a wide range of biotic and abiotic surfaces and often comprise multiple bacterial species⁸¹. These bacteria secrete large amounts of exopolymeric substances (EPS) such as polysaccharides, nucleic acids, lipids and carbohydrates which are thought to mediate adherence, provide mechanical stability and protect from the environment⁸². This extracellular matrix accounts for over 90% of the biofilm content and is crucial for its formation and maintenance⁸³. Many studies have documented that high c-di-GMP concentrations lead to the production of exopolymeric substances and adhesion factors that promote biofilm formation. c-di-GMP can affect biofilm formation through altered gene expression or through posttranslational mechanisms. These mechanisms have been reported for many bacterial species such as *Pseudomonas*^{59,84-86}, *Vibrios*^{64,87,88}, *E. coli*⁸⁹, *Yersinia*^{90,91} and *Salmonella*⁹²⁻⁹⁴.

In *Klebsiella pneumoniae* biofilm formation depends on type III fimbriae, thin hair like protein structures that mediate adherence to surfaces. Expression of these fimbriae is controlled by MrkH, a PilZ-containing transcriptional regulator that activates the expression of fimbrial genes upon binding of c-di-GMP to its PilZ domain. The DGC YfiN and the PDE MrkJ contribute to the regulation of MrkH activity as a function of the cellular c-di-GMP concentrations⁹⁵.

Biofilm formation in *Pseudomonas fluorescens* is posttranslationally controlled by c-di-GMP and the availability of inorganic phosphate⁹⁶. *P. fluorescens* is a plant pathogen that adheres to plant roots by the adhesin LapA. Under high phosphate conditions, c-di-GMP is produced by DGCs and binds to the cytosolic degenerate EAL domain of the effector LapD. This leads to a conformational change in its output domain and to interaction with the periplasmic protease LapG, thereby protecting LapA from cleavage. Low extracellular phosphate concentration is sensed by the two component system PhoR/PhoB which in response activates the expression of the

PDE RapA. Depletion of c-di-GMP releases LapG from LapD leading to subsequent cleavage of the adhesin LapA^{59,60} (Fig. 5).

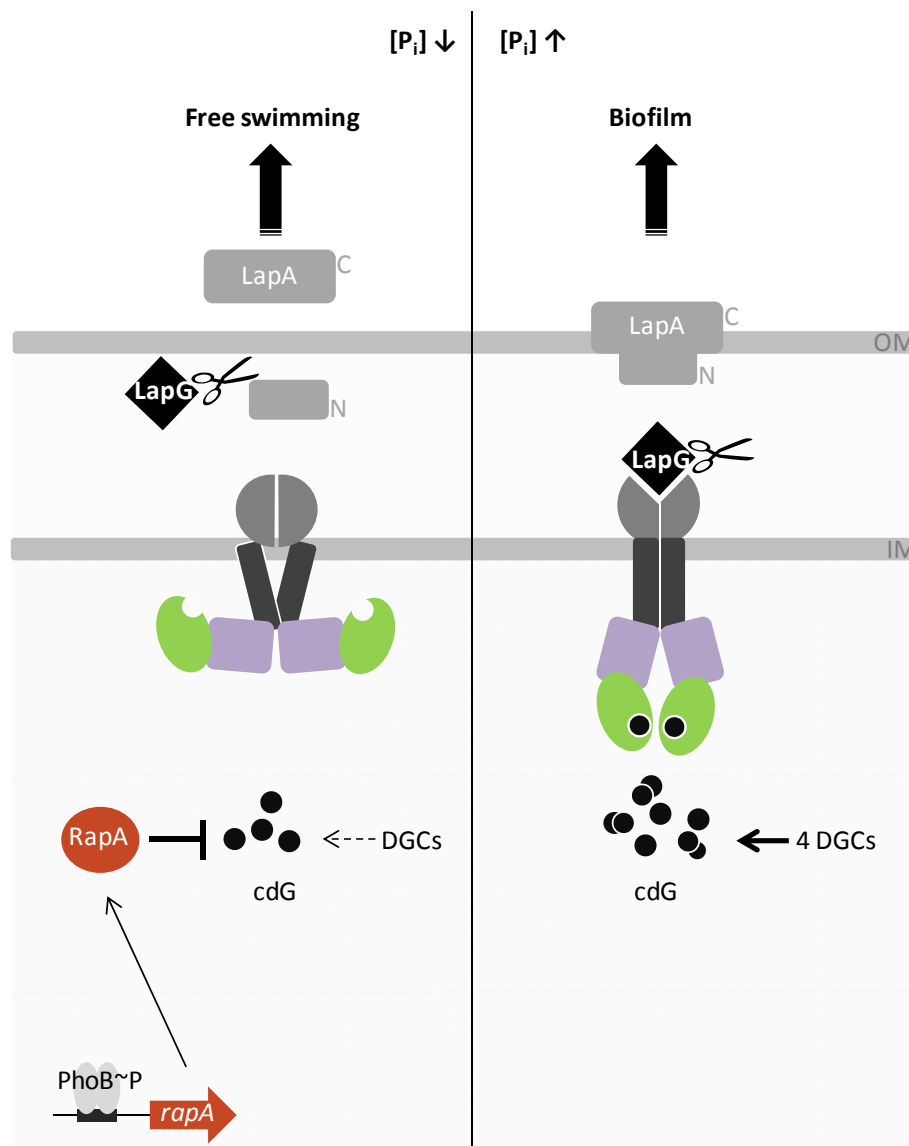


Figure 5: Model for inorganic phosphate and c-di-GMP regulated biofilm formation in *P. fluorescens*. A conformational change of the dimeric c-di-GMP effector protein LapD (violet: GGDEF domain, green: degenerate EAL domain, dark grey: HAMP domain, light grey: output domain) controls the activity of a periplasmic protease LapG (black box) and thereby determines cell adhesion properties. Under high phosphate conditions, c-di-GMP accumulates and binds to the degenerate EAL domain of LapD (green). This leads to a conformational change in its HAMP domains (grey) and allows sequestration of the periplasmic protease LapG (black box). This process protects the adhesin LapA (grey) from proteolytic processing and favors biofilm formation. Low extracellular phosphate activates the two-component system PhoR/PhoB which among other genes induces the transcription of *rapA*. RapA (red) functions as PDE and decreases cellular c-di-GMP concentrations. LapG is relieved from LapD and cleaves LapA thereby promoting its dissociation from the cell membrane. Release of LapA inhibits further attachment and biofilm formation. OM, outer membrane; IM, inner membrane. Adapted from⁹⁶.

1.6.3 c-di-GMP modulates virulence properties

In addition to the role of c-di-GMP in controlling the transition between motile and sessile, biofilm-like bacterial lifestyle, it can modulate virulence properties and virulence gene expression⁹⁷. High levels of c-di-GMP were shown to suppress virulence phenotypes during acute infections, whereas low c-di-GMP concentrations promote biofilm formation which is a virulence factor for the establishment of chronic infections. Therefore c-di-GMP is considered to mediate the transition between acute and chronic infections^{70,71}.

The effect of c-di-GMP on virulence is well studied in the animal pathogen *V. cholerae*⁹⁷. Upon entry into the mammalian host, an unknown signal is thought to activate the two-component system VieSA consisting of the sensor kinase VieS and the response regulator VieA⁹⁸. VieA functions as PDE²⁵ and is strictly required for virulence in mouse models. Its PDE activity is critical for the expression of ToxT, the transcriptional activator of cholera toxin and toxin-regulated pili, the major virulence factors of *V. cholerae*⁹⁹⁻¹⁰¹.

A number of other studies have demonstrated that high c-di-GMP levels repress virulence. In *Salmonella typhimurium* for example invasion into the gastrointestinal epithelial cells is strongly reduced under high c-di-GMP concentrations. This effect is mediated by the biofilm master regulator CsgD which activates genes required for the production of cellulose, capsule and curli fimbriae¹⁰². Expression of these extracellular matrix components interferes with host cell invasion, probably through steric hindrance of the *Salmonella* type III secretion machinery¹⁰³.

Another example that correlates high c-di-GMP concentrations with a reduction of virulence function is described for the plant pathogen *X. campestris*. In response to a diffusible signaling factor (DSF) identified as an unsaturated fatty acid¹⁰⁴ the two-component system RpfCG is activated. The response regulator RpfG is a HD-GYP domain protein that functions as PDE and keeps c-di-GMP concentrations low³¹. It directly interacts with two DGCs in dependence of its conserved GYP motif and regulates a subset of virulence factors, mainly motility related functions, which are essential for full virulence of *X. campestris*^{31,105}.

1.7 Other phenotypes influenced by c-di-GMP

Besides its role in regulating the switch between motile-sessile and virulent-persistent lifestyles, c-di-GMP influences a wide range of other phenotypes such as long-term survival, growth competition, heterocyst development, chemotaxis, heavy metal resistance, phage and antibiotics resistance and photosynthesis^{40,70,106,107}. Moreover, in *C. crescentus* c-di-GMP has been reported to be involved in polar development and cell cycle regulation^{47,56,108,109}.

1.7.1 *Caulobacter crescentus* as model organism for cell cycle and development

Caulobacter crescentus is a gram-negative, rod-shaped α -proteobacterium, which can be isolated from fresh water environments including oceans, streams and lakes¹¹⁰. It is oligoheterotrophic and strictly aerobic. In its natural habitat it is often found attached to submerged biotic and abiotic surfaces including other microorganisms like bacteria and algae¹¹⁰.

The hallmark of the *C. crescentus* life cycle is an asymmetric cell division which results in two morphologically distinct, but genetically identical daughter cells; the so called swarmer and stalked cells (Fig. 6). They have distinct developmental programs reflected by their distinct polar appendages and chromosome replication abilities. The larger stalked cell adheres to surfaces by a membrane protrusion called stalk which contains adhesive polysaccharides at its tip. This so called holdfast mediates very strong and irreversible attachment to solid substrates¹¹¹. DNA replication is strictly restricted to the stalked cell which reinitiates replication almost immediately after cell division^{112,113} thereby working as stem cell continuously producing new swarmer cells¹¹⁴. However, in contrast to many other fast growing prokaryotes, DNA replication is initiated only once per cell cycle¹¹⁵. The smaller swarmer cell is unable to replicate its DNA, but it is motile as it possesses a single polar flagellum and an associated chemotaxis apparatus which allows propelling itself towards a food source. When a nutrient rich environment is reached, the swarmer cell reversibly adheres to the surface by its pili and starts to subsequently eject flagellum. Pili are then retracted to allow the newly formed holdfast to attach irreversibly to the surface. Optimal attachment occurs only during a short time window, when flagellum, pili and holdfast are present at the same time^{116,117}. During the obligate differentiation step from the motile swarmer cell to the sessile stalked cell type the chromosome replication block is relieved, hence the swarmer-to stalked cell transition is also referred to as G1-to S-phase transition in analogy to the G1-phase (gap phase), the S-phase (DNA synthesis phase) and the G2-phase (division phase) in eukaryotic cells.

It is obvious that *C. crescentus* developmental transitions are coordinated with the underlying cell cycle (Fig. 6). The different cell types can be microscopically distinguished by their different morphologies and polar surface structures such as flagellum and stalk. The main advantage of *C. crescentus*, however, lies in the possibility to isolate newborn swarmer cells by density gradient centrifugation. This procedure allows the observation of cell populations at any time point during cell cycle. These features have made *C. crescentus* to a convenient model to study both, bacterial cell cycle and differentiation.

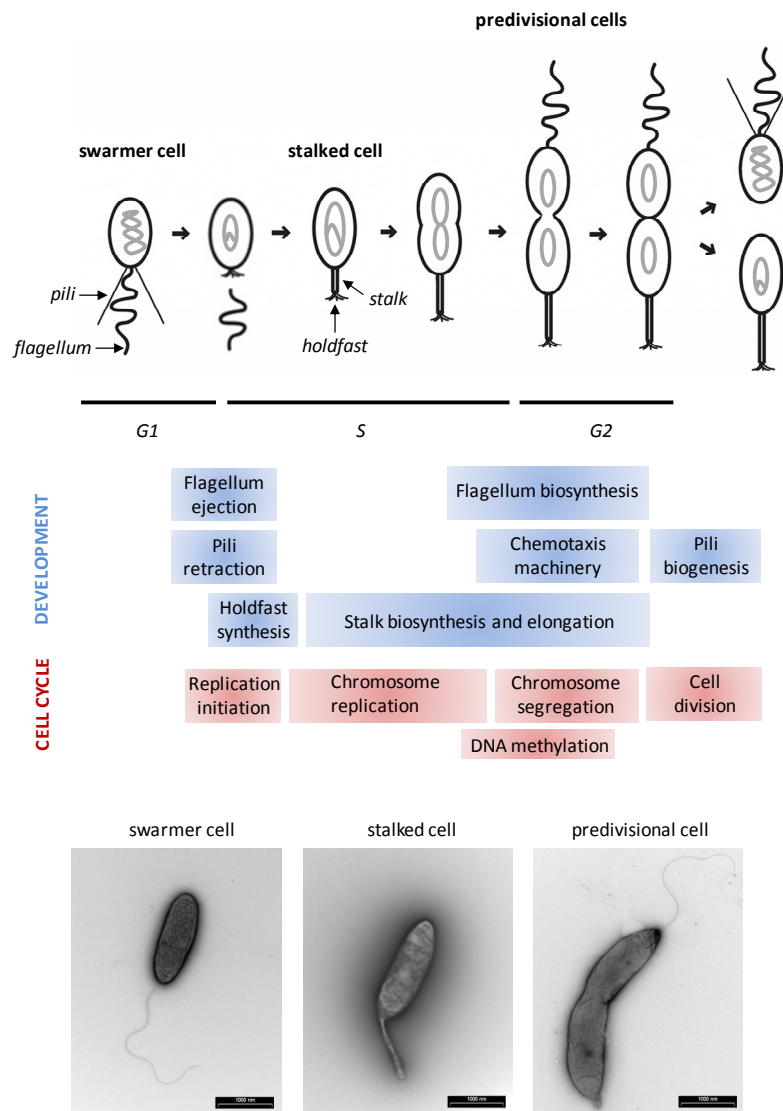


Figure 6: *C. crescentus* cell cycle and development events are tightly coupled. During an obligate cell differentiation process, the motile swarmer cell loses pili and flagellum and replaces them by a structure called stalk which contains an adhesive polysaccharide at its tip, the holdfast. While the chromosome of swarmer cells is quiescent (schematically represented as a grey knot), stalked cells can immediately reinitiate DNA replication (schematically shown in grey “θ” structures). Developmental events are indicated in blue boxes, underlying cell cycle events in red boxes. Electron micrographs of different *C. crescentus* cell types are shown in the lowest panel. Scale bars are equal to 1 μm . Adapted from¹¹⁸.

1.8 C-di-GMP signaling molecules are involved in *C. crescentus* development

Cell cycle-dependent fluctuations of c-di-GMP in the different *C. crescentus* cell types control many aspects of pole development¹¹⁹ such as flagellum, holdfast and stalk biogenesis. So far, several different DGCs and PDEs have been shown to contribute to the asymmetric distribution of c-di-GMP. Among these is the diguanylate cyclase PleD.

PleD is an unorthodox member of the response regulator family of two component signal transduction systems. It contains two N-terminal receiver domains (Rec1 and Rec2) fused to a C-terminal GGDEF domain^{18,20,120}. Upon phosphorylation by two cognate sensor histidine kinases, PleC and DivJ, PleD is activated¹²⁰ and dynamically localizes to the stalked cell pole where it orchestrates pole morphogenesis by yet unknown effector molecules¹⁸ (Fig. 7).

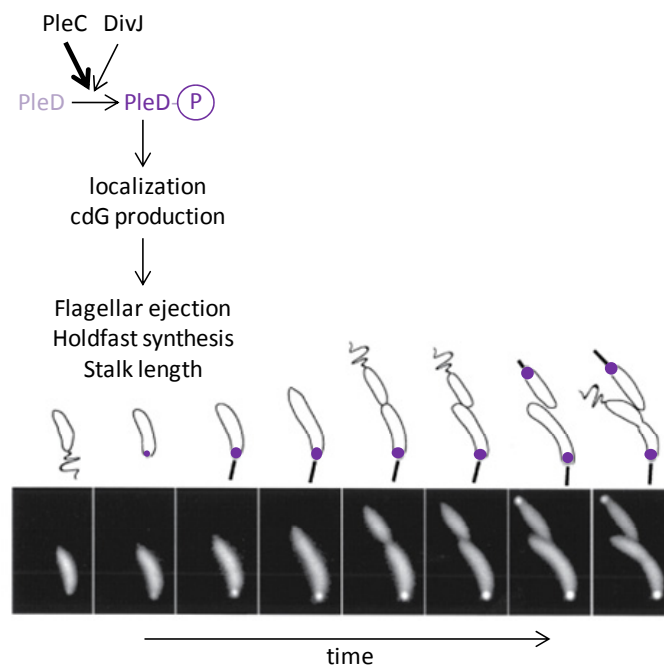


Figure 7: Spatial distribution of the response regulator PleD during *C. crescentus* cell cycle and the upstream components controlling its activity. Time lapse microscopy shows the localization behavior of PleD-GFP during cell cycle. PleD is delocalized in swamer cells. Upon phosphorylation by two cognate histidine kinases, PleC and DivJ, PleD~P is sequestered to the stalked pole where it is involved in flagellar ejection, stalk and holdfast biogenesis. Progression of cell cycle and localization of PleD (violet circles) are shown schematically. Adapted from¹⁸.

A *pleD* deletion mutant fails to efficiently shed flagellum during swarmer-to-stalked cell transition leading to the expression of ectopic flagella in stalked and predivisional cells^{120,121}. This manifests in hypermotile cells^{120,122} and is in contrast to the reduced motility behavior observed on semi solid agar plates. This discrepancy is believed to be due to a chemotaxis defect of *pleD* mutants^{120,123}. Besides its role in flagellar ejection, PleD functions in the correct timing of holdfast and stalk biosynthesis. Holdfast synthesis is delayed in the absence of PleD leading to reduced surface binding properties¹¹⁷ and stalks are strongly shortened compared to wild-type PleD¹²⁰.

Recently, the crystal structures of non-activated and activated PleD have been solved and gave insight into its activation mechanism^{20,21}. They revealed that phosphorylation at the conserved aspartic acid D53 in its Rec1 domain results in the reorientation of two conserved amino acids, T83 and F102, which function as molecular lever and induce conformational changes in the β 4- and β 5-helices of the Rec1 domain^{21,124,125}. This movement promotes rearrangement of both receiver domains, which in turn, facilitate dimerization between Rec1 and Rec2' of an adjacent PleD molecule²¹. A conserved T26 residue plays a critical role in this Rec1-Rec2' mediated dimerization process. While in the non-activated structure this residue sticks out of the Rec1 domain and connects to the Rec2' of an adjacent protomer, the activated structure displays an extended Rec1-Rec2' interface with multiple additional interactions and salt bridges formed between the Rec1 and Rec2' subunits^{20,21}. This tight arrangement of the receiver domains brings two adjacent GTP bound GGDEF domains into close proximity and allows simultaneous nucleophilic attacks of the 3'-hydroxyl group of one GTP onto the α -phosphate of the other GTP. These reactions lead to the formation of c-di-GMP²¹ (Figure 8). The combination of structural analysis and *in vivo* studies with D53, Y26 and active site mutants indicated that phosphorylation induced dimerization is a prerequisite for DGC activity and localization of PleD¹⁰⁸.

Similar to other DGCs, PleD activity can be regulated by inhibitory sites (I-sites) which bind c-di-GMP and mediate feedback inhibition^{20,21}. In PleD three different I-site motifs account for two alternative inhibition modes. The core c-di-GMP binding site is formed by three residues in the GGDEF domain, R359 and R362 of the RxxD motif and R390. Mutations of these so called primary I-site residues (I_p) strongly reduce c-di-GMP binding properties. However, while PleD with mutated R359 and R362 residues completely loses DGC activity, a R390 mutant is active and displays an increased inhibition constant (K_i)²⁴.

In the non-activated PleD structure an intercalated c-di-GMP dimer ($[c\text{-di-GMP}]_2$)⁵³ was shown to crosslink the GGDEF and the Rec2 domain by binding to the primary I-site and to a secondary I-site ($I_{S,Rec2}$). This secondary site is formed by R148 and R178 and is located on the Rec2 domain. Mutation of these residues leads to an increased K_i value. In activated PleD, $[c\text{-di-GMP}]_2$ binding to the primary I-site occurs in the exact same way as in the non-activated structure, but it crosslinks to another residue on an adjacent GGDEF domain, R313 ($I_{S,GGDEF}$). Due to symmetry in activated, dimeric PleD, a second c-di-GMP dimer crosslinks the GGDEF domain of an adjacent PleD molecule. Similar as observed for $I_{S,Rec2}$ mutants, mutation of R313 increased K_i value. In both inhibition modes, c-di-GMP dependent domain crosslinking is thought to reduce the mobility of the GGDEF domains and prevents the productive

arrangement of PleD active sites. This mechanism is called “inhibition by domain immobilization” (Fig. 8).

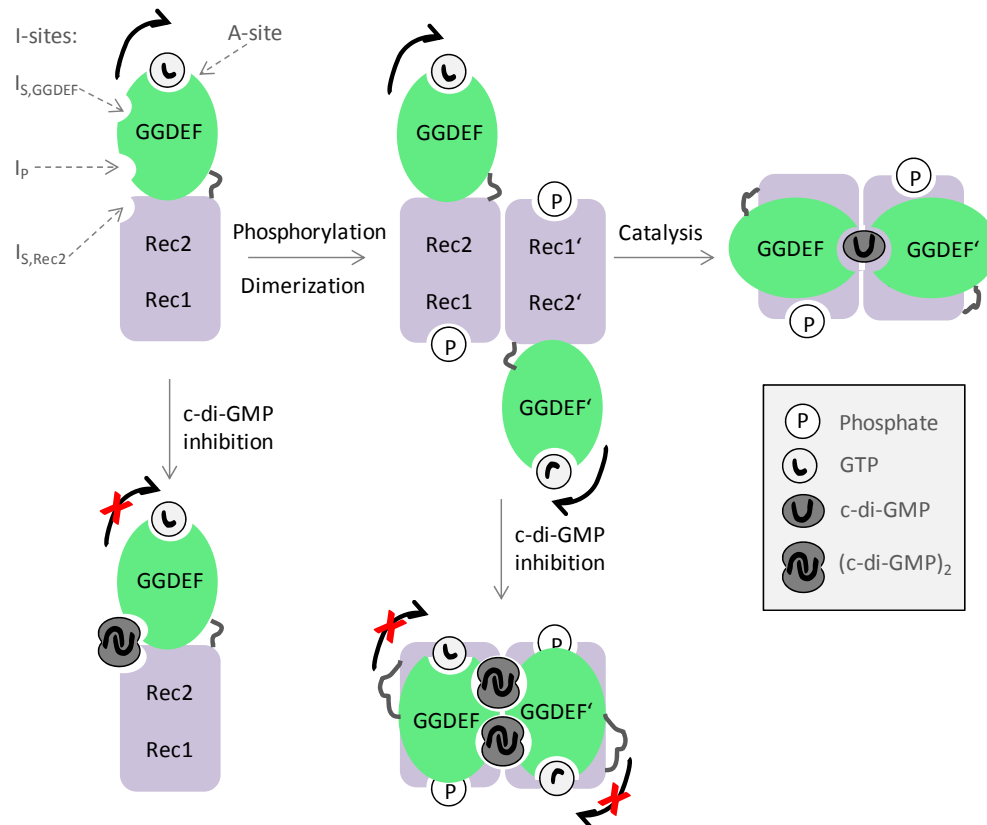


Figure 8: Model for PleD regulation. The catalytic GGDEF domain (green) is connected to its receiver domains (Rec1, Rec2, violet) by a flexible linker and is mobile relative to the receiver domains (black arrow). Phosphorylation (P) of the Rec1 domain leads to conformational changes that promote dimerization of its receiver domains. This brings adjacent GTP-bound GGDEF domains into close proximity and allows the condensation of two GTP molecules into one molecule of c-di-GMP. Two modes of allosteric feedback inhibition involving different I-sites are known (lower panel). Binding of c-di-GMP to the primary (I_p) and one of the secondary I-sites ($I_{S,Rec2}$ or $I_{S,GGDEF}$) can crosslink the GGDEF domain with either the Rec2 domain (first mode of inhibition) or with an adjacent GGDEF' domain (second mode of inhibition). In both cases, this crosslinking reduces mobility (crossed black arrows) and prevents a productive rearrangement of GGDEF active sites (A-site). Adapted from²¹.

Besides PleD, a second DGC, DgcB, was shown to mediate swarmer-to-stalked cell transition. In swarmer cells, DgcB activity is limited by the antagonistic enzyme PdeA, which functions as PDE and keeps c-di-GMP concentrations low. However, during swarmer-to-stalked cell transition, PdeA is targeted to the cell pole where it is degraded by the polar protease complex ClpXP. Localization of both, the substrate PdeA and the protease ClpXP is dependent on the single response regulator CpdR which itself localizes to the cell pole as a function of its phosphorylation state. Proteolytic processing of PdeA relieves DgcB and together with activated PleD leads

to an upshift in c-di-GMP concentration which drives pole morphogenesis. In addition, this mechanism contributes to the degradation of the cell cycle master regulator CtrA and thereby allows entry into S-phase⁴⁷ (Fig. 9).

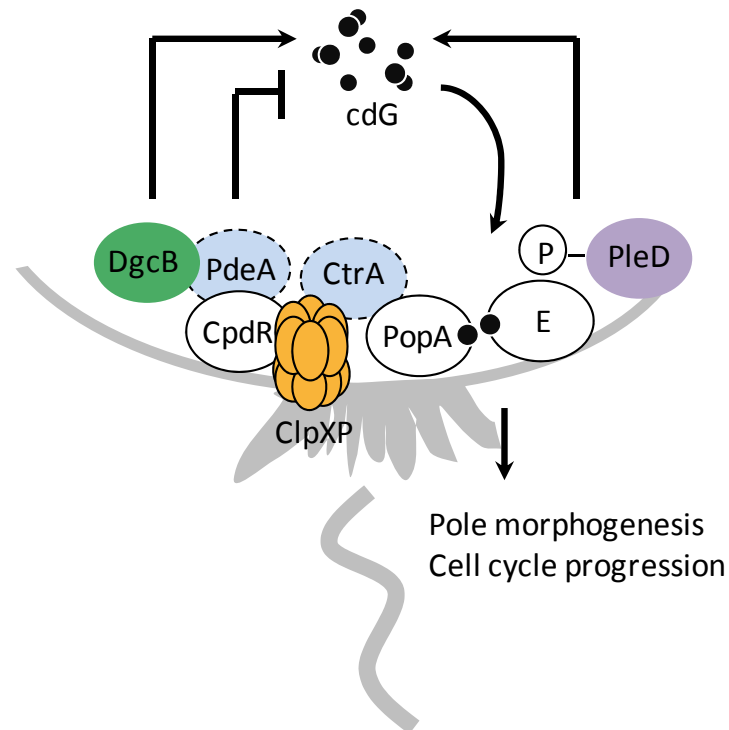


Figure 9: Model for c-di-GMP mediated pole morphogenesis and cell cycle progression. In swarmer cells, DgcB activity (green) is neutralized by the antagonistic enzyme PdeA (blue) which degrades c-di-GMP (cdG, black circles) and keeps c-di-GMP concentrations low. During swarmer-to-stalked cell transition, PdeA is targeted to the pole by CpdR, where it is proteolytically processed by the polar ClpXP complex (orange). This process relieves DgcB and leads together with activated PleD~P (violet) to an upshift in c-di-GMP. This c-di-GMP increase promotes pole morphogenesis through unknown effectors (E) and contributes to the degradation of the replication inhibitor CtrA (blue) to allow cell cycle progression. Adapted from⁴⁷.

1.9 Three oscillating global master regulators control *C. crescentus* cell cycle

In *C. crescentus* correct timing of chromosome replication and cell division relies on periodic fluctuations of three essential global master regulators, CtrA, GcrA, DnaA, and a DNA methyltransferase CcrM¹²⁶⁻¹²⁹. They are organized in a hierarchical transcriptional cascade where every master regulator controls the expression of the next. Together with additional posttranslational modifications such as regulated proteolysis, phosphorylation and specific protein localizations they form an oscillating genetic circuit that ensures the correct activation timing of modular subsystems and numerous downstream targets thereby controlling cell cycle progression^{76,130,131} (Fig. 10).

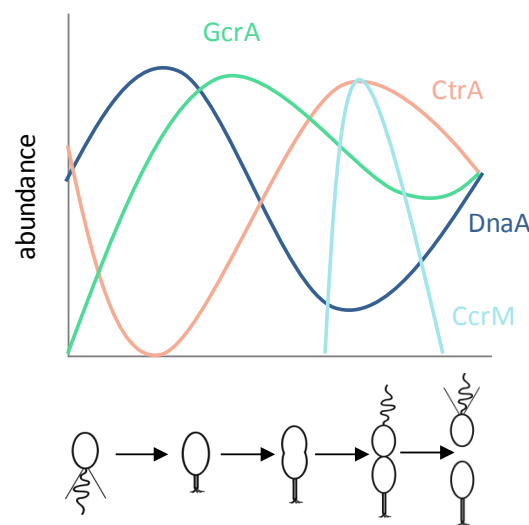


Figure 10: Fluctuations of the three global master regulators CtrA, DnaA, GcrA and the methyltransferase CcrM during cell cycle. Periodic accumulation of these regulators drives cell cycle progression and they successively regulate the cell cycle dependent transcription of over 200 genes. Adapted from¹³².

CtrA is a response regulator which acts as a transcriptional regulator¹³³ for 95 genes involved in chromosome replication initiation, chromosome methylation, cell division and development¹²⁶. In swarmer cells, CtrA is phosphorylated and inhibits chromosome replication initiation¹³⁴. At the same time, it represses the transcription of *ftsZ* and *podJ*^{135,136}, which are required for cell division and polar development^{137,138} and it also represses the transcription of *gcrA*^{127,129}. GcrA is the second cell cycle regulator which controls genes for chromosome replication, cell elongation and polar development by an unknown transcriptional mechanism^{127,139}. During swarmer-to-stalked cell transition, CtrA is proteolytically cleared to allow chromosome replication and at the same time DnaA, a transcriptional activator for chromosome replication, is stabilized and activates the transcription of *gcrA*¹⁴⁰, *ftsZ*,

podJ and genes involved in nucleotide biosynthesis and cell division. Derepression of *gcrA* and concurrent activation by DnaA allows the accumulation of GcrA in stalked cells which eventually turns on *ctrA* transcription in predivisional cells¹²⁷. Together with a positive feedback loop this results in high CtrA concentrations in late predivisional cells¹⁴¹, which does not only shut off *gcrA* transcription, but also activates *ccrM* methyltransferase transcription^{142,143}. At the same time, synthesis of DnaA is stopped and DnaA is removed by degradation through the ClpP protease¹⁴⁰. Newly synthesized CcrM starts to methylate hemimethylated, newly replicated DNA¹⁴⁴ thereby controlling the activity of genes whose expression depends on the methylation state of their promoters. The expression of DnaA for example is down regulated in presence of hemimethylated DNA after replication initiation¹⁴⁵, whereas CtrA transcription is turned on under hemimethylated conditions¹⁴³. CcrM itself is subject to negative autoregulation by methylation of its own promoter¹⁴⁶. To further restrict CcrM activity to the short time window after cell division, CcrM is degraded by the Lon protease¹⁴⁷ (Fig. 11).

The precise timing, teamwork and the correct spatial expression of CtrA, GcrA, DnaA and CcrM is essential for cell cycle progression and development of polar organelles like flagellum, pili and holdfast.

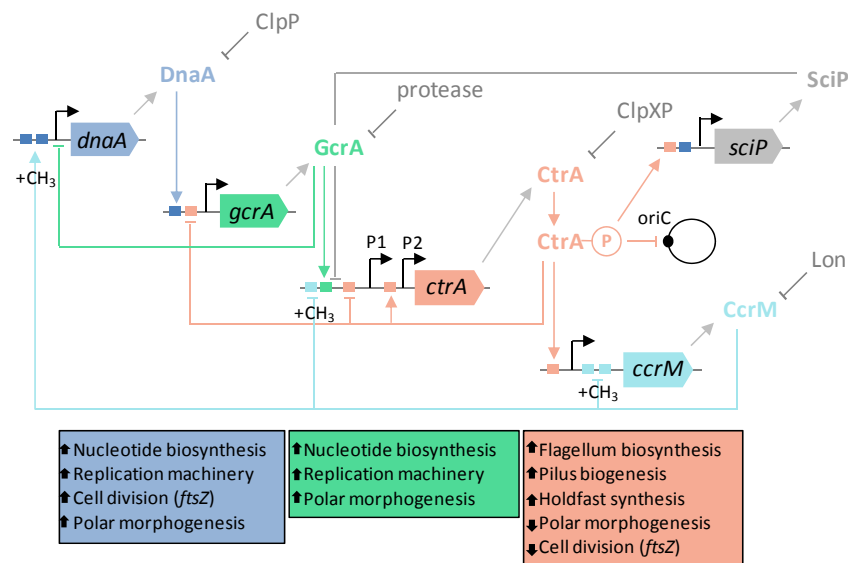


Figure 11: Schematic picture of the *C. crescentus* cell cycle control circuit. Every master regulator activates the transcription of the next and, in case of CtrA and CcrM, inhibits transcription of the previous master regulator in the cascade and *ctrA* transcription is additionally inhibited by SciP. The activity of these cell cycle regulators is posttranslationally controlled by proteolysis, the respective proteases involved are depicted in grey. Promoters (P1 and P2) are indicated with black arrows, the colors of regulatory binding boxes correlate with the color of the master regulator that governs it. +CH₃ represents methylation sensitive promoters. The colored boxes show which functions are regulated by the corresponding master regulator (↑ upregulated, ↓ downregulated). Adapted from¹³⁰.

1.9.1 CtrA controls the cell cycle dependent expression of many target genes and silences the origin of replication

CtrA (cell cycle transcriptional regulator) is the best characterized cell cycle master regulator in *C. crescentus*. It is an essential member of the response regulator family of two component systems and contains a DNA binding output domain¹³³. Typically for this family of response regulators it is activated by phosphorylation of a conserved aspartic acid residue in its receiver domain which serves as phosphoryl acceptor site. Phosphorylated CtrA, CtrA~P, recognizes a specific DNA sequence motif (TTAA-N7-TTAA) in the promoter region of its downstream targets¹¹³. Affinity of CtrA~P binding to this so called CtrA binding box is dependent on the spacing and the conservation of the TTAA elements and is thought to affect temporal expression of CtrA dependent genes^{142,148}. CtrA~P directly controls 95 genes organized in 55 operons¹²⁶. One third of these genes are repressed, two thirds are activated by CtrA. Most repressed genes are maximally expressed when CtrA is degraded during swarmer-to-stalked cell transition and conversely, activated genes are highly expressed after CtrA accumulation in predivisional cells^{126,149}. They encode proteins involved in many diverse cellular processes such as cell division, chromosome methylation, replication initiation and development events like biogenesis of flagellum, pili and holdfast. In addition, CtrA controls the expression of many regulatory genes including operons encoding two component systems and alternative sigma factors which are required for flagellum and stalk formation and proper cell division¹²⁶. In addition to the direct positive and negative regulation of CtrA dependent genes, activated CtrA~P binds directly to five 9-mer sites within the origin of replication (oriC). These sites overlap with an essential DnaA binding box, which is required for DnaA to unwind the DNA and initiate DNA replication. Cooperative binding of phosphorylated CtrA~P to these binding sites is thought to prevent DnaA binding, thereby inhibiting DNA replication initiation in swarmer cells^{150,151}. As cells differentiate into stalked cells, active CtrA~P needs to be removed to permit cell cycle progression.

Correctly timed CtrA activity is crucial for proper cell cycle progression, cell division and development of polar organelles. Active CtrA should appear only at precise times during *C. crescentus* cell cycle, namely in swarmer and in predivisional cells. To ensure temporal restricted CtrA activity, CtrA is redundantly controlled on the levels of transcription, phosphorylation, temporal and spatial regulated proteolysis^{56,127,143,150,152-154}.

1.9.2 CtrA transcription is controlled by two promoters and the methylation state of the DNA

CtrA expression is under control of two promoters P1 and P2 which are active at different time points during cell cycle¹⁴¹. P1 is a weak promoter active in stalked cells. It contains a GANTC methylation site and fires right after replication initiation when the DNA is hemimethylated^{115,143}. In addition, it is stimulated by accumulated GcrA¹²⁷. This allows the production of CtrA in predivisional cells resulting in CcrM activation which methylates freshly replicated DNA thereby repressing P1¹⁴¹. The stronger promoter P2 is under positive feedback control and is driven by the P1- and GcrA-mediated CtrA accumulation in predivisional cells. The resulting burst of CtrA is required in swarmer cell types to inhibit DNA replication initiation¹⁴¹. However, excessive accumulation of CtrA is avoided by SciP which represses *ctrA* transcription. SciP is a transcription factor belonging to the CtrA regulon¹⁵⁵. It accumulates in swarmer cells and represses genes which have been previously activated by CtrA. Among these genes are mainly chemotaxis and flagellar genes. SciP is thought to increase the robustness of cell cycle control¹⁵⁶ (Fig. 11).

However, transcriptional control is not strictly necessary. Cells constitutively transcribing CtrA still proceed through cell cycle¹⁵⁰ suggesting other control mechanisms contributing to the specific CtrA expression and activity during cell cycle.

1.9.3 A phosphorelay couples CtrA phosphorylation and stabilization

In addition to the transcriptional control, the activity of CtrA is modulated by phosphorylation of its conserved aspartic acid. Phosphorylated CtrA displays a higher binding affinity to the downstream target gene promoters and binding to the origin of replication is strongly enhanced when CtrA is phosphorylated¹⁵¹. Phosphorylation of CtrA is mediated by phosphorelay system comprising the membrane bound histidine kinase CckA^{141,157} and the single domain histidine phosphotransferase ChpT. Concurrent to CtrA phosphorylation, the single domain response regulator CpdR is phosphorylated by CckA/ChpT preventing CtrA from being degraded (see below). Therefore, phosphorylation via the CckA/ChpT pathway activates and stabilizes CtrA at the same time¹⁵³.

CckA is active as a kinase in swarmer and predivisional cells and loses its kinase activity during swarmer-to-stalked cell transition to allow CtrA degradation and entry into S-phase^{157,158}. Downregulation of the CckA-ChpT phosphorelay during swarmer-to-stalked cell transition relies on specific protein-protein interactions. The core mechanism is formed by the tyrosine kinase DivL¹⁵⁹ and the single domain response regulator DivK¹⁶⁰. In swarmer cells, DivL and CckA form a polar complex^{161,162} that

promotes CckA kinase activity and thus favors CtrA activity and stability. Upon swarmer-to-stalked cell differentiation, phosphorylated DivK~P levels increase. DivK~P binds directly to DivL preventing DivL from directly stimulating CckA kinase activity¹⁶². In predivisional cells CckA avoids downregulation by DivK~P by localizing at the swarmer pole together with PleC, the main phosphatase for DivK~P¹⁶² (Fig. 12).

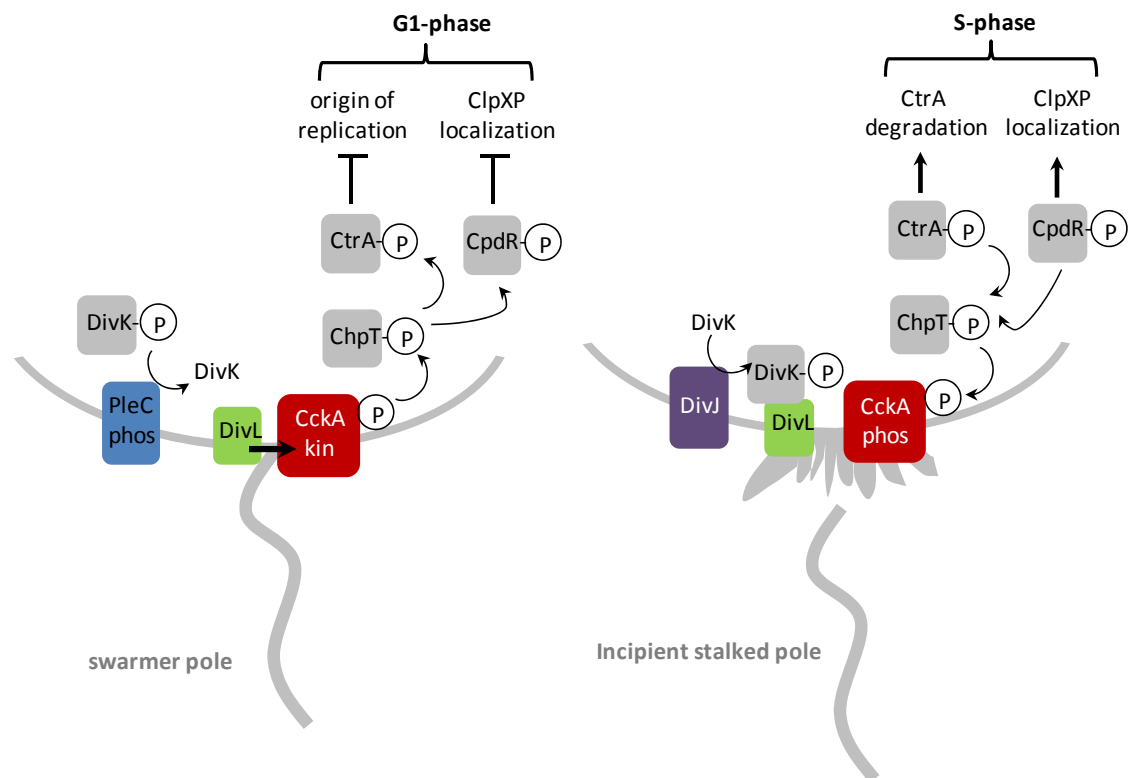


Figure 12: Regulation of the phosphorelay coupling CtrA phosphorylation and stability. In swarmer cells, PleC is active as phosphatase (blue) and dephosphorylates DivK. This allows DivL (green) to stimulate CckA kinase activity (red). The subsequent CckA/ChpT phosphorelay leads to phosphorylation of CtrA and CpdR and at the same time, enhances CtrA stability and prevents it from degradation. Consequently, the origin of replication is inhibited and cells remain in the G1 phase. During swarmer-to-stalked cell transition, the kinase DivJ gets active and phosphorylates DivK which through the binding to DivL inhibits CckA kinase activity and ultimately leads to dephosphorylation of CtrA and CpdR. CtrA can be removed and cells can enter S phase. Adapted from¹⁶².

PleC together with the antagonistic enzyme DivJ at the opposite pole warrant CckA activity in swarmer cells. The stalked pole residing histidine kinase DivJ phosphorylates DivK, whereas the phosphatase PleC at the opposite pole mediates dephosphorylation of DivK. In predivisional cells DivK shuttles between the poles with their opposing enzymatic activities. After cell division, the stalked compartment contains mostly DivK~P, whereas the swarmer cell compartment inherits high

concentrations of dephosphorylated DivK^{109,130}. Dephosphorylation of DivK then allows DivL to promote CckA activity and therefore enhance CtrA activity and stability¹⁶². In addition, *divK* transcription is directly controlled by CtrA¹²⁶. Thus CtrA triggers its own inactivation and degradation by inducing DivK synthesis which feeds back to CckA¹⁵³.

1.9.4 Spatial and temporal regulated proteolysis restricts CtrA activity to swarmer cells

In addition to the transcriptional and phosphorylation control of CtrA, subcellular localization and regulated proteolysis play an important role in the presence of active CtrA. To initiate chromosome replication during swarmer-to-stalked cell differentiation, active CtrA needs to be removed to relieve the origin of replication and to allow access of replication initiation factors like DnaA.

Removal of CtrA during swarmer-to-stalked cell transition is mediated by the essential AAA⁺ protease complex ClpXP whose transcription is controlled by CtrA^{126,154,163}. It consists of one or two hexamers of the ClpX ATPase which recognizes the substrate and energizes its unfolding and translocation into the tetradecamer degradation pore of the ClpP peptidase^{164,165}. Substrate specificity is usually conferred by short N-or C-terminal degradation tags on the adaptor proteins or on the direct substrates¹⁶⁶. However, CtrA contains a bipartite degradation signal where both parts are required, but none of them is sufficient to trigger CtrA degradation alone¹⁶⁷. One determinant consist of its C-terminal hydrophobic amino acid tag (-VAA)¹⁵⁰, the second determinant resides in the first 56 amino acids of its receiver domain which also comprises the phosphoryl acceptor site, but phosphorylation does not affect proteolysis¹⁶⁷. Some of these residues are surface located and are thought to form a binding pocket for an adaptor protein that could enhance ClpXP dependent CtrA degradation¹⁶⁷. However, CtrA degradation by ClpXP *in vitro* is adaptor-independent and CtrA appears to be a direct ClpXP substrate¹⁶³.

Coincident with CtrA clearance in the cell, CtrA dynamically localizes to the incipient stalked pole of newborn stalked cells and to the stalked compartment of predivisional cells. Indeed, CtrA degradation was shown to occur specifically at the incipient stalked pole¹⁶⁷. Consistently, the ClpXP protease complex which is present throughout cell cycle sequesters to the same subcellular site to trigger CtrA degradation during swarmer-to-stalked cell transition forming a polar complex with CtrA *in vivo*^{154,168}. The localization of the protease ClpXP and its substrate CtrA to the same subcellular site ensures the correct timing of CtrA removal during cell cycle.

The polar sequestration of each, CtrA and ClpXP requires dedicated localization factors. ClpXP localization is dependent on the single domain response regulator CpdR which itself sequesters to the pole as a function of its phosphorylation state.

Dephosphorylation of CpdR leads to its localization and to the recruitment of ClpXP via direct interaction thereby preventing CtrA degradation^{56,152}. Conversely, phosphorylated CpdR results in delocalized ClpXP and stabilized CtrA. As already mentioned, CpdR phosphorylation is regulated by the same CckA-ChpT phosphorelay which also controls the phosphorylation of CtrA¹⁵³. Delivery of CtrA to the incipient stalked is dependent on c-di-GMP concentrations in the cell and involves the response regulator protein PopA (Fig. 13).

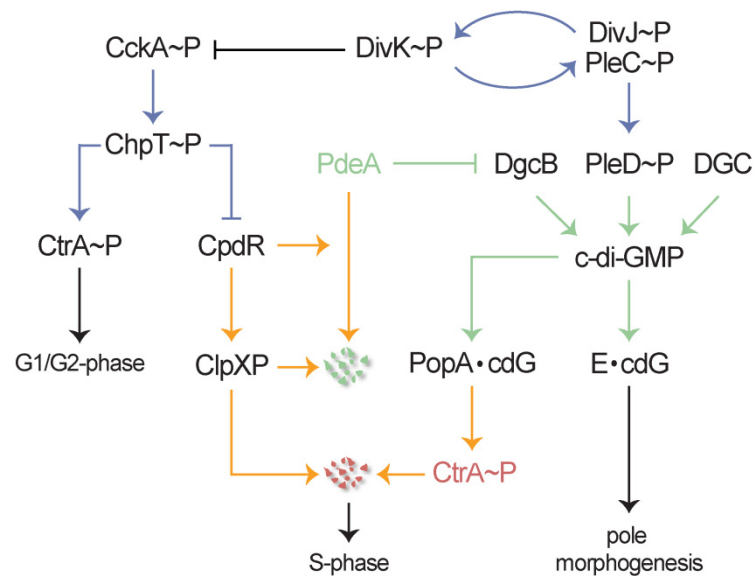


Figure 13: Regulatory network controlling cell cycle progression and pole morphogenesis in *C. crescentus*. Blue arrows indicate phosphorylation dependent processes, green c-di-GMP signaling cascades and orange processes involved in proteolysis of PdeA (green) and CtrA (red). Additional unknown diguanylate cyclases (DGCs) and c-di-GMP (cdG) binding proteins (E) contributing to this network are indicated. Adopted from⁴⁷.

1.10 PopA is a c-di-GMP effector protein involved in both, cell cycle and development

PopA is an unorthodox response regulator having two receiver domains fused to a GGDEF output domain. This domain organization is reminiscent to the diguanylate cyclase PleD and suggested a similar enzymatic function for PopA. However, while phosphorylation and c-di-GMP binding sites (I-sites) are conserved and consistent with this, PopA specifically binds c-di-GMP, the active site motif (A-site) is degenerate and catalytically inactive. These features are typically observed for c-di-GMP effector proteins which modulate cellular behavior as a function of c-di-GMP concentrations.

Mutants lacking PopA fail to localize and to degrade CtrA during swarmer-to-stalked cell transition⁵⁶. This effect is mediated by RcdA, a small adaptor protein that directly interacts with PopA and is required for correct CtrA localization and degradation at the ClpXP occupied stalked pole^{56,168}. Consistent with a role in CtrA degradation, PopA localizes to same subcellular site and interestingly, PopA positioning as well as CtrA localization and degradation are dependent on an intact PopA c-di-GMP binding site⁵⁶. These findings led to a model where PopA, upon c-di-GMP binding, localizes to the ClpXP-occupied stalked pole to promote cell cycle-dependent removal of CtrA through its direct interaction with RcdA⁵⁶. Recently, a second ClpXP substrate, the FtsZ inhibitor KidO, was shown to require PopA for its cell cycle dependent removal¹⁶⁹. This suggests that PopA might have a c-di-GMP dependent function in the delivery of ClpXP dependent substrates to the stalked pole. However, the molecular mechanisms for PopA activation and sequestration as well as polar receptor structures which recognize and retain PopA at the pole are not known yet (Fig. 14).

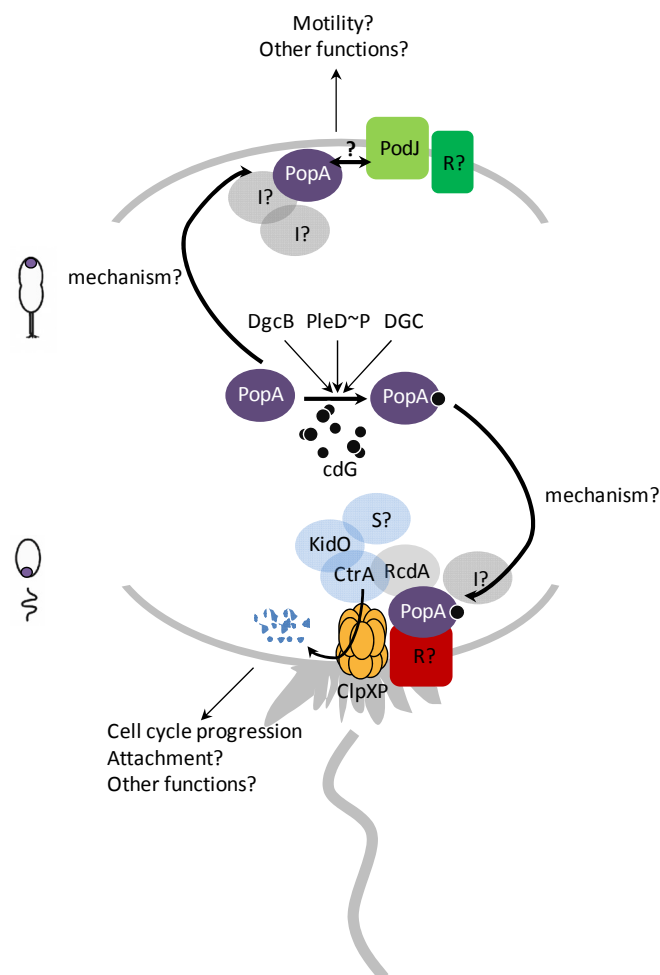


Figure 14: c-di-GMP effector PopA-mediated cell cycle and development control. Stalked pole localization is dependent on an intact c-di-GMP binding site. Upon binding of c-di-GMP (cdG, black circles) PopA is activated and localizes the pole where it is presumably recognized by an unknown

receptor structure (R, red). Through direct interaction with RcdA, PopA recruits CtrA, KidO and maybe other ClpXP substrates (S?, blue) to the pole to license cell cycle progression. It is likely that it interacts with other proteins (I?, grey) that mediate additional developmental functions of PopA such as cell attachment. Sequestration to the incipient flagellated pole requires PodJ and presumably other receptor structures (R?, green). It is not clear whether PopA and PodJ interact directly or if other interacting proteins (I?, grey) mediating additional developmental functions are involved.

PopA belongs to a minority of proteins which localize to both cell poles during cell cycle resulting in a bipolar distribution pattern in stalked and predivisional cells⁵⁶. As mutation of the c-di-GMP binding site does not affect localization to the flagellated pole, another additional targeting mechanism had to be proposed. Indeed it was shown that sequestration to the pole opposite the stalk partially requires the topology factor PodJ⁵⁶. PodJ is a transmembrane protein that is sequestered to the incipient flagellated pole where it mediates polar positioning of proteins involved cell differentiation such as factors for pilus biogenesis, chemotaxis and holdfast^{137,138,170}. The function of PopA at this pole is not known. However, *popA* deletion mutants display a partial motility defect on semi solid agar plates, which correlates with reduced swimming speed and a reduced number of motile cells compared to wild-type¹⁷¹. Moreover, mutants lacking PopA have reduced ability to attach to surfaces¹⁷¹. It is tempting to speculate that PopA might engage developmental functions at the PodJ-dependent pole and it is likely that other interaction partners exist⁵⁶ that mediate these cellular functions (Fig. 14).

2 Aim of the thesis

In the past years, evidence has accumulated suggesting that the bacterial second messenger c-di-GMP is a key regulator of cell cycle control and development in *C. crescentus*. However, many components of the c-di-GMP network as well as their spatial and temporal regulation remain to be investigated. The aim of this work is to understand the activation mechanism and spatial control of the multifunctional c-di-GMP effector protein PopA. Upon c-di-GMP binding, PopA dynamically sequesters to the old cell pole, where it helps to organize the degradation of key cell cycle regulators prior to S-phase entry. This work addresses the following questions: How does c-di-GMP binding lead to the activation and localization of PopA? What are the polar localization signals and determinants required for the dynamic positioning of this protein? And how do these processes 'overlap' with the proposed activation and localization mechanisms of the PleD diguanylate cyclase, a catalytic paralog of PopA? Finally, what are the interaction partners of PopA at the cell pole and what is their role in PopA-mediated cell cycle processes? Together, this work will elucidate the general mechanisms and functional importance of the dynamic cellular behavior of PopA.

3 Results

3.1 Unraveling the Polar Sequestration Mechanism of PopA, a c-di-GMP Effector Protein Involved in *C. crescentus* Cell Cycle Control

Annina Moser, Anna Dürig, Ludwig Zumthor, Tilman Schirmer and Urs Jenal

Statement of my work

All plasmids and strains used in this study have been generated by me, unless otherwise stated in table S1. I phenotypically characterized the Pop_{D55N} mutant (Fig. 2) and I generated and analyzed the putative PopA dimerization mutants (Fig. 3B-D), the primary I-site mutants PopA_{R388A} and PleD_{R359A} (Fig. 4B-F), the PopA secondary I-site mutants (Fig.5), the PopA-GGDEF-GFP fusion (Fig. 6) and I constructed the PopA-PleD hybrids and performed all microscopic and phenotypic analysis (Fig. 7, 8, 9). Furthermore, I developed the PopA-RcdA bacterial two-hybrid screen and analyzed the PopA mutations (Fig. 11). I performed the microscopic analysis to find PopA receptor molecules (Fig. 13A-C) and analyzed PopA localization in PodJ truncation mutants (Fig. 12). PopA purification and all biochemical analysis (Fig. S1B and S1C) except SLS experiments were performed in collaboration with Ludwig Zumthor (Fig. S1D). Finally I constructed putative sulfate-binding mutants in PleD and PopA and analyzed them by microscopy (Fig. 12D-E).

3.1.1 Abstract

The past years have shown that in bacterial cells many regulatory proteins such as transcription factors, signal transduction proteins, and proteases have specific cellular addresses. This suggested that bacteria, similar to their eukaryotic counterparts, exploit protein localization as a general regulatory feature to control different cellular processes. In the α -proteobacterium *Caulobacter crescentus*, cell cycle progression relies on the specific proteolysis of the DNA replication inhibitor CtrA, a process that is coordinated in time and space. While localization of the ClpXP protease is regulated by phosphorylation reactions, polar targeting of CtrA requires PopA and the input from the bacterial second messenger cyclic di-GMP. PopA localizes to the pole and recruits CtrA via its direct interaction with the mediator protein RcdA. Subsequent CtrA clearance promotes S-phase entry. In addition to its function at the ClpXP-occupied old cell pole, PopA localizes to the new cell pole where it exerts a yet unknown function. So far, the molecular mechanisms responsible for the dynamic bipolar localization of PopA are not known. Here we address the mechanisms involved in PopA activation and sequestration to the ClpXP-occupied stalked pole.

PopA is a response regulator with an atypical Rec1-Rec2-GGDEF domain organization that is reminiscent of the diguanylate cyclase PleD. PleD displays a similar overall fold and comparable localization behavior to the stalked pole. However, while PleD localization is mediated by phosphorylation-induced dimerization, we show that phosphorylation is dispensable for PopA localization and function. Instead, conserved primary and secondary binding sites for c-di-GMP within the C-terminal GGDEF domain are required for pole specific function of PopA. This suggested that GGDEF domain crosslinking by c-di-GMP contributes to PopA activation and polar localization. To confirm this and to dissect PopA and PleD-specific localization signals, we generated PopA-PleD hybrid proteins where the GGDEF domain of one protein was grafted onto the receiver domain stem of the other. These studies demonstrated that topological specificity of PleD is mediated by its Rec1-Rec2 stem, while the GGDEF domain encodes the positional information for PopA. A [Rec1-Rec2]_{PleD}-[GGDEF]_{PopA} hybrid protein recognizes both the PleD- and PopA-specific polar addresses, but lacks activity for either pathway. This implied that the PopA GGDEF domain mediates polar localization and that the Rec1-Rec2 stem might be involved in recruiting downstream components of the pathway. In agreement with this we find that RcdA specifically interacts with the first PopA receiver domain. Together these data indicate that the PopA response regulator adopted a novel role as topology specificity factor to dynamically recruit components of the CtrA degradation pathway to the protease occupied pole. Intriguingly, signal

transduction in PopA is reversed as compared to the paradigmatic response regulator family, initiating at the GGDEF domain and exploiting the Rec domains as molecular readout.

3.1.2 Introduction

Dynamic protein localization is an important regulatory feature of diverse bacterial processes. It enables the cell to perform specific functions at specific subcellular sites^{1,2}. Research in the past decade has revealed many structural and regulatory components acting at distinct positions in the bacterial cell. These include factors involved in cytokinesis and chromosome segregation, as well as elements needed for biosynthesis of polar organelles like flagella and pili³. However, in addition to proteins that control morphogenetic processes many regulatory proteins like sensor histidine kinases, transcription factors, proteases and enzymes have specific cellular addresses^{1,4}. Growing evidence from many bacteria indicate that localization is not exclusive to a small number of specific proteins, but rather represents a general regulatory feature of bacterial proteomes⁴. Nevertheless, underlying molecular sequestration mechanisms, structural determinants and polar receptors are poorly understood.

A particularly useful organism to study protein localization to specific subcellular sites is the aquatic α -proteobacterium *Caulobacter crescentus*. It divides asymmetrically and allows the discrimination of old and new cells poles by the visible presence of distinct polar appendages. Cell division results in two genetically identical, but morphologically distinct daughter cells. The swarmer cell progeny is motile and characterized by a single polar flagellum with chemotaxis apparatus and polar pili. The stalked cell progeny is attached to the surface by an adhesive holdfast located at the tip of a protrusion of the cell body called stalk. The daughter cells do not only have different developmental programs reflected by their distinct polar appendages, but also inherit a different replicative potential. Stalked cells can reinitiate DNA replication immediately after cell division, whereas chromosome replication is actively prevented in swarmer cells^{5,6}. The establishment of these swarmer and stalked cell specific programs relies on the specific subcellular distribution of cell fate determinants and regulatory proteins that govern cell cycle progression and polar morphogenesis⁷⁻⁹. E.g. cell cycle progression of the swarmer cell is facilitated by the dynamic and coordinated recruitment of the replication initiation inhibitor CtrA and its cognate protease to the old cell pole¹⁰⁻¹². Replication initiation of the chromosome is licensed through proteolytic removal of CtrA from the cell. Coincident with S-phase entry, the swarmer cell differentiates into the sessile stalked cell, by shedding its flagellum and pili and replacing them with a holdfast and a stalk. These concurrent cell cycle and morphogenetic changes are coordinately controlled by the actions of the bacterial second messenger cyclic di-GMP¹³. Several proteins involved in the production and sensing of the second messenger have been shown to dynamically localize to specific sites in the cell. E.g.

the diguanylate cyclase PleD localizes to the old cell pole where it orchestrates flagellar ejection, stalk and holdfast biogenesis. The c-di-GMP effector protein PopA localizes to the same subcellular site where it is involved in the degradation of CtrA¹⁴⁻¹⁶.

The unorthodox response regulator PleD has two receiver domains fused to a diguanylate cyclase output domain¹⁷. PleD localization is dependent on the phosphorylation by its cognate sensor histidine kinases, PleC and DivJ^{15,16}. Phosphorylation leads to PleD dimerization, activation and localization to the pole where it activates yet unknown effector molecules involved in polar morphogenesis¹⁸. PleD phosphorylation at the conserved aspartic acid D53 of the first receiver domain induces a rearrangement of the receiver domains thereby promoting dimer formation¹⁹. This brings adjacent catalytic active sites (A-sites) of the cyclase domains into close proximity allowing the condensation of two GTP molecules into c-di-GMP¹⁹. Dimerization is the prerequisite for diguanylate cyclase activity and polar localization of PleD¹⁸. The activity of PleD is subject to allosteric inhibition through the non-productive crosslinking of two cyclase domains by their reaction product c-di-GMP. This is accomplished by two complementary c-di-GMP binding sites on adjacent PleD molecules, the primary and secondary I-sites.

The response regulator-like protein PopA has the same domain architecture like PleD and likely originates from PleD through gene duplication. But its GGDEF domain has lost its catalytic activity and instead has adopted a new function as c-di-GMP effector. PopA first localizes to the swarmer cell pole where it functions in motility control. Later on PopA concentrates at the stalked cell pole where it serves to regulate S-phase entry by facilitating the degradation of the replication initiation inhibitor CtrA¹⁴. PopA localization to the incipient swarmer pole is dependent on the swarmer pole specific membrane protein PodJ. Full-length PodJ_L is synthesized in predivisional cells and sequestered to the flagellated pole by a short cytoplasmic tag. PodJ then facilitates the positioning of PopA, the PleC histidine kinase and the pilus assembly factor CpaE to the swarmer pole²⁴⁻²⁶. Based on the observation that both the *popA* and *podJ* mutants show a similar motility defect^{14,27} it was hypothesized that PopA localizes to the flagellated pole to control flagellar motor performance¹⁴.

PopA localization to and function at the stalked pole are dependent on c-di-GMP binding to the conserved RxxD I-site motif¹⁴. During the swarmer-to-stalked cell transition the c-di-GMP concentration increases as a result of diguanylate cyclase activation and phosphodiesterase inactivation. In swarmer cells c-di-GMP levels are kept low by the activity of the phosphodiesterase PdeA, which counteracts the diguanylate cyclase DgcB in this compartment. During swarmer-to-stalked cell transition, PdeA is proteolytically degraded by the ClpXP protease thereby unleashing DgcB activity. At the same time, PleD is activated and, together with

DgcB, causes an upshift in c-di-GMP concentrations²⁰. This upshift not only controls the *C. crescentus* motile-sessile switch but also promotes PopA localization to the stalked pole²⁰. PopA then targets CtrA to the same pole via the mediator protein RcdA that facilitates CtrA localization and eventually degradation by the polar ClpXP protease^{10,12,14,21}. Targeting of ClpXP to the same pole requires the single domain response regulator CpdR in its unphosphorylated state¹². A specific phosphorelay consisting of the sensor kinase CckA and the phosphotransferase protein ChpT controls the phosphorylation status of CpdR and CtrA, thereby coupling activity and stability of the CtrA master cell cycle regulator. While CtrA and CpdR are phosphorylated by CckA in the swarmer cell the phosphate flux through the CckA pathway reverses upon entry into S-phase, thereby inactivating CtrA and sending CpdR to the cell pole to recruit ClpXP^{8,22,23}.

So far, little is known about how c-di-GMP activates PopA and which domain(s) encode the positional information for localization and pole discrimination. To explain its c-di-GMP dependent localization to the stalked pole, we are guided by a model for allosteric control of the PleD diguanylate cyclase, which is based on the elaborate structural knowledge of this protein^{17,19}. According to this model c-di-GMP induced feedback inhibition involves the crosslinking of two adjacent catalytic domains through primary and secondary binding sites. In analogy, c-di-GMP binding could induce a conformational change in PopA by crosslinking two adjacent GGDEF domains. In agreement with such an idea, our experiments show that primary and secondary I-sites are required for PopA localization and CtrA degradation. To address the minimal requirements for PopA localization we analyzed PopA truncation mutants and generated PopA-PleD hybrid proteins by grafting the respective GGDEF domain onto the receiver stem of the counterpart. These experiments indicate that the PopA GGDEF domain contains the positional information for both cell poles. In conclusion, these experiments emphasize the versatility of c-di-GMP signaling proteins and demonstrate that the GGDEF domain has adopted a novel role as targeting factor to localize proteins to specific subcellular compartments in response to c-di-GMP binding.

3.1.3 Results

PopA is a structural homolog of PleD with similar dynamic localization behavior.

PopA and PleD share a similar Rec1-Rec2-GGDEF domain organization but low overall sequence conservation (23% identity). We used CLUSTALW³⁰ sequence alignment to analyze if functional residues of PleD are conserved in PopA. As shown in Fig. 1A, key residues involved in phosphorylation dependent dimerization of PleD^{18,19} are conserved in PopA. In addition, PopA retained key residues of the primary and secondary c-di-GMP binding sites^{18,19}. Structural modeling of PopA using a monomeric version of PleD as a template¹⁷ revealed a very similar overall fold. While the Rec1 and Rec2 domains are virtually identical, the GGDEF domain of PopA is slightly shorter and lacks the last of five central β -sheets (Fig. 1B). Based on these structural homologies and based on their similar localization behavior during the cell cycle, we postulated that the diguanylate cyclase PleD and the c-di-GMP effector protein PopA might share a common activation and localization mechanism.

Regulation of PopA does not require phosphorylation control.

Duerig and coworkers had observed that a single amino acid change in the putative phosphorylation site (D55N) did not alter PopA localization and CtrA degradation during cell cycle¹⁴. The phosphor-acceptor site Asp55 and the main aspartates Asp13 and Asp14 of the acidic pocket essential for Mg^{2+} binding³² and phosphotransfer activity are conserved in PopA. However, a closer analysis of the modeled PopA structure revealed that Asp13 and Asp14 are oriented with their side chains in an outward direction, making it unlikely that coordination of the Mg^{2+} could take place like in PleD. Furthermore, the amino acids Thr83 and Phe102, which undergo rearrangement upon phosphorylation and thereby induce structural changes in the receiver domain in PleD and other response regulators are not conserved in PopA (Fig. 2E). The hydroxyl group containing Ser85 might take over the T83 function, however for F102 no reasonable homologous substitution in PopA exists. Taken together, this indicates that PopA is unlikely being regulated by phosphorylation and that the conserved Asp55 has probably no regulatory function.

Because PopA is a multifunctional protein involved in motility and attachment regulation³¹, a possible role of PopA phosphorylation in swimming behavior, surface attachment, holdfast formation and pili biogenesis was analyzed experimentally. However, in agreement with the observation reported above, a PopA_{D55N} mutant behaved like wild-type PopA in all respects (Fig. 2A-D).

Dimerization via the Rec1/Rec2' interface is not involved in PopA activation and localization.

PopA localization to the stalked pole requires an intact I-site motif¹⁴. Together with the finding that PopA is not regulated by phosphorylation, we hypothesized that c-di-GMP might activate PopA by changing its oligomeric state. This hypothesis was supported by bacterial-two-hybrid analysis and *in vitro* crosslink experiments providing evidence that PopA might oligomerize (Fig. S1A-C). However, biochemical analysis of the PopA oligomerization state by Static Light Scattering (SLS) in the absence of c-di-GMP suggested a monomeric form of PopA at a concentration of 10 μ M (Fig. S1D) and left the question of dimerization inconclusive. A possibility to assess dimerization *in vivo* came from studies with PleD. In PleD monomer-monomer contact between the Rec1 domain and an adjacent Rec2' domain is mediated by three salt bridges that stabilize the dimeric form of PleD¹⁹. Interestingly, in PopA these residues are conserved. Therefore we generated single mutations in this putative Rec1/Rec2' interface of PopA (Rec1: E50, E125, R129; Rec2: R220, R277, E281) and analyzed them with respect to their polar localization (Fig. 3A). All single mutations as well as a the PopA_{R220,R277,E281} triple mutation showed a localization pattern indistinguishable from wild-type (Fig. 3B) and were stably expressed in $\Delta popA$ mutant (Fig. 3C). In agreement with this finding, CtrA was degraded normally during the G1-to-S phase transition in strains expressing these PopA mutants (Fig. 3D). This suggested that these residues either do not constitute the dimer interface of PopA or that PopA localization does not involve PleD-like dimer formation.

Dissection of the primary I-site: R357 and R388, but not D360, are required for PopA localization and CtrA degradation.

Next we focused on the role of the primary I-sites, which form the core c-di-GMP binding unit. In PleD, a c-di-GMP dimer binds to the conserved primary I-site motif (R359, D362, R390) within the GGDEF domain and crosslinks it to an adjacent GGDEF domain over a conserved arginine (R313) referred to as secondary I-site (Fig. 4A). Because this immobilizes the catalytic GGDEF domains in a non-productive conformation, the allosteric product inhibition is called domain immobilization mechanism¹⁹. Substituting Asp359 to alanine did not have an effect on PleD localization (Fig. 4B). In contrast, PopA mutations in the corresponding amino acids R357 and also R388 (corresponds to R390 in PleD) of the primary I-site motif led to a complete abolishment of polar foci at the stalked pole (Fig. 4C and 4D). In accordance, the PopA primary I-site mutants R357A and R388A were unable to support CtrA degradation during G1-to-S transition (Fig. 4F). The failure of these mutant proteins to localize was not due to a general instability effect (Fig. 4E).

To investigate the function of the core c-di-GMP binding sites in localization in more detail, further mutational analysis and dissection of the I-site were performed. In particular, substitutions that were made to dissect feedback inhibition of the diguanylate cyclase DgcA were introduced into PopA³³. PopA_{R357X} (R357A, R357G) mutants failed to localize to the stalked pole and consistent with this, failed to degrade CtrA during cell cycle. Substitutions in Asp360 (D360A, D360E) displayed a partial localization defect, but mutant cells were still able to remove CtrA during G1-to S-phase transition. Mutations in the amino acids V358 and E359 behave similar to wild-type (Fig. 4G). Taken together these data suggest that residues R357 and R388 from the primary I-site motif are strictly required for PopA stalked pole localization and PopA functionality. While Asp360 contributes to PopA function, the residues in between the highly conserved charges of the RXXD motif are not required for PopA function.

Mutations in the secondary I-site have a partial effect on PopA localization and activity.

To further elucidate the role of secondary I-sites in PopA, single and double mutants of conserved secondary I-site candidate aspartic acids (R313, R315 and R317) (Fig. 4A) fused to GFP were engineered. Whereas the $\Delta popA$ mutants expressing PopA_{R315A} or PopA_{R317A} showed a dramatic reduction of stalked pole localization, PopA_{R313A} displayed normal bipolar localization. A R315A R317A double mutant did not show a more severe reduction of stalk pole localization (Fig. 5A and 5B). As the identity of the cell poles is sometimes difficult to distinguish, the PopA_{R315A}, PopA_{R317A} or PopA_{R315A,R317A} mutant proteins were also expressed in a $\Delta podJ$ background that should abolish swarmer pole specific localization. Expression of the mutant forms in this background resulted in an equally reduced number of foci localized to the stalked pole, while no foci at the incipient swarmer pole could be detected (Fig. 5C).

To ensure that the decrease of polar signal was not due to decreased protein levels, immunoblots were carried out with anti-PopA antibodies to demonstrate that the protein levels are comparable to wild-type PopA (Fig. 5D). Analysis of CtrA turnover revealed that despite the partial localization defect, the PopA secondary I-site mutants R315A and R317A as well as the R315AR317A double mutant were still able to degrade CtrA during G1-to S-phase transition (Fig. 5E). In summary these findings suggest that both, the primary and secondary I-sites, contribute to PopA subcellular localization.

The PopA GGDEF contains the c-di-GMP-dependent information for both cell poles.

The expression of individual PopA domains fused to GFP indicated that the GGDEF domain is critical for polar localization (Fig. 6A). Because the GGDEF-GFP fusion was not stable *in vivo*, these results failed to demonstrate that the GGDEF is also sufficient for PopA localization (Fig. 6B). Therefore, we decided to engineer PopA-PleD hybrid proteins to determine the minimal requirements and the structural determinants necessary for PopA and PleD localization to the cell poles. For this, the GGDEF domain of PopA was grafted onto the Rec1-Rec2 domain of PleD and vice versa to generate Hybrid-A and Hybrid-B (Fig. 7A).

The Hybrid-B fusion to GFP was very unstable *in vivo* and did not display a detectable fluorescence signal. In contrast, Hybrid-A fusions were stable and produced robust fluorescence signals (Fig. 7B, C). The majority of predivisional cells expressing a Hybrid-A-GFP fusion protein displayed the bipolar localization pattern typical for PopA localization (42 %). In contrast to predivisional cells expressing wild-type PopA, many cells had no foci (Hybrid-A: 23 %, PopA wild-type: 10%) or only a single focus (Hybrid-A: 35 %, PopA wild-type: 5%) at the stalked pole. The overall signal intensity for the Hybrid-A-GFP fusion is very high compared to the signal intensities observed for PopA-GFP and PleD-GFP. In addition, it is noteworthy that in cells with bipolar localization the signal at the stalked pole is considerably stronger than the signal at the incipient swarmer pole (Fig. 7B). Immunoblot analysis confirmed that the Hybrid-A-GFP fusion is stable and present at about five-fold higher levels than the wild-type PopA-GFP fusion. From these results and from the fact that PleD does not have topological specificity for the flagellated pole, we concluded that Hybrid-A contains the PopA-specific localization signal for the flagellated pole.

However, it was not clear which domain would be responsible for stalked pole localization of Hybrid-A, the PopA GGDEF domain or the receiver domains of PleD or both. Therefore the localization of Hybrid-A-GFP fusion was studied in mutant strains lacking either PleC and DivJ (the upstream components of PleD) or all known diguanylate cyclases of *C. crescentus* (the upstream components of PopA) (*cdG*⁰ strain, S. Abel and U. Jenal, unpublished). In a $\Delta pleC \Delta divJ$ double mutant, Hybrid-A cannot be phosphorylated and PleD fails to be targeted to the pole¹⁶. In the *cdG*⁰ strain, the c-di-GMP input signal for PopA GGDEF domain would be missing and as a consequence PopA would not localize to the stalked pole. As shown in Fig. 7D, a Hybrid-A-GFP fusion localized to the cell poles in a $\Delta pleC \Delta divJ$ mutant strain indicating that the GGDEF domain of PopA alone is able to drive the protein to the stalked pole. In contrast, no polar signal of the Hybrid-A fusion protein was detected in the *cdG*⁰ strain arguing that the PopA GGDEF domain in dependence of c-di-GMP mediates localization to the stalked pole.

To further test the requirement of the PleD dimerization stem, we introduced the amino acid exchange T26A into Hybrid-A. Tyr26 forms a small contact patch between two receiver domains and mediates monomer-monomer interactions in the PleD dimer¹⁹. The Y26A substitution was shown to abolish PleD localization, demonstrating that dimerization is a prerequisite for PleD positioning¹⁸. However, the majority of Hybrid-A_{Y26A}-GFP displayed normal, PopA-like bipolar foci (35 %) similar to wild-type Hybrid-A (Fig. 7E), again arguing that the PopA GGDEF domain is sufficient to tag the hybrid to both cell poles. Next we analyzed the polar distribution pattern of cell expressing Hybrid-A_{R357G}-GFP with a defective I-site. The majority of the cells expressing this mutant hybrid lost localization (40 %) while a relatively large fraction of cells (31 %) retained fluorescent foci at the stalked pole, presumably driven by the PleD receiver domains (Fig. 7E). Together this suggested that the PopA GGDEF domain and the PleD receiver domains independently contribute to the stalked pole localization of Hybrid-A. To test this hypothesis, the Y26A and R357G mutations were combined and localization of the Hybrid-A_{R357G,Y26A}-GFP was analyzed. As expected, the vast majority of cells failed to localize the mutant Hybrid-A completely (78 %) (Fig. 7E), confirming that Hybrid-A contains two individual determinants for stalked pole localization. To exclude that the absence of polar foci is due to unstable mutant proteins, Hybrid-A mutant levels were monitored with immunoblots using anti-GFP antibodies (Fig. 7F).

Taken together these results suggest that the PopA GGDEF domain encodes the positional information for both poles, whereas the receiver domains of PleD contribute to stalked pole localization. The observation that Hybrid-A completely fails to localize to both poles in the *cdG*⁰ strain, while an I-site mutant of Hybrid-A localizes to the stalked pole as efficiently as its PleD counterpart, suggests that PleD activation is abolished in the *cdG*⁰ strain. This is consistent with the observation that PleD also fails to localize to the stalked pole in the *cdG*⁰ strain, while the constitutive active PleD* finds the cell pole in this mutant background (S. Abel and U. Jenal, unpublished).

PopA-PleD Hybrids are correctly targeted to the pole but are non-functional.

The observation that Hybrid-A was able to reach both polar addresses of PleD and of PopA prompted us to analyze the functionality of this hybrid protein. We asked if the Hybrid GFP fusions are able to complement *pleD* or *popA* mutant phenotypes. Since PleD is required for flagellar ejection and degradation of the flagellar anchor protein FliF during the SW-to-ST transition¹⁶ and PopA is important for CtrA degradation during the same cell cycle period, we chose these two proteins as indicators of Hybrid-A functionality. The Hybrid-A protein could not restore FliF degradation in a *pleD* mutant (Fig. 8A). Likewise, Hybrid-A was unable to restore CtrA degradation of

a *popA* mutant (Fig. 8A). Likewise, the Hybrid-B fusion was unable to restore PopA or PleD function.

Interestingly, while Hybrid-A was unable to restore the surface attachment defect of a *pleD* or *popA* mutant, Hybrid-B partially restored this phenotype (Fig. 8B). This suggests that its PleD derived GGDEF domain retained residual diguanylate cyclase activity. In contrast to this observation, both Hybrid proteins were unable to restore motility behavior of the *popA* or *pleD* mutant strains (Fig. 8C).

The first receiver domain of PopA mediates interaction with RcdA.

PopA has been shown to direct RcdA to the stalked pole via direct protein-protein interaction¹⁴. To determine the requirements for this interaction we analyzed if the Hybrid-A fusion protein harboring the PopA GGDEF domain is able to direct RcdA to the cell pole. While RcdA-YFP finds the cell pole when co-expressed with PopA, it fails to localize in the presence of Hybrid-A (Fig. 9). This strongly suggests that the PopA GGDEF domain, although able to localize to the stalked pole, is not sufficient to recruit RcdA to this subcellular site. We further analyzed PopA-RcdA interaction using the bacterial two-hybrid system. Individual PopA domains (Rec1, Rec2, Rec1-Rec2, GGDEF) were C-terminally fused to T25 fragment of the adenylate cyclase and assayed for interaction with RcdA fused C- or N-terminally to the T18 fragment. A positive signal was obtained only for the PopA-Rec1 and RcdA pair (Fig. 10B), whereas all other combinations scored negative (Fig. 10C-10E). This implies that the PopA Rec1 domain is required for interaction with RcdA. This result is consistent with the above observations that Hybrid-A, which lacks the PopA receiver domains, is unable to recruit RcdA to the cell pole. Finally, this result also suggests that the signal transduction flow in PopA is reversed as compared to classical response regulators like PleD. While the C-terminal GGDEF domain of PopA constitutes the input domain, downstream interactions operate through the N-terminal receiver domains.

Identification of PopA surface determinants required for PopA-RcdA interaction, but not for RcdA localization and proteolysis of CtrA.

To probe the molecular details of PopA-RcdA interaction, a genetic screen was set up to isolate PopA mutants that fail to interact with RcdA. We used the bacterial two-hybrid system, which is based on the interaction-mediated reconstitution of a cyclic AMP signaling cascade³⁴. A plasmid-borne copy of the *popA* gene was first mutagenized by passage through an *E. coli* mutator strain (Stratagene, USA) and the resulting mutant alleles were introduced into the bacterial two-hybrid system together with *rcdA* (Fig. 11A). We screened for white colonies indicative of PopA mutants unable to interact with RcdA. In a secondary screen we used immunoblot analysis with anti-PopA antibodies to identify stable full-length PopA versions among

the white clones. Although the frequency of white colonies was within the calculated range ($1.5E^{-2}$, around 4000 colonies were screened), the yield of stable PopA variants was very low, producing only three potential interaction mutations, R272H, G294E and A335T (Fig. 11B). All amino acids altered are located on the surface of the modeled PopA structure. R272 and G294 are positioned in the flexible linker domain connecting the Rec1-Rec2 stem with the GGDEF domain, while A335 is located within the $\alpha 0$ helix of the GGDEF domain (Fig. 11C).

Since RcdA is delocalized in the absence of its interaction partner PopA¹⁴, we assumed that RcdA-PopA interaction is critical for the localization of RcdA and subsequent CtrA degradation. However, the RcdA localization pattern is indistinguishable from wild-type in a strain expressing the *popA*_{R272H} allele as the only copy of *popA* (Fig. 11D). Consistent with this, CtrA degradation during G1-to S-phase transition is normal (Fig. 11E). It is formally possible that PopA-RcdA interaction is not required to localize RcdA to the stalked pole. Alternatively, interaction failure of this particular mutant might be specific for the *E. coli* assay system while it might still interact with RcdA in the natural *Caulobacter crescentus* environment.

Analysis of potential polar receptor proteins for PopA.

The experiments described above addressed mechanisms involved in PopA activation and sequestration to the cell poles. However, the nature of the polar receptor structure required to sequester PopA to the pole remains unknown. One exception is PodJ, which seems to attract PopA to the incipient swarmer pole¹⁴. To confirm this and to dissect the specific requirements of PodJ for this process, the cellular distribution of PopA was studied in several strains expressing truncated PodJ derivatives²⁶. Mutant PodJ589 lacks the transmembrane and the entire periplasmic domain; mutants PodJ639 and PodJ660 truncate within or immediately after the transmembrane domain; all other mutants have progressively shortened periplasmic domains (Fig. 13A). In a *podJ589* mutant, PopA displayed a similar localization defect like a $\Delta podJ$ deletion. In the presence of all other truncated forms, PopA showed the typical bipolar localization pattern (Fig. 13B, C). This demonstrates that the membrane proximal region of PodJ on the cytoplasmic side between amino acids 589 and 639 is critical for PopA targeting to the flagellated pole. In agreement with these findings, Lawler and coworkers report that PodJ589 was unable to localize properly to the nascent flagellar pole while PodJ639 showed near to normal localization behavior²⁶.

Several polarly localized proteins, including TipF, TipN and SpmX, are known to serve as anchoring structures for the successive localization of downstream components and are thus candidates for stalked cell pole specific receptors of

PopA^{24,35-37}. However, mutants lacking TipF, TipN, or SpmX showed wild-type like distribution of PopA, arguing against any of these proteins playing a role as polar receptors for PopA (Fig. 13A-C).

Structural analysis of PleD revealed the existence of a deep positively charged cavity at the bottom of the (Rec1-Rec2')₂ tetramer (Fig. 13D). This cavity contains a buried sulfate molecule that interacts with arginine residues 117 and 121 and their symmetric mates in the tetramer³⁸. This sulfate group increased dimer stability and catalytic efficiency of PleD *in vitro*, while an analogous phosphate moiety had the opposite effect³⁸. As sulfate has a negligible relevance *in vivo* and this pocket is typical for phosphate and phosphate containing ligands³⁹ it was speculated that the receptor could be a phosphorylatable protein, which allows docking of dimeric PleD only in its dephosphorylated state. Interestingly, the arginine residues involved in sulfate binding in the PleD crystal structure are conserved in PopA. To test if these residues are required for PleD and PopA function and localization, the respective point mutations were generated and tested *in vivo*. In PleD two different double mutants were generated replacing R117 and R121 by aspartate or serine residues, respectively, In PopA R118 was replaced by alanine or serine. The mutants were fused to GFP and their localization behavior was analyzed by fluorescence microscopy. As shown in Fig. 13E, PleD mutants (Fig. 4B) show a much stronger polar localization signal as compared to wild-type PleD, comparable to the strong polar signal of the constitutive active mutant PleD* (Fig. 4B). This argues that these residues might indeed be involved modulating PleD polar localization negatively, possibly through the interaction with a polar receptor protein, the phosphorylation status of which might be critical for proper anchoring of the activated PleD dimer. In contrast to PleD, the localization behavior of the PopA mutants were unchanged (Fig. 13F).

3.1.4 Discussion

Bacteria sense and adapt to a wide variety of signals through a complex network of signaling systems. These include the widely used two-component systems, which are based on phosphotransfer reactions from a sensor histidine kinase to its cognate response regulator⁴⁰. Response regulators are composed of a receiver and a regulatory output domain, which can function as DNA binding, enzymatic or protein/ligand binding domain⁴⁰. Phosphorylation of the receiver domain often induces activation of the response regulator through oligomerization⁴¹. The *C. crescentus* response regulator PleD is composed of two receiver domains, which are fused to a GGDEF diguanylate cyclase output domain. Activation of PleD involves phosphorylation of the first receiver domain and results in the dimerization of the molecule via the Rec1-Rec2 stem¹⁹. Here we investigated the signaling mechanisms of the structural homolog of PleD, the orphan response regulator PopA. Like PleD it contains a potential phosphorylation acceptor site within its first receiver domain³² (Fig. 1). However, critical residues for signal transduction are not conserved in PopA (Fig. 2) making it questionable whether phosphorylation of PopA would induce structural changes in its receiver domain. In line with these findings we show that phosphorylation is not required for PopA localization and function *in vivo* (Fig. 2). Moreover, the alternative possibility that the non-phosphorylated form of PopA might be active could be excluded in previous studies³¹. Therefore we suggest a phosphorylation-independent PopA regulation. Similar atypical phosphorylation-independent response regulators have been described before⁴³⁻⁴⁵ and are referred to as PIARR (phosphorylation-independent activation of response regulators). Like PopA, they maintain most of the structural features of canonical receiver domains, but differ in residues directly involved in phosphorylation. It has been speculated that activation of these atypical response regulators occurs through protein-protein interactions^{44,45}. Recently, another Phosphorylation-independent response regulator was described to inversely control motility and extracellular matrix production in *Vibrio cholerae*. VpsT is activated upon binding of c-di-GMP to an atypical extension (helix 6) of its receiver domain. This leads to a conformational change, which induces its dimerization and activation⁴⁶.

Previous studies with PopA suggested that PopA specifically binds c-di-GMP and, in response, changes its dynamic cellular behavior¹⁴. Based on these observations we hypothesized that c-di-GMP binding, rather than phosphorylation, might serve as input signal for PopA. Two c-di-GMP binding sites in the GGDEF domain, referred to as primary and secondary I-sites, were originally identified as allosteric binding sites regulating diguanylate cyclase activity in PleD^{17,19}. Our 3D model of PopA predicted the primary I-site residues R357, D359 and R388 to mediate core c-di-GMP binding

(Fig. 4). While it was shown previously that substitutions of R357 lead to a failure to bind c-di-GMP and PopA activation¹⁴, we show that changing R388 results in a comparable phenotype (Fig. 4). This indicates that, analogous to PleD, both arginine residues are essential for c-di-GMP binding. In contrast, substitutions of D359 led to an intermediate output. While PopA localization to the stalked pole was partially affected in D359 mutants, CtrA degradation was unaltered (Fig. 4). Similar phenotypes were observed for PopA secondary I-site mutants changing residues R315 and R317. This is an interesting finding since it abrogates the strict correlation between polar localization of PopA and CtrA degradation. There are two possible explanations for these experimental findings. First, it is possible that some of the binding mutants have a decreased affinity for c-di-GMP without abolishing binding completely, leading to less efficient polar targeting of PopA. While the residual PopA might be difficult to detect at the cell pole, it could be sufficient to effectively promote CtrA proteolysis. Alternatively, PopA localization to the old cell pole might not be a strict requirement for CtrA degradation. This was postulated recently for certain RcdA mutant proteins that, although delocalized, were still able to facilitate CtrA degradation⁴⁷. However, if this is the case, it is difficult to reconcile the critical role of PopA in CtrA turnover. It is possible that CtrA degradation can be mediated by off-the-pole ClpXP complexes. ClpXP itself but not its localization to the old cell pole is essential⁶⁹. This observation suggested that only a sub-fraction of the protease pool localizes to the pole, while part of the protease remains delocalized. Maybe partially activated but delocalized PopA is able to effectively channel CtrA into this ClpXP pool. If so, one would have to postulate an additional role for PopA in CtrA degradation that goes beyond simple substrate targeting and would involve a more active role in substrate delivery to the protease. Future biochemical experiments should help to elucidate the exact role of PopA and of these mutant variants that show an intermediate localization phenotype *in vivo*.

Little is known about the activation mechanisms of c-di-GMP effector proteins. It is assumed that c-di-GMP induces structural changes that finally alter the output performance of the effector molecule⁴⁸. Relating to PopA, the first activation hypothesis was inspired by the receiver domain-mediated dimerization of PleD. It postulated a c-di-GMP induced conformational change in the PopA receiver domains, which would favor its oligomerization. A similar activation mechanism based on the association of its receiver domains was also reported for the *Pseudomonas aeruginosa* diguanylate cyclase WspR⁴⁹. However, mutations in the modeled receiver domain interface of PopA did not affect PopA stalked pole localization and CtrA degradation. This suggests that the 3D model used is not accurately predicting the dimerization interface or, alternatively, this simple model is incorrect. The alternative assumption that PopA might dimerize via its GGDEF rather

than its receiver domains again originated from the PleD paradigm. In one of the PleD crystals two adjacent GGDEF domains are crosslinked by two c-di-GMP molecules via primary and secondary I-sites. The observation that substitutions of amino acids forming the secondary I-site of PleD alleviated allosteric product inhibition indicated that this conformation has physiological relevance¹⁹. Similarly, mutations of secondary I-site residues of PopA also showed an effect *in vivo*. Moreover, bacterial two-hybrid and *in vitro* disuccinimidyl suberate crosslinking experiments support the idea that PopA is able to form dimers. Further biochemical analysis and attempts to crystallize PopA with or without c-di-GMP were hampered so far by its poor *in vitro* solubility. It is possible that PopA does not use the tight dimerization interface that the receiver domain stem offers to PleD, but instead uses a more flexible GGDEF interface. This would leave a larger surface area provided by the two pseudo-receiver domains to interact with partner proteins that need to be recruited to the cell pole either because they have to be delivered to the ClpXP protease or for other functional reasons (Fig. 14). Finally, one could also think of a model for PopA activation, in which c-di-GMP binding would induce a conformational change that exposes a polar targeting signal or, alternatively, directly crosslinks PopA to a polar receptor via c-di-GMP (Fig. 14). A c-di-GMP-mediated long-range conformational change for example was reported to induce the localization of FimX, a c-di-GMP effector governing type IV pili based twitching motility in *P. aeruginosa*⁵⁰.

In *C. crescentus* many regulatory events such as the cell cycle-dependent proteolysis of CtrA take place at distinct subcellular sites indicating that specific protein localization is essential for the function of spatially restricted processes⁴. However, in many cases the targeting mechanisms and/or polar receptor structures have not been identified yet. PopA belongs to a minority of proteins, which simultaneously localize to both cell poles in stalked and predivisional cells⁴. Localization to the incipient flagellated pole was reported to require the polar transmembrane protein PodJ¹⁴. Here we provide evidence that this targeting relies on the C-terminal cytoplasmic part of PodJ. In the presence of a truncated PodJ that lacks the transmembrane and periplasmic domains and mislocalizes either to non-polar foci or to the stalked pole²⁶, PopA localization was reduced by about half (Fig. 12). This indicates that PodJ has to be anchored and correctly localized in the membrane to recruit PopA. Moreover, these data are in line with bacterial two-hybrid experiments demonstrating a direct and presumably c-di-GMP dependent interaction between PopA and PodJ (A. Moser and U. Jenal, unpublished. See section 3.2). On the other hand these data could argue for additional unknown molecule(s) contributing to PopA swarmer pole localization. It is even possible that such a protein might also provide an explanation for why PopA persists at the incipient

stalked pole although PodJ is proteolytically cleared during swarmer-to-stalked cell transition²⁸. A possible contribution of the “birth-scar” protein TipN^{36,37} to PopA localization could be excluded (Fig. 13), although in a *tipN* deletion mutant other PodJ-recruited proteins such as the switchable kinase/phosphatase PleC and the pilus secretion factor CpaE²⁴ are often misplaced³⁷. PopA function at the incipient swarmer pole is not clear. A *popA* mutant displays a similar reduction in cell motility as described for a *podJ* mutant²⁷. Based on this it was speculated that PopA might mediate the motility specific functions of PodJ at the incipient swarmer pole¹⁴. This is consistent with the finding that PodJ functions as general localization factor for proteins involved in cell differentiation²⁴⁻²⁶. However, this model does not explain the cumulative effect on motility observed in a *popA podJ* double mutant (A. Moser and U. Jenal, unpublished), which indicates separate pathways involved in controlling cell motility. Interestingly, the primary I-site, although not required for localization to the incipient swarmer pole, is needed to sustain normal cell motility³¹. It has been proposed that the primary I-site is needed to maintain proper functioning of the flagellar motor³¹.

Localization to the incipient stalked pole requires intact primary and secondary I-sites and the absence of PopA at this subcellular site correlates with the reported failure of CtrA degradation. However, to date polar receptors recognizing active c-di-GMP bound PopA are not known. In this context we tested SpmX, the earliest known marker of stalked pole development³⁵. However, we show that it does not function as localization factor for PopA and suggest another, SpmX-independent pathway involved in its polar recruitment (Fig. 13).

To identify the minimal requirements for PopA localization and to learn if these requirements are distinct or identical for swarmer and stalked pole, we studied localization behavior and functionality of PopA-PleD hybrid proteins. While a Hybrid-B fusion was completely delocalized and obviously lacked localization signals, we demonstrate that Hybrid-A, featuring the PleD receiver and the PopA GGDEF domain, contains the polar signal(s) and fulfills the structural requirements to localize to the cell poles (Fig. 7). In particular, the bipolar subcellular distribution of Hybrid-A typically observed for PopA wild-type strongly argued that the GGDEF domain is responsible for the observed distribution pattern. It appears to encode at least one signal that mediates localization to both cell poles. Moreover, we show that this signal might be c-di-GMP dependent as expression of Hybrid-A-GFP in a *cdG⁰* strain lacking all known diguanylate cyclases (S. Abel and U. Jenal, unpublished) results in complete delocalization. In line with this, c-di-GMP binding to the primary I-site is needed for stalked pole localization of PopA wild-type, however an intact I-site is not required for localization to the opposite pole¹⁴. This suggests that sequestration to the flagellated pole relies on a c-di-GMP-dependent address rather

than on direct c-di-GMP binding via its I-site. This address might be a polar receptor such as for example PodJ which has been shown to require c-di-GMP for interaction with PopA (A. Moser and U. Jenal, unpublished. See section 3.2).

It is noteworthy that the localization efficiency of Hybrid-A is reduced compared to wild-type PopA showing that its native receiver domains, although alone localization incompetent, contribute to PopA localization. They might stabilize the otherwise unstable GGDEF domain and enhance its localization signal, or alternatively they could mediate direct interactions with other proteins or receptors which help to recruit PopA. The idea of a receiver domain-based interaction platform was supported by co-localization experiments between Hybrid-A and RcdA (Fig. 9). They demonstrate that RcdA is delocalized in presence of Hybrid-A and consistent with this, CtrA cannot be removed during swarmer-to-stalked cell transition (Fig. 8). Additional evidence is provided by bacterial two-hybrid experiments showing that the PopA receiver domain Rec1 is directly interacting with RcdA, whereas Rec2 seems to be not involved in this interaction. Interestingly, a fusion of the receiver domains Rec1Rec2 did not interact with RcdA neither suggesting an interaction inhibitory role for Rec2 (Fig. 10). However, negative interactions of single domains could be due to the instability of fusion proteins and should be interpreted with caution. Moreover, two of three PopA mutants which fail to interact with RcdA in the bacterial two hybrid system are located within its Rec2 domain (Fig. 11). Although not interacting with RcdA, they are still able to recruit RcdA to the pole and consistent with this, CtrA is degraded during swarmer-to-stalked cell transition. The third mutation lying in the GGDEF has not been tested yet. It is possible that the interaction assays in *E. coli* do not completely reflect the situation in *C. crescentus* during swarmer-to-stalked cell transition. The high c-di-GMP concentrations during this time window^{20,51} might change the interaction profile between PopA and RcdA. This effect would be indirect as PopA-RcdA interaction was reported to be I-site independent¹⁴. Another formal possibility to explain this unexpected result assumes that interaction is not ultimately needed for RcdA localization.

Relating to the PleD, our localization studies with Hybrid-A indicated a receiver domain-mediated contribution to stalked pole localization (Fig. 7). Interestingly, this contribution appears to be Phosphorylation- and dimerization-independent and would be in contrast to *in vivo* and *in vitro* studies with wild-type PleD showing that phosphorylation induced dimerization is a prerequisite for localization^{18,19}. To explain this discrepancy between wild-type PleD and Hybrid-A, it is tempting to speculate again that c-di-GMP binding to the PopA GGDEF domain induces dimerization of Hybrid-A and renders additional phosphorylation and dimerization of the PleD receiver domains unnecessary.

In this work we have shown that the c-di-GMP effector PopA is activated by c-di-GMP which leads to its polar localization. In addition, we demonstrated that its GGDEF domain contains the positional information to both poles, whereas its receiver domains serve as interaction platform for other proteins that mediate the multiple functions of PopA at the poles. In the future it will be challenging to identify the exact c-di-GMP dependent activation and sequestration mechanisms of PopA and other c-di-GMP effector proteins.

3.1.5 Material and Methods

Growth Conditions

The bacterial strains and plasmid used in this study are listed in Table S1. *Caulobacter crescentus* strains were grown in peptone yeast extract (PYE⁵², Ely, 1991) or minimal media supplemented with 0.2% glucose or 0.3% D-xylose (M2G or M2X⁵², Ely 1991) at 30°C with constant shaking (150 rpm). When selection was required antibiotics in the following concentrations were added: (solid/liquid media in µg/ml): gentamycin (5/0.5), kanamycin (20/5), nalidixic acid (20/not used) and oxytetracycline (5/2.5). For inducible gene expression the medium was supplemented with 1 mM vanillate or 1 mM IPTG. For synchronization experiments newborn swarmer cells were isolated by Ludox gradient centrifugation⁵³ (Jenal, 1996) and released into fresh minimal medium. When necessary the medium was supplemented with 1 mM Vanillate or 0.3% xylose. For synchronization with inducible constructs, 1 mM vanillate was added to the growth medium 2 h prior synchrony.

E. coli strains were grown in Luria Broth (LB) at 37 °C. When necessary for selection the following antibiotic concentrations were used: (solid/liquid media in µg/ml) ampicillin (100/50), gentamycin (20/15), kanamycin (50/30) and oxytetracycline (12.5/12.5).

Strains and Plasmids

The bacterial strains and plasmid used in this study are listed in Table S1. Strains were constructed and propagated in *E. coli* DH10B and transferred by conjugation⁵² (Ely, 1991) into *C. crescentus* strains. The Strain Arctic^R BL21 (DE3) (Stratagene, USA) was used for protein overexpression and strain MM337⁵⁴ for bacterial two hybrid assays. Other general molecular biology techniques not listed here are described elsewhere⁵⁵. Detailed protocols of strain and plasmid constructions are available on request.

Microscopy

DIC and fluorescence microscopy were performed on a DeltaVision Core (Applied Precision, USA)/Olympus IX71 microscope equipped with an UPlanSApo 100x/1.40 Oil objective (Olympus, Japan) and a coolSNAP HQ-2 (Photometrics, USA) CCD camera. Cells were placed on a patch consisting of 1% agarose in water (Sigma, USA). Images were processed with softWoRx version 5.0.0 (Applied Precision, USA) and Photoshop CS3 (Adobe, USA) software.

For the visualization with electron microscopy, exponential growing *C. crescentus* cultures were applied to glow-discharged, carbon-coated grids and negatively stained with 2 % (w/v) uranylacetate. The samples were viewed in a Philips Morgagni 268D electron microscope at a nominal magnification of 20,000× and an acceleration voltage of 80 kV.

Bacterial Two-Hybrid Analysis

Bacterial Two-Hybrid Analysis was performed according to Karimova and coworkers³⁴. Proteins of interest were fused N or C-terminally to the T18 or T25 fragment of the *B. pertussis* adenylate cyclase. Two microliter of the MM337 culture containing pUT18 and pKT25 derivatives was spotted on a McConkey agar base plate supplemented with 0.1% maltose, kanamycin and ampicillin and grown at 30 °C.

For the PopA-RcdA interaction screen the pKT25 expressing PopA-T25 was propagated in the *E. coli* XL1-Red mutator strain (Stratagene, USA) and isolated. Mutated *popA-T25* was cut out, ligated as a pool into a clean pKT25 vector background transformed together with pUT18C-RcdA into adenylate cyclase deficient MM337. White colonies were collected and tested by α-PopA immunoblot analysis

for full length PopA protein to exclude premature stop codon insertions and instable proteins. Sequencing of the *popA* gene led to the identification of the PopA mutation.

Motility Assays

C. crescentus colonies were spotted onto PYE soft agar plates (0.3% agar) and incubated for 72 h at 30 °C. Plates were then scanned (ScanMaker i800 scanner, Microtek, Germany) and analyzed using Photoshop CS3 (Adobe, CA, USA) and ImageJ (NIH, USA) softwares. For all motility experiments the mean of at least three independent colony sizes is shown. Error bar represent standard deviation.

Attachment Assays

C. crescentus strains were grown in PYE in 96-well microtiter plates (Falcon, USA) for 24 h under constant shaking (200 rpm). After crystal violet (0.3% crystal-violet, 5% isopropanol, 5% methanol) staining of the attached biomass it was dissolved with 20% acetic acid and optical density at 600 nm was measured in a photospectrometer (Genesys6, Thermo Spectronic, USA). For each strain a mean of at least six independent colonies is shown. Error bar represent standard deviation.

Holdfast Staining

An exponential growing *C. crescentus* culture was stained with Oregon Green or Rhodamine coupled wheat germ agglutinin (0.2 mg/ml, Invitrogen, USA). After washing the stained samples were visualized by fluorescence microscopy.

Phage Sensitivity Assay

C. crescentus colonies were streaked through a phage CBK lysate on a PYE plate. After 24 h of growth at 30°C plates could be analyzed. A $\Delta pilA$ strain was used as negative control as this strain is resistant due to the absence of pili.

Microscopy

DIC and fluorescence microscopy were performed on a DeltaVision Core (Applied Precision, USA)/Olympus IX71 microscope equipped with an UPlanSApo 100x/1.40 Oil objective (Olympus, Japan) and a coolSNAP HQ-2 (Photometrics, USA) CCD camera. Cells were placed on a patch consisting of 1% agarose in water (Sigma, USA). Images were processed with softWoRx version 5.0.0 (Applied Precision, USA) and Photoshop CS3 (Adobe, USA) software.

Immunoblots

Antibodies against PopA, CtrA, McpA and GFP were diluted according to ^{14,56,57}. Primary antibodies were detected by HRP-conjugated swine anti-rabbit secondary antibodies (Dako Cytomation, Denmark). Western blots were developed with ECL detection reagents (Western Lightning, Perkin Elmer, USA).

Protein Expression and Purification

PopA was expressed and purified according to Dürig and coworkers¹⁴.

DSS crosslink Assay

Crosslinking of PopA with disuccinimidyl suberate was performed as described in¹⁸. Purified PopA was incubated with 2 mM (DSS, (Pierce) for 0 – 30 min in the presence and absence of 1 mM c-di-GMP. After crosslinking samples were separated on SDS-PAGE and α -PopA immunoblot analysis was performed to detect PopA monomeric and dimeric forms.

SEC-coupled multiangle light scattering (SEC-MALS)

SEC-MALS experiments were carried out using the ÄKTApurifier (GE Healthcare) connected Superdex200 HR10/300 column (GE Healthcare), the three-angle static light scattering detector miniDAWN (Wyatt Technology Corporation) and the differential refractive index detector Optilab rEX (Wyatt Technology Corporation). Bovine serum albumin (Sigma) was used for normalization of the SEC-MALS hardware. Measurements were performed at flow rates of 0.7 ml/min. Concentrations of the eluted protein was monitored by the differential refractive index, which in combination with the light scattering signal was used for the molecular weight calculation using the program ASTRA5.3 (Wyatt Technology Corporation, USA).

Structural Modelling of PopA

The monomeric structure of PopA was modeled by Swiss Model^{58,59} on the basis of a sequence alignment between PleD and PopA which included secondary structure information from the Pfam database⁶⁰. The dimeric PopA model is based on symmetry operations identified in the activated PleD structure¹⁹ by the program modtrafo. Side chain adjustments were done by the program coot⁶¹. The final model was checked with the Anolea Swiss Model output and ProSA^{62,63}. All protein visualizations were made with the program pymol (Version 1.2r3pre, Schrödinger, LLC).

Acknowledgements

We thank Dr. Paul Wassmann for fruitful discussions and Dr. Sören Abel for critical reading of this manuscript. This work was supported by the Deutsche Forschungsgemeinschaft grant JE 442/1-1 554 935.

3.1.6 References

1. Rudner, D.Z. and Losick, R. Protein subcellular localization in bacteria. *Cold Spring Harbor Perspectives in Biology* **2**, (2010).
2. Collier, J. and Shapiro, L. Spatial complexity and control of a bacterial cell cycle. *Current Opinion in Biotechnology* **18**, 333-40 (2007).
3. Goley, E.D., Toro, E., McAdams, H.H. and Shapiro, L. Dynamic chromosome organization and protein localization coordinate the regulatory circuitry that drives the bacterial cell cycle. *Cold Spring Harbor Symposia on Quantitative Biology* **74**, 55-64 (2009).
4. Werner, J.N., Chen, E.Y., Gubermann, J.M., Zippilli, A.R., Irgon, J.J. and Gitai, Z. Quantitative genome-scale analysis of protein localization in an asymmetric bacterium. *Proceedings of the National Academy of Sciences of the United States of America* **106**, 7858-63 (2009).
5. Degnen S.T. and Newton, A. Chromosome replication during development in *Caulobacter crescentus*. *Journal of Molecular Biology* **64**, 671-680 (1972).
6. Marczynski, G.T. and Shapiro, L. Cell-cycle control of a cloned chromosomal origin of replication from *Caulobacter crescentus*. *Journal of Molecular Biology* **226**, 959-77 (1992).
7. Paul, R., Jaeger, T., Abel, S., Wiederkehr, I., Folcher, M., Biondi, E.G., Laub, M.T. and Jenal, U. Allosteric regulation of histidine kinases by their cognate response regulator determines cell fate. *Cell* **133**, 452-61 (2008).
8. Tsokos, C.G., Perchuk, B.S. and Laub, M.T. A dynamic complex of signaling proteins uses polar localization to regulate cell-fate asymmetry in *Caulobacter crescentus*. *Developmental Cell* **20**, 329-41 (2011).
9. Matroule, J.-Y., Lam, H., Burnette, D.T. and Jacobs-Wagner, C. Cytokinesis monitoring during development; rapid pole-to-pole shuttling of a signaling protein by localized kinase and phosphatase in *Caulobacter*. *Cell* **118**, 579-90 (2004).
10. Jenal, U. and Fuchs, T. An essential protease involved in bacterial cell-cycle control. *The EMBO Journal* **17**, 5658-69 (1998).
11. Ryan, K.R., Huntwork, S. and Shapiro, L. Recruitment of a cytoplasmic response regulator to the cell pole is linked to its cell cycle-regulated proteolysis. *Proceedings of the National Academy of Sciences of the United States of America* **101**, 7415-20 (2004).
12. McGrath, P.T., Iniesta, A. a, Ryan, K.R., Shapiro, L. and McAdams, H.H. A dynamically localized protease complex and a polar specificity factor control a cell cycle master regulator. *Cell* **124**, 535-47 (2006).
13. Jenal, U. and Malone, J. Mechanisms of cyclic-di-GMP signaling in bacteria. *Annual Review of Genetics* **40**, 385-407 (2006).
14. Duerig, A., Abel, S., Folcher, M., Nicollier, M., Schwede, T., Amiot, N., Giese, B. and Jenal, U. Second messenger-mediated spatiotemporal control of protein degradation regulates bacterial cell cycle progression. *Genes & Development* **23**, 93-104 (2009).

15. Paul, R., Weiser, S., Amiot, N.C., Chan, C., Schirmer, T., Giese, B. and Jenal, U. Cell cycle-dependent dynamic localization of a bacterial response regulator with a novel di-guanylate cyclase output domain. *Genes & Development* **18**, 715-27 (2004).
16. Aldridge, P., Paul, R., Goymer, P., Rainey, P. and Jenal, U. Role of the GGDEF regulator PleD in polar development of *Caulobacter crescentus*. *Molecular Microbiology* **47**, 1695-708 (2003).
17. Chan, C., Samoray, D., Amiot N.C., Giese, B., Jenal U. and Schirmer, T. Structural basis of activity and allosteric control of diguanylate cyclase. *Proceedings of the National Academy of Sciences of the United States of America* **101**, 17084-9 (2004).
18. Paul, R., Abel, S., Wassmann, P., Beck, A., Heerklotz, H. and Jenal, U. Activation of the diguanylate cyclase PleD by phosphorylation-mediated dimerization. *Journal of Biological Chemistry* **282**, 29170-7 (2007).
19. Wassmann, P., Chan, C., Paul, R., Beck, A., Heerklotz, H., Jenal, U. and Schirmer, T. Structure of BeF3⁻-modified response regulator PleD: implications for diguanylate cyclase activation, catalysis, and feedback inhibition. *Structure* **15**, 915-27 (2007).
20. Abel, S., Chien, P., Wassmann, P., Schirmer, T., Kaefer, V., Laub, M.T., Baker, T.A. and Jenal, U. Regulatory cohesion of cell cycle and cell differentiation through interlinked phosphorylation and second messenger networks. *Molecular Cell* **43**, 550-560 (2011).
21. Chien, P., Perchuk, B.S., Laub, M.T., Sauer, R.T. and Baker, T. a Direct and adaptor-mediated substrate recognition by an essential AAA⁺ protease. *Proceedings of the National Academy of Sciences of the United States of America* **104**, 6590-5 (2007).
22. Biondi, E.G., Reisinger, S.J., Skerker, J.M., Arif, M., Perchuk B.S., Ryan, K.R. and Laub, M.T. Regulation of the bacterial cell cycle by an integrated genetic circuit. *Nature* **444**, 899-904 (2006).
23. Angelastro, P.S., Sliusarenko, O. and Jacobs-Wagner, C. Polar localization of the CckA histidine kinase and cell cycle periodicity of the essential master regulator CtrA in *Caulobacter crescentus*. *Journal of Bacteriology* **192**, 539-52 (2010).
24. Viollier, P.H., Sternheim, N., and Shapiro. Identification of a localization factor for the polar positioning of bacterial structural and regulatory proteins. *Proceedings of the National Academy of Sciences of the United States of America* **99**, 13831-13836 (2002).
25. Hinz, A.J., Larson, D.E., Smith, C.S. and Brun, Y.V. The *Caulobacter crescentus* polar organelle development protein PodJ is differentially localized and is required for polar targeting of the PleC development regulator. *Molecular Microbiology* **47**, 929-41 (2003).
26. Lawler, M.L., Larson, D.E., Hinz, A.J., Klein, D. and Brun, Y.V. Dissection of functional domains of the polar localization factor PodJ in *Caulobacter crescentus*. *Molecular Microbiology* **59**, 301-16 (2006).
27. Wang, S.P., Sharma, P.L., Schoenlein, P.V. and Ely, B. A histidine protein kinase is involved in polar organelle development in *Caulobacter crescentus*. *Proceedings of the National Academy of Sciences of the United States of America* **90**, 630-4 (1993).
28. Chen, J.C., Hottes, A.K., McAdams, H.H., McGrath, P.T., Viollier, P.H. and Shapiro, L. Cytokinesis signals truncation of the PodJ polarity factor by a cell cycle-regulated protease. *The EMBO Journal* **25**, 377-86 (2006).

29. Ponting, C.P., Schultz, J., Milpetz, F. & Bork, P. SMART: identification and annotation of domains from signalling and extracellular protein sequences. *Nucleic Acids Research* **27**, 229-32 (1999).
30. Larkin, M., Blackshields, G, Brown, N.P., Chenna, R., McGettigan, P.A., McWilliam, H., Valentin, F., Wallace, I.M., Wilm, A., Lopez, R., Thompson, J.D., Gibson, T.J. and Higgins, D.G. Clustal W and Clustal X version 2.0. *Bioinformatics* **23**, 2947-8 (2007).
31. Duerig, A. Second messenger mediated spatiotemporal control of cell cycle and development. *PhD thesis* (2008).
32. Hubbard, J. A, MacLachlan, L.K., King, G.W., Jones, J.J. and Fosberry, A.P. Nuclear magnetic resonance spectroscopy reveals the functional state of the signalling protein CheY *in vivo* in *Escherichia coli*. *Molecular Microbiology* **49**, 1191-1200 (2003).
33. Christen, B., Christen, M., Paul, R., Schmid, F., Folcher, M., Jenoe, P., Meuwly, M. and Jenal, U. Allosteric control of cyclic di-GMP signaling. *The Journal of Biological Chemistry* **281**, 32015-24 (2006).
34. Karimova, G., Pidoux, J., Ullmann, A., Ladant, D. A bacterial two-hybrid system based on a reconstituted signal transduction pathway. *Microbiology* **95**, 5752-5756 (1998).
35. Radhakrishnan, S.K., Thanbichler, M. and Viollier, P.H. The dynamic interplay between a cell fate determinant and a lysozyme homolog drives the asymmetric division cycle of *Caulobacter crescentus*. *Genes & Development* **22**, 212-25 (2008).
36. Huitema, E., Pritchard, S., Matteson, D., Radhakrishnan, S.K. and Viollier, P.H. Bacterial birth scar proteins mark future flagellum assembly site. *Cell* **124**, 1025-37 (2006).
37. Lam, H., Schofield, W.B. & Jacobs-Wagner, C. A landmark protein essential for establishing and perpetuating the polarity of a bacterial cell. *Cell* **124**, 1011-23 (2006).
38. Wassmann, P. Elucidation of the regulatory mechanisms of the diguanylate cyclases PleD, DgcA and DgcB by structural and biophysical analysis. *PhD thesis* (2009).
39. Hurley, J.H. GAF domains: cyclic nucleotides come full circle. *Science's STKE* **2003**, PE1 (2003).
40. Gao, R. and Stock, A.M. Biological insights from structures of two-component proteins. *Annual Reviews of Microbiology* **63**, 133-54 (2009).
41. Bachhawat, P., Swapna, G.V.T., Montelione, G.T. and Stock, A.M. Mechanism of activation for transcription factor PhoB suggested by different modes of dimerization in the inactive and active states. *Structure* **13**, 1353-63 (2005).
42. Dyer, C.M. and Dahlquist, F.W. Switched or Not?: the Structure of Unphosphorylated CheY Bound to the N-Terminus of FliM. *Journal of Bacteriology* **188**, 7354-7363 (2006).
43. Schär, J., Sickmann, A. and Beier, D. Phosphorylation-Independent Activity of Atypical Response Regulators of *Helicobacter pylori*. *Journal of Bacteriology* **187**, 3100-3109 (2005).
44. Ruiz, D., Salinas, P., Lopez-Redondo, M.L., Cayuela, M.L. and Marina, A. Phosphorylation-independent activation of the atypical response regulator NblR. *Microbiology* **154**, 3002-3015 (2008).

45. Fraser, J.S., Merlie, J.P., Echols, N., Weisfield, S.R., Mignot, T., Wemmer, D.E., Zusman, D.R., Alber, T. An atypical receiver domain controls the dynamic polar localization of the *Myxococcus xanthus* social motility protein FrzS. *Molecular Microbiology* **65**, 319-32 (2007).
46. Krasteva, P.V., Fong, J.C.N., Shikuma, N.J., Beyhan, S., Navarro, M.V., Yildiz, F.H. and Sondermann, H. *Vibrio cholerae* VpsT regulates matrix production and motility by directly sensing cyclic di-GMP. *Science* **327**, 866-8 (2010).
47. Taylor, J.A., Wilbur, J.D., Smith, S.C. and Ryan, K.R. Mutations that alter RcdA surface residues decouple protein localization and CtrA proteolysis in *Caulobacter crescentus*. *Journal of Molecular Biology* **394**, 46-60 (2009).
48. Hengge, R. Principles of c-di-GMP signalling in bacteria. *Nature Reviews. Microbiology* **7**, 263-73 (2009).
49. De, N., Purruccello, M., Krasteva, P.V., Bae, N., Raghavan, R.V. and Sondermann, H. Phosphorylation-independent regulation of the diguanylate cyclase WspR. *PLoS Biology* **6**, e67 (2008).
50. Qi, Y., Chuah, M.L.C., Dong, X., Xie, K., Luo, Z., Tang, K. and Liang, Z.X. Binding of cyclic diguanylate in the non-catalytic EAL domain of FimX induces a long-range conformational change. *The Journal of Biological Chemistry* **286**, 2910-7 (2011).
51. Christen, M., Kulasekara, H.D., Christen, B., Kulasekara, B.R., Hoffmann, L.R. and Miller S.I. Asymmetrical distribution of the second messenger c-di-GMP upon bacterial cell division. *Science* **328**, 1295-7 (2010).
52. Ely, B. Genetics of *Caulobacter crescentus*. *Methods in Enzymology* **204**, 372-384 (1991).
53. Jenal, U. and Shapiro, L. Cell cycle-controlled proteolysis of a flagellar motor protein that is asymmetrically distributed in the *Caulobacter* predivisional cell. *The EMBO Journal* **15**, 2393-406 (1996).
54. Karimova G. and Ullmann, A.L.D. Bordetella pertussis adenylate cyclase toxin as a tool to analyze molecular interactions in a bacterial two-hybrid system. *International Journal of Medical Microbiology* **290**, 441-445 (2000).
55. Sambrook, J. *Molecular Cloning*. Cold Spring Harbour Press (1989).
56. Tsai, J.-W. and Alley, M.R.K. Proteolysis of the *Caulobacter* McpA chemoreceptor is cell cycle regulated by a ClpX-dependent pathway. *Journal of Bacteriology* **183**, 5001-5007 (2001).
57. Domian, I.J., Quon, K.C. and Shapiro, L. Cell type-specific phosphorylation and proteolysis of a transcriptional regulator controls the G1-to-S transition in a bacterial cell cycle. *Cell* **90**, 415-24 (1997).
58. Arnold, K., Bordoli, L., Kopp, J. and Schwede, T. The SWISS-MODEL workspace: a web-based environment for protein structure homology modelling. *Bioinformatics* **22**, 195-201 (2006).
59. Schwede, T. SWISS-MODEL: an automated protein homology-modeling server. *Nucleic Acids Research* **31**, 3381-3385 (2003).

60. Finn, R.D., Mistry, J., Tate, J., Coggill, P., Heger, A., Pollington, J.E., Gavin, L.O., Gunasekaran, P., Ceric, G., Forslund, K., Holm, L., Sonnhammer, E.L.L., Eddy, S.R., Bateman, A. The Pfam protein families database. *Database* **38**, 211-222 (2010).
61. Emsley P., and Coot, C.K.: model-building tools for molecular graphics. *Acta Crystallographica. Section D. Biological Chrystallography* **60**, 2126-2130 (2004).
62. Sippl, M.J. Recognition of errors in three-dimensional structures of proteins. *Proteins* **17**, 355-362 (1993).
63. Wiederstein, M. and Sippl, M.J. ProSA-web: interactive web service for the recognition of errors in three-dimensional structures of proteins. *Nucleic Acids Research* **35**, W407-10 (2007).
64. Evinger, M. and Agabian, N. Envelope-associated nucleoid from *Caulobacter crescentus* stalked and swarmer cells. *Journal of Bacteriology* **132**, 294-301 (1977).
65. Simon, R., Prieffer, U. and Puhler, A. A broad host range mobilization system for *in vivo* genetic engineering: Transposon mutagenesis in gram-negative bacteria. *Biotechnology* 784-790 (1983).
66. Roberts, R.C., Toochinda, C., Avedissian, M., Baldini, R.L., Gomes, S.L. and Shapiro, L. Identification of a *Caulobacter crescentus* operon encoding *hrcA*, involved in negatively regulating heat-Inducible transcription , and the chaperone gene *grpE*. *Journal of Bacteriology* **178**, 1829-1841 (1996).
67. Kovach, M.E., Elzer, P.H., Hill, S.D., Robertson, G.T., Farris, M.A., Roop, Martin, R. and Peterson, K.M. Four new derivatives of the broad-host-range cloning vector pBBR1MCS, carrying different antibiotic-resistance cassettes. *Gene* **166**, 175-6 (1995).
68. Thanbichler, M., Iniesta, A.A. and Shapiro, L. A comprehensive set of plasmids for vanillate- and xylose-inducible gene expression in *Caulobacter crescentus*. *Nucleic Acids Research* **35** (2007).

3.1.7 Figures and Figure Legends

Figure 1: Sequence and structure comparison of the c-di-GMP effector protein PopA and the diguanylate cyclase PleD.

A. A schematic view of the domain architectures and a sequence alignment between PopA and PleD are shown. The three different domains are indicated by different colors. The active site in PleD is boxed in blue, the conserved primary I-sites are highlighted in green, secondary I-site of PleD and possible conserved secondary I-sites of PopA are boxed in white, residues important for signal transduction in PleD and PopA are shown in yellow and conserved residues of the Rec1/Rec2' dimerization interface of PleD and residues of the putative PopA dimerization interface are shown in black. [*] Identical residue, [:] conserved substitution, [.] semi conserved substitution.

B. The X-ray structure of native monomeric PleD¹⁷ and the modeled structure of PopA using native PleD as template are depicted. The GGDEF domain is colored green, the Rec1 domain red and the Rec2 domain yellow. The active site and the I-site bound to (c-di-GMP)₂ are indicated with arrows.

Figure 2: A PopA_{D55N} is not required for PopA function.

Swimming behavior on semi solid agar plates, attachment on polystyrene surfaces, amount of holdfast stained with Oregon green coupled wheat germ agglutinin (Invitrogen, USA) and resistance to phage CBK reflecting the absence of pili were analyzed for CB15 wild-type, CB15 $\Delta popA$ mutant and CB15 $\Delta popA$ strain expressing either PopA wild-type GFP-fusion or PopA_{D55N}-GFP fusion.

- A. A PopA_{D55N} mutants swims like wild-type CB15.
- B. D55 does not play a role in attachment. It attaches similarly to wild-type CB15.
- C. PopA_{D55N} produces similar levels of holdfast like wild-type. The upper panels reflect the DIC channel, FITC the Oregon green channel.
- D. A PopA_{D55N} expresses pili like wild-type. A $\Delta pilA$ strain was used as a phage CBK resistant strain as it has no functional pili.
- E. Comparison of the PleD Rec1/Rec2 interface with the modeled situation in PopA viewed along the quasi-two-fold axis. The conserved phosphoryl acceptor sites are highlighted in yellow, the conserved residues involved in signal transduction are boxed.

Figure 3: Dimerization over the Rec1/Rec2' interface is not involved in PopA stalked pole localization and CtrA degradation.

A. Comparison of the PleD Rec1/Rec2' stem domains (red/yellow) and the modeled Rec1/Rec2' domains (green/purple) of PopA. The marked residues define the dimerization interface of PleD. The respective conserved residues in the putative Rec1-Rec2' interface of PopA are indicated as well. A schematic drawing of the situation in PleD is included in the panel below. Dashed lines show the mentioned dimerization interface residues of PleD.

B. PopA single and triple mutants of the putative Rec1/Rec2' interface do not affect PopA stalked pole localization. The localization of putative PopA dimerization interface mutants expressing C-terminal GFP was analyzed by fluorescence microscopy. Polar localization is indicated schematically in the lowest panels. The following single mutants were used: PopA wild-type, PopA_{E125A}, PopA_{R277A}, PopA_{E50A}, PopA_{R220A}, PopA_{R129A}, PopA_{E281A} and the triple mutation PopA_{R220AR277AE281A}.

C. The PopA-GFP mutants are expressed in $\Delta popA$. The stability of the microscopically analyzed PopA mutants was assayed by α -PopA immunoblot analysis. Strains are mentioned in B.

D. PopA single and triple mutants of the putative Rec1/Rec2' interface do not affect CtrA degradation during cell cycle. α -CtrA immunoblots of synchronized cultures of the strains mentioned in B. were performed to monitor CtrA levels during cell cycle.

Figure 4: PopA primary I-sites are required for correct localization to the stalked pole.

A. A closer view into the I-site of activated PleD bound to $(c\text{-di-GMP})_2$ ¹⁹ and into the modeled I-site of PopA. Side chains of the I-site residues are shown together with surrounding secondary structure elements. The core residues important for c-di-GMP binding (primary I-sites) are circled and the dashed circles show the secondary I-sites. A schematic drawing of the I-site region in PleD is included. It shows how adjacent GGDEF domains are crosslinked together with $(c\text{-di-GMP})_2$ bound to the I-sites. Residues important for this crosslinking are circled.

B. The primary I-site of PleD is not required for polar localization. PleD primary I-site mutants expressing C-terminal GFP in $\Delta pleD$ background were analyzed for their localization by fluorescence microscopy. The following mutants were used: PleD wild-type, PleD* and PleD_{R359A}. Localization is illustrated in the schematic panels on the right.

C. PopA primary I-site mutants are needed for correct localization to the stalked pole. PopA primary I-site mutants expressing C-terminal GFP in $\Delta popA$ background were analyzed for their localization by fluorescence microscopy. The following

mutants were used: PopA wild-type, PopA_{R357G} and PopA_{R388A} (referred to as secondary I-site mutants).

D. Statistical analysis of the localization data in predivisional cells. ST pole: localization to the stalked pole, SW pole: localization to the incipient swarmer pole, two foci: bipolar localization, no focus: no polar localization observed.

E. The PopA I-site mutants are stably expressed in $\Delta popA$. The levels of the PopA I-site mutants were assayed by α -PopA immunoblot analysis.

F. Correct primary I-sites are needed for CtrA degradation. α -CtrA immunoblots of synchronized cultures were performed to follow CtrA levels during cell cycle.

G. The arginine R357 of the I-site motif is required for PopA localization and CtrA degradation whereas the aspartic acid D360 is dispensable for CtrA degradation but not for localization. The amino acid mutations in the I-site are indicated in blue and the conserved residues are highlighted in red. CtrA levels of synchronized cultures using α -CtrA immunoblot and localization were analyzed by fluorescence microscopy for each of the mutants.

Figure 5: Secondary I-site mutants have a partial effect on PopA stalked pole localization and CtrA degradation.

Putative secondary I-site candidates in PopA were mutated and fused C-terminally to GFP. Their localization was studied in a $\Delta popA$ and in a $\Delta popA \Delta podJ$ background by fluorescence microscopy. $\Delta popA$ or $\Delta popA \Delta podJ$ expressing the following PopA-GFP alleles were studied: PopA_{R313A}, PopA_{R315A}, PopA_{R317A} and PopA_{R315AR317A} (referred to as secondary I-site mutants). PopA wild-type and PopA_{R357G} were used as controls. Localization is illustrated schematically in the lowest panels.

A. PopA secondary I-site mutants have a partial effect on PopA stalked pole localization. The localization to the incipient swarmer pole is not affected.

B. Statistical analysis of the localization data. Localization was counted in predivisional cells. ST pole: localization to the stalked pole, SW pole: localization to the incipient swarmer pole, two foci: localization to both poles and no focus: no localization observed.

C. PopA secondary I-site mutants have a partial effect on PopA stalked pole localization. In agreement with Duerig and coworkers¹⁴ no PopA localization to the incipient swarmer pole is observed in a $\Delta podJ$ background.

D. The PopA-GFP fusions are expressed in $\Delta popA$. Their levels were assayed by α -PopA immunoblot analysis.

E. PopA secondary I-site mutants are not needed for correct CtrA degradation. CtrA levels of the PopA mutants during cell cycle were checked by α -CtrA immunoblots.

Figure 6: The GGDEF domain is critical for PopA localization.

- A. Single PopA domains were C-terminally fused to GFP and their localization was analyzed by fluorescence microscopy. The following mutants were used: PopA-Rec1-GFP, PopA-Rec1-Rec2-GFP and PopA-GGDEF-GFP. Full length PopA-GFP was used as control. Schematic drawing of the localization are shown in the panels on the right.
- B. PopA-GGDEF alone is not stable. The levels of the PopA truncated mutants were tested by α -PopA immunoblots.

Figure 7: The PopA GGDEF domain contains the polar localization information.

- A. Schematic domain representation of PopA and PleD wildtype and of the constructed PopA-PleD-Hybrid proteins A and B. Active sites, I-sites and P-sites are indicated.
- B. Hybrid A localizes to the cell poles whereas no signal was observed for Hybrid B. The localization of the Hybrid proteins A and B fused to GFP was analyzed in $\Delta popA$ and $\Delta pleD$ backgrounds by fluorescence microscopy. PopA and PleD wild-type GFP fusions in $\Delta popA$ and $\Delta pleD$ were used as controls. Schematic localization drawings are included in the panel on the right.
- C. Stability of the PopA-PleD-Hybrid fusions and PopA and PleD wild-type controls was tested by α -PopA immunoblots.
- D. c-di-GMP has an effect on Hybrid-A localization, whereas phosphorylation is not required for its localization. The localization pattern of the GFP tagged Hybrid proteins A and B and the controls PopA and PleD wild-types were studied in $\Delta pleD$ $\Delta divJ$ and cdG^0 backgrounds.
- E. Mutation of both, Y26A and R359G leads to delocalization of the Hybrid-A protein. The localization of Hybrid-A-GFP alleles with point mutations in Y26A, R359G and Y26AR359G was analyzed in a $\Delta popA$ background by fluorescence microscopy. Polar foci are illustrated in the schematic pictures. Statistical analysis of the localization data in predivisional cells is provided. ST pole: localization to the stalked pole, two foci: localization to both poles and no focus: no localization observed, mislocalized: unpolar foci distributed all over the cell.
- F. Hybrid-A-GFP mutants are stably expressed. Stability of the Hybrid-A-GFP protein and the mutants Hybrid-A_{R357G}-GFP, Hybrid-A_{Y26A}-GFP, Hybrid-A_{R357G,Y26A} was tested by α -GFP immunoblots. NA1000 and $\Delta popA$ were used as controls.

Figure 8: The PopA-PleD-Hybrid proteins are not able to complement FliF and CtrA stabilization, the attachment and the motility defect of $\Delta popA$ and $\Delta pleD$ mutants.

A. The GFP tagged Hybrid-A and Hybrid-B proteins in $\Delta popA$ or $\Delta pleD$ backgrounds were analyzed for their complementation of the $\Delta popA$ CtrA stabilization and the $\Delta pleD$ FliF stabilization phenotype. Synchronized cultures were tested by immunoblot analysis with α -CtrA and α -FliF. α -McpA and α -GFP blots were used as controls for synchronization quality and stability of the hybrid proteins, respectively. NA1000, $\Delta popA$ and $\Delta pleD$ with empty plasmid as well as PopA-GFP and PleD-GFP fusions were used as controls.

B. The Hybrid-A and Hybrid-B-GFP in $\Delta popA$ or $\Delta pleD$ backgrounds were quantified for their ability to attach to polystyrene surfaces. CB15 wild-type, $\Delta popA$ and $\Delta pleD$ with empty plasmid and PopA-GFP and PleD-GFP in the respective backgrounds were used as controls.

C. Swimming behavior on semi-solid agar plates was scored for CB15 wildtype, $\Delta popA$ and $\Delta pleD$ empty plasmids and $\Delta popA$ or $\Delta pleD$ expressing either PopA or PleD wild-type -GFP of PopA-PleD-Hybrid-GFP.

Figure 9: The PopA Rec domains are needed for the localization of RcdA.

$\Delta popA$ cells expressing RcdA-YFP and either PopA wild-type or Hybrid-A-CFP from plasmids were analyzed by fluorescence microscopy for their colocalization. Schematic drawing of the localization are shown in separate panels.

Figure 10: PopA Rec1 is needed to interact with RcdA.

- A. pKT25-PopA interacts directly with RcdA-pUT18 and pUT18C-RcdA. Controls with empty vectors are negative.
- B. pKT25-PopA-Rec1 interacts directly with RcdA-pUT18 and pUT18C-RcdA. Controls with empty vectors are negative.
- C. PopA-Rec2 does not interact with RcdA.
- D. PopA-Rec1-Rec2 does not interact with RcdA.
- E. PopA-GGDEF does not interact with RcdA.

Figure 11: The interaction between PopA and RcdA involves R272H, which is located in the in the flexible linker domain between Rec2 and GGDEF domain.

A. Schematic representation of the bacterial Two-Hybrid system used to screen for PopA mutants which do not interact anymore with RcdA. PopA and RcdA are fused to T25 and T18 fragments of CyaA. As a consequence of PopA-RcdA interaction, catabolic genes like the maltose utilization genes are expressed leading to red color on McConkey agar base maltose plates. If PopA contains a mutation in a

critical residue for interaction (shown as asterisk), colonies stay white indicating an impaired protein interaction.

B. PopA directly interacts with RcdA. The PopA mutations R272H, G294E and A335T were found to stay white, indicating that they do not interact with RcdA anymore. The respective panels are shown with arrows.

C. The residues R272H, G294E and A335T lie on the surface of the modeled PopA structure. The location of the residues R272H, G294E and A335T on the structural model of PopA is shown. The GGDEF domain is colored in green, Rec1 in red, Rec2 in yellow and the flexible linker region between Rec2 and GGDEF is shown in light grey. Zoom-in views of the respective residues are depicted in the lower panels.

D. A PopA_{R272H} mutant localizes to the cell poles and colocalizes RcdA at the stalked pole. $\Delta popA$ cells expressing RcdA-YFP and either PopA wild-type or PopA_{R272H}-CFP from plasmids were analyzed by fluorescence microscopy for their colocalization. Schematic drawing of the localization are shown in separate panels.

E. The stability of PopA-GFP fusions was tested by α -PopA immunoblot analysis. NA1000 and $\Delta popA$ were used as controls.

F. A $\Delta popA$ mutant expressing PopA_{R272H} degrades CtrA similar to the wild-type. Synchronized cultures of $\Delta popA$ expressing either PopA wild-type CFP or PopA_{R272H}-CFP were probed with α -CtrA to compare CtrA levels during cell cycle. α -McpA immunoblots were used as a quality control for synchronization.

Figure 12: PopA localization to the incipient swarmer pole requires correct polar PodJ localization.

A. Schematic representation of PodJ. The N-terminal part lies in the cytosol, the C-terminal part in the periplasm. CC: coiled-coil domains, TM: transmembrane domain, TPR: tetratricopeptide repeats, PG: peptidoglycan binding domain. The positions of stop codon insertion are indicated by arrows. Adapted from²⁶.

B. PopA cannot localize to the incipient swarmer pole in presence of a cytosolic not membrane anchored version of PodJ. The localization of PopA-GFP in $\Delta popA$ $\Delta podJ$ strains expressing PodJ truncated at several different positions was analyzed by fluorescence microscopy. The following PodJ truncation mutants were used: PodJ truncated at amino acid position 589, 639, 660, 757, 794, 829 and 921. PopA-GFP in $\Delta popA$ and in $\Delta popA$ $\Delta podJ$ was used as control.

C. Statistical analysis of PopA-GFP in the different PodJ truncation mutant strains in predivisional and stalked cell types. ST pole: localization to the stalked pole, SW pole: localization to the incipient swarmer pole, two foci: bipolar localization, no focus: no polar localization observed.

Figure 13: PopA localization to the poles is not affected in $\Delta spmX$, $\Delta tipF$ and $\Delta tipN$ mutants.

A. SpmX does not control PopA localization to the poles. NA1000 $\Delta popA$ and NA1000 $\Delta popA \Delta spmX$ expressing PopA-GFP from plasmid were compared in their ability to localize to the cell poles by fluorescence microscopy. Schematic pictures of the localization are depicted in the panels on the right.

B. TipF has no influence on PopA localization to the poles. NA1000 $\Delta popA$ and NA1000 $\Delta popA \Delta tipF$ expressing PopA-GFP from plasmid were compared in their ability to localize to the cell poles by fluorescence microscopy. Schematic pictures of the localization are depicted in the panels on the right.

C. TipN does not affect PopA localization to the poles. NA1000 and NA1000 $\Delta tipF$ expressing PopA-GFP from plasmid were compared in their ability to localize to the cell poles by fluorescence microscopy. Schematic pictures of the localization are depicted in the panels on the right.

D. The x-ray structure of an activated PleD dimer is shown. Residues involved in sulfate binding are boxed in black. The Rec1 domain is shown in red, the Rec2 domain in yellow. The GGDEF domains are omitted for clarity.

E. Mutation of putative sulfate binding residues R117 and R121 in PleD do not affect its localization. The strains NA1000 $\Delta pleD$ expressing PleD_{R117SR121S}-GFP or PleD_{R117DR121D} from plasmid were analyzed by fluorescence microscopy for their subcellular localization. NA1000 $\Delta pleD$ expressing PleD-GFP wild-type and the non phosphorylatable allele PleD_{D53N}-GFP were used as controls. Schematic pictures are given in the panels on the right.

F. Mutation of the putative binding residue R118 in PopA did not change the bipolar localization pattern of PopA. The strains NA1000 $\Delta popA$ expressing PopA wild-type GFP, the mutants PopA_{R118A}-GFP or PopA_{R118S}-GFP were analyzed for their subcellular distribution. Schematic pictures are presented in the panels on the right.

Figure 14: Reversed signal transduction in PopA compared to classical response regulators

A. Signal transduction in PleD involves phosphorylation (P) of a conserved aspartic acid in its C-terminal receiver domain (violet). This leads to a domain rearrangement (red arrow) which activates its N-terminal GGDEF output domain (green) and induces dimerization.

B. Signal transduction in PopA involves c-di-GMP binding (cdG) to conserved I-sites within the C-terminal GGDEF domain (green). This leads to conformational changes (red arrow) that either allows monomeric PopA to get crosslinked to polar receptors (dark blue, R) or alternatively, c-di-GMP crosslinks adjacent GGDEF domains and the resulting dimeric PopA is recognized by polar receptors (dark blue).

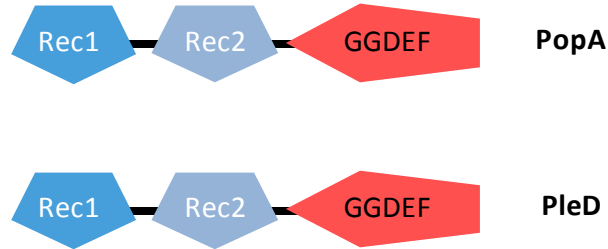
Its receiver domains (violet) mediate interactions with downstream components (I) of the PopA pathway.

Figure S1: Weak evidences for and against the dimerization model of PopA.

- A. Evidence for dimerization: PopA slightly interacts with itself. PopA-PopA protein interactions were analyzed with the bacterial two-hybrid system on McConkey agar base plates supplemented with 0.1% maltose. Positive interaction scores in red, negative score white. 1) PopA fused to pKT25 and to pUT18C. 2) pKT25 and pUT18C empty vectors (negative control). 3) PopA fused to pKT25 and RcdA fused to pUT18C (positive control).
- B. Evidence for dimerization: PopA runs at the molecular weight of the dimer species. Purified PopA-H₆ was crosslinked with 2 mM DSS in the presence of 1 mM c-di-GMP and analyzed by α -PopA immunoblot analysis.
- C. Evidence for dimerization. Purified PopA-H₆ in two different concentrations was analyzed in the presence and absence of c-di-GMP by non denaturing gel electrophoresis.
- D Evidence against PopA dimerization: PopA appears as a clear monomer at a concentration of 10 μ M in static light scattering experiments. They were performed with purified PopA-H₆. The grey curve represents the molar mass distribution and the thick red line indicates the molar mass of PopA. Values for polydispersity, molar mass, statistical errors and final PopA concentration are indicated.
- E. Evidence against PopA dimerization: PopA-PopA interactions were analyzed in the bacterial two-hybrid system on minimal plates containing maltose. Positive interactors survive, negative interactors die. 1) PopA fused to pKT25 and to pUT18C. 2) PopA_{R357G} fused to pKT25 and pUT18C. 3) pKT25 and pUT18C empty vectors (negative control). 4) pKT25-zip and pUT18-zip (positive control). 5) PopA fused to pKT25 and RcdA fused to pUT18C.

Figure 1

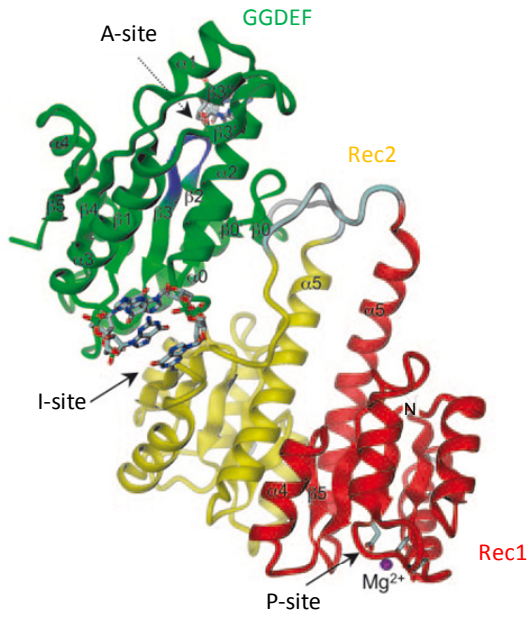
A



PopA	MAVDARILIVAFDDVRAGPLAEGLDRLGWRITARGPYAALAALGDLPIEAVIYDMASAG	60
PleD	--MSARILVDDIEANVRLLEAKLTAEYEVSTAMDGPTALAMAARDLFDIILLVMMPG	58
	:.****:* :... * * :.. ** . :*** . : : : : . *	
PopA	PETQTLARRLKA AVAPRRLPVIAISEPN-ADFRSQSFDL---TLSPPLHPSQAALRLES	115
PleD	MDGFTVCRK LKDDP TTRHIPVVLITALDGRGDRIQGLESGASIFLTKPIDDVMLFARVRS	118
	: * : : * * : : * : : : * * : : * : * : : * : * : : * : * : *	
PopA	LVRTAIAEEEFELRLETFGERRLDLPEPLDAP-YRILAVGEPAPQFLALSNAIQASGA	174
PleD	LTRFKLVIDELRREASGRRMGVIAGAAARLDGLGGRVLI VDDNERQAQRVA AELGVEHR	178
	*. * :. : : * : : * : : * : : * : : * : : * : : * : : * : : *	
PopA	EVVGAF TAYTAFDYLHERP FDSVVLWAGDSQEQALSIAAGMRRNTRIFHIPALLYLKAES	234
PleD	PVIESDPEKAKIS--AGGPVDLIVNAAAKNFDGLRFTAALRSEERTQLPVLAMVDPDD	236
	* : . : . : : : * * * : : * : : : * : : : * : : : * : : : * : : *	
PopA	YVTMSEAFHRGVSDV ASPETPEGETAMRVMELARSFRRGESIRGAL EKARSSGLMDAATG	294
PleD	RGRMVKALEIGVNDILSRPIDPQELSARVKTQIQRKRYTDYLRNNLDHSL ELAVTDQLTG	296
	* : * : : * * : * : * : * : * : * : * : * : * : * : * : * : *	
PopA	LFTRDLFAAHLARLASAARRSRPLSICVLRVADKPE TVWARQNGWLDRAIPQIGSMVGR	354
PleD	LHNRRYMTGQLDSLVRATLGGDPVSALLIDIDFFKKINDTFGHDIGDEV LREFALRLAS	356
	* . * : : : * * : * : * : * : * : : : : : : : * . : : : . : . *	
PopA	LVRVEDTPARLATEVFALALPATNQNAACAAAEIRIAAVIGCTAFDAGEDRAPFVCEFDIG	414
PleD	NVRAIDLPCRYGGEEFV VIMPDTALADALRIAEIRIMHVS GSPFTVAHGREMLNVTISIG	416
	** . * * * . * * : : * * * * * : : : * : : * : : * : : * : : *	
PopA	VAEVQ-PGEGAVKALERAAAAALKREAG-----	441
PleD	VSATAGEGDTP EALLKRADEGVYQAKASGRNAVVGKAA	454
	* : . * : . * : * * . . : : *	

B

Native PleD structure



PopA modeled with native PleD as template

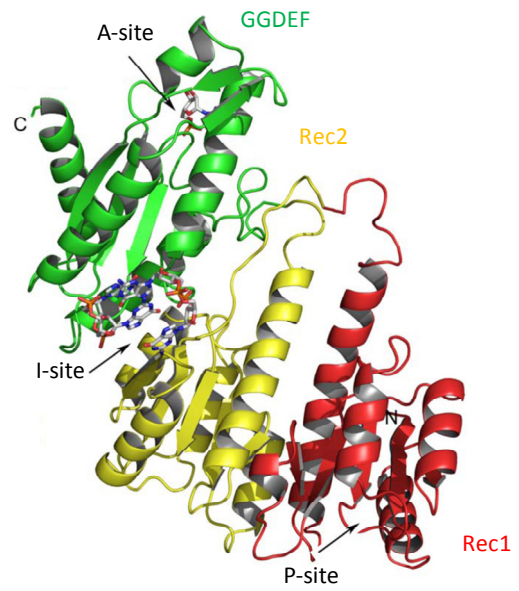
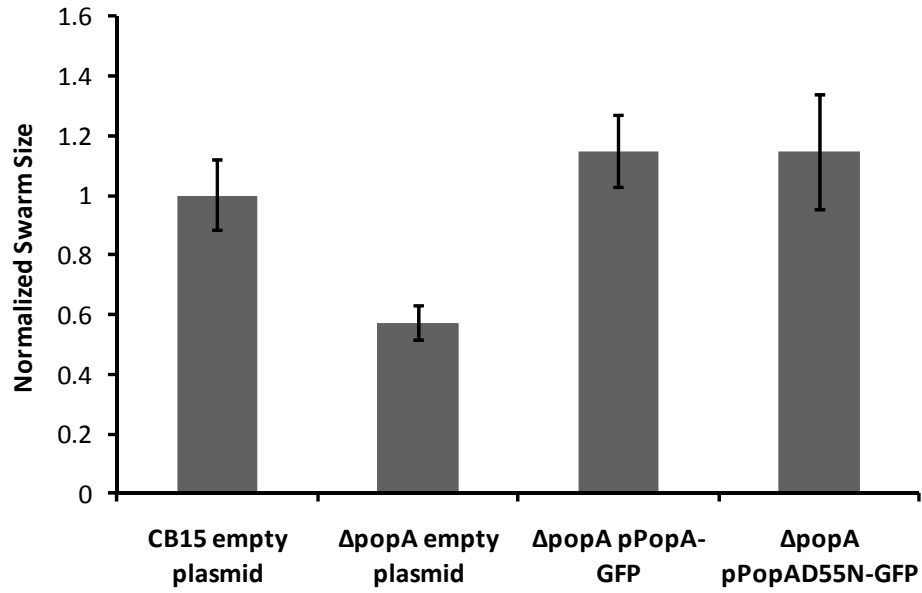
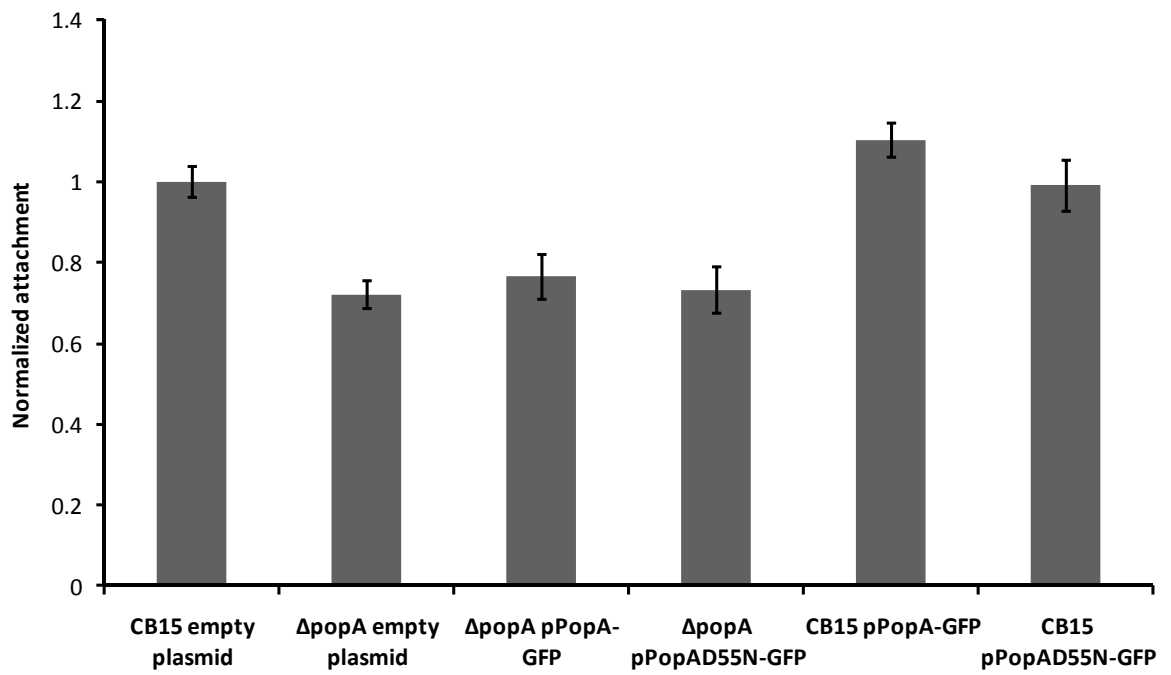


Figure 2

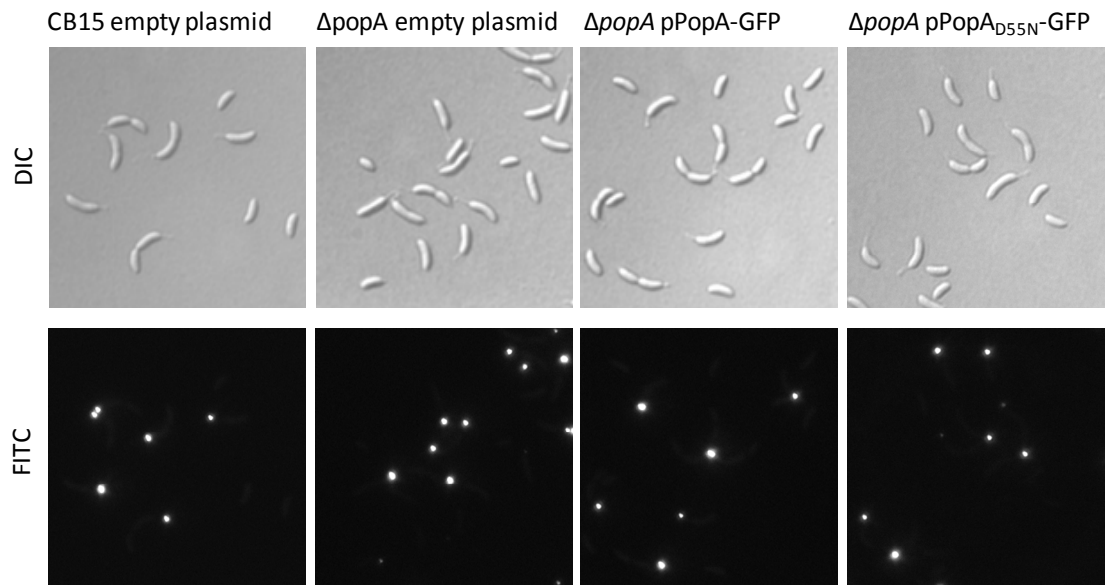
A



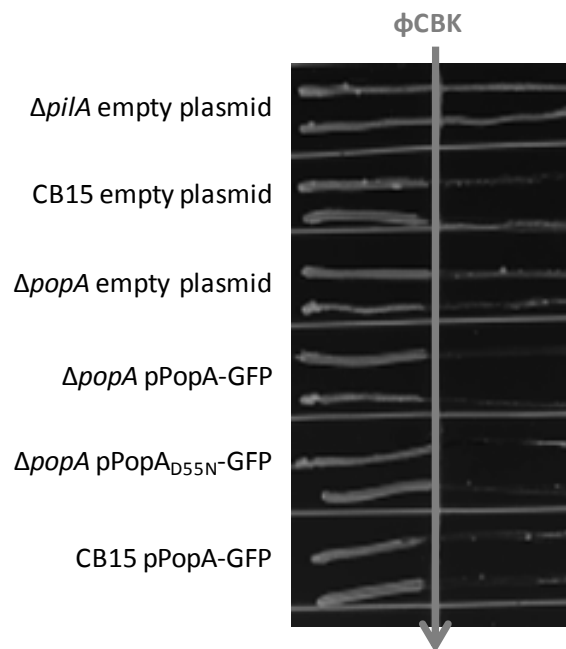
B



C

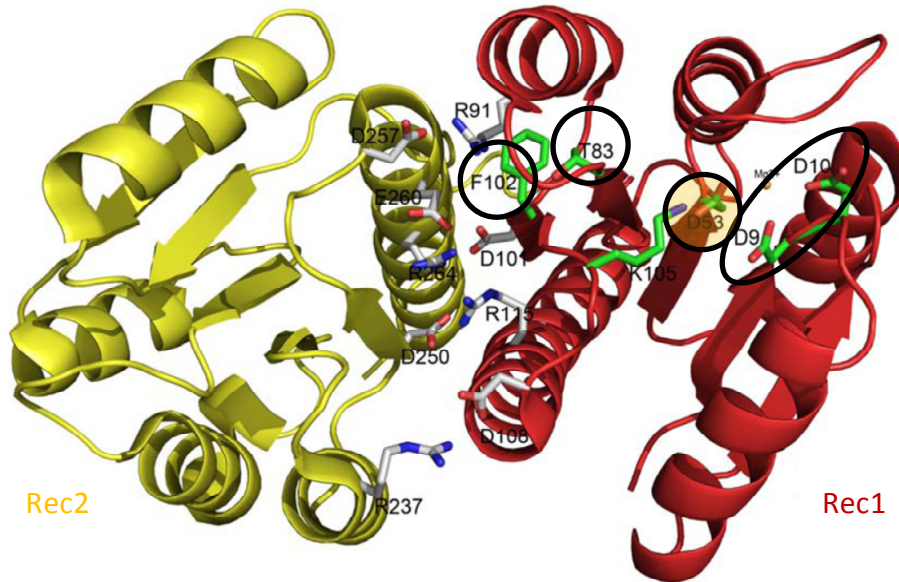


D



E

PleD Rec1/Rec2 interface



PopA modeled Rec1/Rec2 interface

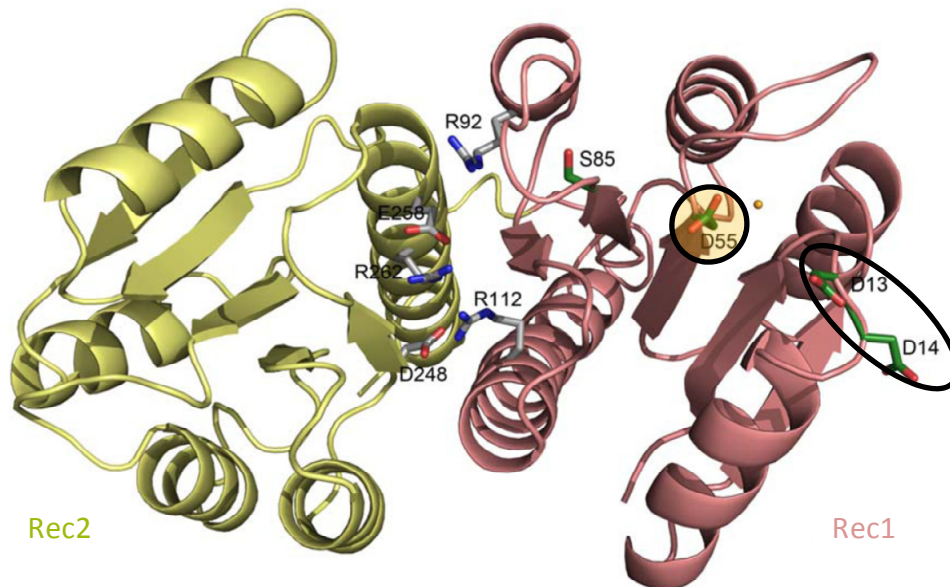
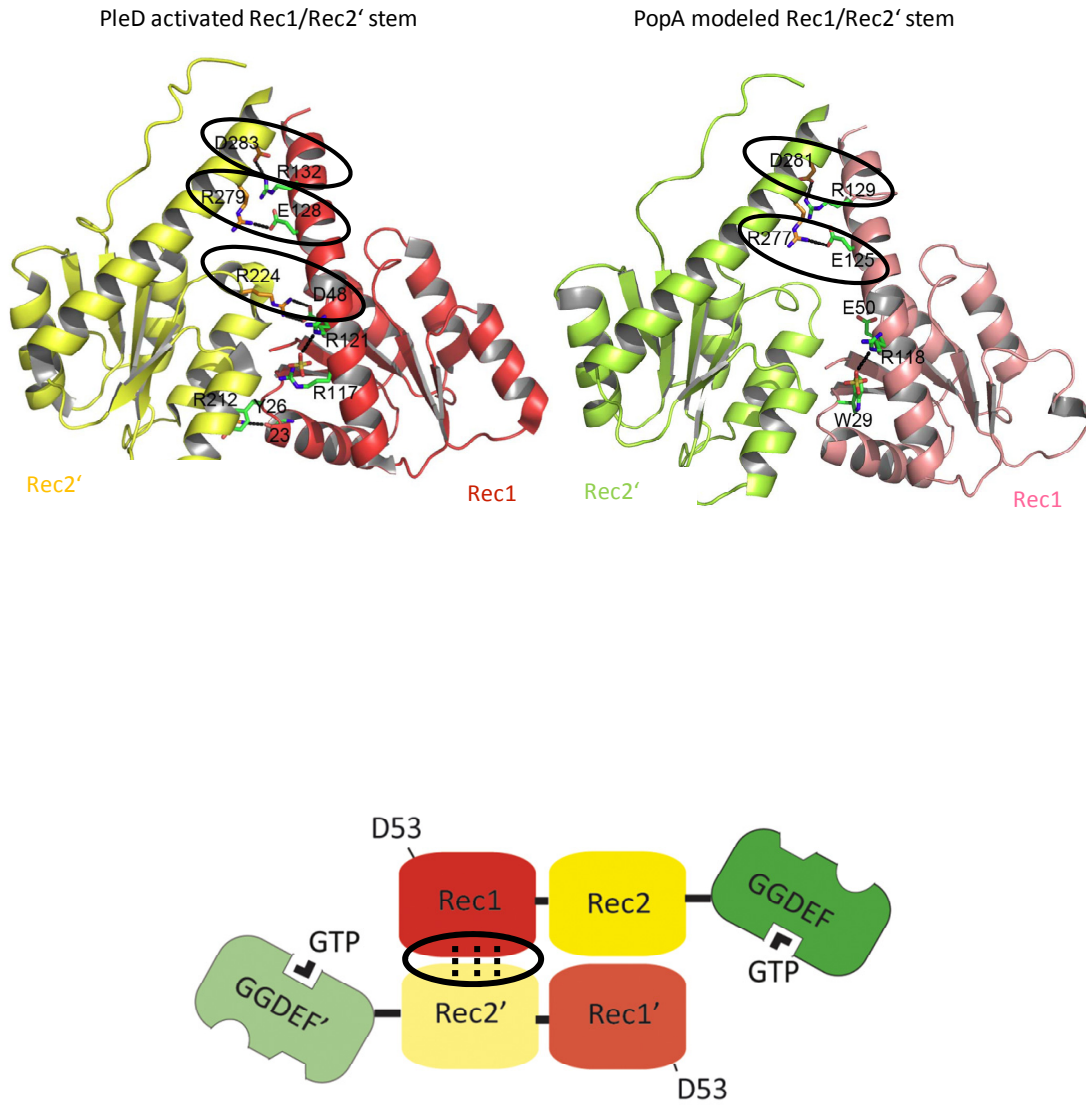
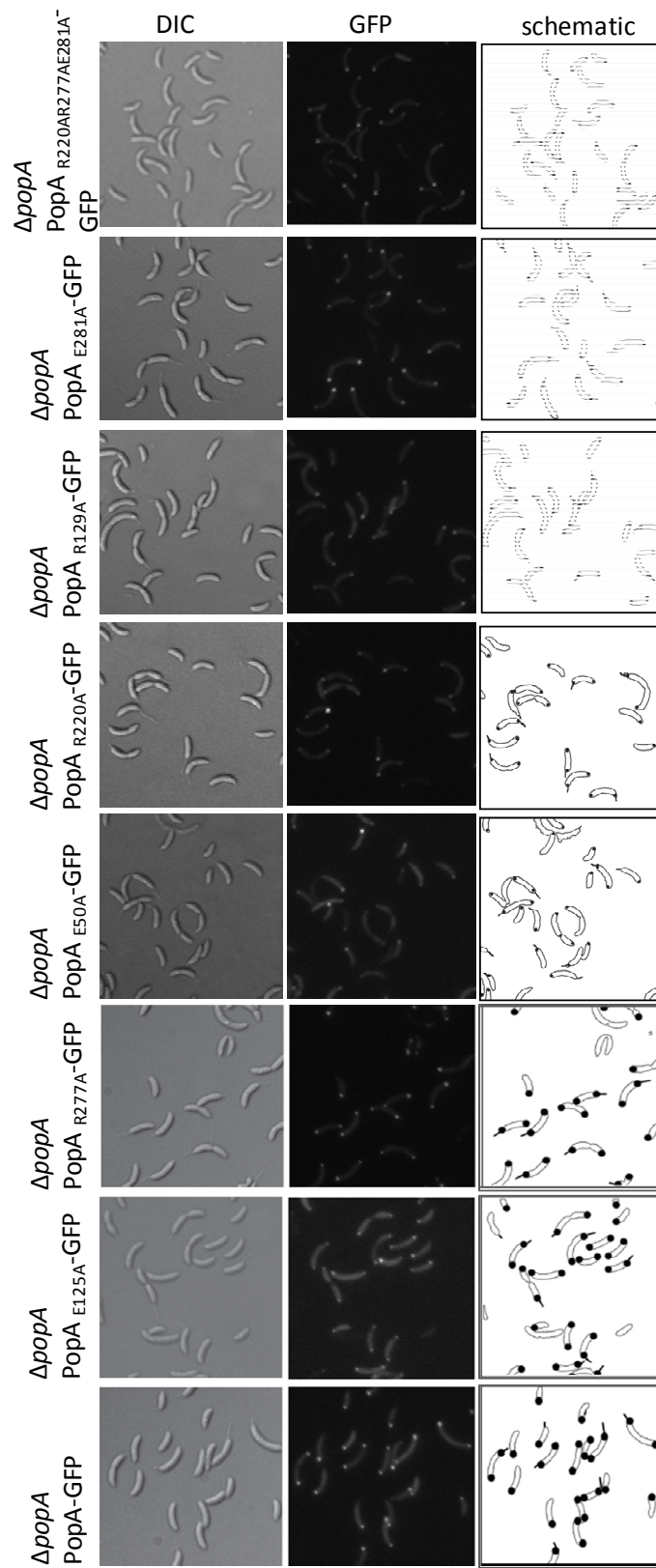


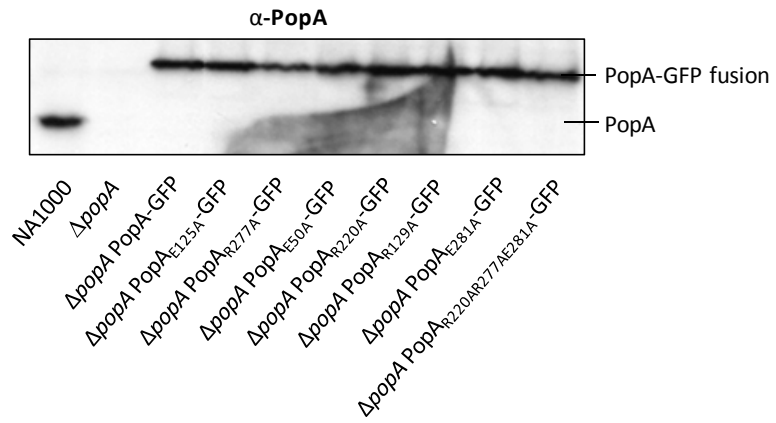
Figure 3

A



B

C



D

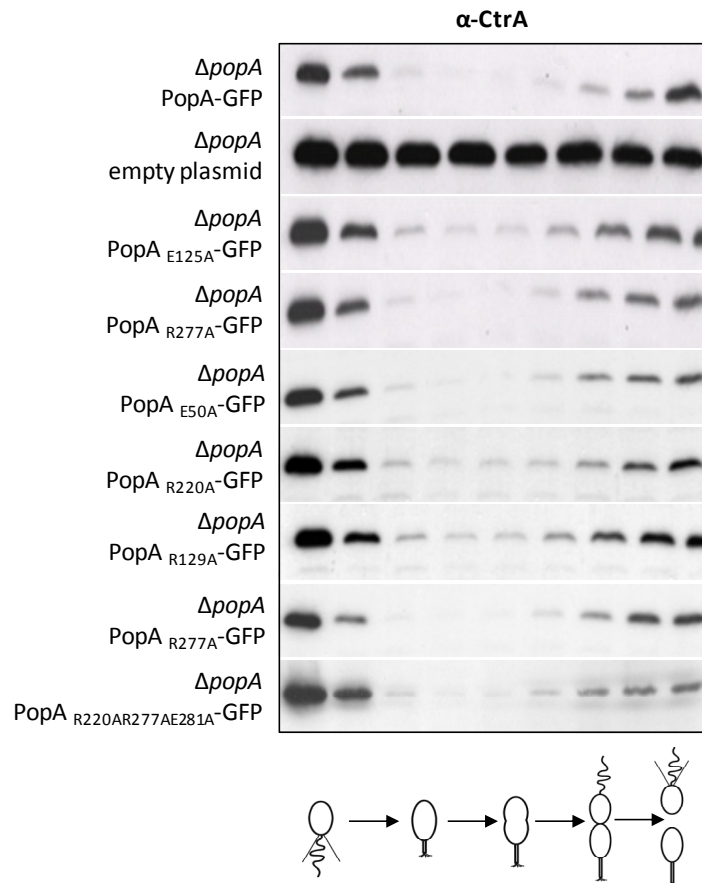
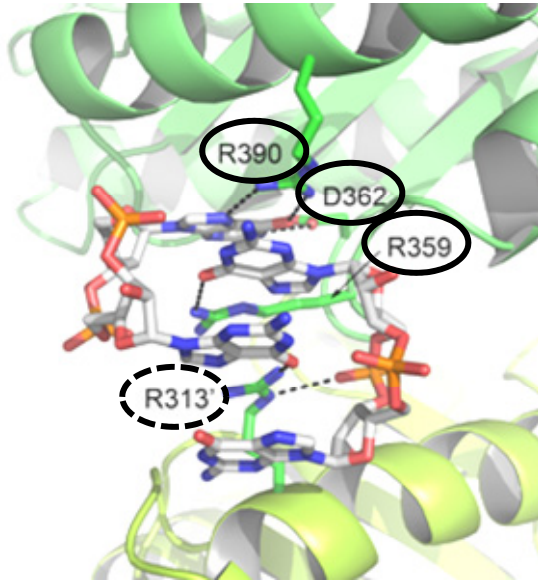


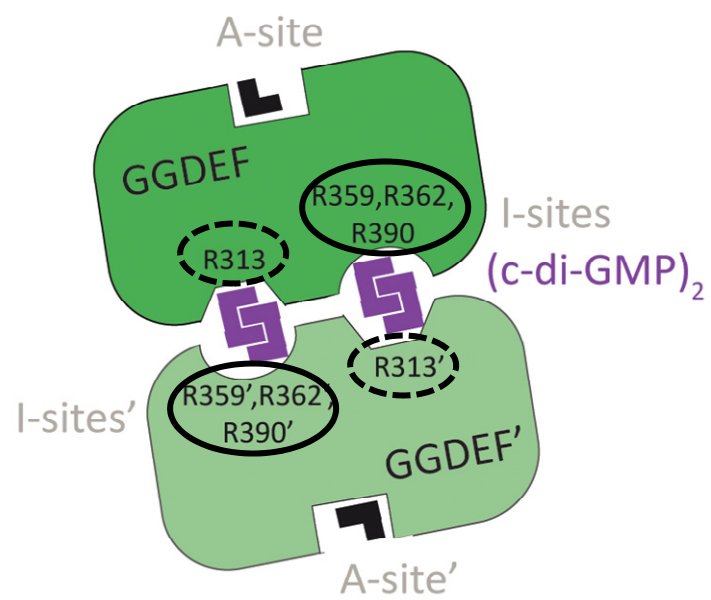
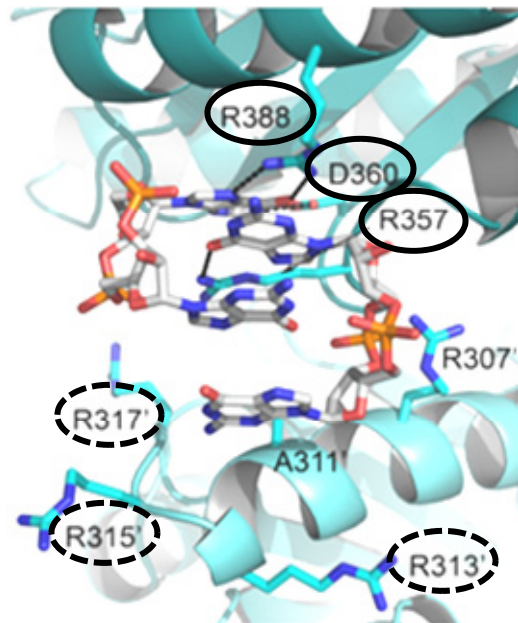
Figure 4

A

PleD I-site

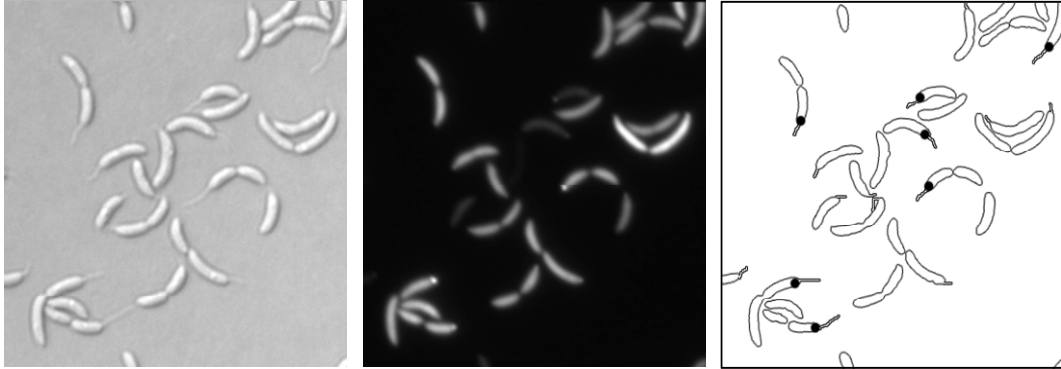


modelled PopA I-site

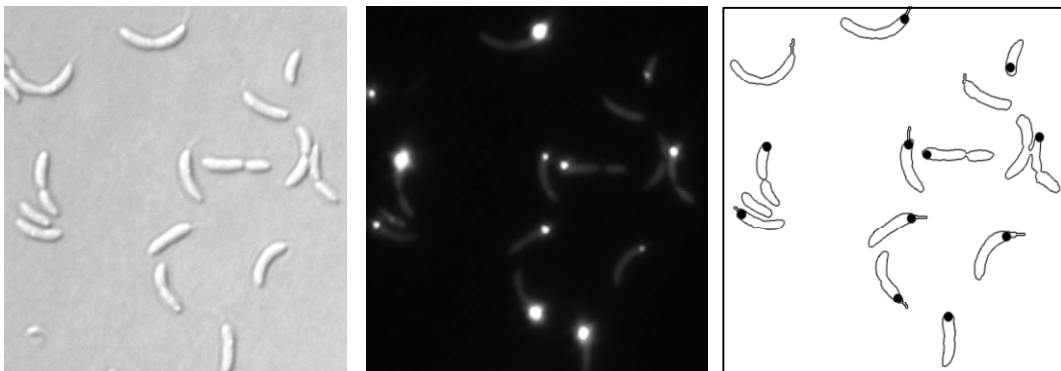


B

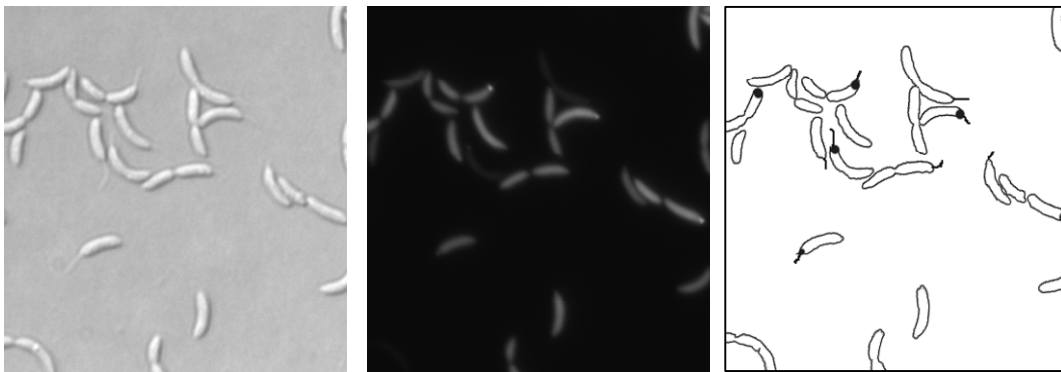
ΔpleD PleD-GFP



ΔpleD PleD*-GFP



ΔpleD PleD_{R359A}-GFP

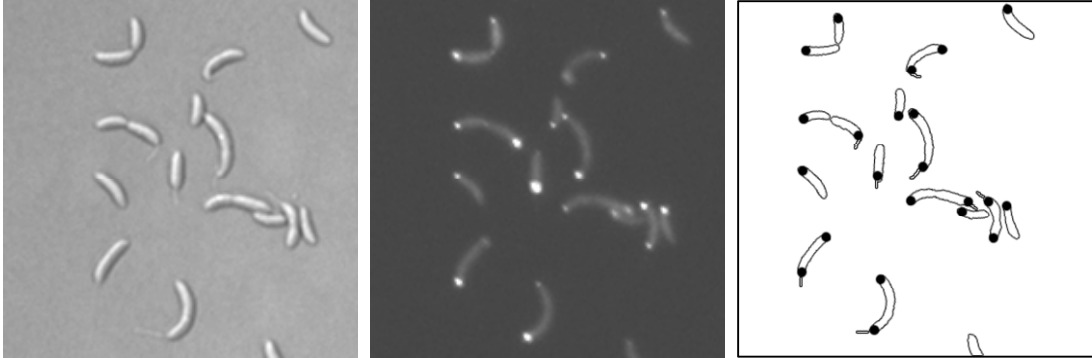
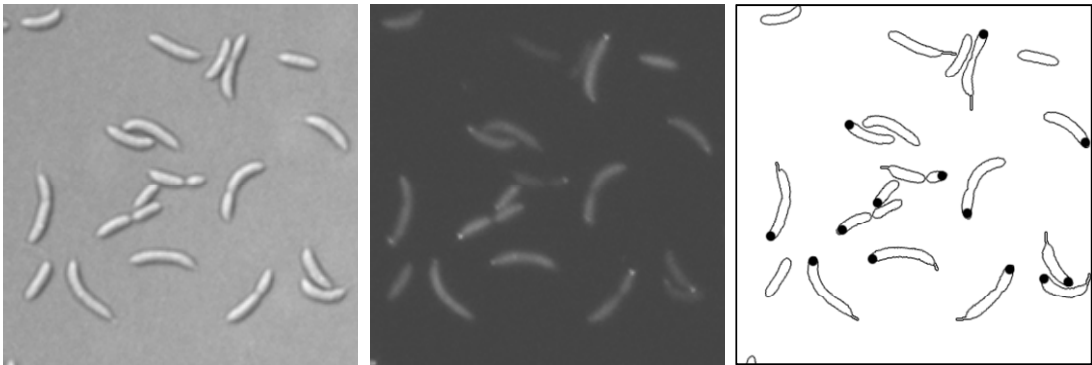
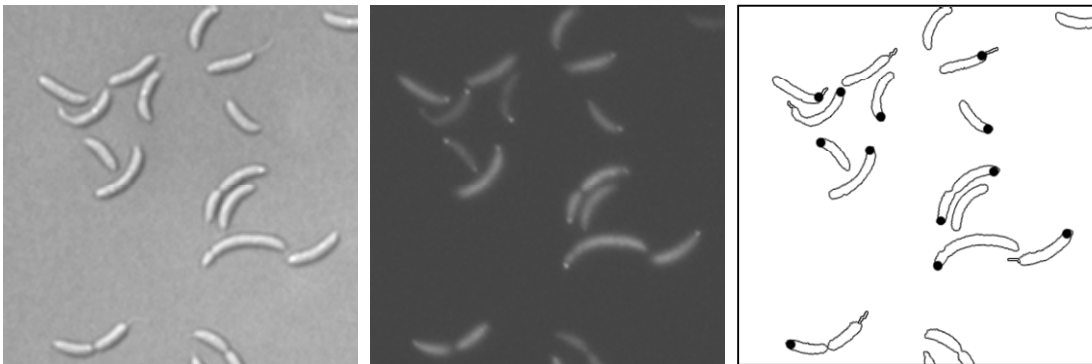


DIC

GFP

schematic

C

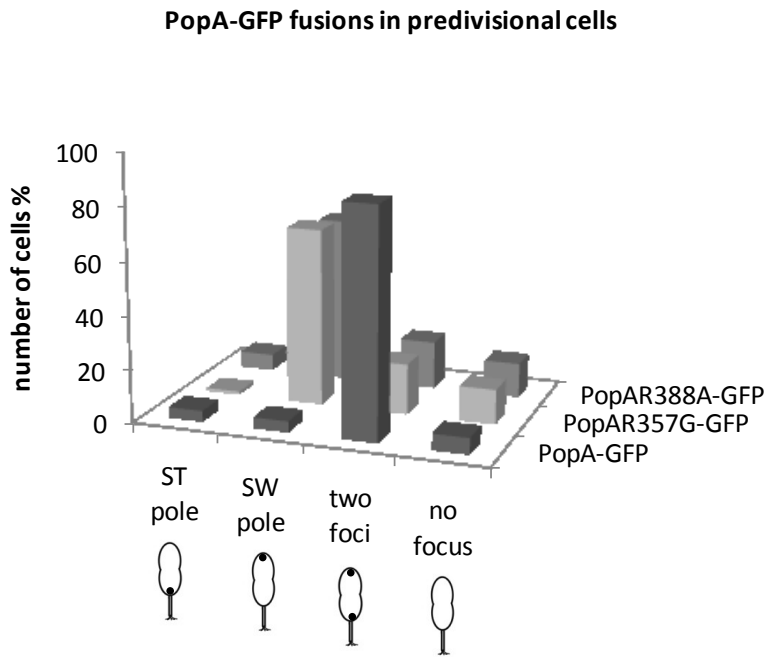
 $\Delta popA$ PopA-GFP $\Delta popA$ PopA_{R357G}-GFP $\Delta popA$ PopA_{R388A}-GFP

DIC

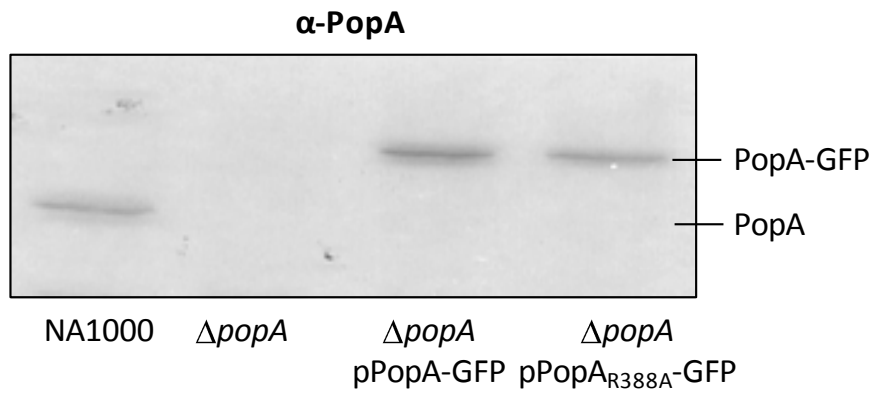
GFP

schematic

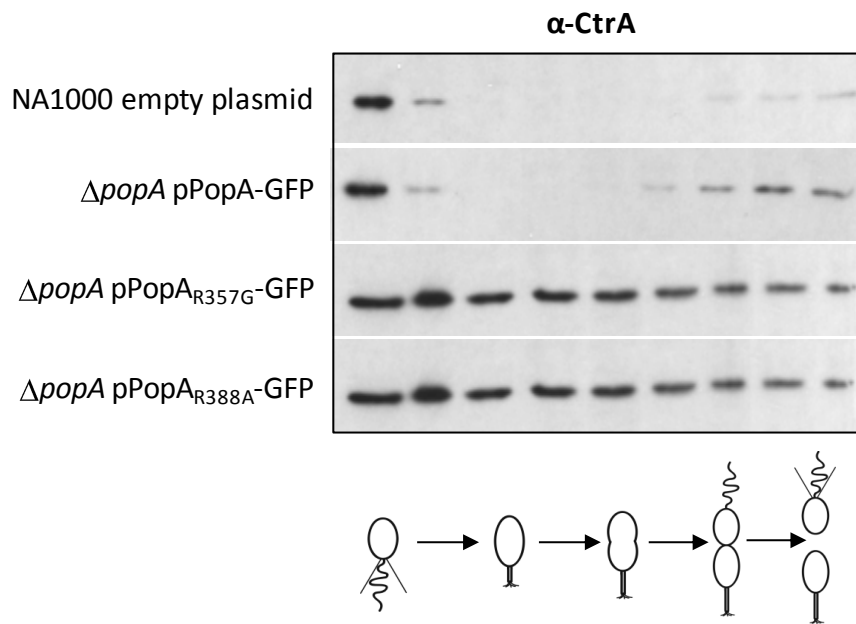
D



E



F



G

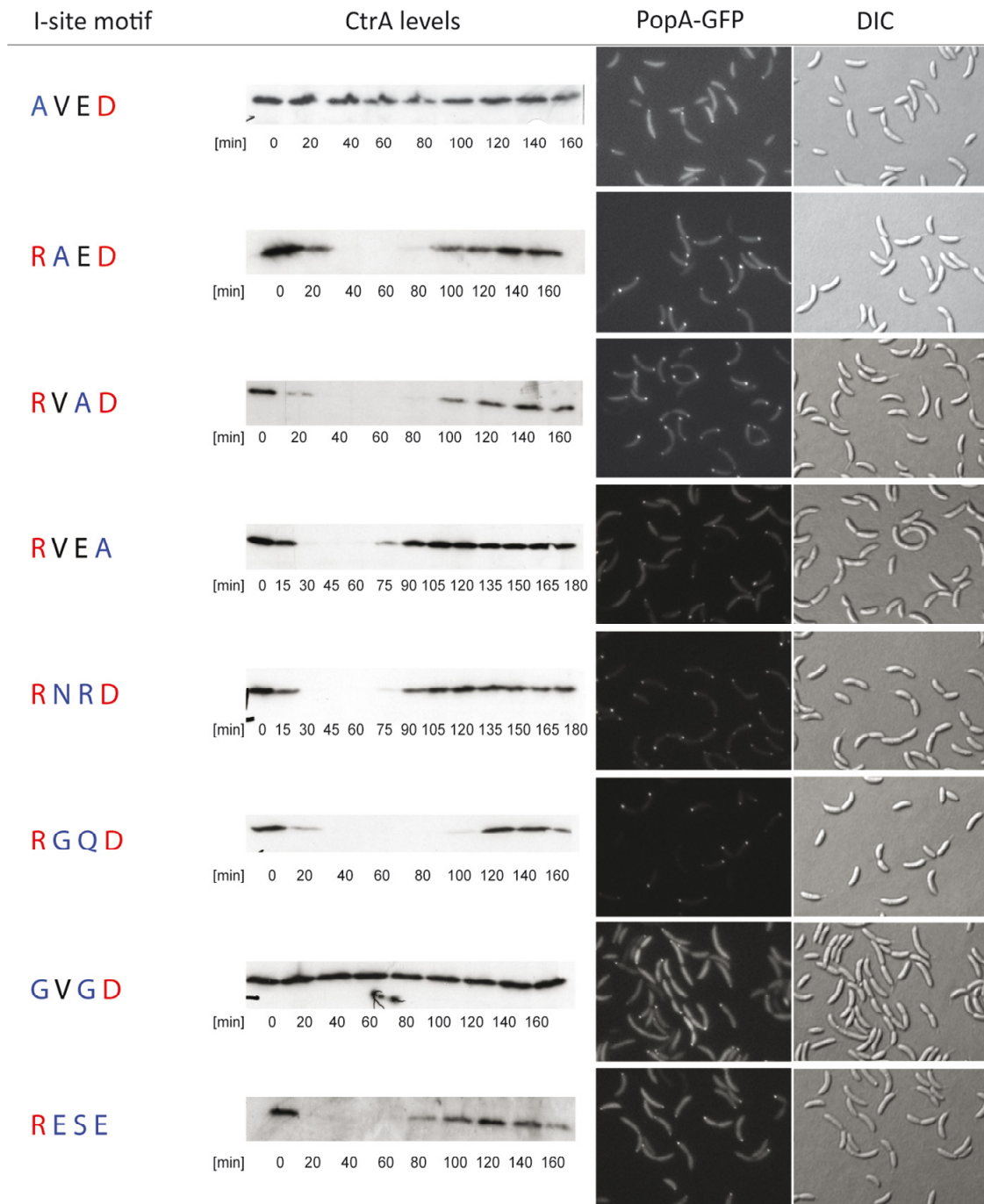
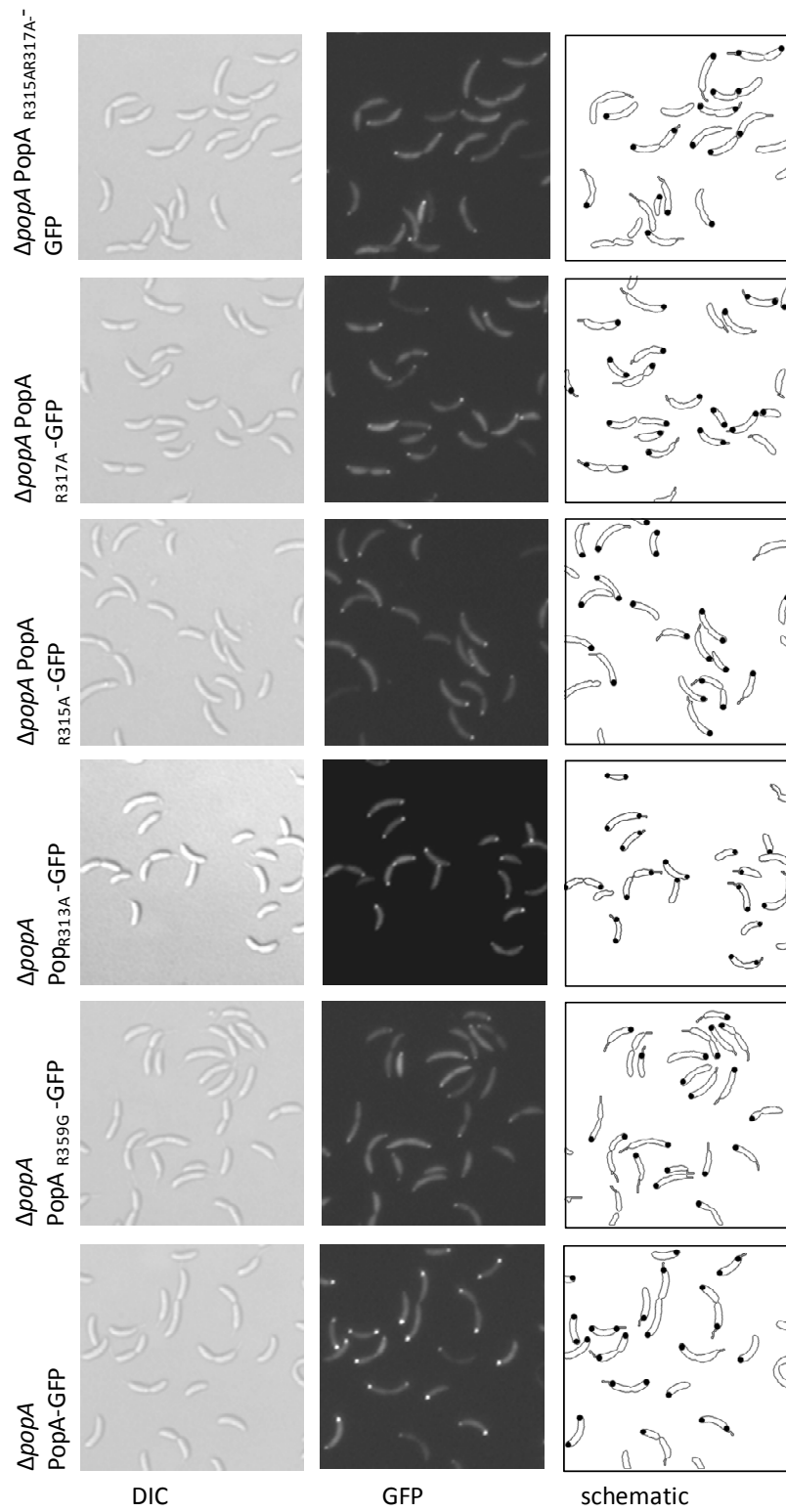
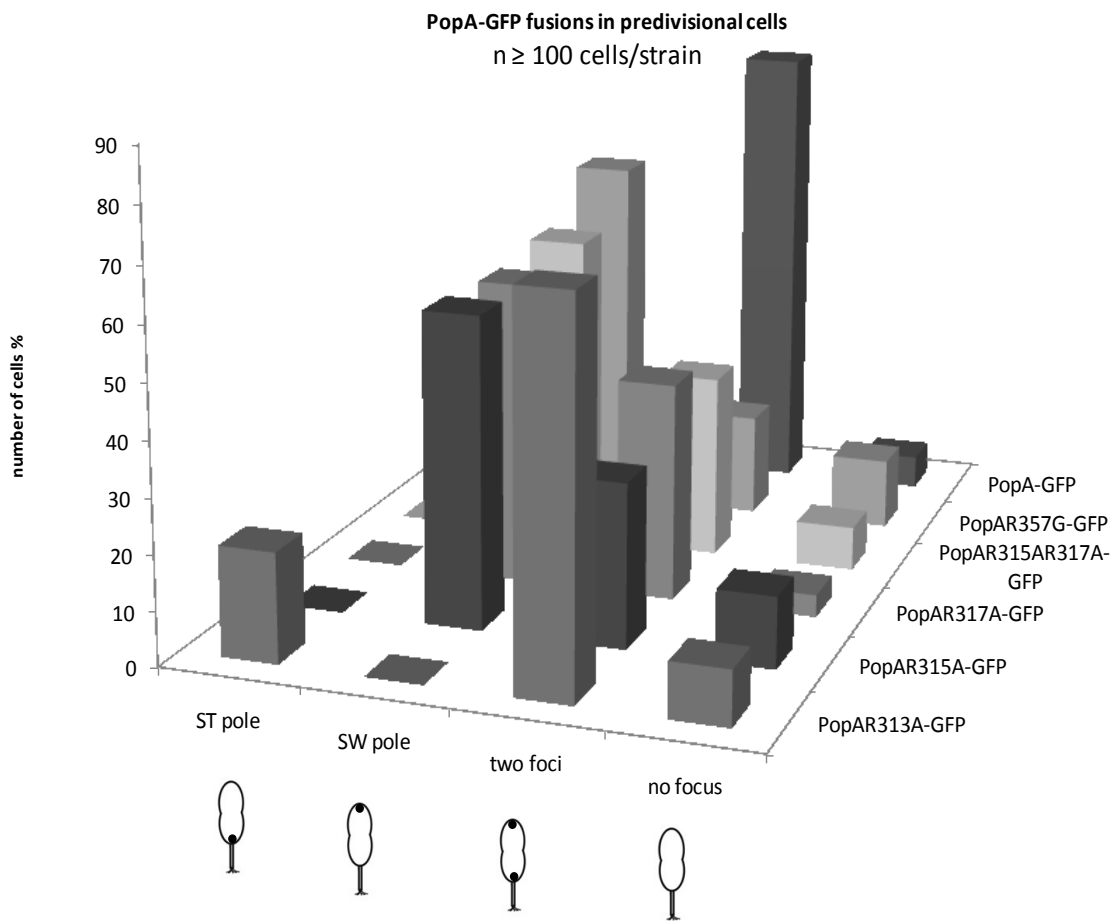


Figure 5

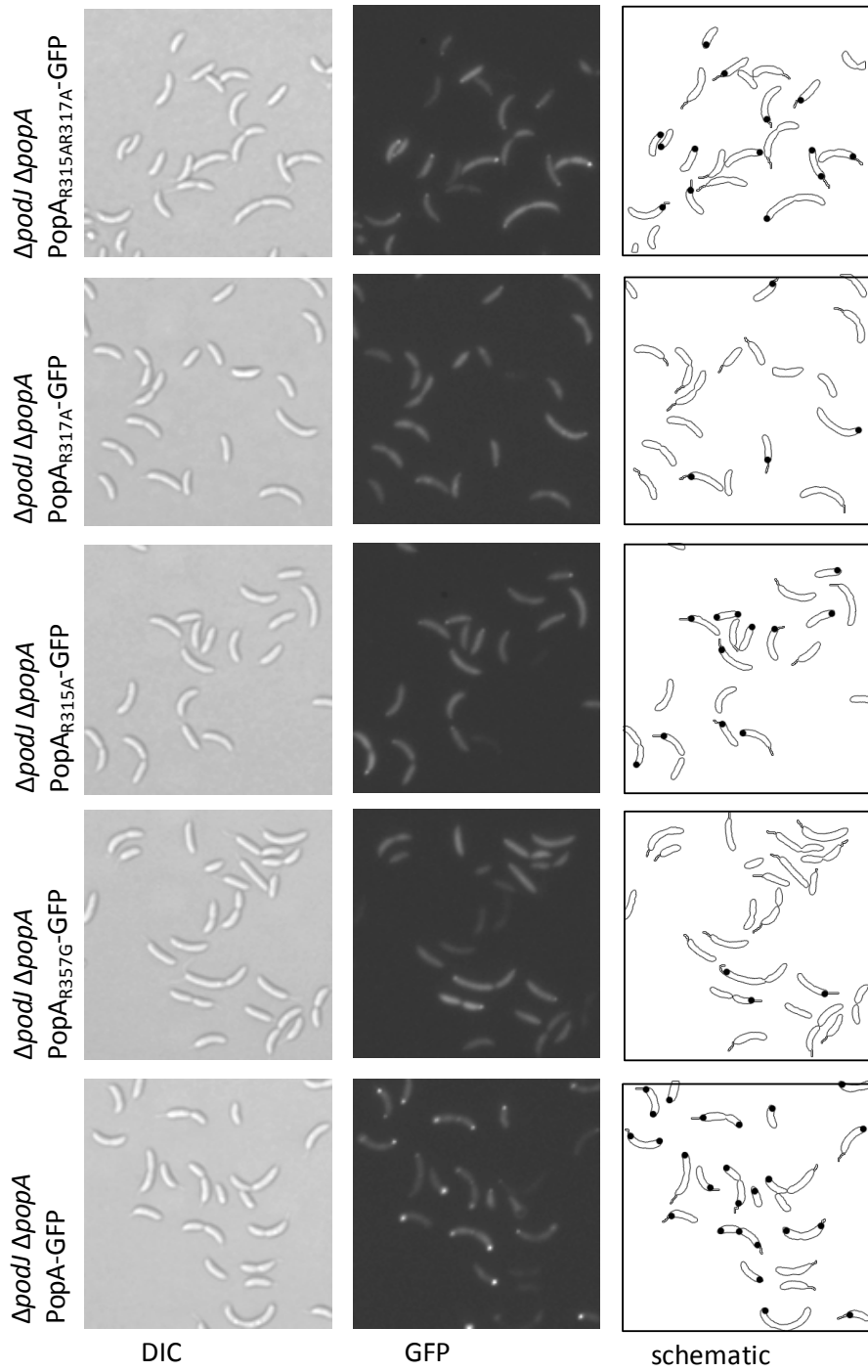
A



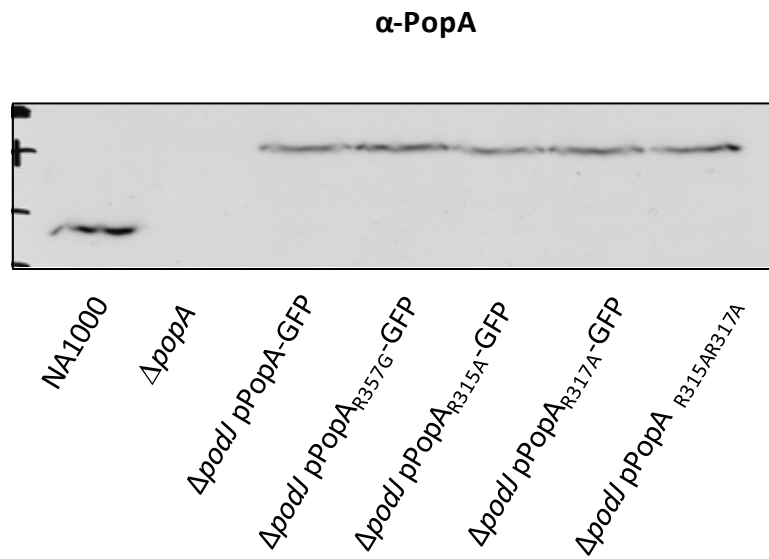
B



c



D



E

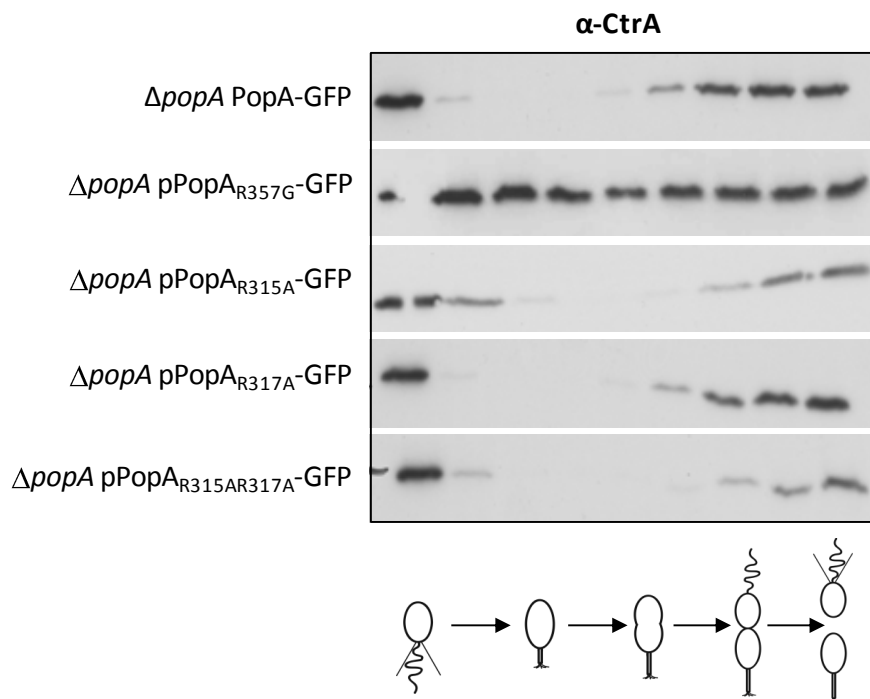
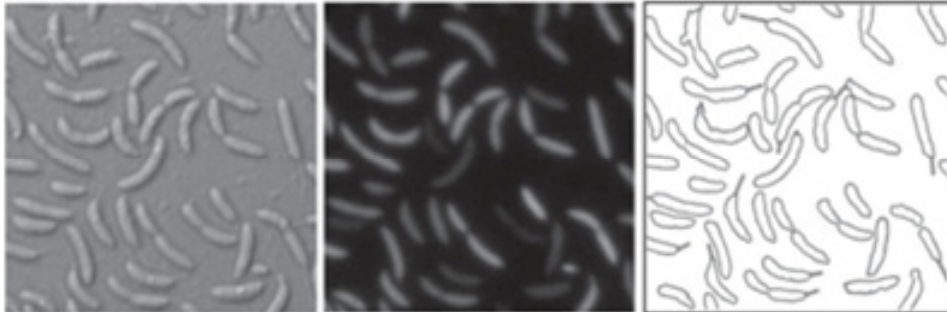
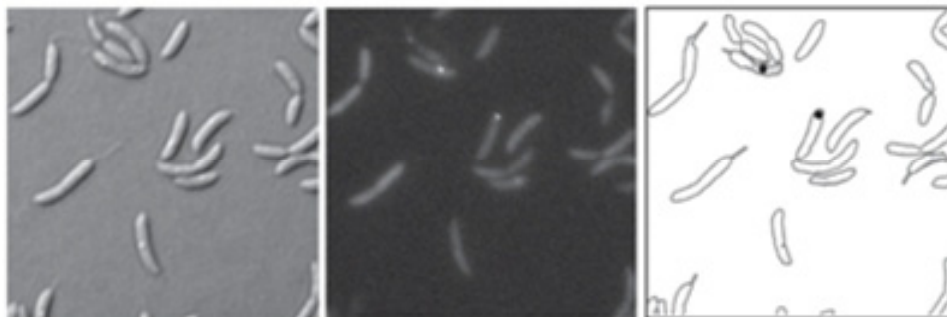
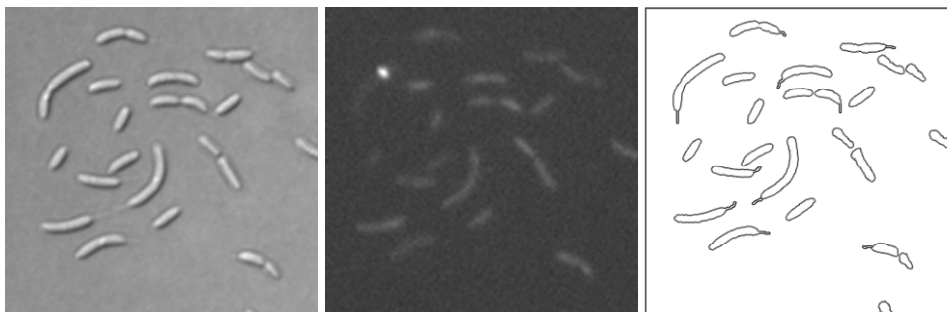
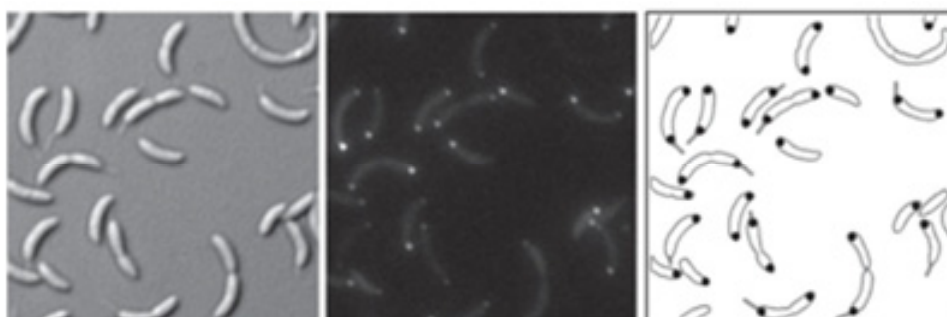


Figure 6

A

ΔpopA pRec1-GFP*ΔpopA* pRec1-Rec2-GFP*ΔpopA* pGGDEF-GFP*ΔpopA* pRec1-Rec2-GGDEF-GFP

DIC

GFP

schematic

B

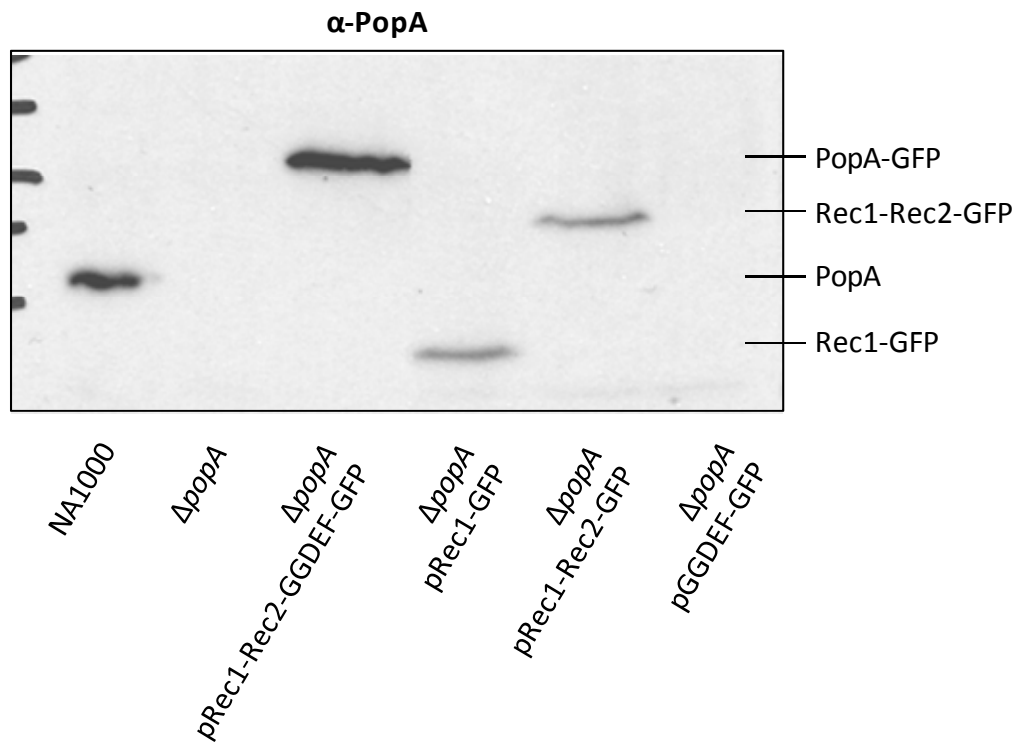
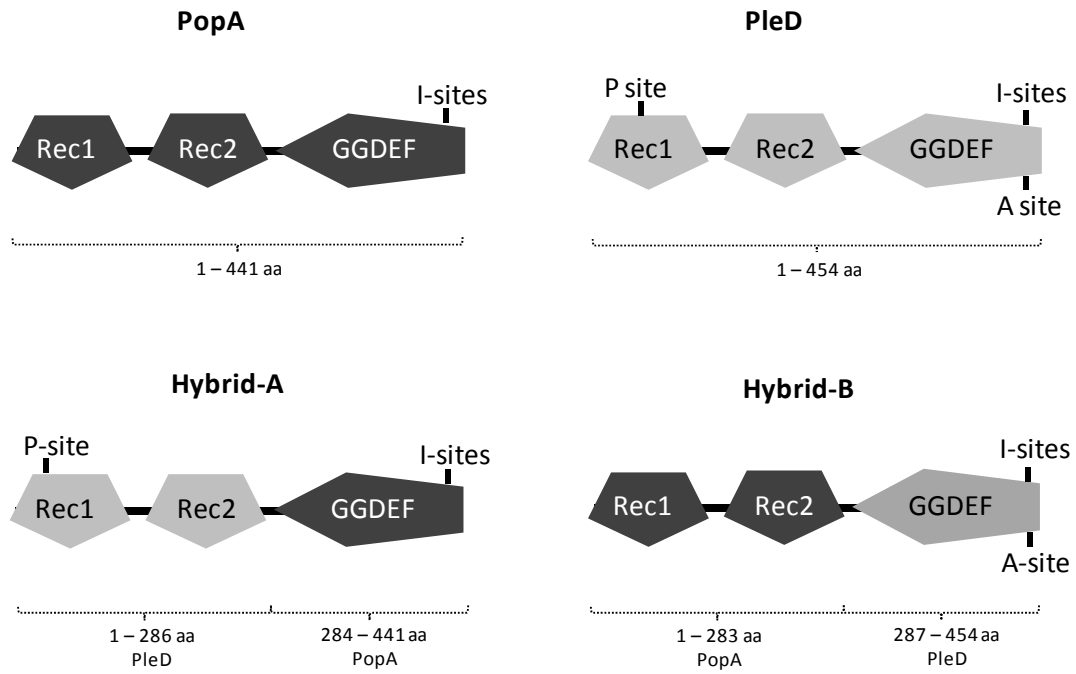
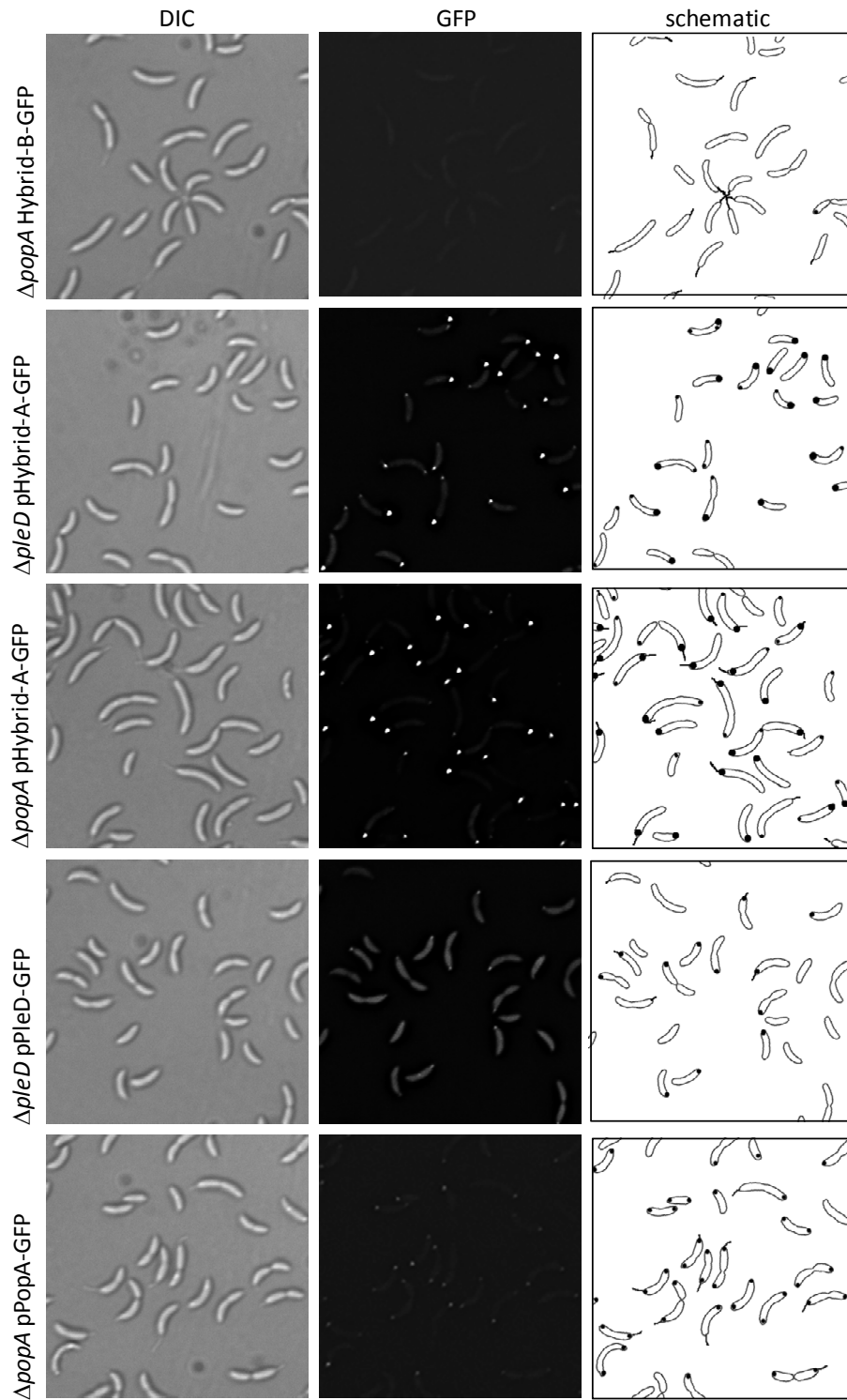


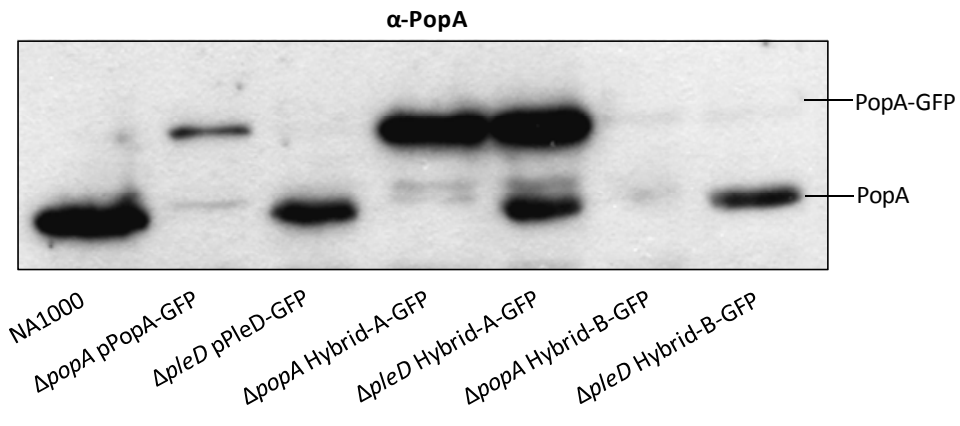
Figure 7

A

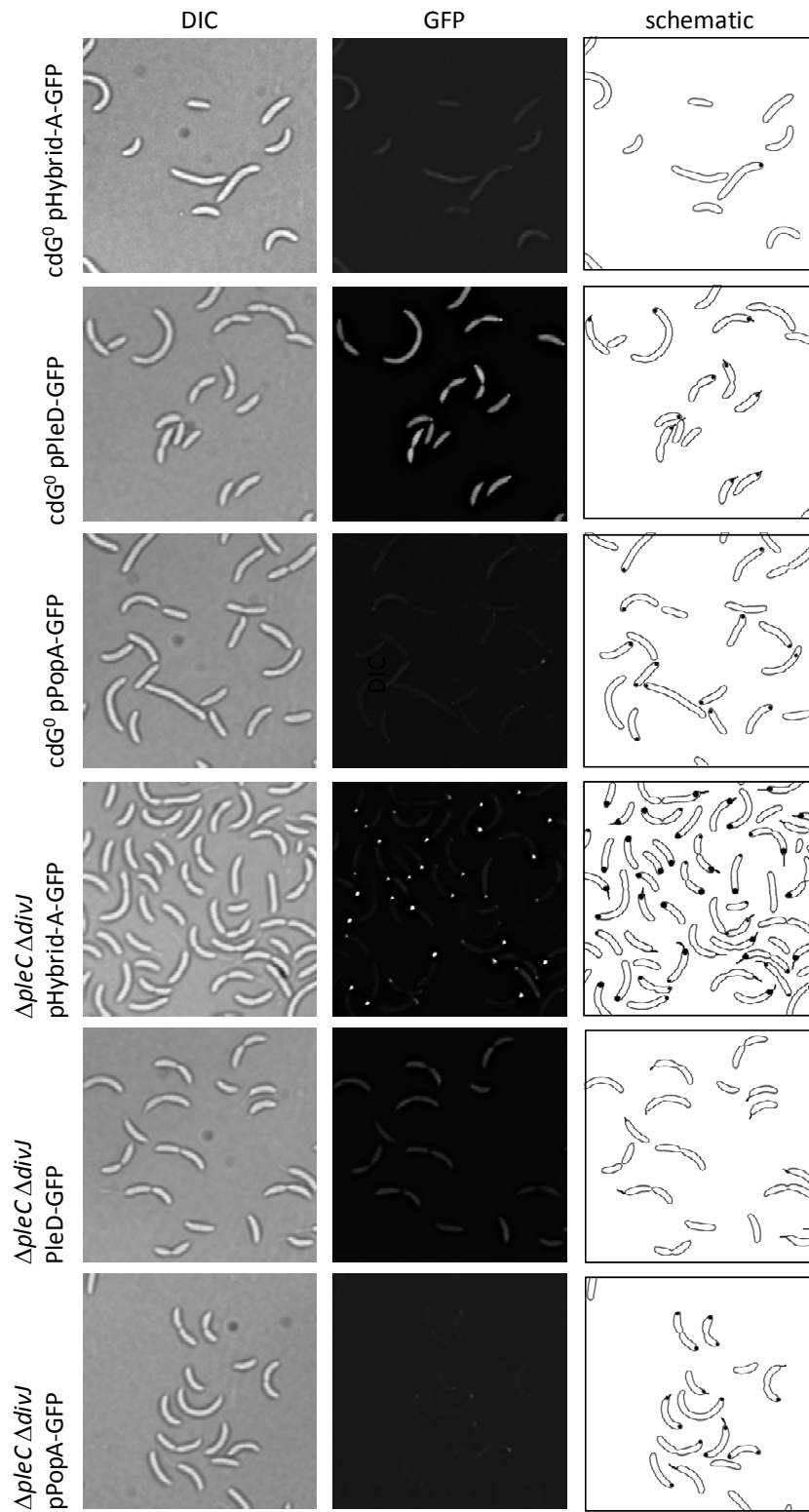


B

C

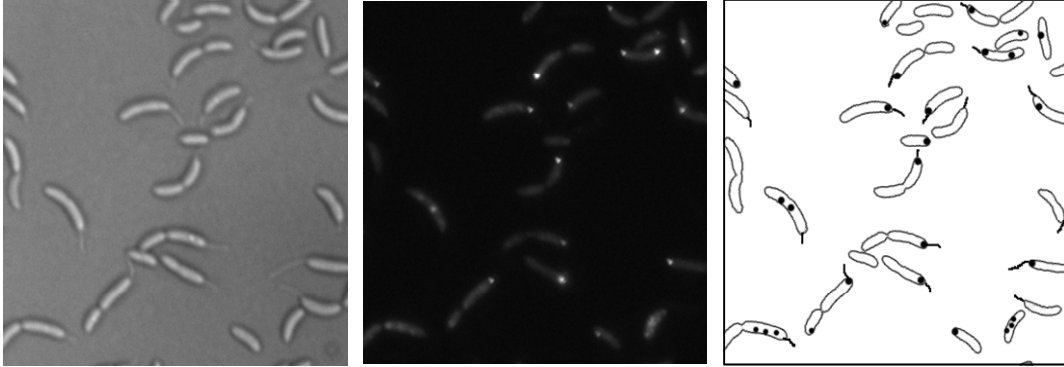


D

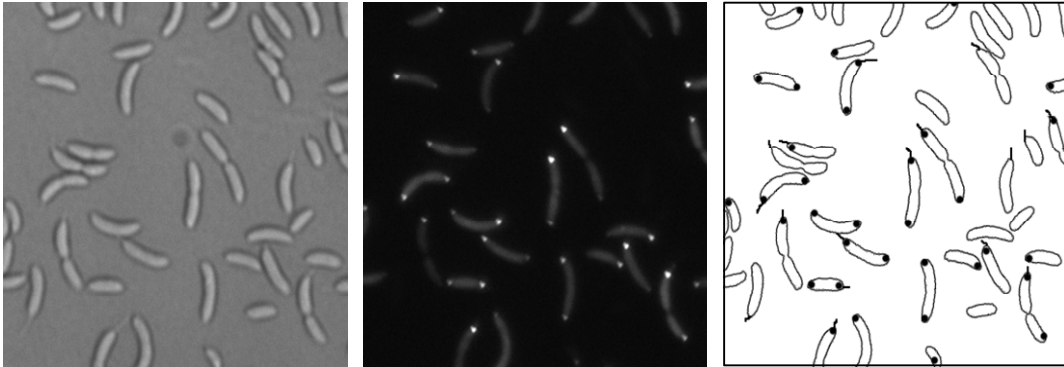


E

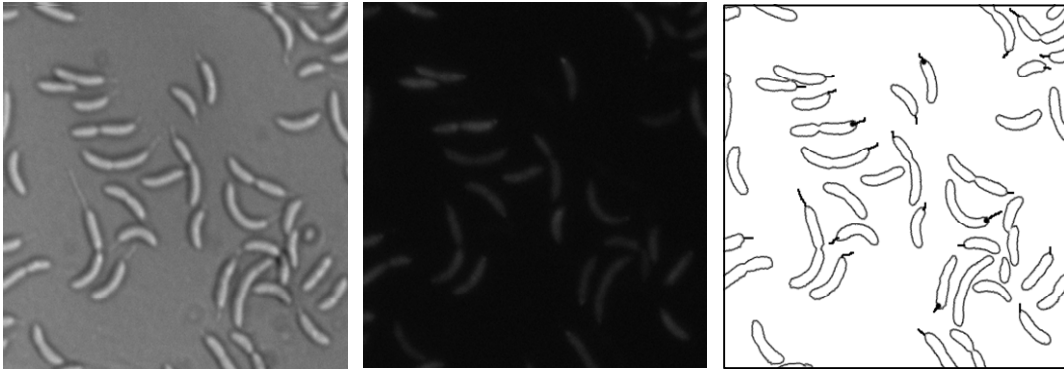
$\Delta popA$ pHybrid- A_{R357G} -GFP



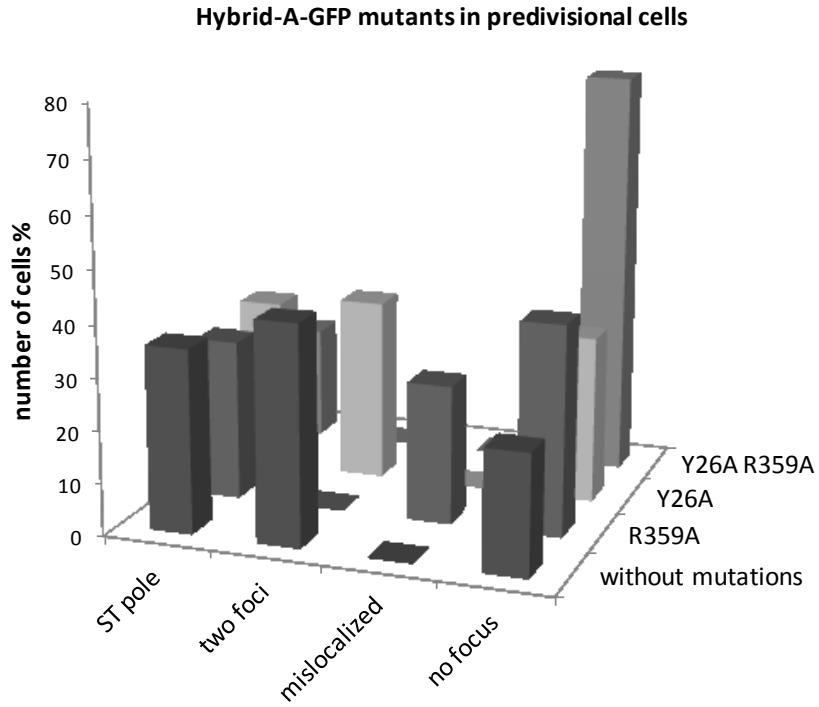
$\Delta popA$ pHybrid- A_{Y26A} -GFP



$\Delta popA$ pHybrid- $A_{R357G,Y26A}$ -GFP



E cont.



F

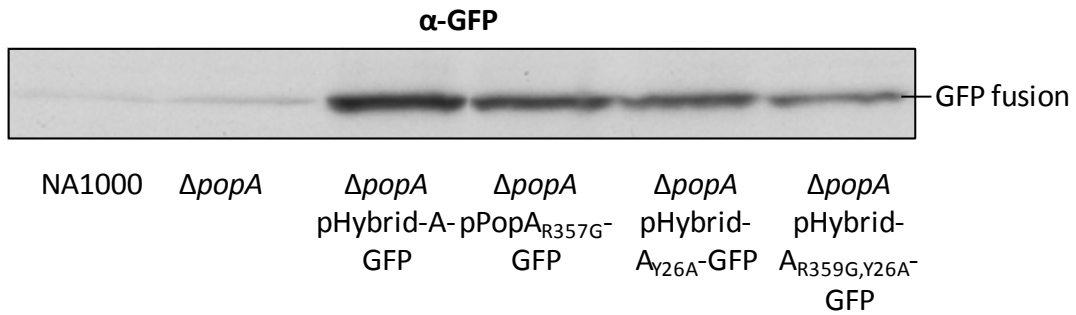
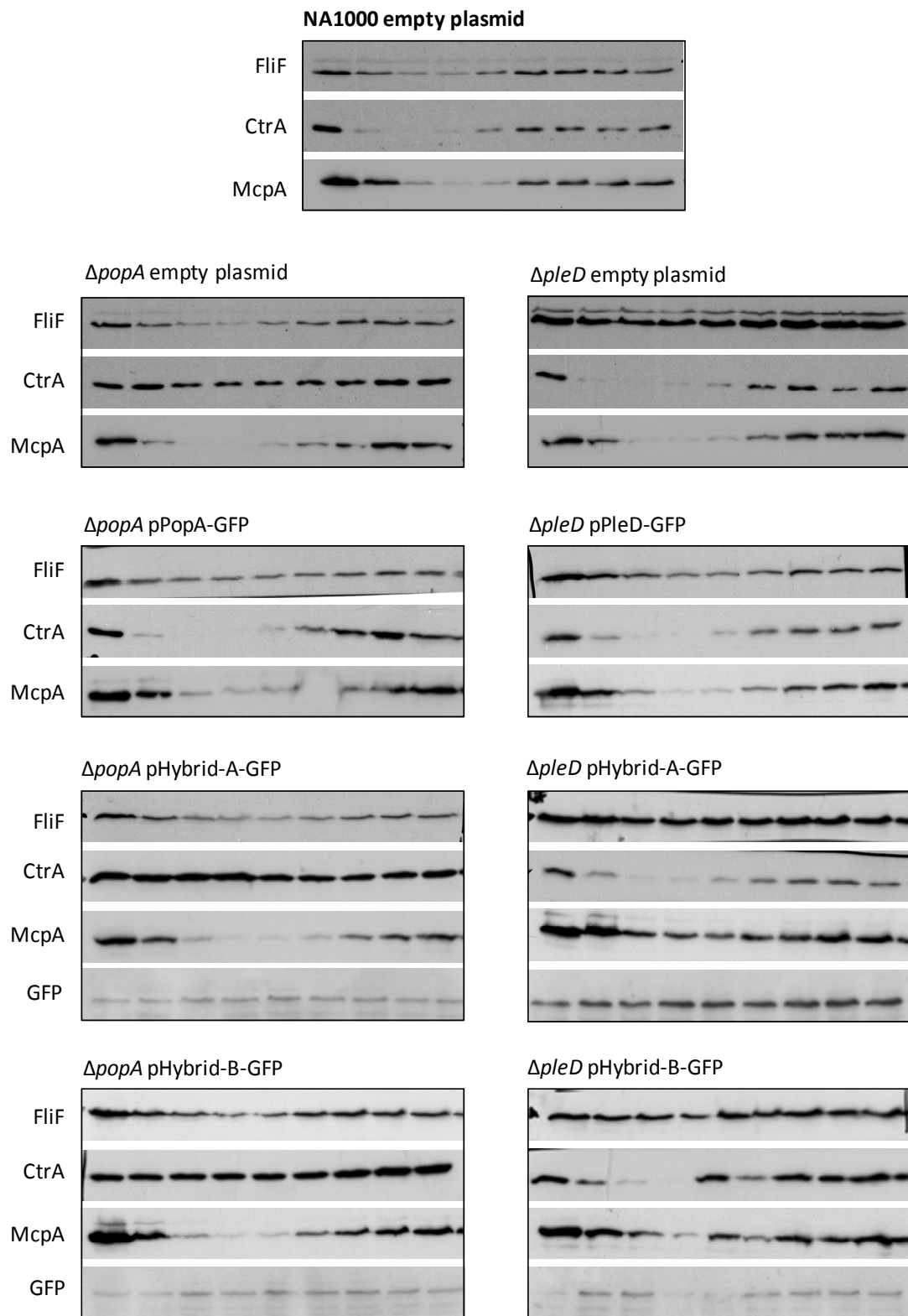
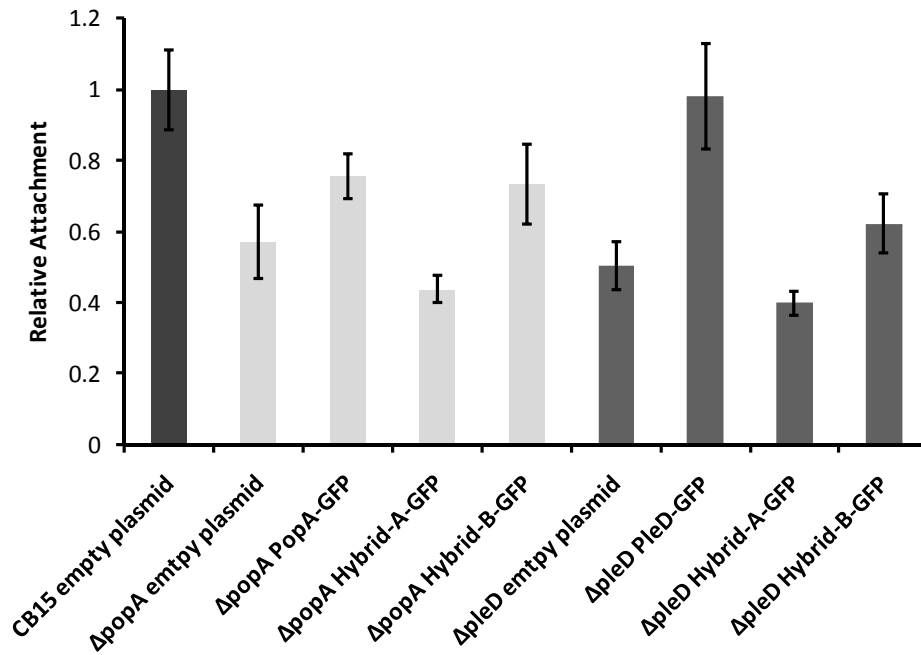


Figure 8

A



B



C

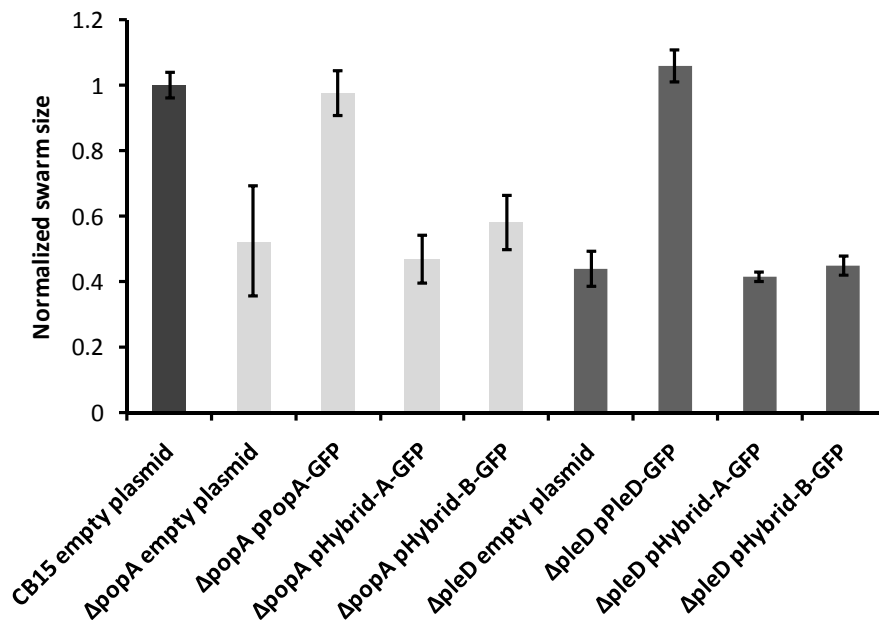


Figure 9

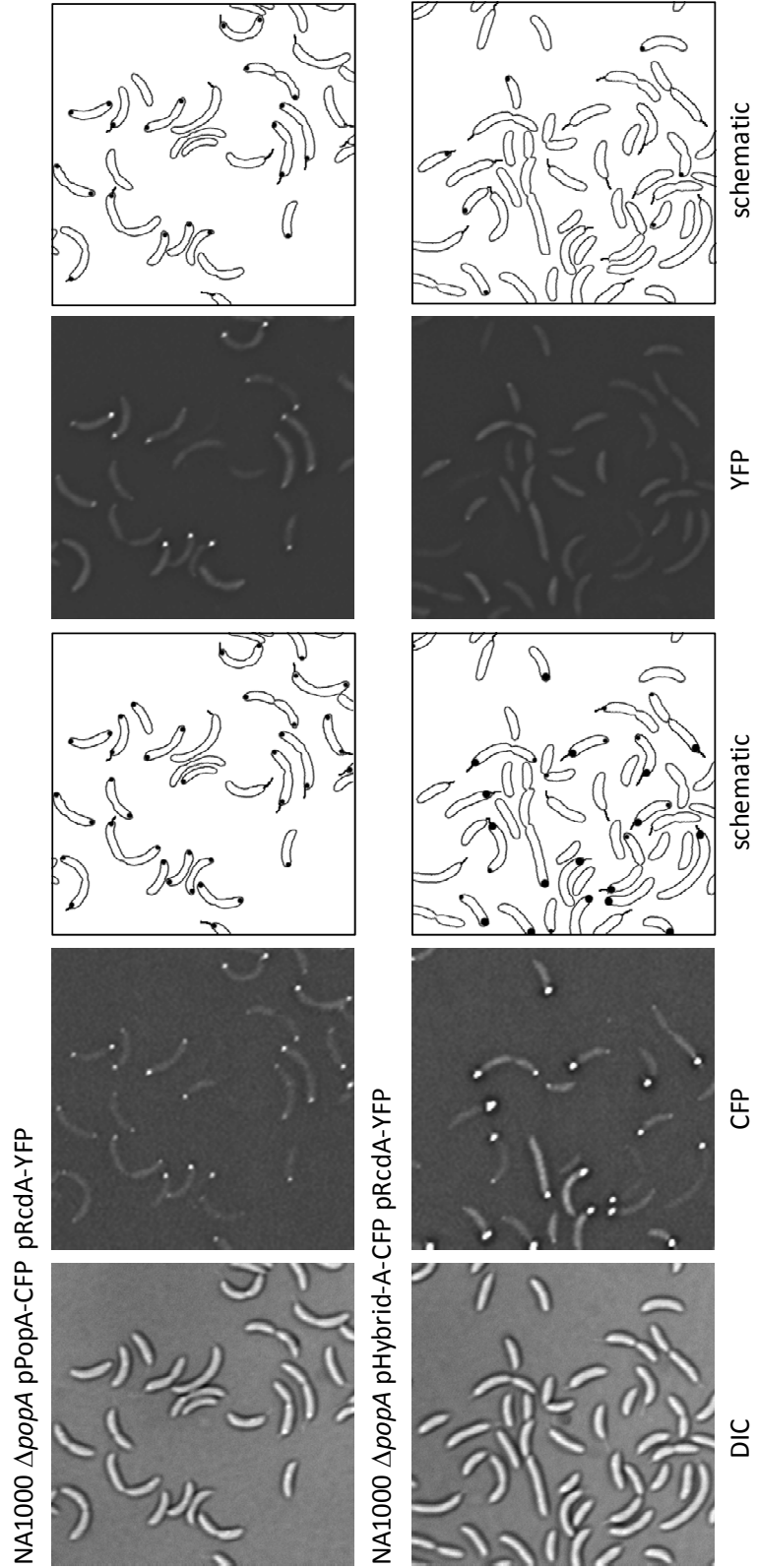
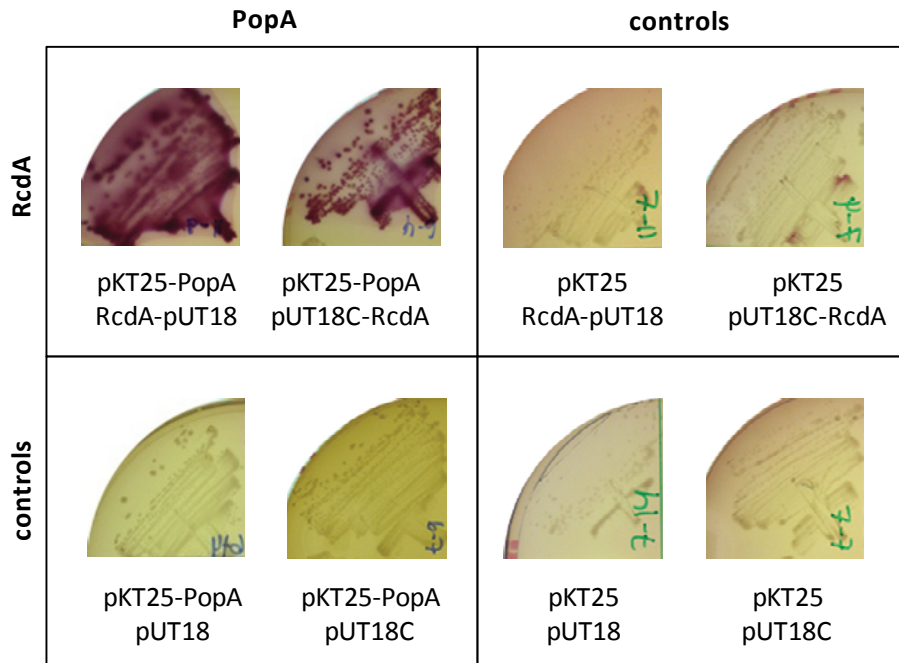
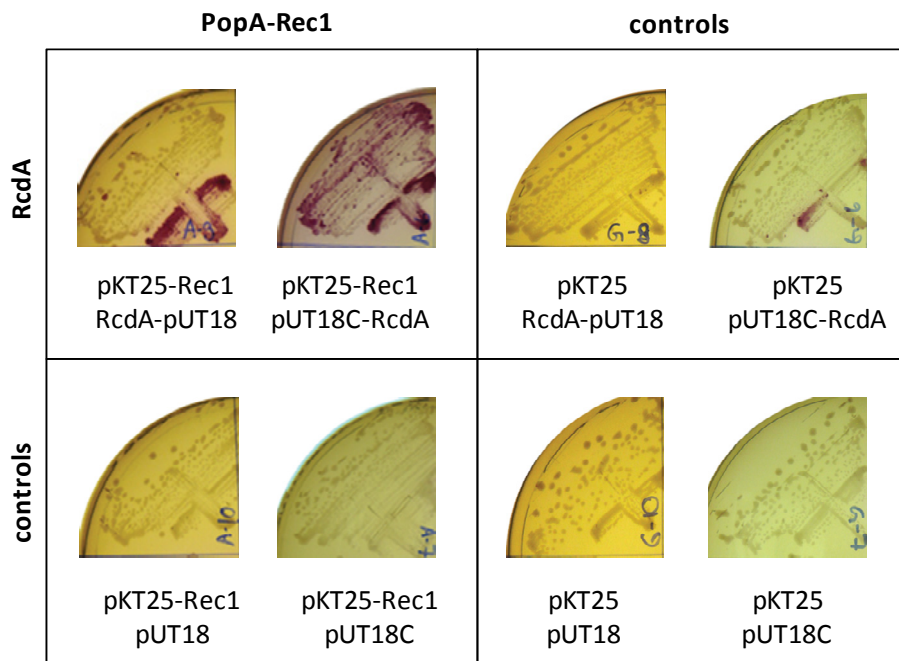


Figure 10

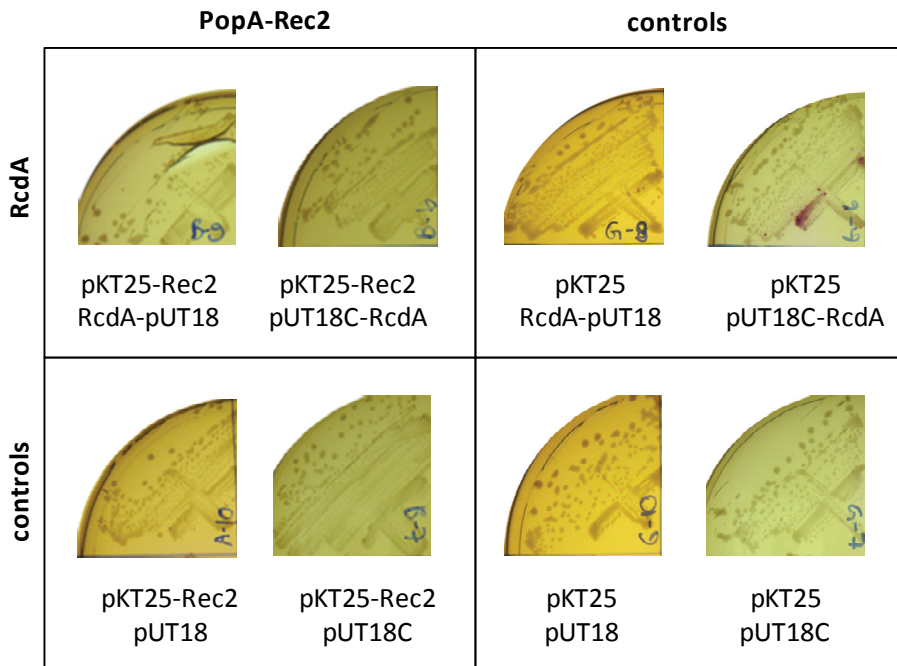
A



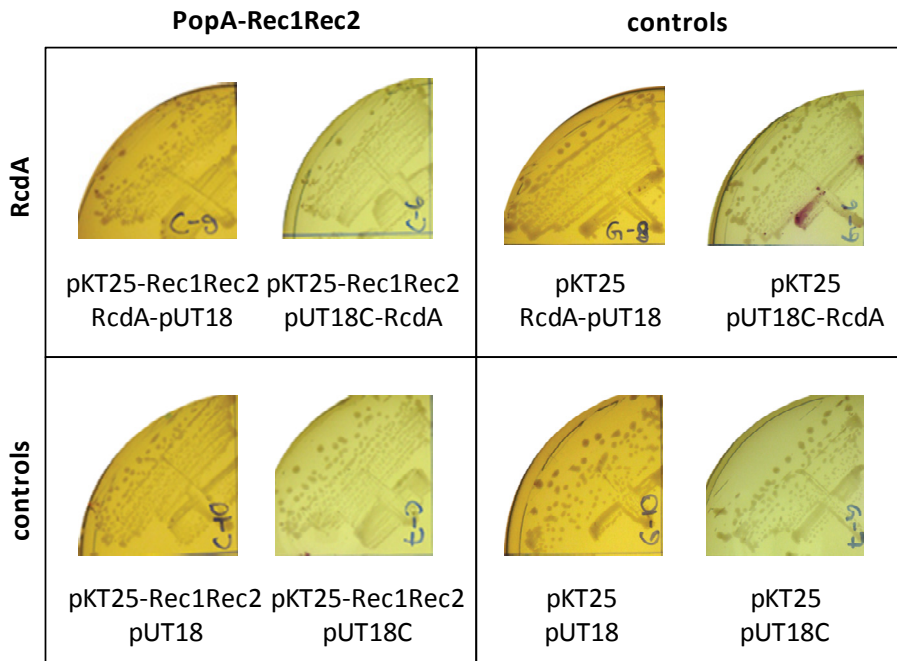
B



C



D



E

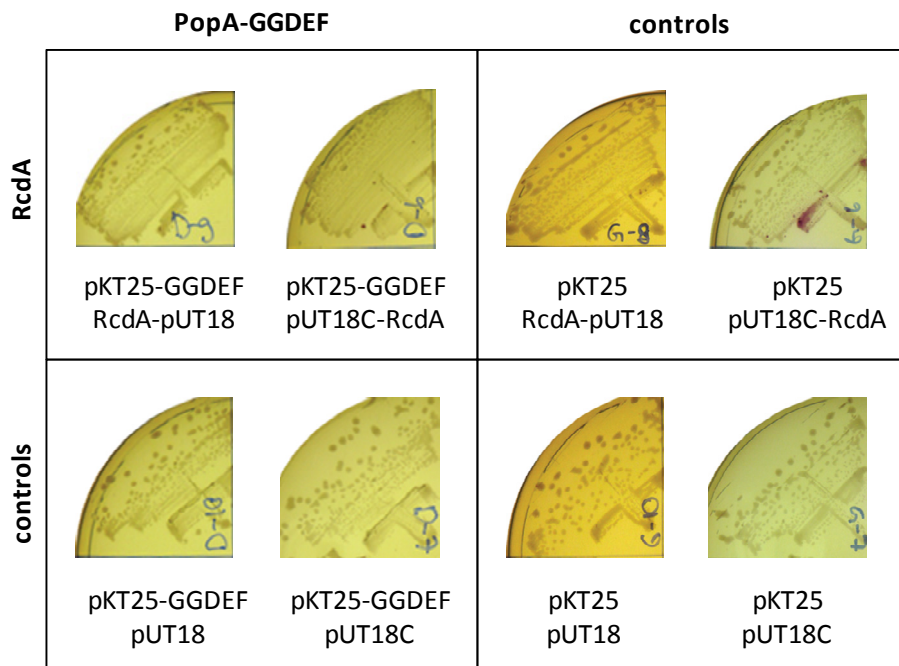
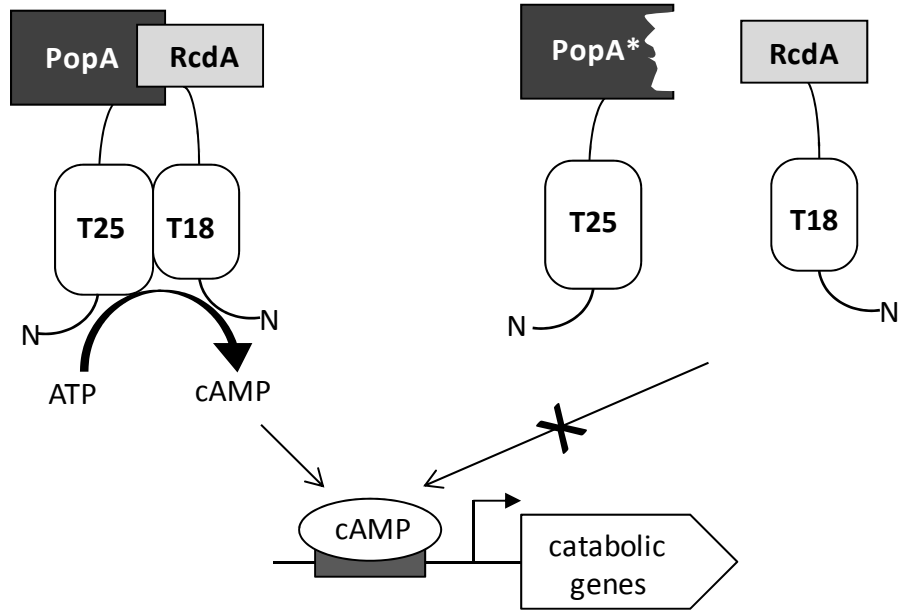
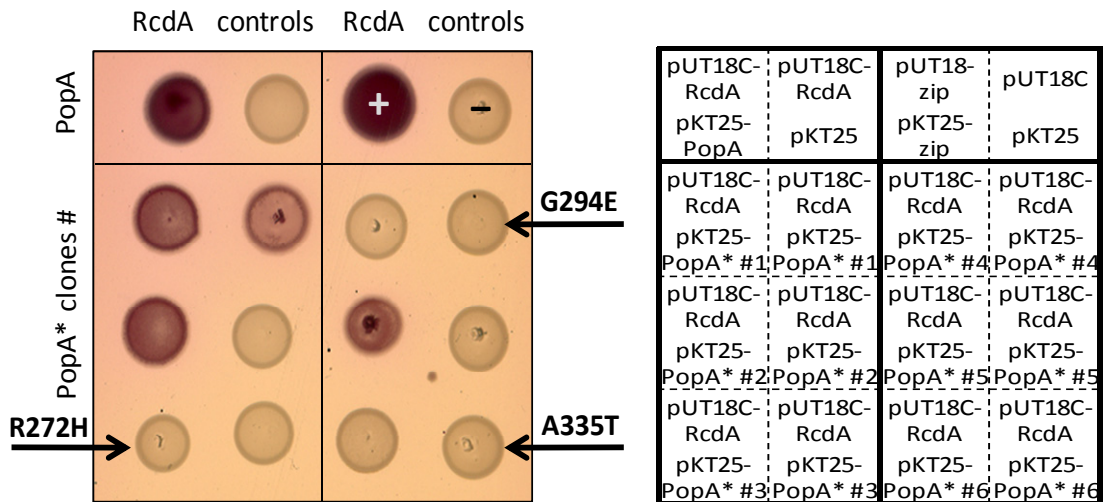


Figure 11

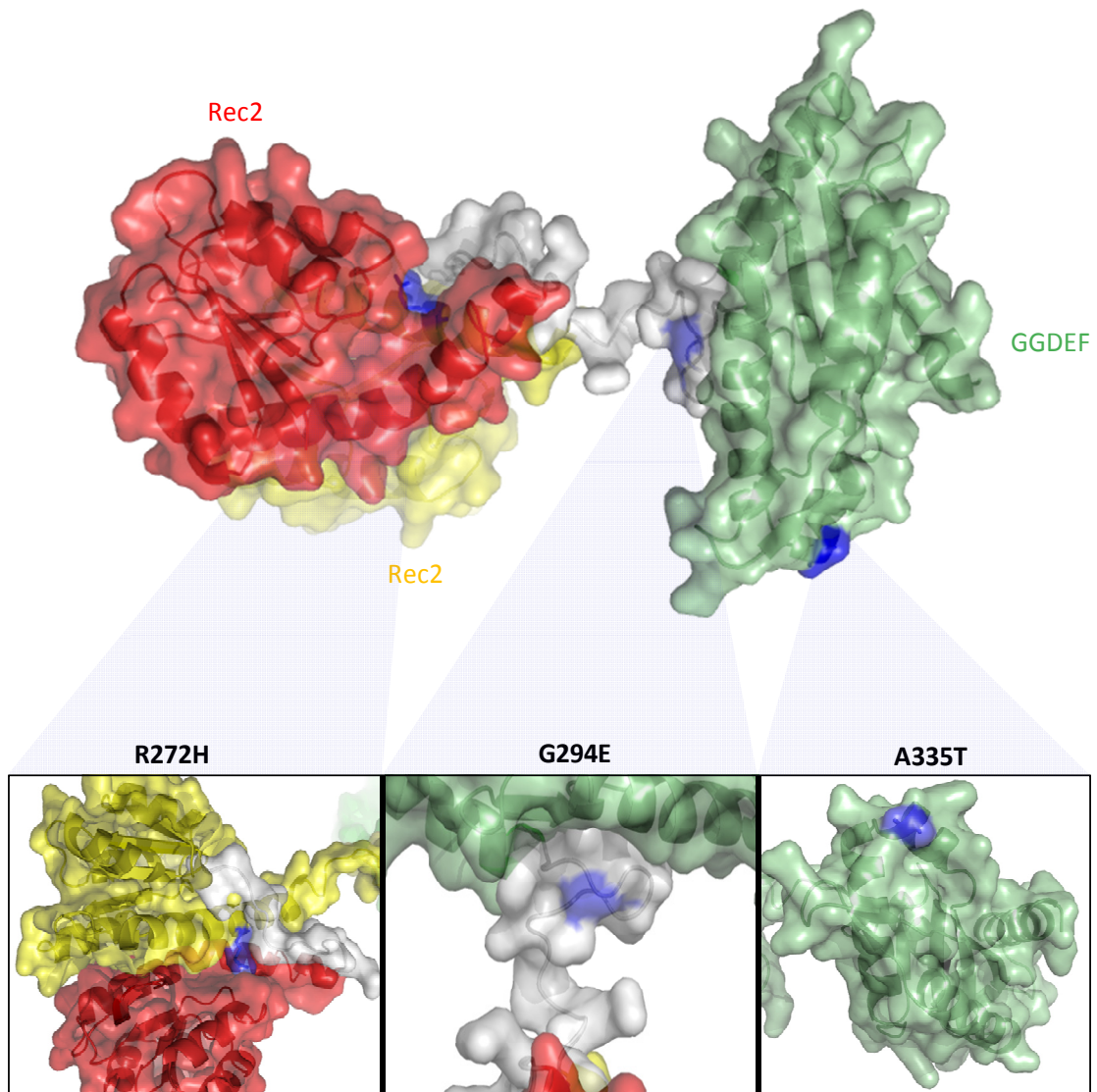
A



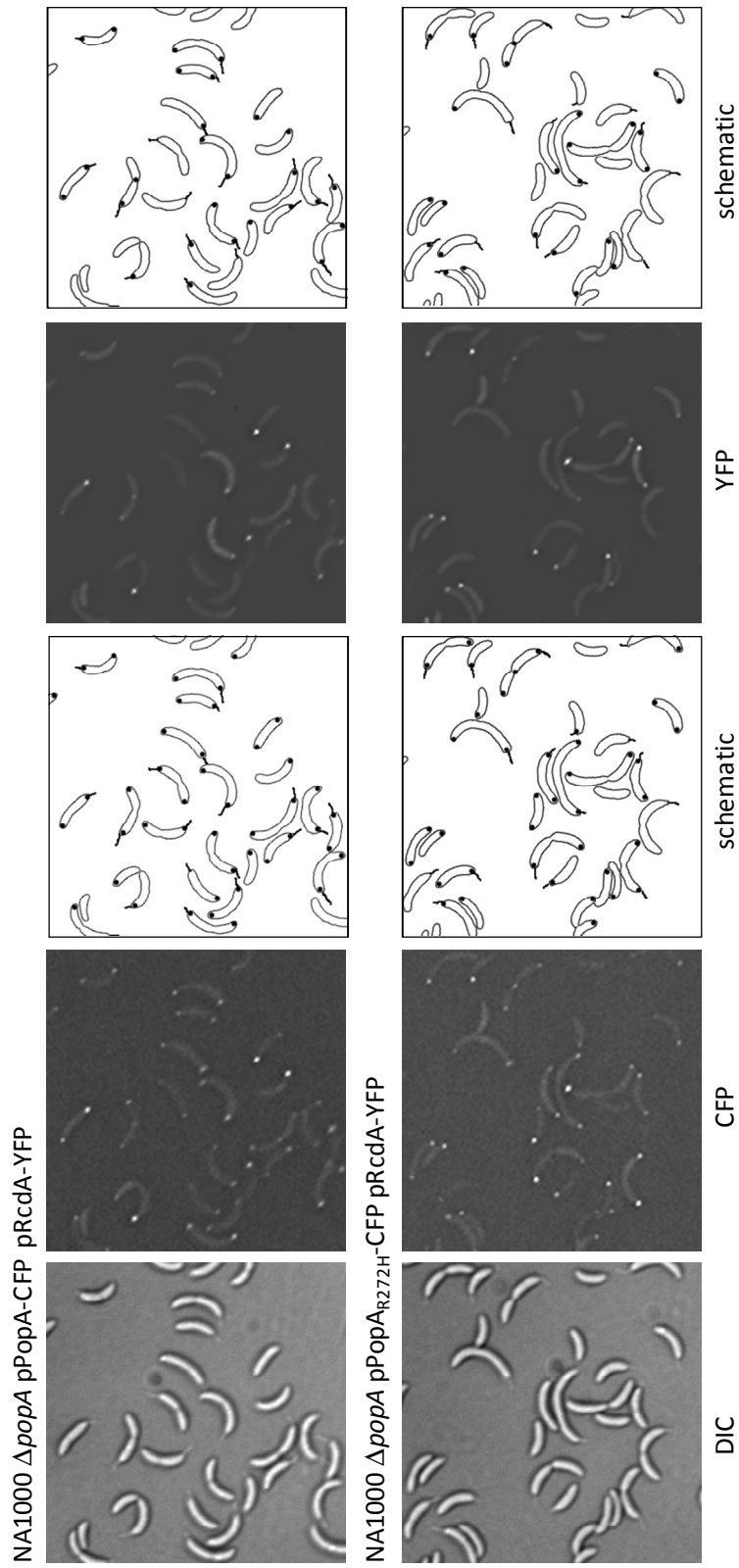
B



C



D



E

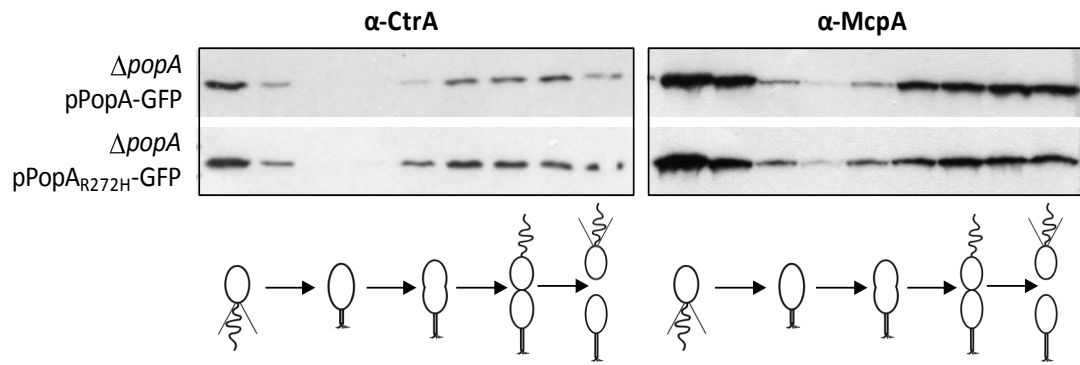
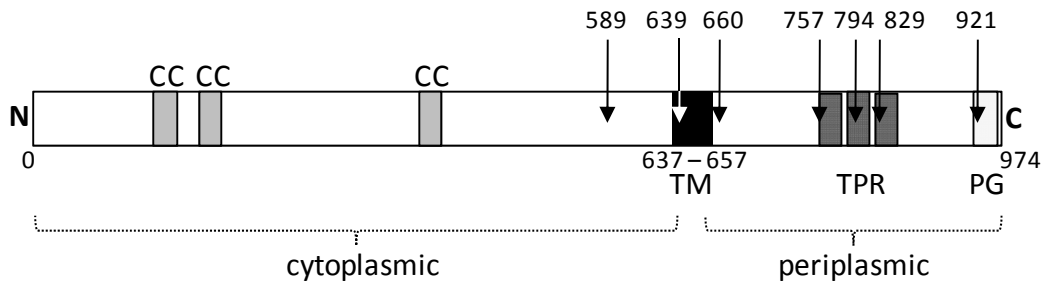
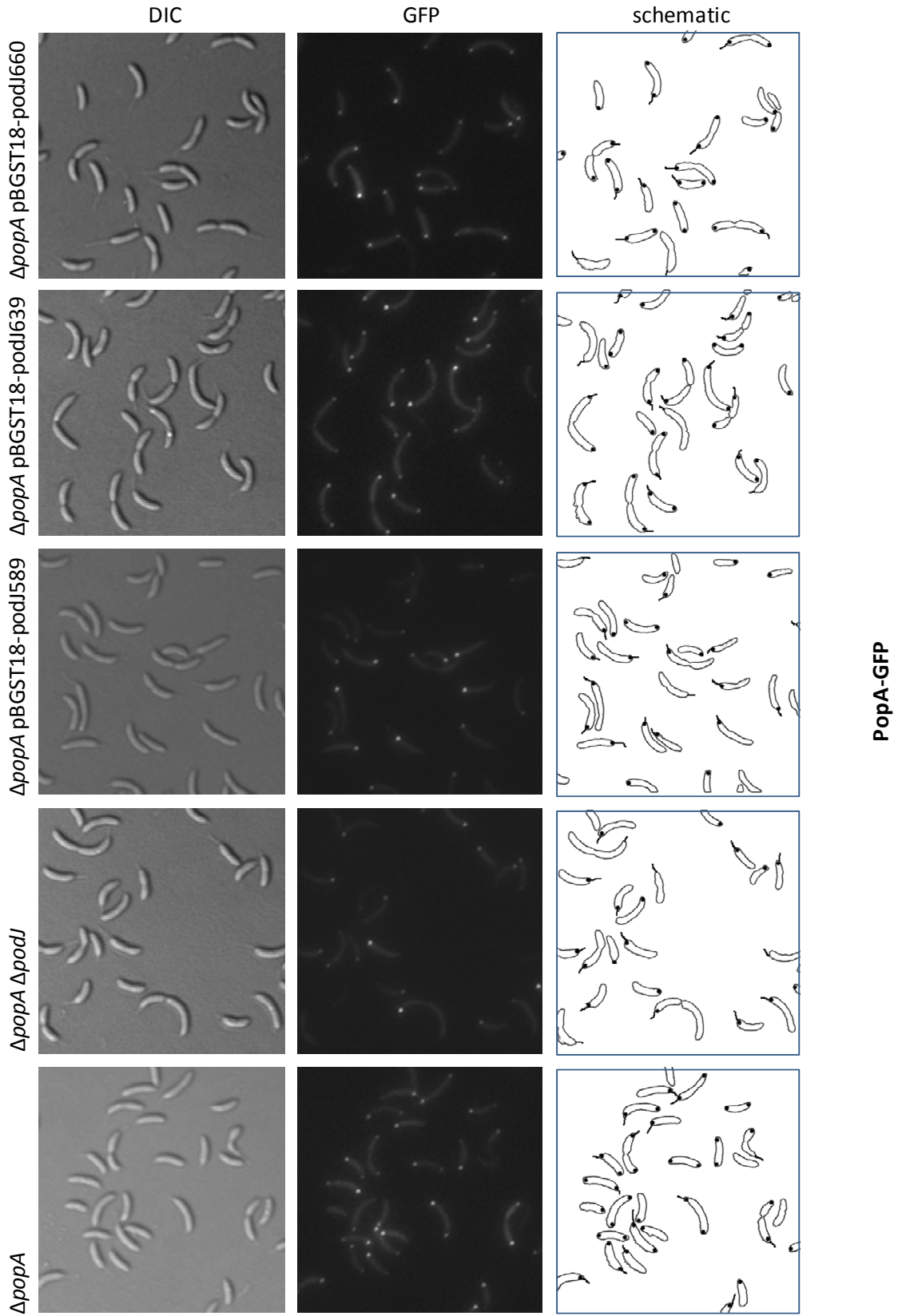


Figure 12

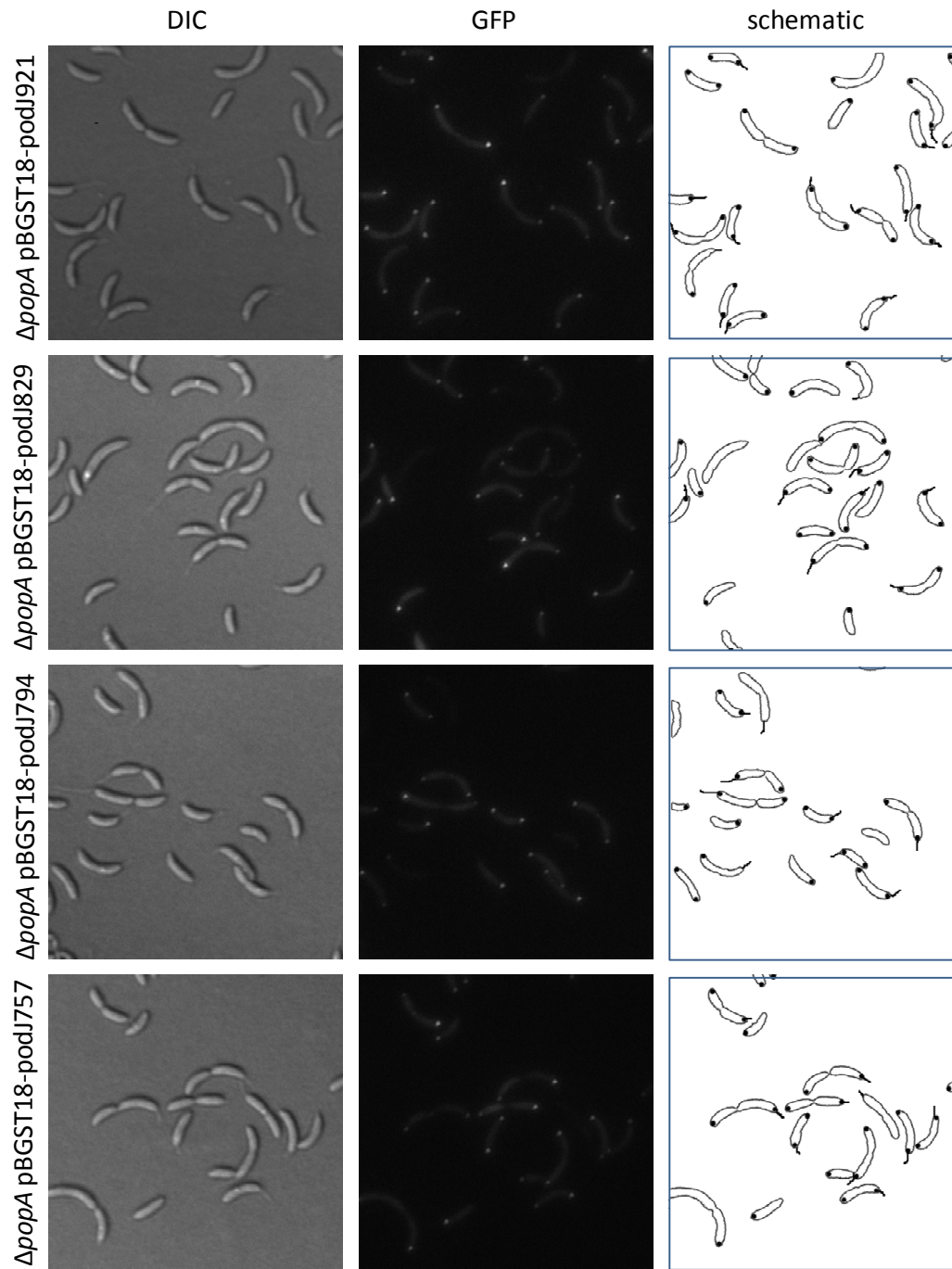
A



B



B cont.



C

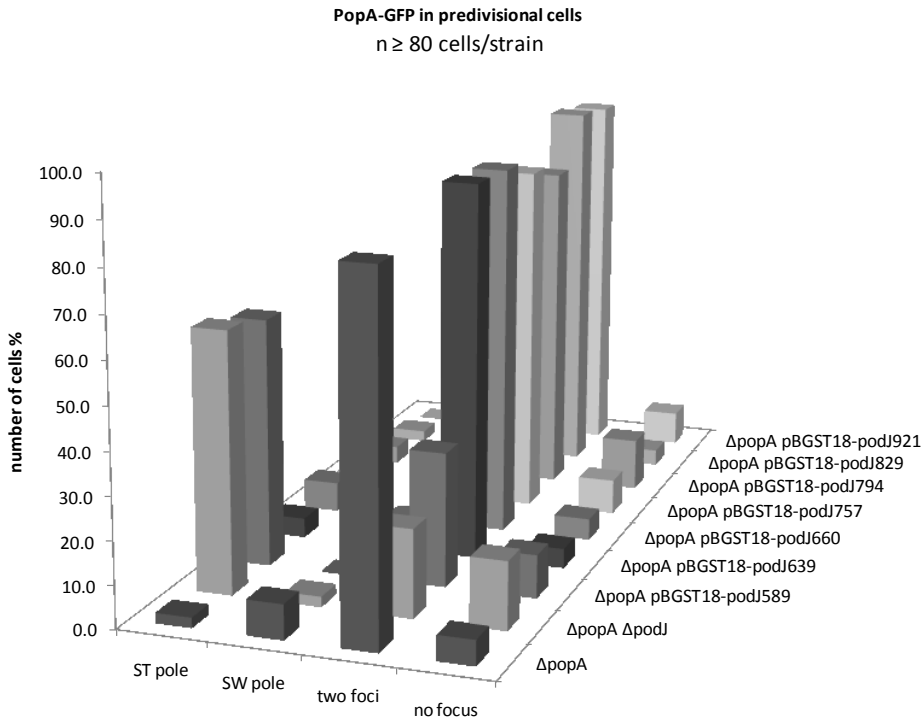
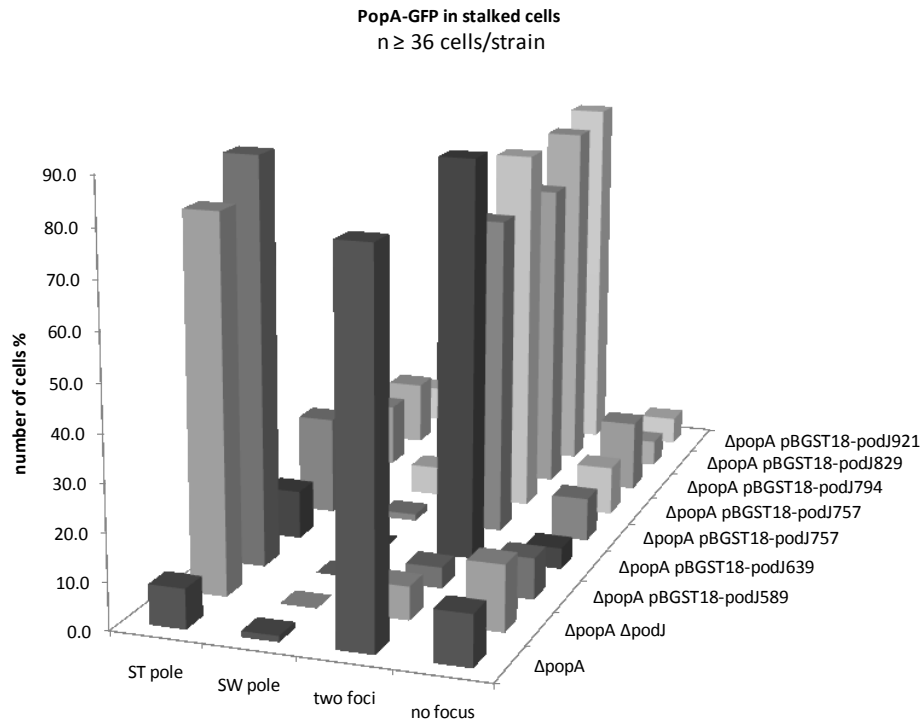
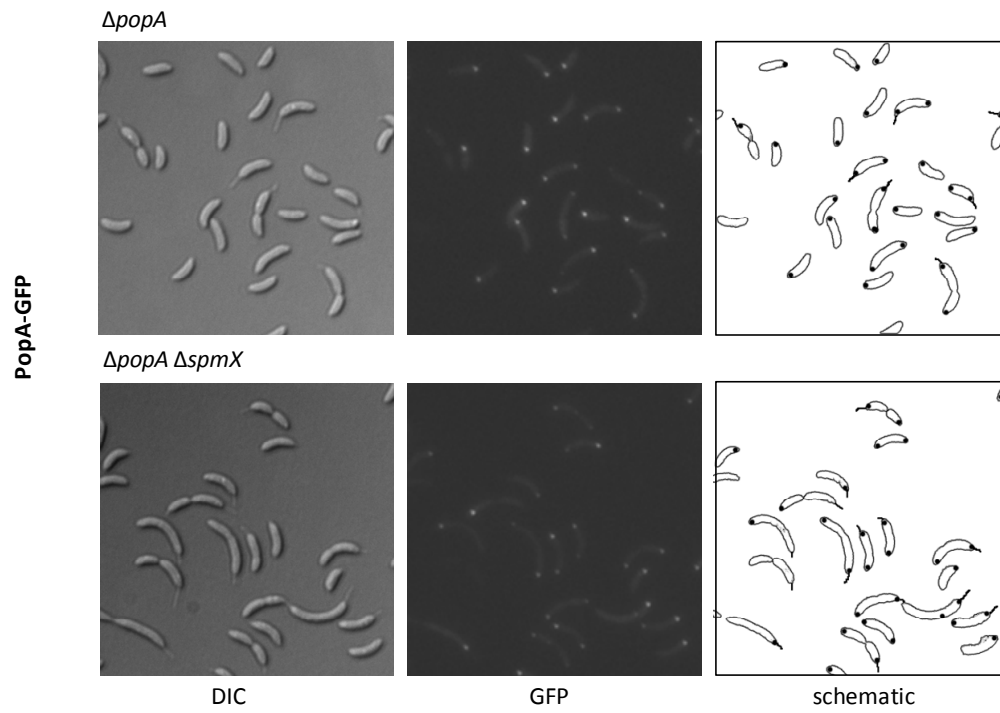
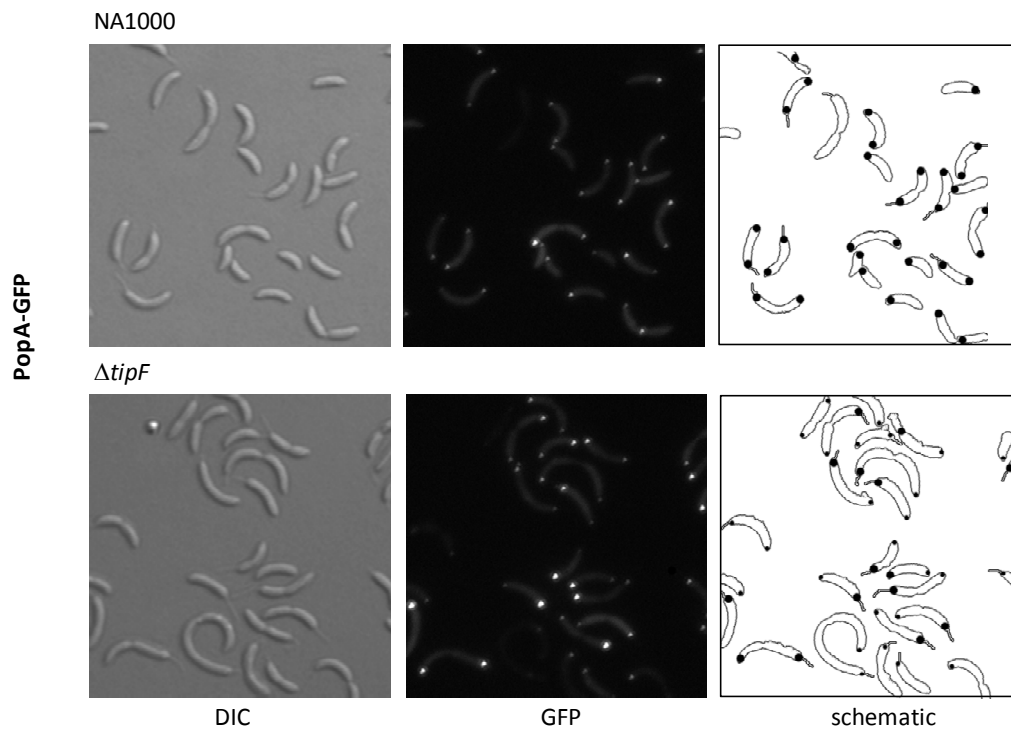


Figure 13

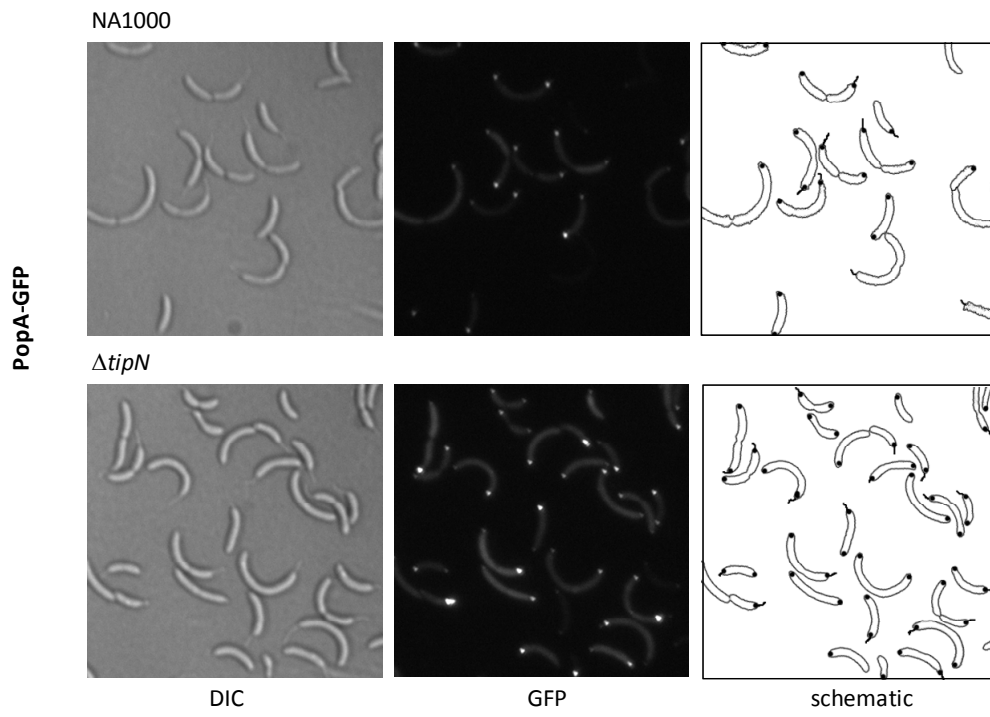
A



B

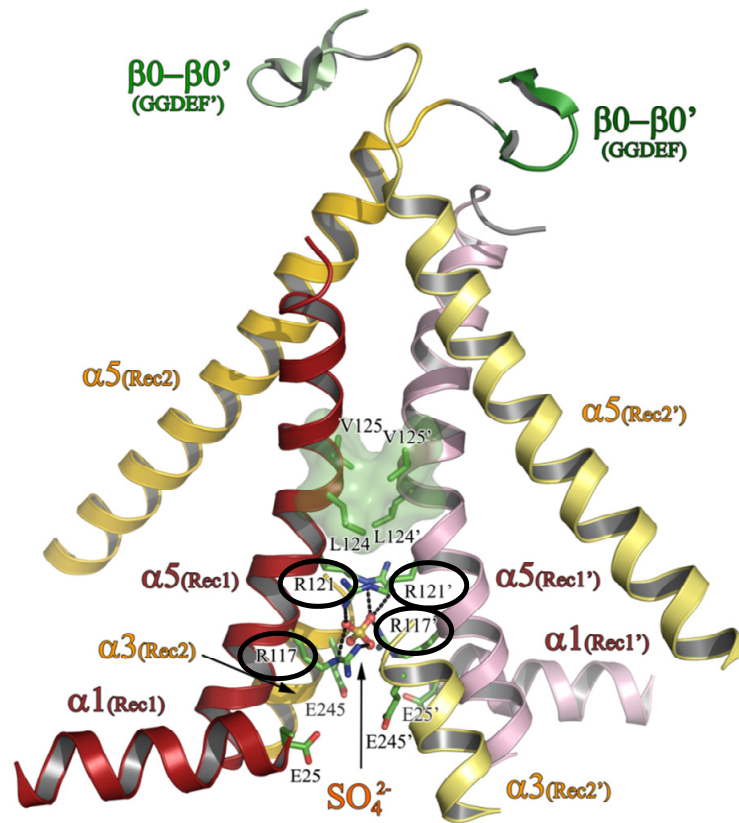


C

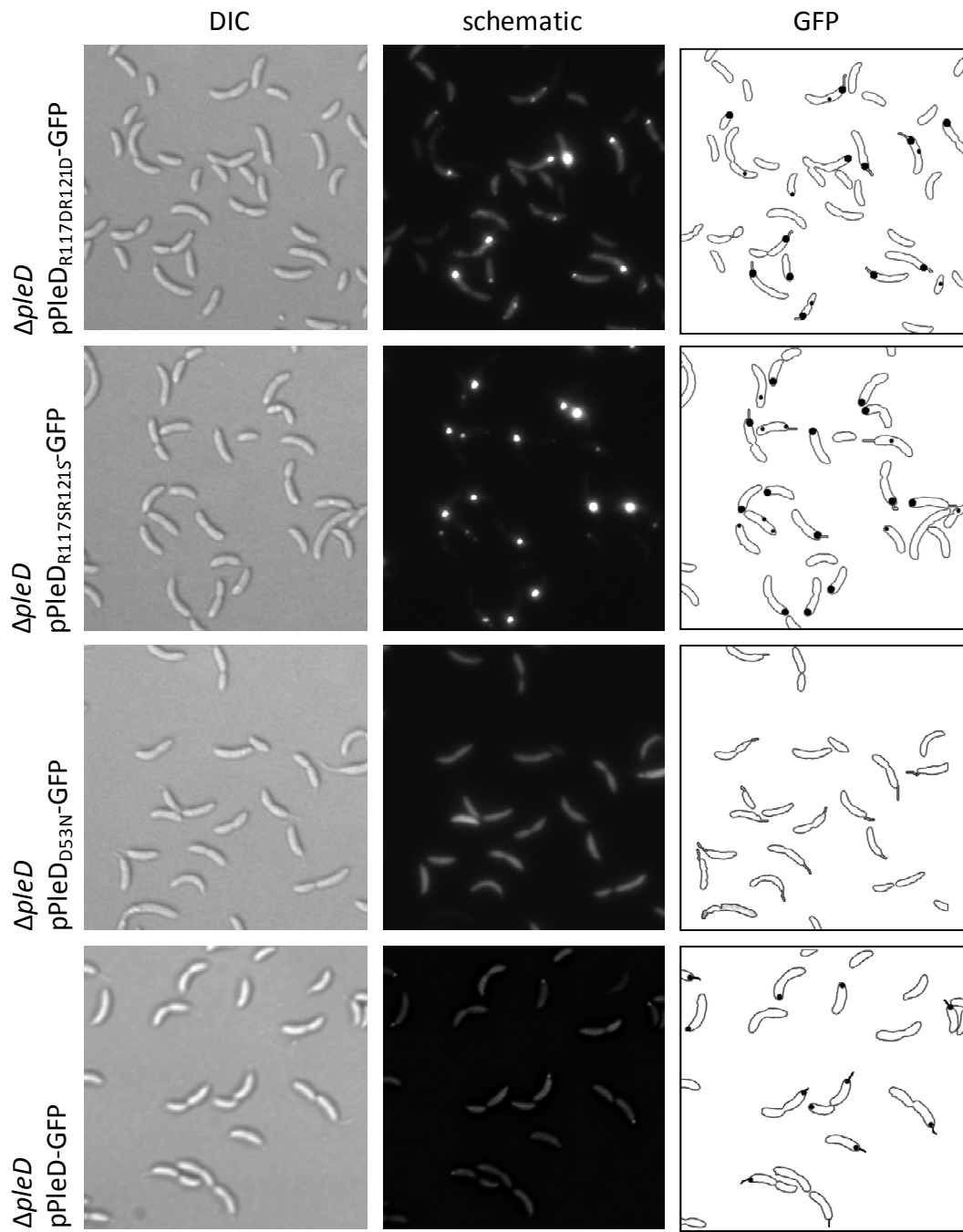


D

PleD activated dimer

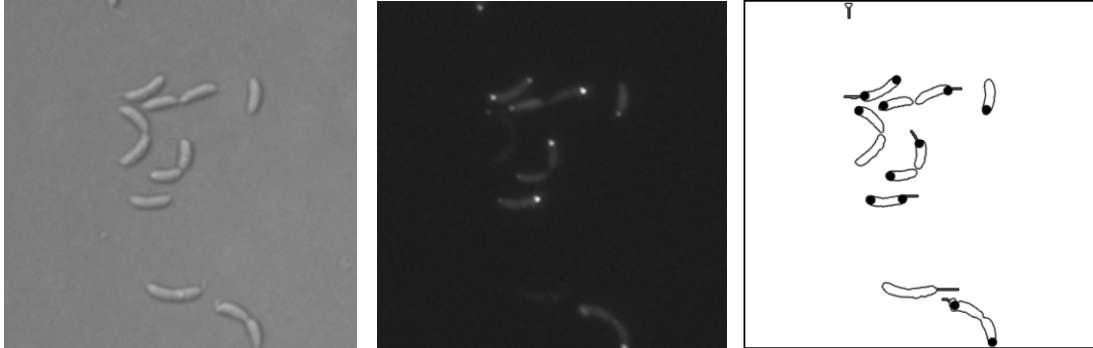


E

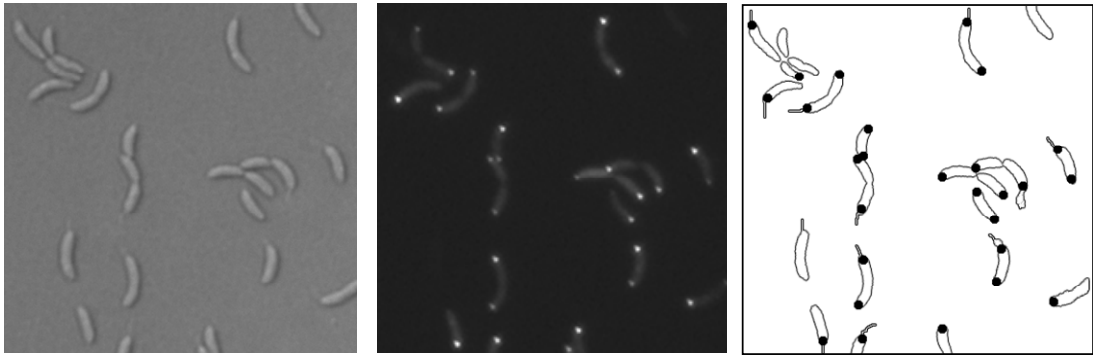


F

ΔpopA pPopA-GFP



ΔpopA pPopA_{R118A}-GFP



ΔpopA pPopA_{R118S}-GFP

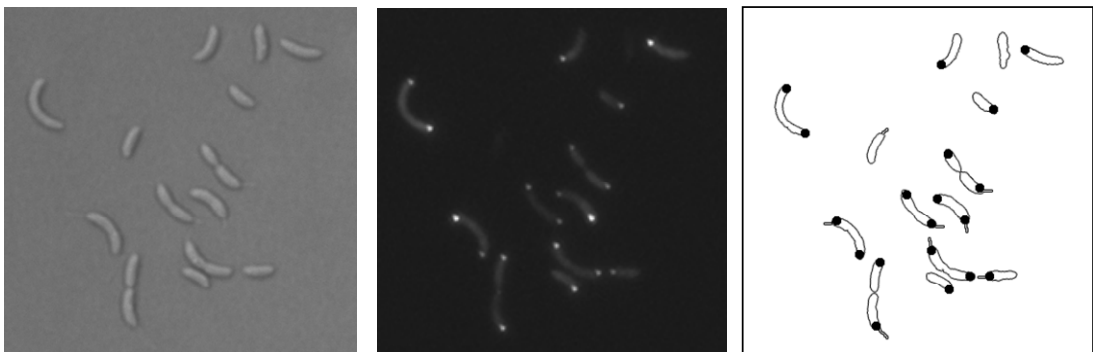
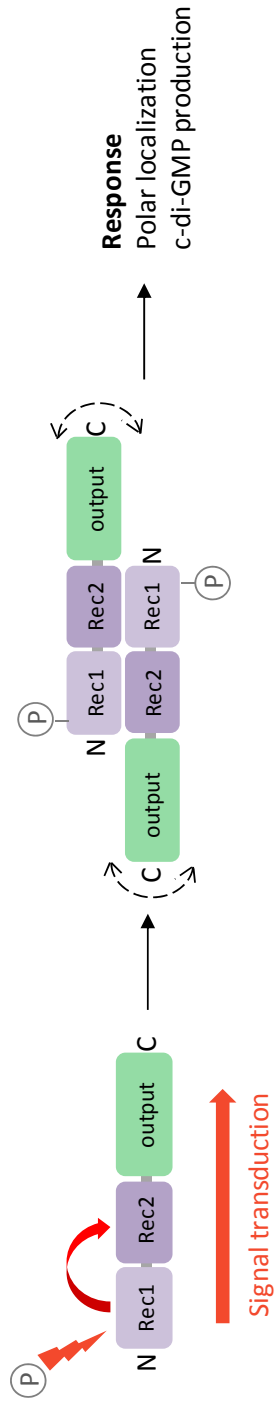


Figure 14

A



B

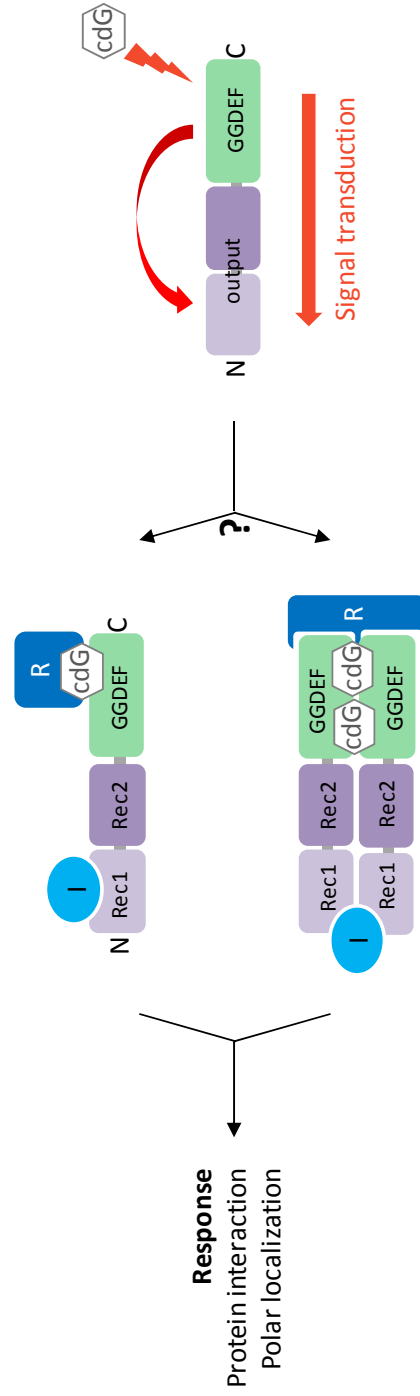
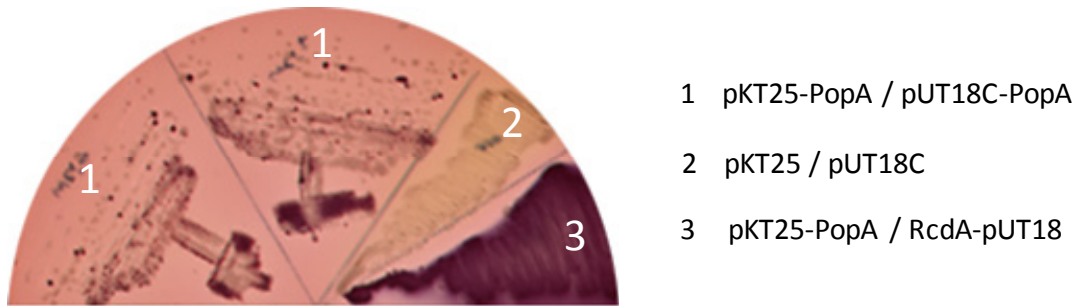
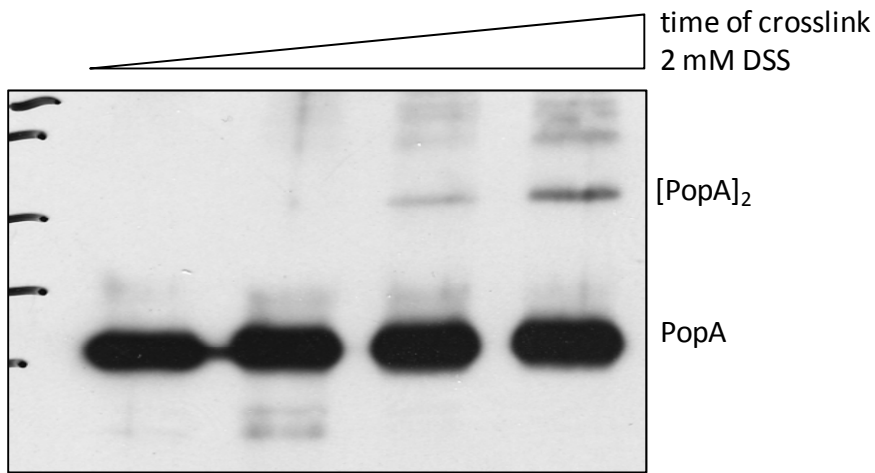


Figure S1

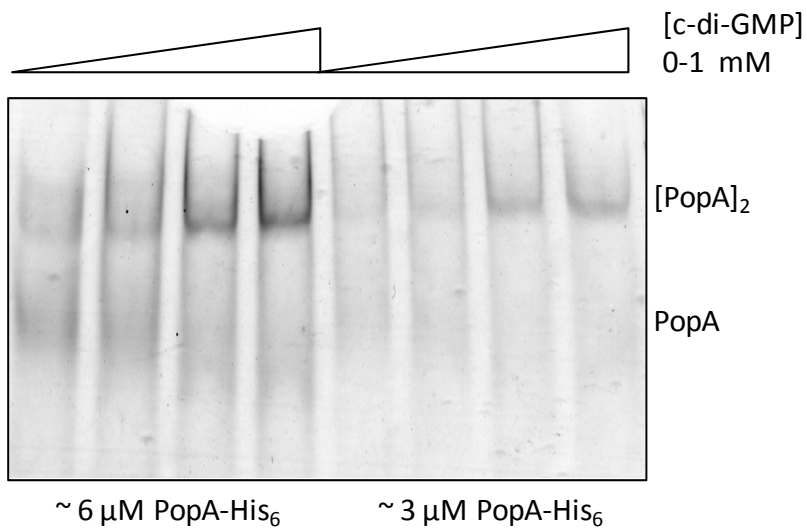
A



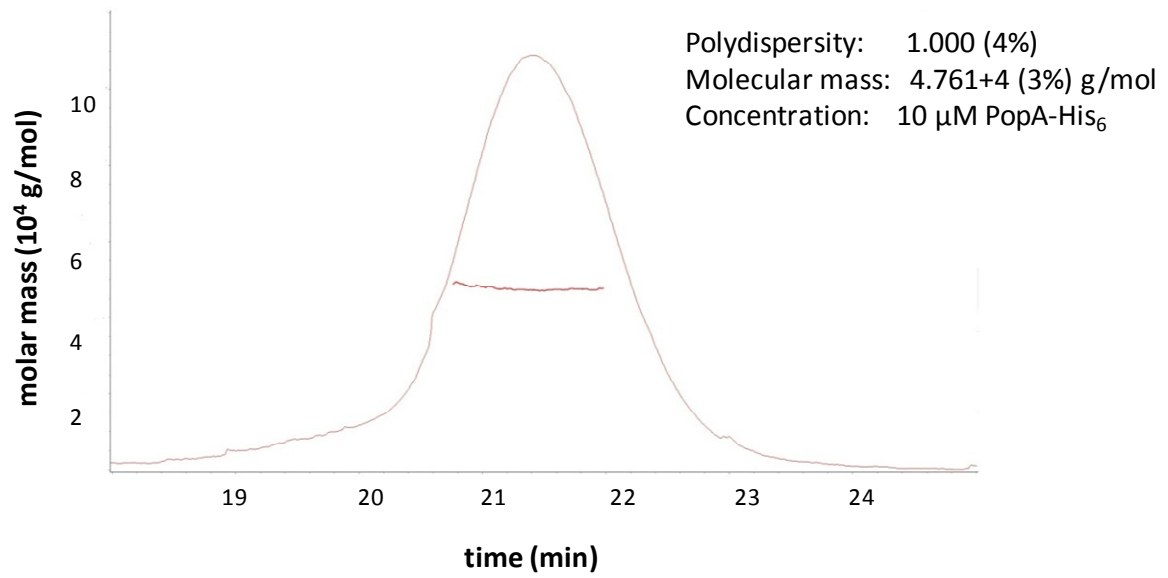
B



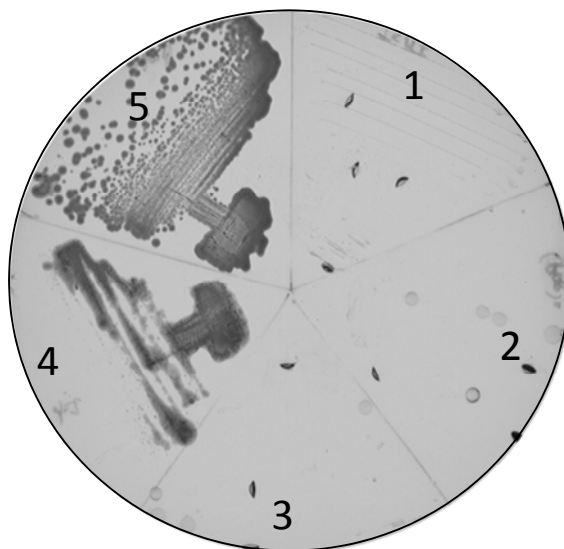
C



D



E



- 1 pKT25-PopA / pUT18C-PopA
- 2 pKT25-PopA_{R357G} / pUT18C-PopA_{R357G}
- 3 pKT25 / pUT18C
- 4 pKT25-zip / pUT18-zip
- 5 pKT25-PopA / pUT18C-RcdA

3.1.8 Table S1

***C. crescentus* Strains**

Name	Description	Reference or Source
UJ4248	NA1000 $\Delta ropA$ and plasmid pAD115	This study
UJ4249	NA1000 $\Delta ropA$ and plasmid pAD116	This study
UJ4250	NA1000 $\Delta ropA$ and plasmid pAD117	This study
UJ4251	NA1000 $\Delta ropA$ and plasmid pAD118	This study
UJ4252	NA1000 $\Delta ropA$ and plasmid pAD119	This study
UJ4253	NA1000 $\Delta ropA$ and plasmid pAD120	This study
UJ4254	NA1000 $\Delta ropA$ and plasmid pAD121	This study
UJ4255	NA1000 $\Delta ropA$ and plasmid pAD122	This study
UJ4334	NA1000 $\Delta ropA$ and plasmid pAD131	This study
UJ4394	NA1000 $\Delta ropA \Delta podJ$ and plasmids pBGST18-podJ589, pAD5	This study
UJ4395	NA1000 $\Delta ropA \Delta podJ$ and plasmids pBGST18-podJ639, pAD5	This study
UJ4396	NA1000 $\Delta ropA \Delta podJ$ and plasmids pBGST18-podJ660, pAD5	This study
UJ4397	NA1000 $\Delta ropA \Delta podJ$ and plasmids pBGST18-podJ757, pAD5	This study
UJ4398	NA1000 $\Delta ropA \Delta podJ$ and plasmids pBGST18-podJ794, pAD5	This study
UJ4399	NA1000 $\Delta ropA \Delta podJ$ and plasmids pBGST18-podJ921, pAD5	This study
UJ4400	NA1000 $\Delta ropA \Delta podJ$ and plasmids pBGST18-podJ829, pAD5	This study
UJ4485	NA1000 $\Delta ropA$ and plasmid pAM16	This study
UJ4496	NA1000 $\Delta ropA$ and plasmid pAM14	This study
UJ4497	NA1000 $\Delta ropA$ and plasmid pAM15	This study
UJ4529	NA1000 $\Delta ropA$ and plasmid pAM13	This study
UJ4674	NA1000 $\Delta ropA$ and plasmid pAM17	This study
UJ4697	NA1000 $\Delta ropA \Delta spmX$ and plasmid pAD5	This study
UJ4698	NA1000 $\Delta ropA \Delta spmX$	This study
UJ4767	CB15 $\Delta ropA$ and pMR20	This study
UJ4769	CB15 $\Delta ropA$ and plasmid pAD19	This study
UJ4790	CB15 and pMR20	This study
UJ4794	NA1000 $\Delta ropA$ and plasmid pAM37	This study
UJ4795	NA1000 $\Delta ropA$ and plasmid pAM38	This study
UJ4832	NA1000 $\Delta ropA$ and plasmid pAM40	This study
UJ4884	NA1000 $\Delta ropA$ and plasmid pAM42	This study
UJ4933	NA1000 $\Delta ropA$ and plasmid pAM44	This study
UJ4935	NA1000 $\Delta ropA \Delta podJ$ and plasmid pAM44	This study
UJ4936	NA1000 $\Delta ropA \Delta podJ$ and plasmid pAM37	This study
UJ4937	NA1000 $\Delta ropA \Delta podJ$ and plasmid pAM42	This study
UJ5002	NA1000 $\Delta tipF$ and plasmid pAD5	This study
UJ5113	NA1000 $\Delta ropA$ and plasmid pAM46	This study
UJ5117	NA1000 $\Delta ropA$ and plasmid pAM48	This study
UJ5119	NA1000 $\Delta ropA$ and plasmid pAM45	This study
UJ6004	CB15 $\Delta pleD$ and plasmid pAM79	This study
UJ6005	CB15 $\Delta ropA$ and plasmid pAM79	This study
UJ6006	CB15 $\Delta pleD$ and plasmid pAM78	This study

UJ6007	CB15 $\Delta popA$ and plasmid pAM78	This study
UJ6008	CB15 $\Delta pleD$ and plasmid pAM81	This study
UJ6009	CB15 $\Delta popA$ and plasmid pAM80	This study
UJ6015	NA1000 $\Delta popA$ and plasmids pAM82, pAD106	This study
UJ6016	NA1000 $\Delta popA$ and plasmid pAM83	This study
UJ6017	NA1000 $\Delta popA$ and plasmid pAM84	This study
UJ6043	NA1000 $\Delta pleD$ and plasmid pAM89	This study
UJ6045	NA1000 $\Delta popA$ and plasmid pAM86	This study
UJ6062	NA1000 $\Delta popA$ and plasmids pAD84, pAD106	This study
UJ6063	NA1000 $\Delta popA$ and plasmids pAM87, pAD106	This study
UJ6146	NA1000 $\Delta popA$ and plasmid pAM96	This study
UJ6148	NA1000 $\Delta popA$ and plasmid pAM97	This study
UJ6149	NA1000 $\Delta tipN$ and plasmid pAD5	This study
UJ6192	NA1000 cdG ⁰ strain and plasmid pAM81	This study
UJ6193	NA1000 cdG ⁰ strain and plasmid pAM80	This study
UJ6194	NA1000 $\Delta pleC \Delta divJ$ and plasmid pAM81	This study
UJ6195	NA1000 $\Delta pleC \Delta divJ$ and plasmid pAM80	This study
UJ6196	NA1000 cdG ⁰ strain and plasmid pAM79	This study
UJ6197	NA1000 $\Delta pleC \Delta divJ$ and plasmid pAM79	This study
CB15	<i>C. crescentus</i> wild-type strain	ATCC 19089
NA1000	Synchronizable laboratory strain of CB15	64
UJ1000	NA1000 $\Delta pleC \Delta divJ$	16
UJ1581	NA1000 $\Delta podJ$	P. Viollier
UJ2827	NA1000 $\Delta popA$	14
UJ284	NA1000 $\Delta pleD$	16
UJ3160	NA1000 $\Delta popA$ and plasmid pAD5	14
UJ3565	NA1000 $\Delta popA$ and plasmid pAD30	14
UJ3635	NA1000 $\Delta tipN$	36
UJ3638	NA1000 $\Delta tipF$	36
UJ3640	NA1000 $\Delta popA \Delta podJ$	14
UJ3666	NA1000 $\Delta popA \Delta podJ$ and plasmid pAD5	14
UJ3672	NA1000 $\Delta popA \Delta podJ$ and plasmid pAD30	14
UJ4331	NA1000 $\Delta popA$ and plasmid pAD128	14
UJ4333	NA1000 $\Delta popA$ and plasmid pAD130	14
UJ4687	NA1000 $\Delta spmX$	35
UJ2756	NA1000 $\Delta pleD$ and plasmid pSA12	S. Abel
UJ5065	NA1000 cdG ⁰ strain	S. Abel

***E. coli* Strains**

Name	Description	Source or Reference
MM337	<i>E. coli</i> K-12 <i>araD139 flbB5301 ptsF25 rbsR relA1 rpsL150-</i> (arg-F-lac)U169-cya	34
DH10B	<i>F</i> ⁻ <i>mcrA</i> D(<i>mrr</i> ⁻ <i>hsd</i> RMS ⁻ <i>mcrBC</i>) f80 <i>dlacZ</i> M15 <i>DlacX</i> 74 endA1 <i>rec1</i> deoR D(<i>ara</i> , <i>leu</i>)7697 <i>araD139 galU nupG rpsL thi pro</i> ⁻ <i>hsd</i> ⁺ <i>recA</i> RP4-2-Tc::Mu-Tn7	65

S-17	F ⁻ , lambda (-), thi, pro, recA, restriction (-) modification (+), RP4 derivative integrated into the chromosome with Tet::Mu, Km::T7	65
Arctic ^R	BL21 (DE3) arctic express strain for protein expression	Stratagene
Epicurian Coli [®]	<i>endA1 gyrA96 thi-1 hsdR17 supE44 relA1 lac mutD5</i>	Stratagene
XL1-Red	<i>mutS mutT Tn10 (Tetr)a</i>	

Plasmids

Name	Description	Source or Reference
pAM13	pMR20; <i>popA_{E125}-gfp</i> under the control of <i>popA</i> promoter	This study
pAM14	pMR20; <i>popA_{R129A}-gfp</i> under the control of <i>popA</i> promoter	This study
pAM15	pMR20; <i>popA_{R220A}-gfp</i> under the control of <i>popA</i> promoter	This study
pAM16	pMR20; <i>popA_{R277A}-gfp</i> under the control of <i>popA</i> promoter	This study
pAM17	pMR20; <i>popA_{E281A}-gfp</i> under the control of <i>popA</i> promoter	This study
pAM37	pMR20; <i>popA_{R317A}-gfp</i> under the control of <i>popA</i> promoter	This study
pAM38	pMR20; <i>popA_{R220AR277AE281A}-gfp</i> under the control of <i>popA</i> promoter	This study
pAM40	pMR20; <i>popA_{E50A}-gfp</i> under the control of <i>popA</i> promoter	This study
pAM42	pMR20; <i>popA_{R315A}-gfp</i> under the control of <i>popA</i> promoter	This study
pAM44	pMR20; <i>popA_{R315AR317A}-gfp</i> under the control of <i>popA</i> promoter	This study
pAM45	pMR20; <i>popA_{R118S}-gfp</i> under the control of <i>popA</i> promoter	This study
pAM46	pMR20; <i>popA_{R313A}-gfp</i> under the control of <i>popA</i> promoter	This study
pAM48	pMR20; <i>popA_{R118D}-gfp</i> under the control of <i>popA</i> promoter	This study
pAM55	pKT25; <i>popA_{R272H}</i> C-terminal fused to T25 fragment	This study
pAM58	pMR20; <i>pleD_{R117SR121S}-gfp</i> under the control of <i>divK</i> promoter	This study
pAM59	pMR20; <i>pleD_{R117DR121D}-gfp</i> under the control of <i>divK</i> promoter	This study
pAM70	pUT18C; <i>popA_{R357G}</i> C-terminal fused to T18 fragment	This study
pAM78	pRVGFPC-2; <i>popA_{Rec1Rec2}pleD_{GGDEF}-gfp</i> (Hybrid-B) under the control of vanillate promoter	This study
pAM79	pRVGFPC-2; <i>pleD_{Rec1Rec2}popA_{GGDEF}-gfp</i> (Hybrid-A) under the control of vanillate promoter	This study
pAM80	pRVGFPC-2; <i>popA-gfp</i> under the control of vanillate promoter	This study
pAM81	pRVGFPC-2; <i>pleD-gfp</i> under the control of vanillate promoter	This study
pAM82	pRVGFPC-2; <i>pleD_{Rec1Rec2}popA_{GGDEF}-Cfp</i> (Hybrid-A) under the control of vanillate promoter	This study
pAM83	pRVGFPC-2; <i>pleD_{Rec1Rec2}popA_{GGDEF,R357G}-gfp</i> (Hybrid-A _{R357G}) under the control of vanillate promoter	This study
pAM84	pRVGFPC-2; <i>popA_{R357G}-gfp</i> under the control of vanillate promoter	This study
pAM86	pMR20; <i>popA_{R388A}-gfp</i> under the control of <i>popA</i> promoter	This study
pAM87	pMR20; <i>popA_{R272H}-gfp</i> under the control of <i>popA</i> promoter	This study
pAM89	pMR20; <i>pleD_{R359A}-gfp</i> under the control of <i>divK</i> promoter	This study
pAM94	pKT25; <i>popA_{G294E}</i> C-terminal fused to T25 fragment	This study
pAM95	pKT25; <i>popA_{A335T}</i> C-terminal fused to T25 fragment	This study
pAM96	pRVGFPC-2; <i>pleD_{Rec1Rec2,Y26A}popA_{GGDEF}-gfp</i> (Hybrid-A _{Y26A}) under the control of vanillate promoter	This study

pAM97	pRVGFPC-2; <i>pleD</i> _{Rec1Rec2,Y26A} <i>popA</i> _{GGDEF,R357G} - <i>gfp</i> (Hybrid-A _{R357G}) under the control of vanillate promotor	This study
pAD115	pMR20; <i>popA</i> _{R357A} - <i>gfp</i> under the control of <i>popA</i> promotor	This study
pAD116	pMR20; <i>popA</i> _{V358A} - <i>gfp</i> under the control of <i>popA</i> promotor	This study
pAD117	pMR20; <i>popA</i> _{E359A} - <i>gfp</i> under the control of <i>popA</i> promotor	This study
pAD118	pMR20; <i>popA</i> _{D360A} - <i>gfp</i> under the control of <i>popA</i> promotor	This study
pAD119	pMR20; <i>popA</i> _{V358NE359R} - <i>gfp</i> under the control of <i>popA</i> promotor	This study
pAD120	pMR20; <i>popA</i> _{V358GE359Q} - <i>gfp</i> under the control of <i>popA</i> promotor	This study
pAD121	pMR20; <i>popA</i> _{R357GE359G} - <i>gfp</i> under the control of <i>popA</i> promotor	This study
pAD122	pMR20; <i>popA</i> _{V358EE359SD360E} - <i>gfp</i> under the control of <i>popA</i> promotor	This study
pAD131	pMR20; <i>popA</i> <i>GGDEF</i> - <i>gfp</i> under the control of <i>popA</i> promotor	This study
pAD5	pMR20; <i>popA</i> - <i>gfp</i> under the control of <i>popA</i> promotor	14
pAD8	pNPTS138; suicide vector to generate a clean <i>popA</i> deletion	14
pAD19	pMR20; <i>popA</i> _{D55N} - <i>gfp</i> under the control of <i>popA</i> promotor	14
pAD30	pMR20; <i>popA</i> _{R357G} - <i>gfp</i> under the control of <i>popA</i> promotor	14
pAD50	pUT18C; <i>rcdA</i> C-terminal fused to T18 fragment	14
pAD56	pUT18; <i>rcdA</i> N-terminal fused to T18 fragment	14
pAD67	pUT18; <i>popA</i> N-terminal fused to T18 fragment	14
pAD84	pMR20; <i>popA</i> -CFP under the control of <i>popA</i> promotor	14
pAD90	pKT25; <i>popA</i> _{R357G} C-terminal fused to T25 fragment	14
pAD90	pKT25; <i>popA</i> _{R357G} C-terminal fused to T25 fragment	14
pAD92	pUT18; <i>popA</i> _{R357G} N-terminal fused to T18 fragment	14
pAD106	pBBR-MCS-5; <i>rcdA</i> - <i>yfp</i> under control of <i>rcdA</i> promotor	14
pAD128	pMR20; <i>popA</i> <i>Rec1</i> - <i>gfp</i> under the control of <i>popA</i> promotor	14
pAD130	pMR20; <i>popA</i> <i>Rec1-Rec2</i> - <i>gfp</i> under the control of <i>popA</i> promotor	14
pAD141	pKT25; <i>popA</i> C-terminal fused to T25 fragment	14
pAD143	pUT18C; <i>popA</i> C-terminal fused to T18 fragment	14
pAD160	pKT25; <i>popA</i> <i>Rec1</i> C-terminal fused to T25 fragment	14
pAD161	pKT25; <i>popA</i> <i>Rec2</i> C-terminal fused to T25 fragment	14
pAD162	pKT25; <i>popA</i> <i>Rec1-Rec2</i> C-terminal fused to T25 fragment	14
pAD163	pKT25; <i>popA</i> <i>GGDEF</i> C-terminal fused to T25 fragment	14
pET21c::PdpA	pET21c; <i>popA</i> C-terminal fused to His ₆	14
pBGST18-podJ58	pBGST18; vector to insert stop codon in <i>podJ</i> at position 589	26
pBGST18-podJ63	pBGST18; vector to insert stop codon in <i>podJ</i> at position 639	26
pBGST18-podJ66	pBGST18; vector to insert stop codon in <i>podJ</i> at position 660	26
pBGST18-podJ75	pBGST18; vector to insert stop codon in <i>podJ</i> at position 757	26
pBGST18-podJ79	pBGST18; vector to insert stop codon in <i>podJ</i> at position 794	26
pBGST18-podJ82	pBGST18; vector to insert stop codon in <i>podJ</i> at position 829	26
pBGST18-podJ92	pBGST18; vector to insert stop codon in <i>podJ</i> at position 921	26
pKT25	pSU40 derivative with T25 fragment of CyaA. C-terminal fusions	54
pKT25- <i>zip</i>	pKT25 derivative with leucine zipper of GCN4	54
pUT18C	pUC19 derivative with T18 fragment of CyaA. C-terminal fusions	54
pUT18C- <i>zip</i>	pUT18C derivative with leucine zipper of GCN4	54
pUT18	pUC19 derivative with T18 fragment of CyaA. N-terminal fusions	54
pSA12	pMR20; <i>pleD</i> - <i>gfp</i> under the control of <i>divK</i> promotor	S. Abel

pSA13	pMR20; <i>pleD</i> _{D53N} - <i>gfp</i> under the control of <i>divK</i> promoter	S. Abel
pSA15	pMR20; <i>pleD</i> *- <i>gfp</i> under the control of <i>divK</i> promoter	S. Abel
pMR20	Tet ^R low copy number and broad host range vector	66
pET21c	Amp ^R high copy number expression vector	Novagen
pBBR-MCS-5	Gent ^R , broad host range and cloning vector	67
pRVCFPC-5	pRK2 derivative, Tet ^R low copy number vector	68
pRVGFPC-2	pRK2 derivative, Kan ^R low copy number vector	68
pNPTS138	Kan ^R , suicide vector with <i>sacB</i> gene and <i>oriT</i>	M.R.K. Alley
pBGST18	pRK2 derivative, Kan ^R , oriT	M.R.K. Alley

3.2 Identifying New Interaction Partners of PopA, a c-di-GMP Effector Protein Involved in Cell Cycle Control and Development of *Caulobacter Crescentus*

Annina Moser, Anna Dürig, Svetlana Ponti, and Urs Jenal

Statement of my work

All plasmids and strains used in this study have been generated by me, unless otherwise stated in table S1. I performed large scale co-immunoprecipitation experiments (Fig.1, S1) and I did the bioinformatic analysis of two new interaction partners (Fig. 3, 8). I confirmed interactions in the bacterial two-hybrid system (Fig. 2, S2) and generated clean deletions and overexpression constructs of the interaction partners and analyzed them with respect to growth, motility, flagellum, attachment and pili (Fig. 4, 9, S3-S4, S6-S7). All DIC and fluorescence microscopy followed by statistical analysis were done by me (Fig. 5, 10, S5, S8). I cloned and purified the interaction partners for expression and antibody generation. Synchronizations and immunoblots were done in close collaboration with Svetlana Ponti (Fig. 6, 7, 11, S9).

3.2.1 Abstract

Caulobacter crescentus undergoes a characteristic asymmetric cell division, which is tightly coupled to cellular differentiation events and makes this organism a convenient model to study the regulation of the bacterial cell cycle and development. In the recent years growing evidence linked the action of bacterial second messenger cyclic di-GMP signaling proteins with these processes.

The c-di-GMP effector protein PopA is involved in both, cell cycle progression control and polar development. Upon binding of c-di-GMP PopA localizes to the protease ClpXP occupied old cell pole where it recruits ClpXP substrates such as the replication inhibitor CtrA and the NADPH binding protein KidO to the pole to facilitate their cell cycle dependent degradation. Localization to the opposite pole requires the general topology factor PodJ which does not only target PopA to this subcellular site but also other proteins involved in *C. crescentus* polar development.

Here we identify two new direct PopA interaction partners, CC1462 and CC2616, and show that both localize to the cell poles in a PopA-dependent manner. We show that CC1462 is a ClpXP substrate, which requires PopA to localize to the ClpXP-occupied pole and to be eliminated during the swarmer-to-stalked cell transition. However, the significance of CC1462 degradation remains unclear. While the CC1462 gene is located in a flagellar gene cluster, its deletion did not affect flagellar assembly and function. In contrast, CC1462 overexpression decreased cell motility, a phenotype whose molecular basis has not been fully investigated yet. In contrast to CC1462, the levels of the annotated guanine deaminase CC2616 remain stable throughout cell cycle suggesting that CC2616 belongs to a new class of PopA-dependent proteins, which are not proteolytically processed. While it is not clear whether CC2616 indeed acts as enzyme or adopted a novel regulatory function, its deletion led to an increase in attachment and a decrease in motility, a phenotype observed for strain having elevated c-di-GMP levels. Altogether, these data strengthen the view that the c-di-GMP effector PopA is at the core of a protein degradation platform that elicits important cell cycle decisions through ClpXP mediated degradation of key regulators.

3.2.2 Introduction

The freshwater α -proteobacterium *Caulobacter crescentus*¹ divides asymmetrically resulting in two morphologically distinct, but genetically identical daughter cells; the motile swarmer cell and the sessile and surface adherent stalked cell. Chromosome replication is strictly restricted to the stalked cell^{2,3}. In contrast, the swarmer cell first has to undergo an obligate differentiation process before it can initiate replication and cell division. During this transition it loses its polar flagellum and chemotaxis apparatus and replaces it by a membrane protrusion called stalk and an adhesive holdfast at its tip. The essential response regulator CtrA is a key regulatory factor driving this differentiation step and promoting cell cycle progression. In swarmer cells, phosphorylated CtrA directly binds to the origin of replication thereby inhibiting DNA replication initiation⁴. This inhibition is relieved during swarmer-to-stalked cell transition by inactivation of CtrA through concomitant dephosphorylation and ClpXP-dependent degradation thereby allowing replication to start at the onset of S-phase⁵⁻⁷. The correct timing of CtrA degradation is ensured by coincident dynamic recruitment of ClpXP protease and the substrate to the same subcellular site, the old cell pole. This process is orchestrated by two dedicated polar targeting factors, which are themselves localized through the bacterial second messenger cyclic di-GMP and by phosphorylation cascades^{8,9}.

Timed polar positioning of the protease complex ClpXP relies on the polar localization of the single domain response regulator CpdR in dependence of its phosphorylation state. Dephosphorylated CpdR accumulates at the pole and recruits ClpXP via direct interaction¹⁰. Phosphorylation of CpdR by a phosphorelay comprising CckA sensor kinase and ChpT phosphotransferase prevents localization of CpdR and, as a consequence, localization of ClpXP. Since CckA also phosphorylates CtrA itself, this pathway elegantly controls both activation and stabilization of this master cell cycle regulator in the swarmer cell¹¹.

Localization of the substrate CtrA to the old cell pole is triggered by an upshift in cyclic di-GMP during the swarmer-to-stalked cell transition. In swarmer cells, c-di-GMP concentrations are kept low by the action of the phosphodiesterase PdeA. During cell differentiation, PdeA is recruited transiently to the ClpXP occupied pole where it is destroyed in a ClpXP-dependent manner, similarly to CtrA. The specific release of the PdeA antagonist DgcB together with the simultaneous activation of the diguanylate cyclase PleD increases c-di-GMP prior to S-phase entry and contributes to the polar recruitment of the c-di-GMP effector PopA⁹. Specific binding of c-di-GMP to a conserved binding pocket (I-site) causes PopA to dynamically reposition to the cell pole, where it directly recruits the mediator protein RcdA, which is required to attract CtrA to the same pole^{8,12}. The observation that ClpXP-

dependent degradation of PdeA depends on CpdR, but not PopA, establishes a clear order of events with ClpXP localization and PdeA degradation preceding targeting of PopA and destruction of CtrA⁹.

PopA is also recruited to the incipient flagellated pole, a process that requires the cell polarity factor PodJ. In stalked cells full length PodJ (PodJ_L) localizes to the incipient flagellated pole where it mediates polar positioning of the histidine kinase/phosphatase PleC and the pilus assembly factor CpaE¹³⁻¹⁵. Proteolytic processing by the periplasmic protease PerP in late predivisional cells creates a shorter PodJ version (PodJ_S), which is responsible for holdfast formation and swarming motility^{15,16}. PodJ_S remains at the flagellated pole after cytokinesis and is degraded by the metalloprotease MmpA during swarmer-to-stalked cell transition¹⁶. The function of PopA at the PodJ occupied pole is not known. However, the observation that a $\Delta podJ$ mutant displays the same motility defect like a $\Delta popA$ mutant arguing that PopA might engage motility-specific functions at the flagellated pole⁸. In addition to its role in CtrA degradation control and cell motility, PopA appears to be important for attachment to surfaces suggesting that PopA is a protein with multiple functions at distinct subcellular sites⁸.

So far, the molecular basis for PopA localization to the cell poles and its exact developmental functions are not understood. To explain the dynamic and multifunctional behavior of PopA, additional factors have to be postulated which help coordinating differential localization to the poles to exert pole-specific functions. Localization requires general or PopA-specific receptor structures that would allow PopA to distinguish between swarmer and stalked pole. PodJ is such a general topology factor for the flagellated pole^{13,14}. But while PodJ is required for PopA localization to this subcellular site⁸, a PodJ-independent mechanism has to be proposed for the stalked pole, as PodJ is degraded during swarmer-to-stalked cell transition^{13,16} while PopA persists at the pole. Moreover, additional general or PopA-specific c-di-GMP signaling modules may feed into the PopA pathway. This assumption is supported by the observation that the two major diguanylate cyclases DgcB and PleD are not sufficient to drive PopA to the cell pole⁹. Moreover, the two branches leading to CtrA and ClpXP localization, respectively, need to converge and thus might need to be physically interlinked. One candidate for such a function is RcdA, which appears to directly interact with CpdR⁸. This could explain the observation that PopA contributes to CpdR and ClpX localization during swarmer-to-stalked cell transition⁸. But while PopA and RcdA interact with each other, neither of these proteins interacts directly with CtrA⁸. It is thus clear that additional factors are involved in the formation and function of a macromolecular degradasome complex at the cell pole.

Here we identify two new PopA interaction partners, CC1462 and CC2616. CC1462, a hypothetical protein sequesters to the cell poles in a PopA-dependent manner and is degraded by the protease ClpXP during swarmer-to-stalked cell transition. Mutants lacking CC1462 have no obvious phenotype leaving the function of CC1462 unclear. It is possible that the interaction of CC1462 with PopA relates primarily to its delivery to the ClpXP protease. However, neither CtrA nor KidO, the other known PopA-dependent ClpXP substrates directly interact with PopA. CC2616 is annotated as guanine deaminase, an enzyme catalyzing the conversion of guanine to xanthine. It appears to inversely regulate motility and attachment, but its exact function is not known. Consistent with its direct interaction with PopA, its localization to the cell poles is dependent on PopA and CpdR, suggesting a possible role as molecular linker between the phosphorylation and the c-di-GMP dependent branch of the network controlling CtrA degradation.

3.2.3 Results

Identification of two new PopA interaction partners.

To identify additional components involved in PopA function, large scale co-immunoprecipitation experiments were performed with lysates from a $\Delta popA$ strain expressing a *popA-flag* allele under the control of *popA* promoter. To optimize conditions, immunoblots against the known PopA interaction partner RcdA⁸ were used. They verified that RcdA specifically co-immunoprecipitates with PopA-*flag* and is not detected in precipitates of a strain lacking PopA (Fig. 1A). Two prominent bands consistently appeared, but were absent in control precipitates from a $\Delta popA$ strain expressing untagged PopA and were subsequently analyzed by tandem mass spectrometry (Fig. 1B). The functionality of PopA-*flag* was confirmed by complementation assays (Fig. S1). This strategy led to the identification of two new interacting proteins, CC1462 and CC2616.

CC1462 and CC2616 directly interact with PopA, but not with components of the CtrA degradation machinery.

To verify if the newly identified proteins CC1462 and CC2616 are direct interaction partners of PopA, the proteins were cloned into the bacterial two-hybrid system¹⁷, which is based on the reconstruction of the cAMP signaling cascade. In this system, specific protein-protein interactions lead to the ability to catabolize maltose and the appearance of red colonies on McConkey agar base maltose plates. All possible fusions between PopA, CC1462, CC2616 and T18 or T25 complementary fragments of the adenylate cyclase from *Bordetella pertussis* were generated and tested. In addition, the interaction of PopA with the soluble N-terminal part of the transmembrane protein PodJ was assayed, because PodJ has been reported to mediate PopA localization to the flagellated pole⁸ and could directly interact with PopA as well. Strong positive interactions were detected for PopA and CC1462. PopA and CC2616 scored red on McConkey agar base maltose plates as well, although the interactions were less distinct and not all fusion combinations led to red colonies (positive combinations: pUT18C-PopA/pKT25-CC2616 and pKT25-PopA/CC2616-pUT18C). Moreover, a weak, but continuously observed interaction between pUT18C-PopA and pKT25-PodJ was detected (Fig. 2A).

Many PopA cellular functions require an intact I-site motif, e.g. localization to the stalked pole, the polar recruitment of RcdA and the degradation of CtrA during cell cycle. However, for the interaction between PopA and RcdA an intact I-site is not needed suggesting that the two proteins interact in a c-di-GMP independent manner⁸. This prompted us to analyze if a PopA I-site mutant (PopA_{R357G}) can still interact with CC1462, CC2616 and PodJ in the bacterial two-hybrid system. Indeed,

positive interactions of PopA I-site mutant with CC1462 and CC2616 were unchanged, whereas interaction with the cytoplasmic part of PodJ seemed to be reduced in presence of a PopA I-site mutant (Fig. 2B) suggesting that PopA/PodJ interaction might be c-di-GMP dependent.

Finally, we analyzed cross-interaction between CC1462 and CC2616 and with components of the CtrA degradation machinery. However, all interaction pairs scored negative (Fig. S2). Taken together, these findings strongly argue, that CC1462, CC2616 and PodJ are direct interaction partners of PopA.

CC1462 is a hypothetical protein encoded within a flagellin gene cluster.

CC1462 is a 15 kDa hypothetical protein, which is located within the *C. crescentus* α -flagellin gene cluster^{18,19}. Besides the CC1462 gene it contains *fjlL*, *fjlK* and *fliJ* coding for class IV flagellins and for FlaF and FlbT, which are involved in late flagellar gene translation control^{20,21}. Moreover, this locus contains five hypothetical proteins (Fig. 3A). Homologs of CC1462 are found throughout the bacterial kingdom, even in bacteria lacking flagella, arguing that its function might not be directly linked to the flagellar motor. In contrast to most of the homologs, CC1462 is annotated with an N-terminal extension. Since a peptide within this elongated N-terminus was identified in the mass spectrometry analysis of the PopA co-immunoprecipitation experiments we assume that this difference in length is not due to an annotation error. Paralogs of CC1462 could not be found in *C. crescentus* (SSDB Paralog Search²²).

Pfam database analysis of the CC1462 protein^{23,24} revealed a 40 amino acids stretch with homology to FlaG domains. Their role is often associated with the flagellum, but studies to elucidate their exact function in the CC1462 homologs *flaG* and *ORF3* in *Pseudomonas fluorescence* and *Vibrio anguillarum* remain contradictory^{25,26}. The structure of another FlaG domain protein, *YvyC* from *Bacillus subtilis*, was solved in 2009²⁷ (PDB: 2HC5). It consists of a three-helix bundle and three β -strands arranged in an antiparallel manner. HHpred²⁸ analysis predicted a similar structure for CC1462, although one α -helix is missing and the elongated N-terminal end appears as unstructured region (Fig. 3B). Similarly to CC1462, the *yvyC* gene is flanked by flagellins and flagellin-specific chaperones²⁹, but its cellular function remains unclear.

Overexpression of CC1462 leads to a slight reduction in cell motility.

Besides its role in cell cycle control⁸, PopA seems to be part of a regulatory network controlling cell motility and surface attachment. Although a $\Delta popA$ mutant has an intact single polar flagellum, it shows reduced motility on semi solid agar plates³⁰. As the coding sequence of the PopA interactor CC1462 is associated with flagellar genes we addressed the question, if CC1462 is required for optimal PopA-dependent motility. A CC1462 deletion mutant was generated in *C. crescentus* CB15 wild-type and its laboratory adapted derivative NA1000³¹. Growth rates and morphologies of strains harboring the deletion were similar to wild-type (data not shown), as were surface attachment and expression of pili (Fig. S3). Motility scored on semi solid agar plates was indistinguishable from wild-type and a $\Delta popA \Delta CC1462$ double mutant displayed the same phenotype as a $\Delta popA$ single mutant (Fig. 4A). Consistently, electron microscopy and immunoblot analysis confirmed the presence of a single polar flagellum and similar flagellin levels in these mutants (Fig. 4B). Overexpression of CC1462 from an IPTG inducible plasmid led to a 20% decrease in motility in CB15 and $\Delta popA$ when compared to the non-induced samples (Fig. 4C). Similar effects are observed in the NA1000 background. Differences in growth rates were not observed (Fig. S4).

In summary, deletion of CC1462 has no phenotype whereas overexpression of CC1462 leads to a slight reduction of *C. crescentus* cell motility.

CC1462 localizes to the cell poles in a PopA-dependent manner.

PopA localization to the incipient flagellated pole is dependent on PodJ⁸. While PodJ is degraded during G1-to-S transition and disappears from the differentiating pole¹⁴, PopA is retained. This speaks for an additional factor that retains PopA at the old stalked pole. To test whether CC1462 fulfills this function, PopA localization in a $\Delta CC1462$ strain was analyzed. PopA displayed the same typical bipolar localization pattern in a $\Delta CC1462$ mutant (Fig. S5A) strongly indicating that CC1462 does not mediate PopA polar localization. Likewise, CC1462 does not affect RcdA localization to the cell pole (Fig. S5C and S5D). It has been reported that PopA interferes with CpdR localization during G1-to-S transition, although a direct interaction between these proteins could not be shown⁸. This raised the question, if CC1462 mediates the PopA contribution to CpdR localization. However, CpdR localization was not affected in a $\Delta CC1462$ mutant (Fig. S5B), arguing against such a hypothesis.

In a next step, C- and N-terminal YFP tagged versions of CC1462 were expressed from a plasmid-borne vanillate inducible promoter to analyze its subcellular distribution in different mutant backgrounds. In agreement with its specific interaction with PopA, both N- and C-terminal YFP tagged CC1462 fusion proteins localized to the cell poles in a PopA-dependent manner. Interestingly, C-terminal

fusions led to a much brighter overall signal indicating that a C-terminal tag might stabilize the protein and obscure the physiological localization behavior of the protein (Fig. 5A). Thus, the N-YFP-CC1462 fusion protein was used to test CC1462 localization in mutant backgrounds that affect its partner PopA. In summary, CC1462 strictly followed the differential localization pattern of PopA in all strains tested, emphasizing its tight interaction with and functional dependency of PopA (Fig. 5B). In particular, PopA and CC1462 localization to the flagellated pole is eliminated in a *podJ* mutant (Fig. 5B). Likewise, a strain lacking all diguanylate cyclases (cdG^0 , S. Abel and U. Jenal, unpublished) is unable to localize PopA and CC1462 to the stalked pole. It is important to note that while PopA still localizes to the presumable flagellated pole (cell polarity is obscured in the cdG^0 strain) CC1462 shows a diffuse fluorescence or non-polar foci in this strain. Likewise, CC1462 fails to localize to both poles in a strain expressing a PopA I-site mutant (Fig. 5C). Together this argues that in order to recruit CC1462 to the cell poles, PopA needs to be in its c-di-GMP activated state. Finally, the expression of a single cyclase, PleD, in the cdG^0 strain rescues both PopA and CC1462 localization (Fig. 5B). Also, RcdA or CpdR were not required for localization of CC1462 to the cell poles (Fig. 5D and 5E).

CC1462 deletion mutants do not affect CtrA degradation.

In *popA* mutants, RcdA and CtrA fail to localize to the stalked pole resulting in stabilized CtrA⁸. To test if CC1462 is involved in controlling CtrA turnover, CtrA levels were monitored in synchronized cultures of the *CC1462* mutant by immunoblot analysis. As shown in Fig. 6A, CC1462 does not influence CtrA degradation nor does its absence restore CtrA degradation in the $\Delta popA$ mutant background. This argues against CC1462 playing a role as positive or negative factor in PopA-mediated CtrA degradation. Similarly, overexpression of CC1462 could not block CtrA degradation (Fig. 6B).

In summary, these data suggest that CC1462 is not involved in CtrA degradation control. This is consistent with the observation that RcdA localization is not impaired in $\Delta CC1462$ mutants (Fig. S5C).

Cell cycle-dependent degradation of CC1462 requires ClpX.

The assembly and subsequent ejection of the flagellum are tightly coupled to the *C. crescentus* cell cycle. Upon flagellar ejection, some of its structural components are specifically degraded³³⁻³⁵. CC1462 is encoded in a flagellin cluster and has a C-terminally exposed hydrophobic amino acid (Fig. 3A), a hallmark of protease substrate recognition³⁶. To address the question, if CC1462 is also subject of degradation, CC1462 protein levels were monitored during cell cycle with polyclonal antibodies raised against CC1462. We found that protein levels in $\Delta popA$, $\Delta rcdA$ and

$\Delta cpdR$ mutants were elevated compared to wild-type, whereas $\Delta pleD$ and $\Delta CC2616$ mutants showed no effect on CC1462 levels (Fig. 7A).

In a next step, CC1462 levels were analyzed during cell cycle in wild-type and the mutants $\Delta popA$, $\Delta rcdA$ and $\Delta cpdR$. In wild-type, CC1462 was degraded during G1-to-S phase transition, whereas in the $\Delta popA$, $\Delta rcdA$ and $\Delta cpdR$ deletion mutants CC1462 was stabilized (Fig. 7B). This pattern is similar to the CtrA degradation pattern in wild-type and the respective mutants, although CtrA and CC1462 degradation patterns differ in time suggesting that CtrA is eliminated before CC1462. The observed cell cycle degradation pattern of CC1462 together with the requirement of this process for PopA, RcdA, and CpdR suggested that ClpXP might be involved in timed destruction of CC1462. To test this, we made use of a xylose inducible copy of a dominant negative ATPase mutant of the essential ClpX subunit of the ClpXP protease³⁷. As shown in Fig. 7C, induction of the $clpX^{ATP*}$ allele lead to a rapid accumulation of both CtrA and CC1462, while levels of FliF, a ClpAP substrate³⁴, were not affected. Taken together, these results demonstrate that CC1462 is degraded during the G1-to-S transition by ClpXP after the degradation of CtrA has taken place.

CC2616 is a guanine deaminase homolog.

The *CC2616* gene is located in a gene cluster together with genes encoding components for xanthine degradation. In addition, three hypothetical genes are part of this locus. Pfam database search²³ revealed that CC2616 protein possesses an aminohydrolase domain and belongs to the subfamily of guanine deaminases (Fig. 8A). Guanine deaminases are ubiquitous metallo enzymes catalyzing the hydrolytic deamination of guanine to xanthine (Fig. 8B). This reaction irreversibly removes purine bases from the cellular pool, which then relieves the PurR-mediated repression of purine biosynthesis genes^{38,39}.

Using the guanine deaminase Blr3380 from *B. japonicum* as a template (R. Agarwal, unpublished, PDB: 2OOD), an HHpred-based²⁸ model structure of CC2616 was generated (Fig. 8C). This structure shows the typical TIM barrel fold of amidohydrolases, which contain an active site bound to a divalent cation⁴⁰. Alignment of CC2616, the well known guanine deaminase YgfP from *E. coli*⁴¹ and the guanine deaminase from human brain⁴¹ showed that the well conserved zinc binding motif is conserved arguing that CC2616 could indeed have aminohydrolase activity (Fig. 8D).

A *CC2616* deletion inversely influences attachment and motility.

In order to elucidate the cellular function of CC2616, a clean deletion of *CC2616* was generated in *C. crescentus* CB15 wild-type. Growth rates and morphologies of the

strains harboring the deletion were similar to wild-type (data not shown). However, deletions showed reduced motility and surface attachment properties (Fig. 9A and 9B), a phenotype generally associated with increased levels of c-di-GMP⁴². Importantly, the motility and attachment phenotype could not be complemented by introducing a wild-type CC2616 copy on a vanillate inducible plasmid (Fig. S6).

As *C. crescentus* uses the flagellum, pili and holdfast for optimal attachment^{43,44}, CC2616 mutants were also analyzed for their ability to build holdfast and pili. They were not affected in the deletion mutants (Fig. S7). However, increased pili expression and a timing difference in holdfast biogenesis cannot be excluded yet.

CC2616 localization is dependent on PopA and CpdR.

As described for CC1462, we also examined if CC2616 could play a role as localization factor or connector protein for PopA, RcdA and CpdR. However, microscopic analysis revealed that CC2616 is dispensable for PopA, RcdA and CpdR localization as their cellular distributions remained unaltered in Δ CC2616 deletion mutants (Fig. S8). As expected from these results, CtrA turnover during cell cycle was not altered in a CC2616 mutant and CC2616 could not rescue CtrA degradation in a Δ popA mutant. Cell cycle regulated levels of the chemoreceptor McpA³² were monitored as synchronization quality control (Fig. S9).

All players involved in cell cycle control dynamically localize to the cell pole. Moreover, a general protein localization screen by Werner and coworkers⁴⁵ identified CC2616 as being positioned to the cell pole. To verify polar localization, a C-terminal CC2616-YFP fusion protein was expressed from a plasmid-borne vanillate inducible promoter. CC2616 localized to both cell poles, however, the large fraction of cells displayed one focus at the stalked pole (50 %), whereas 20% of the cells showed a bipolar distribution pattern. Consistent with its direct interaction with PopA, CC2616 subcellular distribution was strictly dependent on PopA (Fig. 10A) and examination of CC2616 levels during cell cycle using antibodies raised against purified hexahistidine tagged CC2616 showed that C2616 protein was always present during cell cycle (Fig. 11).

Surprisingly, CC2616 localization was dramatically reduced in a Δ cpdR mutant, indicating that CpdR is required for its localization or robust maintenance at the cell pole. Since CpdR is required for polar positioning of the ClpXP protease¹⁰ we wanted to exclude that the CpdR effect on CC2616 is indirect. When CC2616-YFP distribution was analyzed in a strain with conditional expression of *clpP*, coding for the peptidase subunit of the protease, CC2616 localization was unchanged under ClpP depletion conditions (Fig. 10D). This experiment suggested that the role of CpdR for polar localization of CC2616 cannot be explained indirectly through ClpXP. In contrast, RcdA, CC1462 and PleD are not required for CC2616 localization (Fig. 10A, B).

Immunoblots against CC2616 confirm that CC2616-YFP fusions are stably expressed in $\Delta popA$ and $\Delta cpdR$ mutants (Fig. 10C). It is important to note that CC2616-YFP seems to be partially processed. However, the fact that the extent of processing seems to be very similar in all three strains tested argues against the possibility that one of the processed derivatives (e.g. YFP alone) is responsible for the differential localization behavior.

3.2.4 Discussion

CC1462 is a new member of the PopA-mediated class of ClpXP substrates

In this study we identified CC1462, a new ClpXP substrate of unknown function. Like other ClpXP substrates CC1462 is directed to the cell pole by the c-di-GMP effector protein PopA and is removed by the polar ClpXP protease during swarmer-to-stalked cell transition. In *C. crescentus*, several cell cycle-regulated proteins are specifically degraded during a particular stage of the cell cycle to provide characteristic protein fluctuation patterns^{46,47}. These include not only proteins involved in flagellar function^{33,34} and chemotaxis³², but also proteins required for cell division, cell cycle progression, DNA methylation and c-di-GMP signaling^{7,9,49,50}. Among them are only a few known ClpXP substrates. These include the replication inhibitor CtrA^{5,6}, the swarmer cell specific phosphodiesterase PdeA⁹, the ClpXP localization factor CpdR⁵⁰ and the NAD(P)H-binding regulator KidO⁵¹. All of these substrates sequester to the stalked pole during G1-S transition and require the polar ClpXP protease to be degraded. Substrate specificity is usually conferred by short hydrophobic tails exposed at the N- or C-terminus or by substrate-specific adaptor proteins^{9,36}. CC1462, although a ClpXP substrate, does neither contain an N-terminal nor the classical C-terminal recognition motif, but it contains a short hydrophobic stretch at the C-terminus, which is interrupted by three negatively or uncharged amino acids and ends with a final alanine (Fig. 3). While CtrA, CpdR and KidO display completely hydrophobic C-termini, PdeA also lacks the conserved motif (Fig. 12). However, altering its last two amino acids to negatively charged residues leads to stabilization of PdeA⁹. This suggests that in *C. crescentus* other motifs might be involved in substrate recognition and one can speculate that the final alanine at the C-terminus of CC1462 might be sufficient as signal. It is equally possible that CC1462 degradation, like PdeA, requires a specific adaptor protein. The observation that CC1462 degradation requires CpdR points in this direction. CpdR is a bifunctional protein that acts both as polar localization factor for ClpXP and as specific Phosphorylation-dependent adaptor protein to deliver PdeA to the ClpXP protease⁹. CC1462 degradation also requires RcdA, the exact function of which is still unknown. While RcdA is not required for ClpXP-mediated degradation of CtrA *in vitro*⁶ such experiments could help clarify the potential role of CpdR or RcdA for CC1462 degradation.

Degradation of different ClpXP substrates during the G1-to S-phase transition follows a specific order and timing. PdeA is the earliest known substrate to be degraded and does not require the PopA pathway. This is consistent with the idea that PdeA keeps c-di-GMP concentrations low in swarmer cells and that its degradation contributes to the c-di-GMP upshift that eventually targets PopA to the

cell pole and initiates the next wave of ClpXP-mediated degradation, which includes CtrA and KidO⁹. For these two substrates, PopA seems to serve primarily as recruitment factor^{9,51}. Also, degradation of both CtrA and KidO requires RcdA. So far no adaptor protein is known for CtrA and, in contrast to PdeA, its degradation by ClpXP *in vitro* was found to be adaptor independent⁶. It is possible that the PopA pathway serves primarily to increase the CtrA concentration in the proximity of ClpXP to efficiently mediate its degradation. The bifunctional protein KidO inhibits Z-ring formation and plays a role in establishing the swarmer cell program. It has to be degraded during swarmer-to-stalked cell transition to license cytokinesis and chromosome replication initiation⁵¹. Next, CC1462 and CpdR are removed in a ClpXP-dependent manner. It is assumed that CpdR removal turns off the degradation pathway at the stalked pole after cells have initiated chromosome replication and prevents the degradation of newly synthesized CtrA in the predivisional cell⁵⁰. We found that CC1462 degradation takes place about 20 minutes after CtrA (Fig. 7). Thus, CC1462 turnover is similarly delayed compared to CtrA as the degradation of CpdR. It is important to note that the requirements for the degradation of CC1462 are different from those for CtrA. Not only CC1462 directly interacts with PopA, but it does not require RcdA not for its polar localization, but instead CpdR for efficient degradation by ClpXP. Whether CpdR degradation also requires RcdA is not known, but it is formally possible that the two proteins are organized in the same hierarchy class of ClpXP substrates. It is formally even possible that CC1462 could be involved in the degradation of CpdR and in turning off the degradation pathway after chromosome replication has started.

The molecular and cellular function of CC1462 and the rationale for its PopA- and ClpXP-dependent removal during the cell cycle are not clear. The *CC1462* gene is located in a flagellar gene cluster implying a function in cell motility or possibly the cellular organization of the motor complex (Fig. 3). However, deleting *CC1462* had no observable effect on flagellar assembly or function (Fig. 4). This is in agreement with experiments from Faulds-Pain and coworkers¹⁹ in *C. crescentus* showing that a *CC1462* deletion did not affect motility analyzed on swarm agar plates. However, these findings are in contrast with observations made in homologous proteins from *Pseudomonas fluorescens* and *Vibrio anguillarum*. In these organisms, insertion mutants led to an elongated flagellum and had effects on cell motility^{25,26}. While in *P. fluorescens* motility was 50% increased, deletion of this ORF in *V. anguillarum* led to 11 % decrease in motility. Yet no complementation experiments were presented in these studies and it can thus not be excluded that they were due to polar effects of the inserted sequences. Interestingly, overexpression of CC1462 led to a significant decrease in motility on semisolid agar plates (Fig. 4). The molecular basis for this is not known, but might be related to the drastic change in CC1462 protein levels

during the cell cycle under these conditions (Fig. 6). Since this phenotype is specific for motility (surface attachment is not affected), it is possible that overexpression specifically impacts cell motility or chemotaxis, phenotypes which are known to be connected to decreased swarm sizes⁵². A careful analysis of motor composition and performance under these conditions could help clarify this issue.

An important difference between CC1462 and other proteins interacting with PopA physically or functionally (RcdA, CtrA, KidO) is its positioning to the flagellated pole. While other PopA-dependent ClpXP substrates localize to the old cell pole immediately before they are degraded, CC1462 localizes primarily to the stalked cell pole in stalked cells and shows a bipolar localization pattern in a large fraction of predivisional cells (Fig. 5). This strongly argues that it is recruited to the flagellated pole relatively early during the division cycle. This behavior speaks against CC1462 being only a target of the PopA-ClpXP pathway and suggests that it functionally interacts with PopA at the flagellated pole long before the degradation pathway is activated. This suggests that CC1462 has a swarmer cell specific function that might be obscured by our superficial phenotypic analysis or by functional redundancy of this particular pathway. E.g. the flagellum has been postulated to play a role as sensory device for the adaptation of bacteria to their life on surfaces. It is possible that CC1462 is not important for motility per se, but plays a role in a downstream process leading to switch to sessility.

CC2616 is a guanine deaminase homolog that interacts with PopA without being degraded during cell cycle

The CC2616 protein is recruited to the cell poles in a PopA dependent manner (Fig. 10), but in contrast to CC1462, this protein is not degraded during the cell cycle (Fig. 11). CC2616 is annotated as a guanine deaminase, an enzyme that is found throughout all kingdoms of life. They catalyze the hydrolytic deamination from guanine to xanthine⁴⁰. This reaction irreversibly eliminates the guanine base from further utilization as guanylate nucleotide by the salvage pathway⁵³. However, analysis of the *C. crescentus* metabolic pathways in the KEGG database²² shows that xanthine can be degraded into urate, but further enzymes to metabolize urate into carboxylate and ammonia are not conserved.

Two types of guanine deaminases have evolved separately⁴⁰. Plant, archaeal and some bacterial deaminases belong to the cytidine deaminase-like protein family, while mammalian, insect, fungal and some bacterial guanine deaminases belong to the TIM barrel metallohydrolyase superfamily. The latter are characterized by a specific nine-residue sequence that is involved in cation binding, predominantly Zn²⁺. This motif is conserved in CC2616. In addition to this motif, many eukaryotic and some bacterial guanine deaminases contain a specific tetrapeptide at their C-

terminus. This motif is present on many signaling proteins and can be recognized by PDZ domain proteins⁵⁴. PDZ interactions work as scaffolds and help to cluster membrane-anchoring proteins, cytoskeletal elements and signaling proteins and might be involved in polarity establishment in prokaryotes⁴⁰. However, this second specific C-terminal tetrapeptide is not conserved in CC2616 making it unlikely that CC2616 is recognized by a PDZ domain protein.

So far, it is not clear if CC2616 acts as guanine deaminase or has acquired a novel protein function. However, it is tempting to speculate that CC2616 is an active enzyme and plays a role in the regulation of the c-di-GMP pool. In higher eukaryotes for example, guanine deaminases have adopted additional functions. It was shown that expression of guanine deaminases is tissue specific and restricted to certain areas in the brain⁵³, where they play a role in the regulation of dendrite branching⁵⁵. It is thought, that neurons use guanine deaminases to regulate neuronal signaling⁵⁶ by reducing the amount of free guanylate nucleotides such as cGMP and GTP, which are needed for the activity of small GTPases and cGMP dependent protein kinases⁵⁶. Our finding that deletion of CC2616 leads to increased attachment and decreased motility (Fig. 9), an effect seen for strains with elevated c-di-GMP levels^{42,57} is consistent with the idea that this guanine deaminase might decrease the GTP levels normally used for the synthesis of c-di-GMP. Alternatively, CC2616 could act directly on the c-di-GMP pool by inactivating c-di-GMP via deamination, instead of hydrolytic cleavage. In both cases, one would expect to detect increased levels of c-di-GMP in a CC2616 mutant strain.

Interestingly, CC2616, like CC1462 (see above) localizes to both cell poles (Fig. 10). The observation that CC2616 predominantly localizes to the stalked pole of predivisional cells and that a relatively small fraction of predivisional cells shows bipolar distribution of CC2616 argues that CC2616 arrives at the flagellated pole at a late time point, immediately before or after cytokinesis takes place. Localization to both poles depends on PopA and CpdR. While the PopA requirement for swarmer pole localization can easily be rationalized (PopA also localizes to this site), CpdR presumably is inactive and delocalized in swarmer cells. Therefore, the swarmer pole localization of CC2616 and a possible involvement of CpdR in this process need to be evaluated more carefully. However, CpdR clearly plays a role in CC2616 positioning to the stalked pole. Since ClpXP does not seem to degrade CC2616, it is unlikely that the protease is involved in this process. It is possible that CC2616 acts as a linker between the Phosphorylation-dependent CpdR and the c-di-GMP-dependent PopA branch of the network controlling the timing of CtrA, KidO and CC1462 degradation. However, the role of CC2616 is unclear as it does not have an influence on the degradation of ClpXP substrates and is not binding directly to any of the proteins involved in CtrA degradation.

This brings up the question why an enzyme involved in purine catabolism is targeted to the pole? A possible explanation could be that PopA and/or CpdR control its activity by sequestration. Evidence for localized activity of enzymes comes from the *C. crescentus* diguanylate cyclase PleD where activation and subcellular localization are coupled⁵⁸. Another example was reported in *Synechococcus elongatus* where the activity of the histidine kinase CikA, which is part of the cyanobacterial circadian clock is coupled to its subcellular localization⁵⁹. Sometimes bacterial regulatory proteins also localize to the cell poles without having a direct function at those positions. This was observed for the sensor kinase CckA which ultimately phosphorylates CtrA and CpdR in swarmer cells. It was shown that localization of CckA to the incipient flagellated pole in predivisional cells is important to generate a protected microenvironment to avoid downregulation by its own inhibitor⁶⁰. A similar strategy for CC2616 would be conceivable as well.

PopA interacts with multiple proteins

Although PopA is a relatively small protein, it interacts with at least four proteins at different subcellular sites; RcdA, PodJ, CC1462 and CC2616 (Fig. 2). This raises the question about potential binding sites on PopA and about the cellular requirements for efficient binding. We showed previously that PopA uses its N-terminal receiver domains as interaction platform for RcdA and CC1462 (A. Moser and U. Jenal, unpublished. See section 3.1) and the data presented here suggest c-di-GMP-independent binding between PopA and these proteins. However, whether RcdA and CC1462 compete for overlapping binding sites or whether binding occurs independently is not clear yet. In an alternative scenario, RcdA and CC1462 would bind cooperatively to PopA, but as these proteins localize independently from each other, this possibility seems to be rather unlikely. For CC2616 and PodJ, the PopA domains required for interaction are not known, although our experiments argue that PodJ interacts stronger with c-di-GMP activated PopA. This suggests that c-di-GMP can modulate binding properties between PodJ and PopA. Analyzing cellular functions and localization of these proteins while overexpressing other interaction partners will help to elucidate the binding properties of these proteins to PopA.

Growing evidence suggests the existence of a macromolecular protease complex localized at the stalked pole. This complex is dynamically assembled around the ClpXP protease in response to phosphorylation and c-di-GMP dependent stimuli to control the localized degradation of key substrate proteins. PopA is an important component of this polar “degradasome” and its role might be to deliver substrates such as CtrA, KidO and CC1462 to the protease. However, PopA also localizes proteins like CC2616, which are not proteolytically processed. It is possible that CC2616 plays a subtle role in the degradasome machinery and that PopA helps to

organize this function. Alternatively, CC2616 (and CC1462) function are unrelated to the actual degradation processes. PopA would then be involved in several pathways, possibly as a coordinating platform. One can speculate that localization of PopA to the incipient flagellated pole is linked to its function in cell motility, stalk biogenesis and holdfast formation. Since CC1462 and CC2616 are not involved in these processes, it is likely that more proteins interact with PopA mediating these PopA-dependent phenotypes.

3.2.5 Material and Methods

Growth Conditions

The bacterial strains and plasmid used in this study are listed in Table S1. *Caulobacter crescentus* strains were grown in peptone yeast extract (PYE⁶¹) or minimal media supplemented with 0.2% glucose or 0.3% D-xylose (M2G or M2X⁶¹) at 30°C with constant shaking (150 rpm). When selection was required antibiotics in the following concentrations were added: (solid/liquid media in µg/ml): gentamycin (5/0.5), kanamycin (20/5), nalidixic acid (20/not used) and oxytetracycline (5/2.5). For inducible gene expression the medium was supplemented with 1 mM vanillate or 1 mM IPTG. For synchronization experiments newborn swarmer cells were isolated by Ludox gradient centrifugation⁶² and released into fresh minimal medium. When necessary the medium was supplemented with 1 mM Vanillate or 0.3% xylose. For synchronization with inducible constructs, 1 mM vanillate was added to the growth medium 2 h prior synchrony.

E. coli strains were grown in Luria Broth (LB) at 37 °C. When necessary for selection the following antibiotic concentrations were used: (solid/liquid media in µg/ml) ampicillin (100/50), gentamycin (20/15), kanamycin (50/30) and oxytetracycline (12.5/12.5).

Strains and Plasmids

The bacterial strains and plasmid used in this study are listed in Table S1. Strains were constructed and propagated in *E. coli* DH10B and transferred by conjugation⁶¹ into *C. crescentus* strains. The Strain Arctic^R BL21 (DE3) (Stratagene, USA) was used for protein overexpression and strain MM337⁶³ for bacterial two hybrid assays. Other general molecular biology techniques not listed here are described elsewhere⁶⁴. Detailed protocols of strain and plasmid constructions are available on request.

Microscopy

DIC and fluorescence microscopy were performed on a DeltaVision Core (Applied Precision, USA)/Olympus IX71 microscope equipped with an UPlanSApo 100x/1.40 Oil objective (Olympus, Japan) and a coolSNAP HQ-2 (Photometrics, USA) CCD camera. Cells were placed on a patch consisting of 1% agarose in water (Sigma, USA). Images were processed with softWoRx version 5.0.0 (Applied Precision, USA) and Photoshop CS3 (Adobe, USA) software.

For the visualization with electron microscopy, exponential growing *C. crescentus* cultures were applied to glow-discharged, carbon-coated grids and negatively stained with 2 % (w/v) uranylacetate. The samples were viewed in a Philips Morgagni 268D electron microscope at a nominal magnification of 20,000× and an acceleration voltage of 80 kV.

Coimmunoprecipitation Experiments

The coimmunoprecipitation experimental procedure is based on McGrath and coworkers¹². Briefly, 1 l exponential growing culture was harvested and washed with 20 mM HEPES pH 7.4, 100 mM NaCl, 20 % glycerol. After resuspension the buffer was supplemented with 0.05% Triton X, protease inhibitor (1 x Complete Mini Protease Inhibitor, Roche) and DNaseI (Fermentas, USA). Cells were French pressed and clarified lysates were precleared for 30 min at 4 °C with 30 µl of protein A agarose beads (Invitrogen, USA)/ml of lysate. Supernatants were collected and mixed with 20 µl of protein A agarose beads linked to M2 monoclonal antibody (Sigma-Aldrich, USA) and incubated over night at 4°C. Samples were washed 5-6 times with 20 mM HEPES pH 7.4, 100 mM NaCl, 20 % Glycerol-containing protease inhibitor. After the last centrifugation step the pellet was mixed with SDS loading dye and incubated at 37°C for 30 min to remove the precipitated samples from the beads.

Bacterial Two-Hybrid Analysis

Bacterial Two Hybrid Analysis was performed according to Karimova and coworkers¹⁷. Proteins of interest were fused N or C-terminally to the T18 or T25 fragment of the *B. pertussis* adenylate cyclase. Two microliter of the MM337 culture containing pUT18 and pKT25 derivatives was spotted on a McConkey agar base plate supplemented with 0.1% maltose, kanamycin and ampicillin and grown at 30 °C.

Protein Expression and Purification

E. coli BL21 (DE3) (Stratagene, USA) carrying either His₆-CC1462 or His₆-CC2616 expression plasmids were grown in LB to an OD₆₀₀ of 0.5. Expression was induced by adding IPTG to a final concentration of 1 mM for 2 h at 30°C. Cells were harvested by centrifugation, resuspended in 50 mM Na-phosphate pH 8, 500 mM NaCl, 5 mM imidazole and lysed by French pressing. Clarified lysates were loaded on a HP HisTrap column (GE Healthcare, UK) attached to an ÄKTApurifier (GE Healthcare, UK). Protein was eluted by raising the imidazole concentration to 500 mM. Further purification and buffer exchange were performed by size exclusion chromatography on a Superdex-75 column (GE Healthcare, UK) using 1 x PBS (phosphate buffered saline) pH 7.4 for CC1462 and 1 x PBS pH 7.4, 2 mM DTT, 10% glycerol as a buffer. The protein fractions were lyophilized for antibody production.

Antibody Production and Immunoblots

CC1462 and CC2616 fused to an N-terminal His₆ tag were purified as described above. Lyophilized protein samples were injected into rabbits for polyclonal antibody production (Josman, LLCTM, USA). Antibodies against CC1462 were diluted 1:1000, antibodies against CC2616 1:5000. Antibodies against PopA, CtrA, McpA, RcdA and GFP were diluted described in the cited publications^{5,8,32}. Primary antibodies were detected by HPR-conjugated swine anti-rabbit secondary antibodies (Dako Cytomation, Denmark). Western blots were developed with ECL detection reagents (Western Lightning, Perkin Elmer, USA).

ClpP Depletion Experiment

C. crescentus cultures expressing xylose dependent ClpP⁷ and a C-terminal CC2616-GFP fusion protein under the control of vanillate promoter (non induced) were shifted from xylose containing medium (M2GX) to restrictive conditions (M2G) for 9 h. Levels of ClpP and CC2616-GFP were monitored immunologically by α -ClpP and α -CC2616 antibodies. Localization of CC2616-GFP was analyzed by DIC and fluorescence microscopy (described above).

Motility Assays

C. crescentus colonies were spotted onto PYE soft agar plates (0.3% agar) and incubated for 72 h at 30 °C. Plates were then scanned (ScanMaker i800 scanner, Microtek, Germany) and analyzed using Photoshop CS3 (Adobe, USA) and ImageJ (NIH, USA) softwares. For all motility experiments the mean of at least three independent colony sizes is shown. Error bars represent standard deviation.

Attachment Assays

C. crescentus strains were grown in PYE in 96-well microtiter plates (Falcon, USA) for 24 h under constant shaking (200 rpm). After crystal violet (0.3% crystal-violet, 5% isopropanol, 5% methanol) staining of the attached biomass it was dissolved with 20% acetic acid and optical density at 600 nm was measured in a photospectrometer (Genesys6, Thermo Spectronic, USA). For each strain a mean of at least six independent colonies is shown. Error bar represent standard deviation.

Holdfast Staining

An exponential growing *C. crescentus* culture was stained with Oregon Green or Rhodamine coupled wheat germ agglutinin (0.2 mg/ml, Invitrogen, USA). After washing the stained samples were visualized by fluorescence microscopy.

Phage Sensitivity Assay

C. crescentus colonies were streaked through a phage CBK lysate on a PYE plate. After 24 h of growth at 30°C plates could be analyzed. A $\Delta pilA$ strain was used as negative control as this strain is resistant due to the absence of pili.

Acknowledgements

We thank Fabienne Hamburger for strains and plasmids, Suzette Moes and Dr. Paul Jenö for mass spectrometry analysis, Vesna Olivieri and Ursula Sauder for electron micrographic pictures of *C. crescentus* and Dr. Jutta Nesper for critical reading of this manuscript. This work was supported by the Deutsche Forschungsgemeinschaft grant JE 442/1-1 554 935.

3.2.6 References

1. Poindexter, J.S. The *Caulobacters*: Ubiquitous unusual bacteria. *Microbiological Reviews* **45**, 123-179 (1981).
2. Degnen S.T. and Newton, A. Chromosome replication during development in *Caulobacter crescentus*. *Journal of Molecular Biology* **64**, 671-680 (1972).
3. Marczynski, G.T. and Shapiro, L. Cell-cycle control of a cloned chromosomal origin of replication from *Caulobacter crescentus*. *Journal of Molecular Biology* **226**, 959-77 (1992).
4. Quon, K.C., Yang, B., Domian, I.J., Shapiro, L. and Marczynski, G.T. Negative control of bacterial DNA replication by a cell cycle regulatory protein that binds at the chromosome origin. *Proceedings of the National Academy of Sciences of the United States of America* **95**, 120-5 (1998).
5. Domian, I.J., Quon, K.C. & Shapiro, L. Cell type-specific phosphorylation and proteolysis of a transcriptional regulator controls the G1-to-S transition in a bacterial cell cycle. *Cell* **90**, 415-24 (1997).
6. Chien, P., Perchuk, B.S., Laub, M.T., Sauer, R.T. and Baker, T. a Direct and adaptor-mediated substrate recognition by an essential AAA+ protease. *Proceedings of the National Academy of Sciences of the United States of America* **104**, 6590-5 (2007).
7. Jenal, U. and Fuchs, T. An essential protease involved in bacterial cell-cycle control. *The EMBO Journal* **17**, 5658-69 (1998).
8. Duerig, A., Abel, S., Folcher, M., Nicollier, M., Schwede, T., Amiot N., Giese, B. and Jenal, U. Second messenger-mediated spatiotemporal control of protein degradation regulates bacterial cell cycle progression. *Genes & Development* **23**, 93-104 (2009).
9. Abel, S., Chien, P., Wassmann, P., Schirmer, T., Kaefer, V., Laub, M.T., Baker, T.A. and Jenal, U. Regulatory Cohesion of Cell Cycle and Cell Differentiation through Interlinked Phosphorylation and Second Messenger Networks. *Molecular Cell* **43**, 550-560 (2011).
10. Iniesta, A.A., McGrath, P.T., Reisenauer, A., McAdams, H.H. and Shapiro, L. A phospho-signaling pathway controls the localization and activity of a protease complex critical for bacterial cell cycle progression. *Proceedings of the National Academy of Sciences of the United States of America* **103**, 10935-40 (2006).
11. Biondi, E.G., Reisinger, S., Skerker, J.M., Arif, M., Perchuk, B.S., Ryan, K.R. and Laub, M.T. Regulation of the bacterial cell cycle by an integrated genetic circuit. *Nature* **444**, 899-904 (2006).
12. McGrath, P.T., Iniesta, A. a, Ryan, K.R., Shapiro, L. and McAdams, H.H. A dynamically localized protease complex and a polar specificity factor control a cell cycle master regulator. *Cell* **124**, 535-47 (2006).
13. Viollier, P.H., Sternheim, N. and Shapiro, L. Identification of a localization factor for the polar positioning of bacterial structural and regulatory proteins. *Proceedings of the National Academy of Sciences of the United States of America*, 13831-13836 (2002).

14. Hinz, A.J., Larson, D.E., Smith, C.S. and Brun, Y.V. The *Caulobacter crescentus* polar organelle development protein PodJ is differentially localized and is required for polar targeting of the PleC development regulator. *Molecular Microbiology* **47**, 929-41 (2003).
15. Lawler, M.L., Larson, D.E., Hinz, A.J., Klein, D. and Brun, Y.V. Dissection of functional domains of the polar localization factor PodJ in *Caulobacter crescentus*. *Molecular Microbiology* **59**, 301-16 (2006).
16. Chen, J.C., Hottes, A.K., McAdams, H.H., McGrath, P.T., Viollier, P.H. and Shapiro, L. Cytokinesis signals truncation of the PodJ polarity factor by a cell cycle-regulated protease. *The EMBO Journal* **25**, 377-86 (2006).
17. Karimova G., Pidoux J., Ullmann A., Ladant, D. A bacterial two-hybrid system based on a reconstituted signal transduction pathway. *Microbiology* **95**, 5752-5756 (1998).
18. Ely, B., Ely, T.W., Crymes, W.B. and Minnich, S. A. A family of six flagellin genes contributes to the *Caulobacter crescentus* flagellar filament. *Journal of Bacteriology* **182**, 5001-4 (2000).
19. Faulds-Pain, A. Birchall, C., Aldrige, C., Smith, W.D, Grimaldi, G., Nakamura, S., Miyata, T., Gray, J., Li, G., Tang, J.X., Namba, K., Minamino, T. and Aldridge P.D. Flagellin redundancy in *Caulobacter crescentus* and its implications for flagellar filament assembly. *Journal of Bacteriology* **193**, 2695-707 (2011).
20. Llewellyn, M., Dutton, R.J., Easter, J., O'donnol, D. and Gober, J.W. The conserved flaF gene has a critical role in coupling flagellin translation and assembly in *Caulobacter crescentus*. *Molecular Microbiology* **57**, 1127-42 (2005).
21. Anderson, P.E. and Gober, J.W. FlbT, the post-transcriptional regulator of flagellin synthesis in *Caulobacter crescentus*, interacts with the 5' untranslated region of flagellin mRNA. *Molecular Microbiology* **38**, 41-52 (2000).
22. Aoki K F, Kanehisa, M. Using the KEGG database resource. *Current Protocols in Bioinformatics* Unit 1.12 (2005).
23. Sonnhammer, E.L., Eddy, S.R. and Durbin, R. Pfam: a comprehensive database of protein domain families based on seed alignments. *Proteins* **28**, 405-20 (1997).
24. Finn, R.D., Mistry, J., Tate, J., Coggill, P., Heger, A, Pollington, J.E., Gavin, O.L., Gunasekaran, P., Ceric, G., Forslund, K., Holm, L., Sonnhammer, E.L.L., Eddy, S.R. and Bateman, A. The Pfam protein families database. *Database* **38**, 211-222 (2010).
25. McGee, K., Hörstedt, P. and Milton, D.L. Identification and characterization of additional flagellin genes from *Vibrio anguillarum*. *Journal of Bacteriology* **178**, 5188-98 (1996).
26. Capdevila, S., Martínez-Granero, F.M., Sánchez-Contreras, M., Rivilla, R. and Martín, M. Analysis of *Pseudomonas fluorescens* F113 genes implicated in flagellar filament synthesis and their role in competitive root colonization. *Microbiology* **150**, 3889-97 (2004).
27. Eletsky, A., Sukumaran, D.K., Xiao, R., Acton, T., Rost, B., Montelione, G. and Szyperski, T. NMR structure of protein YvyC from *Bacillus subtilis* reveals unexpected structural similarity between two PFAM families. *Proteins* **76**, 1037-1041 (2009).
28. Söding, J., Biegert, A. and Lupas, A.N. The HHpred interactive server for protein homology detection and structure prediction. *Nucleic Acids Research* **33**, W244-8 (2005).

29. Chen, L. and Helmann, J.D. The *Bacillus subtilis* sigma D-dependent operon encoding the flagellar proteins FliD, FliS, and FliT. *Journal of Bacteriology* **176**, 3093-101 (1994).
30. Duerig, A. Second messenger mediated spatiotemporal control of cell cycle and development. *PhD thesis* (2008).
31. Marks, M.E., Castro-Rojas C.M., Teiling, C., Du, L., Dpatral, V., Walunas, T.L. and Crosson, S. The genetic basis of laboratory adaptation in *Caulobacter crescentus*. *Journal of Bacteriology* **192**, 3678-88 (2010).
32. Tsai, J.-W. and Alley, M.R.K. Proteolysis of the *Caulobacter* McpA chemoreceptor is cell cycle regulated by a ClpX-dependent pathway. *Journal of Bacteriology* **183**, 5001-5007 (2001).
33. Grünenfelder, B., Gehring, S. and Jenal, U. Role of the cytoplasmic C-terminus of the FliF motor protein in flagellar assembly and rotation. *Journal of Bacteriology* **185**, 1624-1633 (2003).
34. Grünenfelder, B., Tawfilis, S., Gehrig, S., Østeras, M., Eglin, D. and Jenal, U. Identification of the protease and the turnover signal responsible for cell cycle-dependent degradation of the *Caulobacter* FliF motor protein. *Journal of Bacteriology* **186**, 4960-4971 (2004).
35. Jenal, U. The role of proteolysis in the *Caulobacter crescentus* cell cycle and development. *Research in Microbiology* **160**, 687-95 (2009).
36. Flynn, J.M., Neher, S.B., Kim, Y.I., Sauer, R.T. and Baker, T. a Proteomic discovery of cellular substrates of the ClpXP protease reveals five classes of ClpX-recognition signals. *Molecular Cell* **11**, 671-83 (2003).
37. Potocka, I., Thein, M., Østeras, M., Jenal, U. and Alley, M.R.K. Degradation of a *Caulobacter* soluble cytoplasmic chemoreceptor is ClpX-dependent. *Journal of Bacteriology* **184**, 6635-6641 (2002).
38. Meng, L.M. and Nygaard, P. Identification of hypoxanthine and guanine as the co-repressors for the purine regulon genes of *Escherichia coli*. *Molecular Microbiology* **4**, 2187-92 (1990).
39. Zalkin, H. and Ebbole, D.J. Organization and regulation of genes encoding biosynthetic enzymes in *Bacillus subtilis*. *Journal of Biological Chemistry* **263**, 1595-8 (1988).
40. Fernández, J.R., Byrne, B. and Firestein, B.L. Phylogenetic analysis and molecular evolution of guanine deaminases: from guanine to dendrites. *Journal of Molecular Evolution* **68**, 227-35 (2009).
41. Maynes, J.T., Yuan, R.G. and Snyder, F.F. Identification, expression, and characterization of *Escherichia coli* guanine deaminase. *Journal of Bacteriology* **182**, 4658-60 (2000).
42. Hengge, R. Principles of c-di-GMP signalling in bacteria. *Nature Reviews Microbiology* **7**, 263-73 (2009).
43. Assaf, L. and Jenal, U. Holdfast formation in motile swarmer cells optimizes surface attachment during *Caulobacter crescentus* development. *Journal of Bacteriology* **188**, 5315-5318 (2006).
44. Bodenmiller, D., Toh, E. and Brun, Y.V. Development of surface adhesion in *Caulobacter crescentus*. *Journal of Bacteriology* **186**, 1438-1447 (2004).

45. Werner, J.N., Chen, E.Y., Gubermann, J.M., Zippilli, A.R., Irgon, J.J. and Gitai, Z. Quantitative genome-scale analysis of protein localization in an asymmetric bacterium. *Proceedings of the National Academy of Sciences of the United States of America* **106**, 7858-63 (2009).
46. Grünenfelder, B., Rummel, G., Vohradsky, J., Röder, D., Langen, H. and Jenal, U. Proteomic analysis of the bacterial cell cycle. *Proceedings of the National Academy of Sciences of the United States of America* **98**, 4681-6 (2001).
47. Laub, M.T. Global analysis of the genetic network controlling a bacterial cell cycle. *Science* **290**, 2144-2148 (2000).
48. Kelly, A.J., Sackett, M.J., Din, N., Quardokus, E. and Brun, Y.V. Cell cycle-dependent transcriptional and proteolytic regulation of FtsZ in *Caulobacter*. *Genes & Development* **12**, 880-93 (1998).
49. Wright, R., Stephens, C., Zweiger, G., Shapiro, L. and Alley, M.R. *Caulobacter* Lon protease has a critical role in cell-cycle control of DNA methylation. *Genes & Development* **10**, 1532-1542 (1996).
50. Iniesta, A.A. and Shapiro, L. A bacterial control circuit integrates polar localization and proteolysis of key regulatory proteins with a phospho-signaling cascade. *Proceedings of the National Academy of Sciences of the United States of America* **105**, 16602-7 (2008).
51. Radhakrishnan, S.K., Pritchard, S. and Viollier, P.H. Coupling prokaryotic cell fate and division control with a bifunctional and oscillating oxidoreductase homolog. *Developmental Cell* **18**, 90-101 (2010).
52. Skerker, J.M., Prasol, M.S., Perchuk, B.S., Biondi, E.G. and Laub, M.T. Two-component signal transduction pathways regulating growth and cell cycle progression in a bacterium: a system-level analysis. *PLoS Biology* **3**, e334 (2005).
53. Paletzki, R.F. Cloning and characterization of guanine deaminase from mouse and rat brain. *Neuroscience* **109**, 15-26 (2002).
54. Sheng, M. and Sala, C. PDZ domains and the organization of supramolecular complexes. *Annual Reviews of Neuroscience* 1-29 (2001).
55. Akum, B.F., Chen, M., Gunderson, S.I., Riefler, G.M., Scerri-Hansen, M.M. and Firestein, B.L. Cypin regulates dendrite patterning in hippocampal neurons by promoting microtubule assembly. *Nature Neuroscience* **7**, 145-52 (2004).
56. Wennerberg, K., Rossman, K.L. and Der, C.J. The Ras superfamily at a glance. *Journal of Cell Science* **118**, 843-6 (2005).
57. Jenal, U. and Malone, J. Mechanisms of cyclic-di-GMP signaling in bacteria. *Annual Review of Genetics* **40**, 385-407 (2006).
58. Paul, R., Abel, S., Wassmann, P., Beck, A., Heerklotz, H. and Jenal, U. Activation of the diguanylate cyclase PleD by phosphorylation-mediated dimerization. *Journal of Biological Chemistry* **282**, 29170-7 (2007).
59. Zhang, X., Dong, G. and Golden, S.S. The pseudo-receiver domain of CikA regulates the cyanobacterial circadian input pathway. *Molecular Microbiology* **60**, 658-68 (2006).

60. Tsokos, C.G., Perchuk, B.S. and Laub, M.T. A dynamic complex of signaling proteins uses polar localization to regulate cell-fate asymmetry in *Caulobacter crescentus*. *Developmental Cell* **20**, 329-41 (2011).
61. Ely, B. Genetics of *Caulobacter crescentus*. *Methods in Enzymology* **204**, 372-384 (1991).
62. Jenal, U. and Shapiro, L. Cell cycle-controlled proteolysis of a flagellar motor protein that is asymmetrically distributed in the *Caulobacter* predivisional cell. *The EMBO Journal* **15**, 2393-406 (1996).
63. Karimova G, Ullmann A, Ladant, D. *Bordetella pertussis* adenylate cyclase toxin as a tool to analyze molecular interactions in a bacterial two-hybrid system. *International Journal of Medical Microbiology* **290**, 441-445 (2000).
64. Sambrook, J. *Molecular Cloning*. Cold Spring Harbour Press (1989).
65. Evinger, M. and Agabian, N. Envelope-associated nucleoid from *Caulobacter crescentus* stalked and swarmer cells. *Journal of Bacteriology* **132**, 294-301 (1977).
66. Aldridge, P., Paul, R., Goymer, P., Rainey, P. and Jenal, U. Role of the GGDEF regulator PleD in polar development of *Caulobacter crescentus*. *Molecular Microbiology* **47**, 1695-708 (2003).
67. Ackermann, M., Schauerte, A., Stearns, S.C. and Jenal, U. Experimental evolution of aging in a bacterium. *BMC Evolutionary Biology* **10**, 1-10 (2007).
68. Simon, R., Prieffer, U. & Puhler, A. A broad host range mobilization system for *in vivo* genetic engineering: Transposon mutagenesis in gram-negative bacteria. *Biotechnology* **784-790** (1983).
69. Khan, S.R., Gaines, J., Roop, R.M. and Farrand, S.K. Broad-host-range expression vectors with tightly regulated promoters and their use to examine the influence of TraR and TraM expression on Ti plasmid quorum sensing. *Applied and Environmental Microbiology* **74**, 5053-62 (2008).
70. Thanbichler, M., Iniesta, A.A and Shapiro, L. A comprehensive set of plasmids for vanillate- and xylose-inducible gene expression in *Caulobacter crescentus*. *Nucleic Acids Research* **35** (2007).
71. Roberts, R.C., Toochinda, C., Avedissian, M., Baldini, R.L., Gomes, S.L. and Shapiro, L. Identification of a *Caulobacter crescentus* operon encoding *hrcA*, involved in negatively regulating heat-inducible transcription, and the chaperone gene *grpE*. *Journal of Bacteriology* **178**, 1829-1841 (1996).

3.2.7 Figures and Figure Legends

Figure 1: PopA interacts with CC1462 and CC2616 *in vivo*.

A. CC1462 and CC2616 are interacting with PopA. Cell lysates of a $\Delta popA$ strain expressing C-terminal *flag*-tagged PopA from plasmid were immunoprecipitated with a monoclonal antibody recognizing the M2-epitope. The precipitates were run on SDS-PAGE and stained with Colloidal Blue Staining Kit (Invitrogen, USA). Two bands are visible in the immunoprecipitates with flag-tagged PopA, but are not present in the immunoprecipitates from a $\Delta popA$ strain expressing untagged PopA. The proteins CC2616 (≈ 50 kDa) and CC1462 (≈ 15 kDa) identified by tandem mass spectrometry are indicated with arrows.

B. The known interaction partner RcdA can be immunoprecipitated with *flag*-tagged PopA. α -PopA and α -RcdA immunoblot analysis from the precipitated samples show that RcdA is present in samples of tagged PopA, but it cannot be detected in samples of a $\Delta popA$ empty plasmid extract.

Figure 2: CC1462, CC2616 and PodJ_{cyt} interact directly with PopA.

The Bacterial Two-Hybrid System was used to validate the coimmunoprecipitation data of PopA. Positive interactions score in red on McConkey agar base plates with maltose, negative interactions in white. Detailed representation of the used constructs is shown in the panels on the right. For the membrane protein PodJ a truncated cytosolic version, PodJ_{cyt} was used.

A. PopA directly interacts with CC1462, CC2616 and weakly with PodJ_{cyt}.

B. PopA_{R357G} (I-site mutant) interacts directly with CC1462, CC2616, but not with PodJ_{cyt}.

Figure 3: CC1462 is a hypothetical protein encoded in a flagellin gene cluster.

A. Genetic organization of the α -flagellin locus in *C. crescentus*. The hypothetical gene *CC1462* (black arrow) is flanked by *fljK,L* and *J* flagellin genes and lies in the same locus of the flagellin translation regulators FlbT and FlaF and the regulatory protein FlaEY (grey arrows). The *CC1462* gene product contains a stretch with homology to FlaG domains (grey) and exhibits hydrophobic amino acids at its C-terminal end (high lightened in black, the hydrophobic amino acids are underlined). The peptide identified by mass spectrometry analysis is shown as ticked box.

B. The NMR structure of the FlaG domain protein YvyC from *B. subtilis* (blue, PDB: 2HC5) is compared to the modeled structure of CC1462 (green) using YvyC as a template. A peptide identified by mass spectrometry in the elongated N-terminus is depicted in red.

Figure 4: Overexpression of CC1462 influences swimming behavior.

- A. $\Delta CC1462$ clean deletion mutants do not affect motility. Swimming behavior on semi solid agar plates was quantified for wild-type, $\Delta popA$, $\Delta CC1462$ and $\Delta popA \Delta CC1462$ mutants. Mutants were generated in *C. crescentus* CB15 and NA1000 wild-types.
- B. $\Delta CC1462$ mutants are flagellated like wild-type and contain the same flagellin levels. Electron micrographic pictures show the presence of flagellum in swarmer cells of NA1000, $\Delta popA$ and $\Delta CC1462$ mutants. Flagellar protein levels were analyzed by α -flagellin immunoblots. NA1000 and $\Delta flgH$ (part of the flagellar basal body, Brown, 2009) were used as controls.
- C. Overexpression of CC1462 influences motility. Swimming behavior of CB15 and CB15 $\Delta popA$ expressing CC1462 from an IPTG inducible plasmid and the respective strains with empty plasmids was analyzed. Strains were compared under non induced and induced (0.5 mM IPTG) conditions. α -CC1462 immunoblots to test the overexpression are shown below the graph. CB15 and $\Delta CC1462$ were used as controls.

Figure 5: CC1462 localizes to the cell poles in a PopA-dependent manner.

- A. CC1462 localizes to the cell poles in a PopA-dependent manner. The localization of C-terminal and N-terminal tagged CC1462-YFP fusions on a vanillate inducible plasmid (non induced) was analyzed by fluorescence microscopy in the presence and absence of PopA. Polar foci are schematically shown in the right panels. Statistical analysis of the YFP-CC1462 localization in predivisional and stalked cell types is presented. SW pole: localization to the incipient swarmer pole, ST pole: localization to the stalked pole, two foci: bipolar localization, no focus: no polar localization, mislocalized: foci at any position.
- B. YFP-CC1462 strictly follows the PopA localization pattern. PopA-GFP localization on plasmid under the control of *popA* promoter was analyzed in NA1000, $\Delta podJ$, cdG^0 and cdG^0 expressing PleD from plasmid and compared to YFP-CC1462 localization in the same strain backgrounds. Schematic localization representations are shown in the panels below.
- C. YFP-CC1462 is completely delocalized in the presence of a PopA_{R357G} (I-site) mutant. The localization of an N-terminal YFP-CC1462 fusion under the vanillate promoter (non induced) was analyzed in $\Delta popA$ expressing PopA I-site mutant under the *popA* promoter. Schematic drawings of the localization pattern are included in the right panels. Immunoblots against PopA and CC1462 show the presence of PopA and CC1462 derivatives respectively.

D. RcdA and CpdR are dispensable for CC1462 Localization. YFP-1462 localization was analyzed in *rcdA::hyg* and $\Delta cpdR$ strain backgrounds by fluorescence microscopy.

E. Statistical analysis of the YFP-CC1462 localization in predivisional and stalked cell types in *rcdA::hyg* and $\Delta cpdR$ mutants. SW pole: localization to the incipient swarmer pole, ST pole: localization to the stalked pole, two foci: bipolar localization, no focus: no polar localization, mislocalized: foci at any position.

Figure 6: CC1462 is not involved in CtrA degradation.

A. CtrA degradation is not affected in *CC1462* deletion mutants. α -CtrA immunoblots of synchronized *C. crescentus* cultures were used to check CtrA levels during cell cycle. The following strains were compared: NA1000, $\Delta popA$, $\Delta CC1462$ and $\Delta CC1462 \Delta popA$. Quality of synchronization was tested by α -McpA immunoblots.

B. *CC1462* overexpression does not change CtrA degradation pattern. CtrA levels of NA1000 and NA1000 overexpressing *CC1462* on plasmid (non induced) were analyzed by α -CtrA immunoblots. The levels of *CC1462* in the wild-type and in the overexpressing situation during cell cycle are shown in the right panels.

Figure 7: CC1462 protein is cell cycle regulated and degraded by ClpXP.

A. *CC1462* protein levels are elevated in $\Delta popA$, *rcdA::hyg*, $\Delta cpdR$ mutants. α -*CC1462* immunoblot analysis of *C. crescentus* mixed exponential growing cultures to check the protein levels in different mutant backgrounds: $\Delta popA$, *rcdA::hyg*, $\Delta cpdR$, $\Delta pleD$ and $\Delta CC2616$. Samples from NA1000 and $\Delta CC1462$ were used as controls.

B. PopA, RcdA and CpdR are needed for cell cycle dependent degradation of *CC1462*. α -*CC1462* immunoblot experiments of synchronized cultures were performed to follow *CC1462* protein levels. α -CtrA blots were used as controls.

C. *CC1462* is degraded by ClpXP. *CC1462* levels were monitored by α -*CC1462* immunoblots while expressing an inactive dominant negative copy of the ClpX ATPase from the xylose promoter. This expression leads to an accumulation of ClpXP substrates over time. Addition of glucose represses the xylose promoter and ClpXP substrates can be degraded. CtrA and FliF serve as positive and negative controls.

Figure 8: CC1462 is a guanine deaminase homolog.

A. Genetic organization of the gene cluster containing *CC2616* (black arrow). Genes upstream of *CC2616* encode components of the xanthine degradation machinery or are annotated as hypothetical genes (grey arrows). The *CC2616* gene product is annotated as a guanine deaminase. It has an amino acid stretch

homologous to the amidohydrolase domain which contains the active site motif (dark grey) with strongly conserved residues underlined.

B. Guanine deaminases (GDA) catalyze the hydrolytic deamination from the purine base guanine to xanthine.

C. CC2616 has the typical amidohydrolase TIM barrel fold. The x-ray structure of the guanine deaminase Blr3380 from *B. japonicum* (PDB 2OOD, unpublished) is shown in green. A Zn²⁺ cation is bound to the active site of the enzyme. The structure of CC2616 is modeled (blue) using Blr3380 as a template.

D. CC2616 has a well conserved Zn²⁺ binding site. A sequence alignment of CC2616 and the guanine deaminase YgfP from *E. coli* and human brain guanine deaminase is shown. A strongly conserved nine-residue motif (black box) can be identified. It is found in other amidohydrolase family members that have been shown to coordinate the heavy metal ion zinc.

Figure 9: A CC2616 deletion inversely influences motility and attachment.

Swimming behavior on semi solid agar plates and attachment on polystyrene surfaces were analyzed for CB15, $\Delta popA$, $\Delta CC2616$ and $\Delta CC2616 \Delta popA$ double mutant.

A. A $\Delta CC2616$ mutant decreases motility by 20% compared to CB15.

B. A $\Delta CC2616$ mutant attaches 20% better than a wild-type CB15 strain.

Figure 10: CC2616 localization is dependent on PopA and CpdR.

A. Polar localization pattern of CC2616-YFP on a low copy vanillate inducible plasmid (non-induced) was analyzed in NA1000 wild-type and the mutants $\Delta CC2616$, $\Delta popA$, $rcdA::hyg$, $\Delta cpdR$, $\Delta CC1462$ and $\Delta pleD$ by fluorescence microscopy. Polar foci are indicated in the schematic representations in the panels on the right.

B. CC2616 localization requires PopA and CpdR. A statistical analysis of the CC2616 localizations in stalked and predivisional cells in the different backgrounds is shown. SW: localization to the incipient swarmer pole, ST: localization to the stalked pole, two foci: bipolar localization, no focus: no polar localization.

C. CC2616-YFP is expressed in a $\Delta cpdR$ mutant. CC2616-YFP levels were tested under non-induced and induced (1 mM vanillate) conditions by α -CC2616 immunoblots. CB15 and $\Delta CC2616$ were used as controls.

D. CC2616 localization is independent of ClpP. The localization of CC2616-YFP was studied on a low copy plasmid under the vanillate promoter in a ClpP depletion strain by fluorescence microscopy. Xylose is needed for the cells to express ClpP, addition of glucose leads to ClpP depletion. Polar foci are shown in the schematic drawings in the right panels. Depletion of ClpP and presence of CC2616-YFP was controlled by α -CC2616 and α -ClpP immunoblots. Statistical analysis of the CC2616

localization pattern in a ClpP depletion strain is presented for predivisional and stalked cells.

Figure 11: CC2616 protein levels do not oscillate during cell cycle.

CC2616 is present throughout the cell cycle. CC2616 immunoblot experiments of synchronized cultures were performed to follow CC2616 protein levels. α -CtrA and α -McpA blots were used as controls.

Figure 12: Hydrophobic C-termini of *C. crescentus* ClpXP substrates

The C-termini of known ClpXP substrates are shown. Whereas CtrA, KidO and CpdR display the classical hydrophobic dipeptide at their C-terminus that is known to confer substrate specificity, this motif is absent in CC1462 and PdeA. The classical dipeptide is illustrated in red, general hydrophobic amino acids are underlined.

Figure S1: PopA-*flag* is functional in terms of motility and CtrA degradation.

A $\Delta popA$ strain expressing either PopA-*flag* or untagged PopA was constructed for immunoprecipitation experiments. The functionality of PopA-*flag* was tested in a motility assay and CtrA levels during cell cycle were monitored.

A. PopA-*flag* complements the $\Delta popA$ motility defect. The following strains were compared: NA1000 wild-type, $\Delta popA$ and $\Delta popA$ expressing untagged and flag tagged PopA.

B. PopA-*flag* complements the $\Delta popA$ CtrA stabilization effect. Synchronized cultures were analyzed by α -CtrA immunoblots for CtrA levels during cell cycle. $\Delta popA$ was compared with $\Delta popA$ expressing PopA or PopA-*flag*.

Figure S2: CC1462, CC2616 and PodJ_{cyt} do not interact with components of the CtrA degradation machinery.

Bacterial Two-Hybrid Analysis of the new PopA interaction partners with components of the CtrA degradation machinery. Positive interactions score in red, negatives in white. Detailed representation of the used constructs is shown in the panels on the right. For the membrane protein PodJ a truncated cytosolic version, PodJ_{cyt} was used.

A. No other interactions can be detected for CC1462 with PodJ_{cyt}, CC2616, CtrA, CpdR, ClpX, ClpP and PleD. Interaction with RcdA is inconclusive due to autoactivation of pKT25-RcdA with empty pUT18 vectors.

B. No interaction was obtained for CC2616 with itself, PodJ_{cyt}, CtrA, RcdA, CpdR, ClpX, ClpP and PleD. The fusion pKT25-RcdA shows positive interaction with the empty plasmids pUT18 and pUT18C which suggests false positive interaction.

Figure S3: CC1462 attaches like wild-type and expresses pili.

CC1462 clean deletion and CC1462 overexpressing strains on IPTG inducible plasmids were analyzed for their ability to attach on polystyrene surfaces and for their resistance to phage CBK.

- A. CC1462 does not influence attachment and cannot rescue the attachment defect of a $\Delta popA$ mutant. NA1000 does not attach and is therefore used as negative control.
- B. Overexpressing CC1462 under induced and non induced conditions in CB15 and $\Delta popA$ does not change their attachment capacity. NA1000 does not attach therefore is used as negative control.
- C. $\Delta CC1462$ expresses pili. The resistance to phage CBK reflects the absence of pili. CB15, $\Delta popA$, $\Delta CC1462$ and $\Delta popA \Delta CC1462$ were streaked through a CBK phage lysate (shown as grey arrow) and growth after the lysate was observed. A $\Delta pilA$ strain was used as a resistant control.
- D. Overexpressing CC1462 does not affect the presence of pili. Wild-types CB15 and NA1000 and $\Delta popA$ overexpressing CC1462 on IPTG inducible plasmid were analyzed for their resistance to phage CBK (grey arrow) under induced and non induced conditions.

Figure S4: The CC1462 overexpression effect on motility is not due to a growth defect.

- A. Overexpression of CC1462 results in decreased motility. Swimming behavior was quantified for NA1000 wild-type and $\Delta popA$ and the respective strains overexpressing CC1462 on an IPTG inducible plasmid.
- B. Overexpressing CC1462 did not affect growth. Growth of the following strains was monitored by OD₆₆₀ over time: NA1000, $\Delta popA$, $\Delta CC1462$, $\Delta popA \Delta CC1462$ and the respective strains overexpressing CC1462 on an IPTG inducible plasmid.

Figure S5: PopA, RcdA and CpdR do not require CC1462 for polar localization.

- A. CC1462 is not a localization factor for PopA. PopA-GFP localization on plasmid under the control of *popA* promoter was analyzed by fluorescence microscopy in a $\Delta popA$ and a $\Delta popA \Delta CC1462$ double mutant. Schematic drawings of the localization are depicted on the right panel. Statistical analysis of the localization pattern in predivisional and stalked cells is presented below the microscopic pictures.
- B. CpdR localization is independent of CC1462. CpdR-YFP localization on a xylose inducible plasmid was analyzed in NA1000 and $\Delta CC1462$ mutant. Statistical analysis of the localization pattern is shown below. One focus: polar localization, no focus: no polar localization, no signal: no fluorescent signal observed.

C. CC1462 is dispensable for RcdA localization. RcdA-YFP localization on plasmid under the control of *rcdA* promoter was analyzed in NA1000 and Δ CC1462. Statistical analysis of the localization pattern is shown below. SW pole: localization to the incipient swarmer pole, ST pole: localization to the stalked pole, two foci: bipolar localization, no focus: no polar localization.

D. The stability of RcdA and CpdR-YFP fusions was assessed by α -RcdA and α -GFP immunoblots. NA1000 and *rcdA::hyg* were used as controls.

Figure S6: CC2616 expressed under the control of vanillate promoter cannot complement the attachment and motility defect of a Δ CC2616 deletion mutant.

A. CC2616 does not complement the attachment phenotype of a Δ CC2616 mutant. CC2616 expressed under induced and non induced conditions in CB15, Δ *popA*, Δ CC2616 and Δ *popA* Δ CC2616 double mutant were analyzed for their attachment to polystyrene surfaces. Overexpression was monitored by α -CC2616 immunoblots and is shown below the graph.

B. CC2616-YFP does not complement the attachment phenotype of a Δ CC2616 mutant. CC2616-YFP expressed under induced and non induced conditions in CB15 and Δ *popA* were analyzed for their attachment to polystyrene surfaces.

C. Overexpressing CC2616 does not increase motility of CB15 and Δ *popA* mutant. Swimming behavior was checked for CB15 and Δ *popA* expressing CC2616-YFP.

Figure S7: A CC2616 deletion mutant produces holdfast and expresses pili like wild-type.

Amount of produced holdfast stained with rhodamin coupled wheat germ agglutinin (Invitrogen, USA) and resistance to phage CBK reflecting the absence/presence of pili were analyzed for CB15, Δ *popA*, Δ CC2616 and Δ CC2616 Δ *popA* double mutant.

A. A Δ CC2616 mutant shows similar amounts of holdfast compared to CB15 wild-type.

B. A Δ CC2616 possesses functional pili. The mentioned strains were streaked through a CBK phage lysate indicated by a grey line. Δ *pilA* strain was used as a phage CBK resistant control.

Figure S8: PopA, RcdA and CpdR do not require CC2616 for polar localization.

Polar localization patterns of PopA, RcdA and CpdR were compared in wildtype and Δ CC2616 mutant by fluorescence microscopy. Polar foci are indicated in the schematic representations in the panels on the right. Statistical analysis of the localization in stalked and predivisional cell types is provided in the graphs below the

microscopic pictures. SW: localization to the incipient swarmer pole, ST: localization to the stalked pole, two foci: bipolar localization, no focus: no polar localization.

A. PopA-GFP localization on a low copy plasmid under the control of *popA* promoter is similar to wild-type in a $\Delta CC2616$ mutant.

B. RcdA-YFP expressed from a medium copy plasmid under *rcdA* promoter localizes normally in a $\Delta CC2616$ mutant.

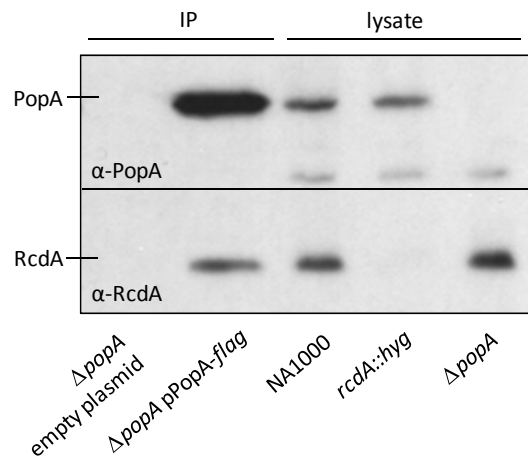
C. CpdR-YFP localization on a low copy plasmid under the xylose promoter is not affected in a $\Delta CC2616$ mutant.

Figure S9: CC2616 does not affect CtrA degradation pattern and cannot rescue the CtrA stabilization effect of a $\Delta popA$ mutant.

CtrA levels during *C. crescentus* cell cycle were monitored by α -CtrA immunoblots comparing NA1000, $\Delta popA$, $\Delta CC2616$ and $\Delta popA \Delta CC2616$ double mutant with each other. α -McpA blots were used to control quality of the synchronization.

Figure 1

A



B

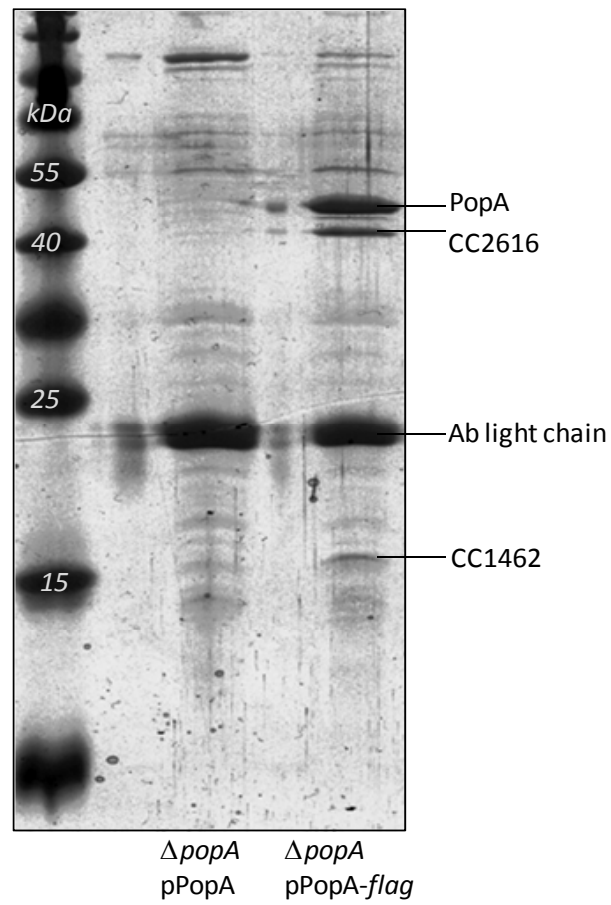
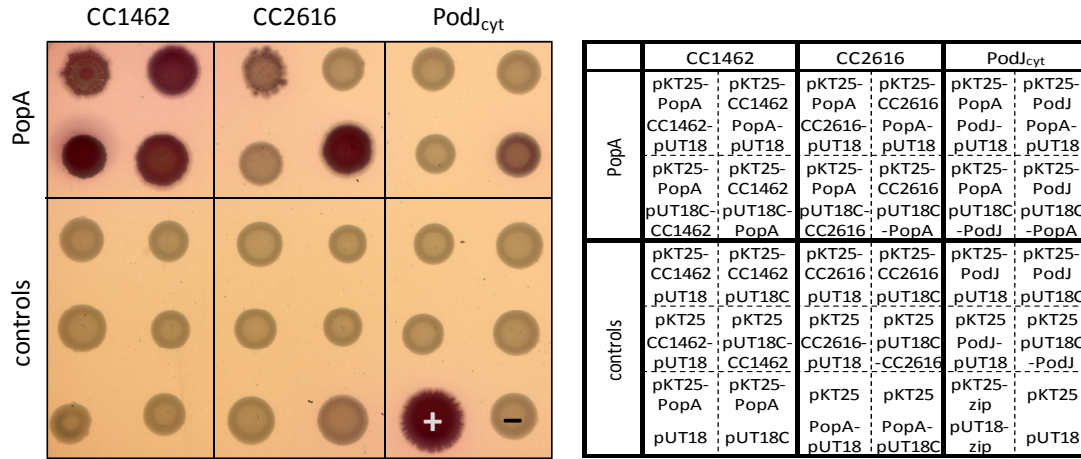


Figure 2

A



B

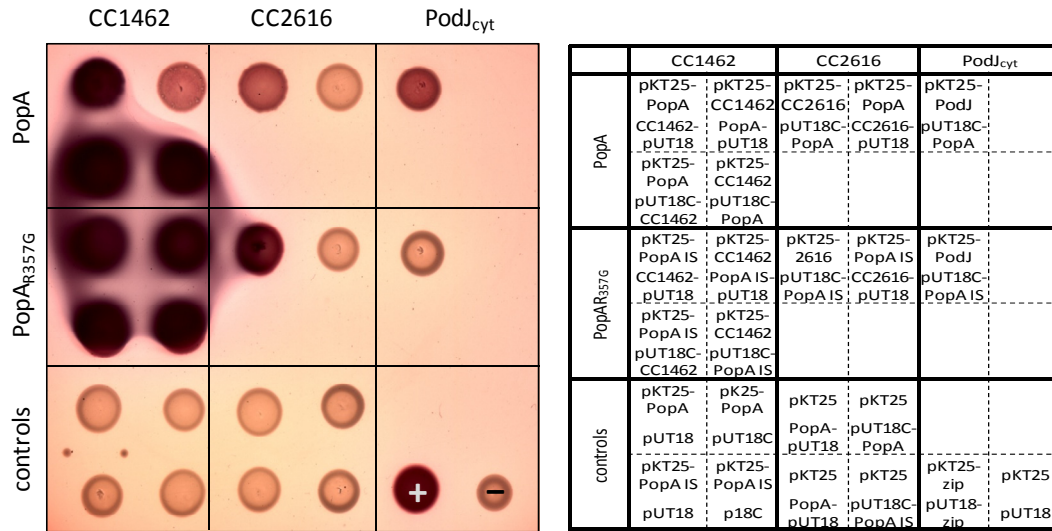
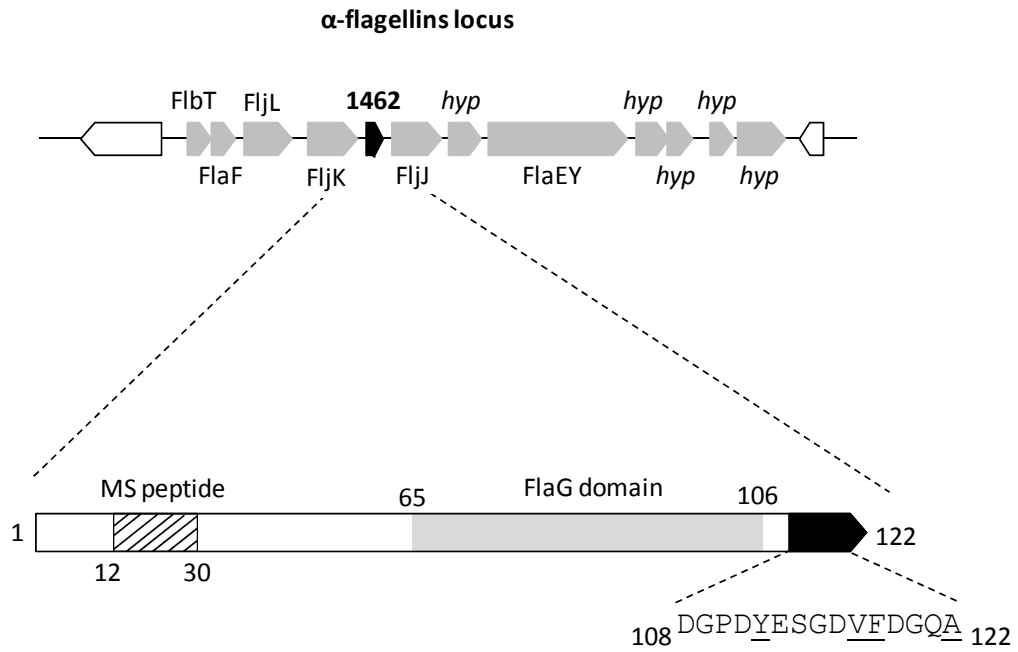


Figure 3

A



B

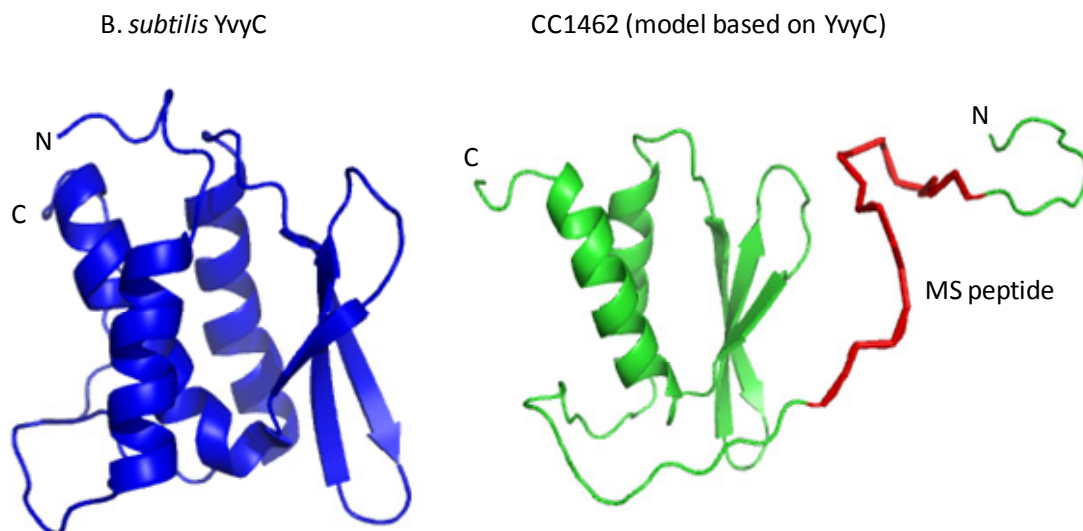
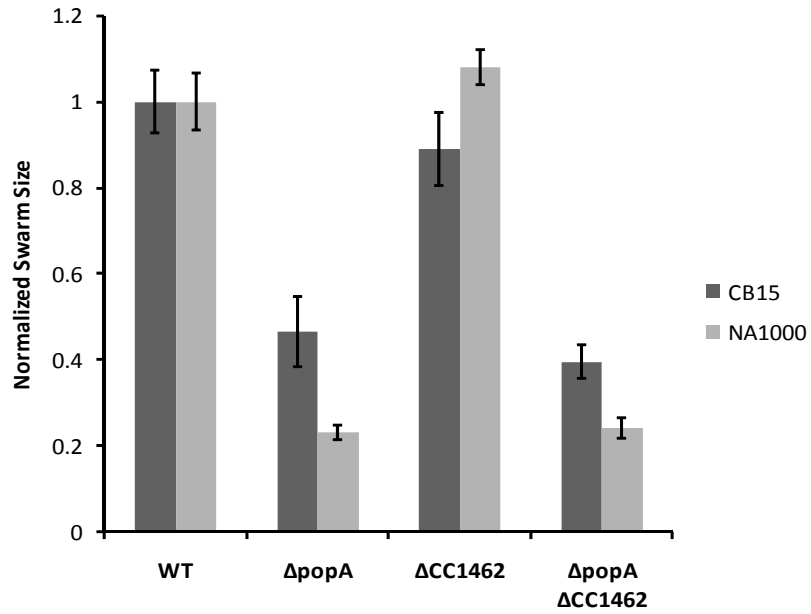
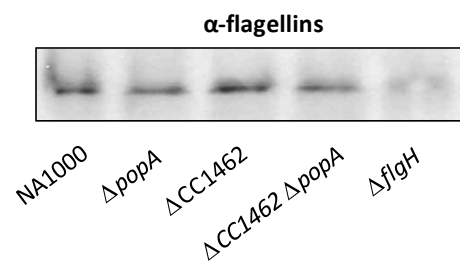
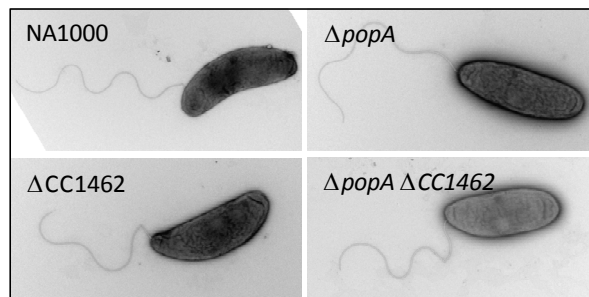


Figure 4

A



B



C

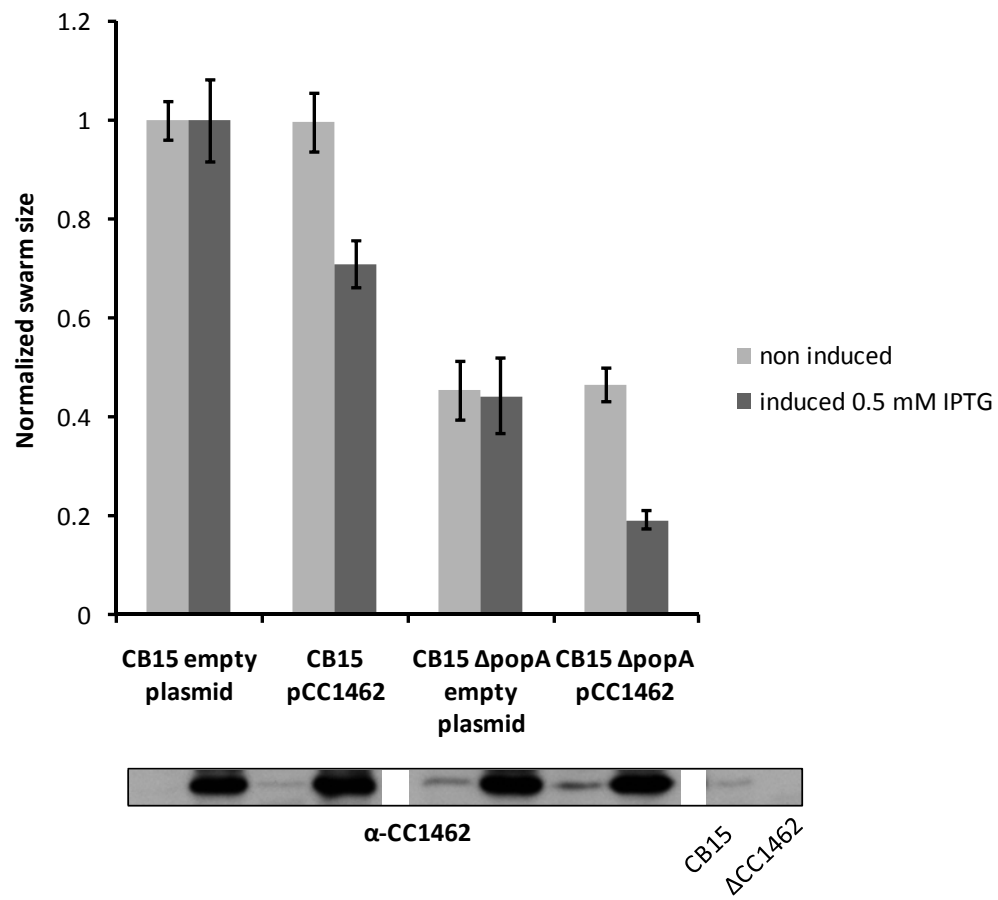
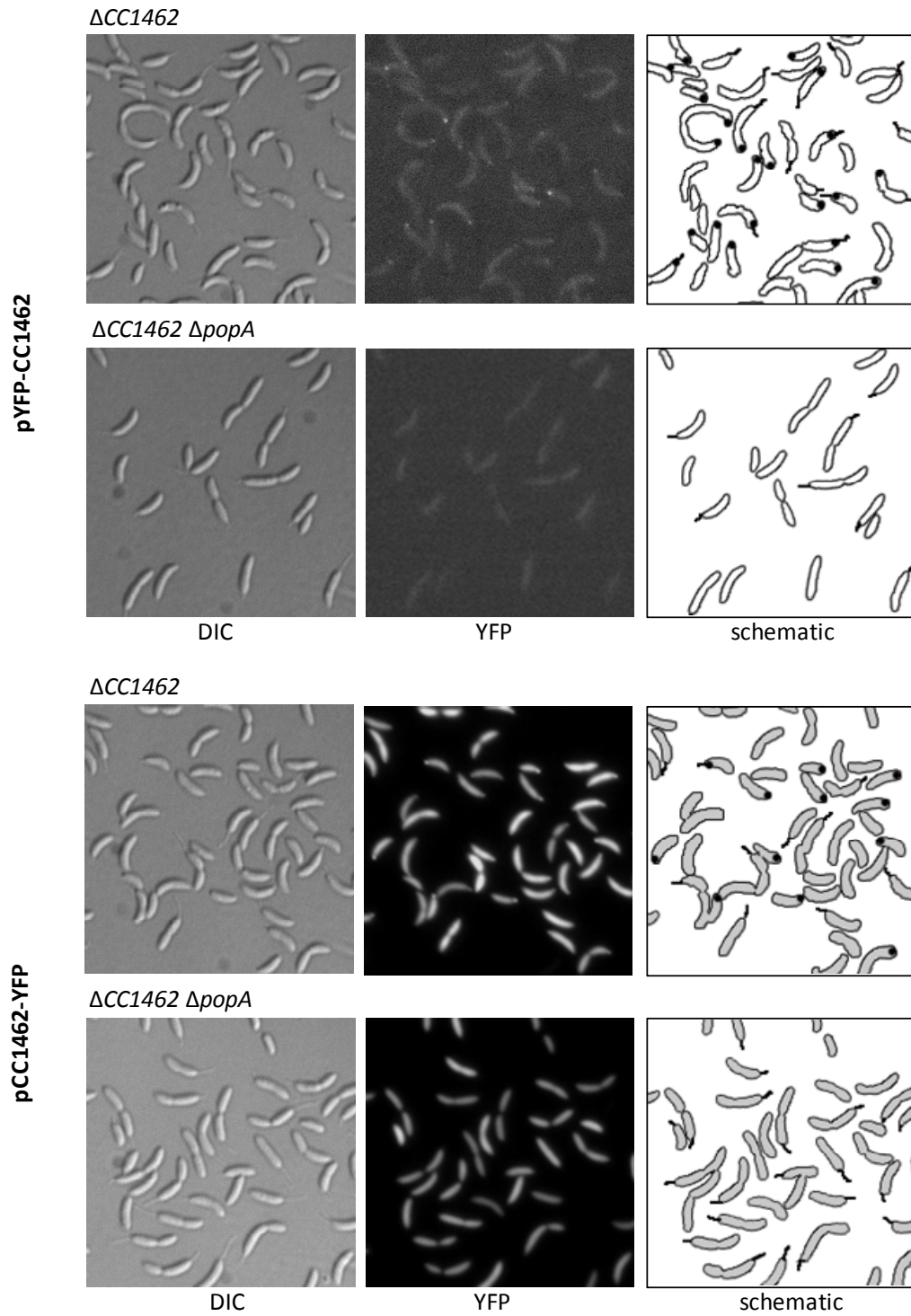
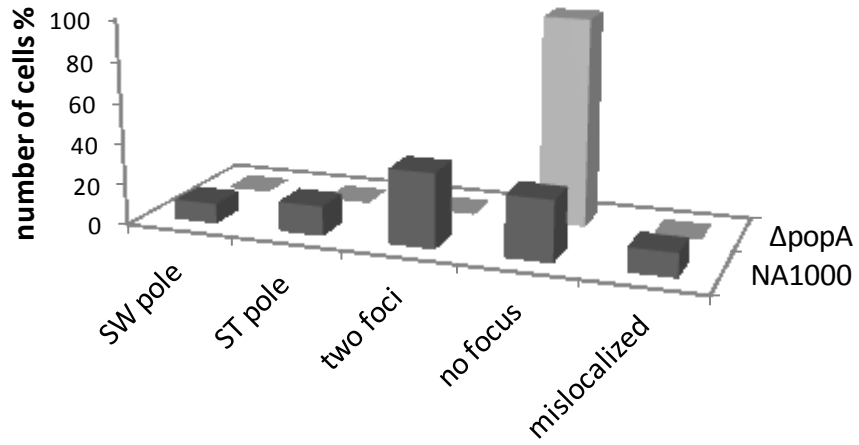


Figure 5

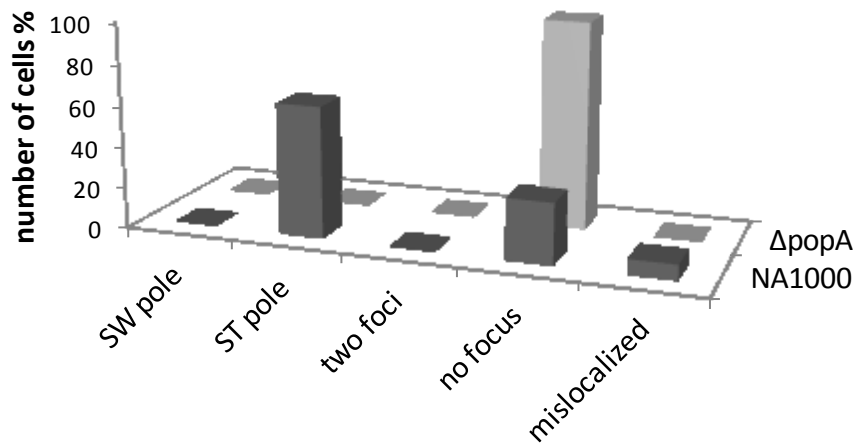
A



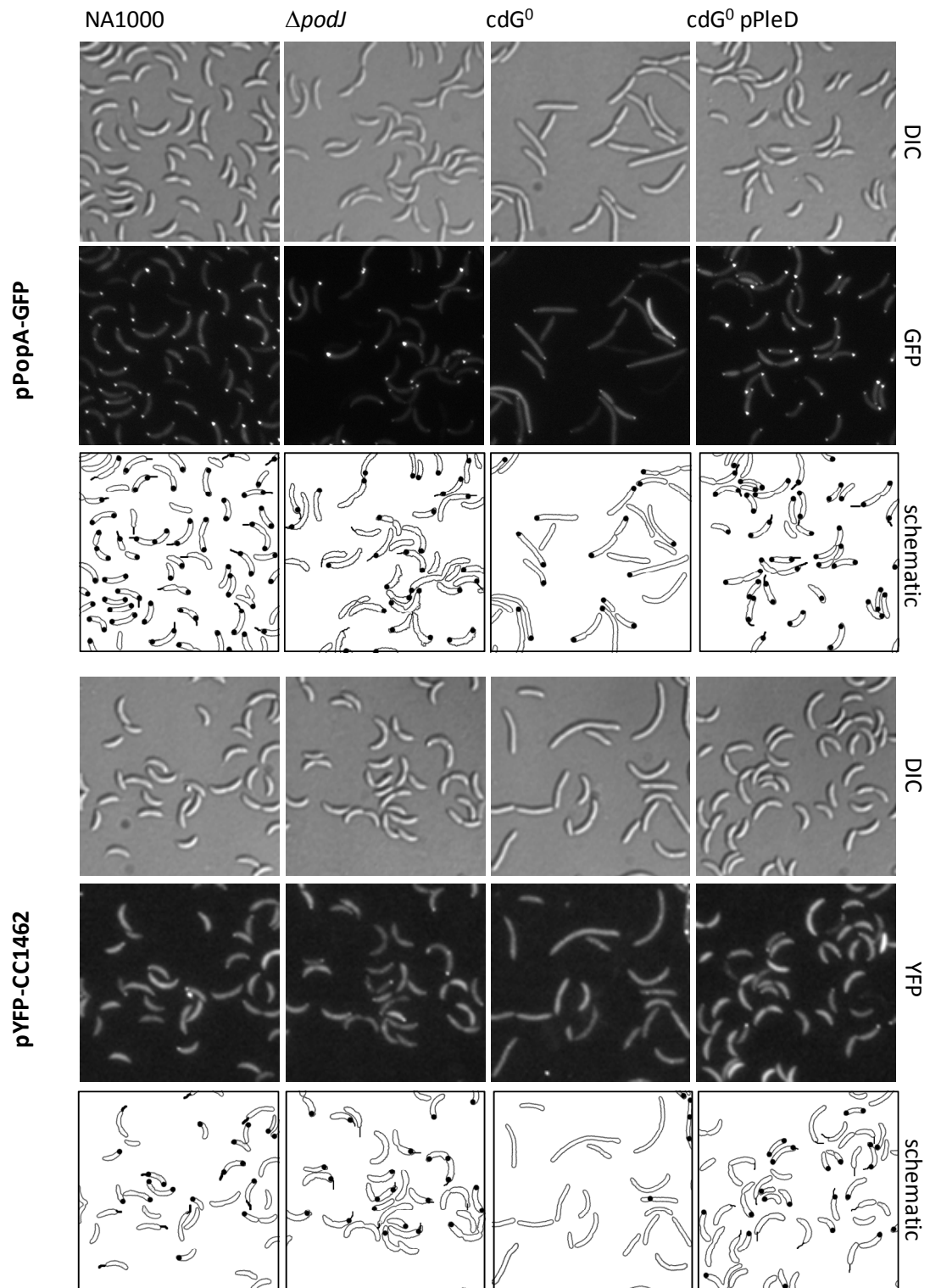
YFP-CC1462 in predivisinal cells



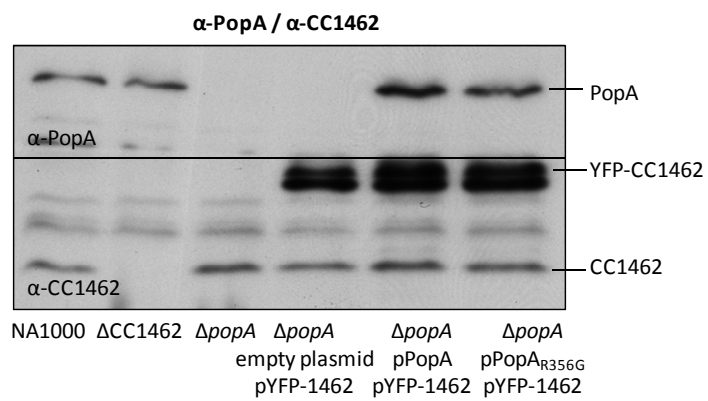
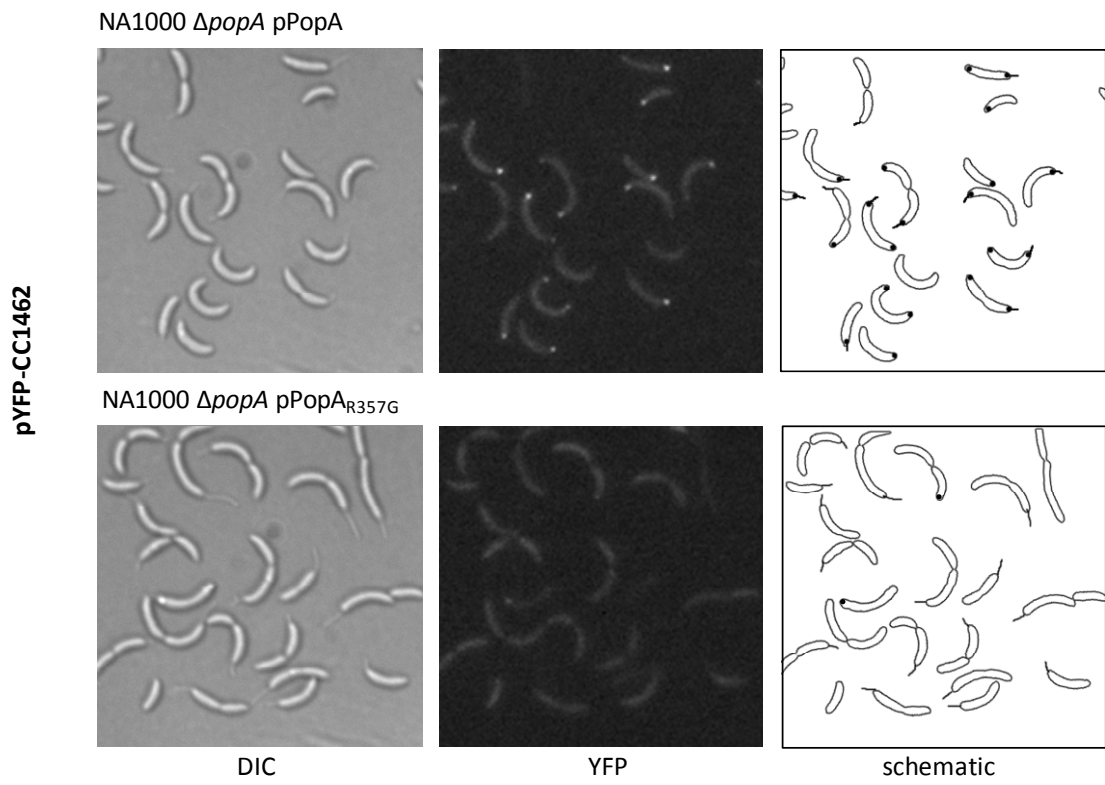
YFP-CC1462 in stalked cells



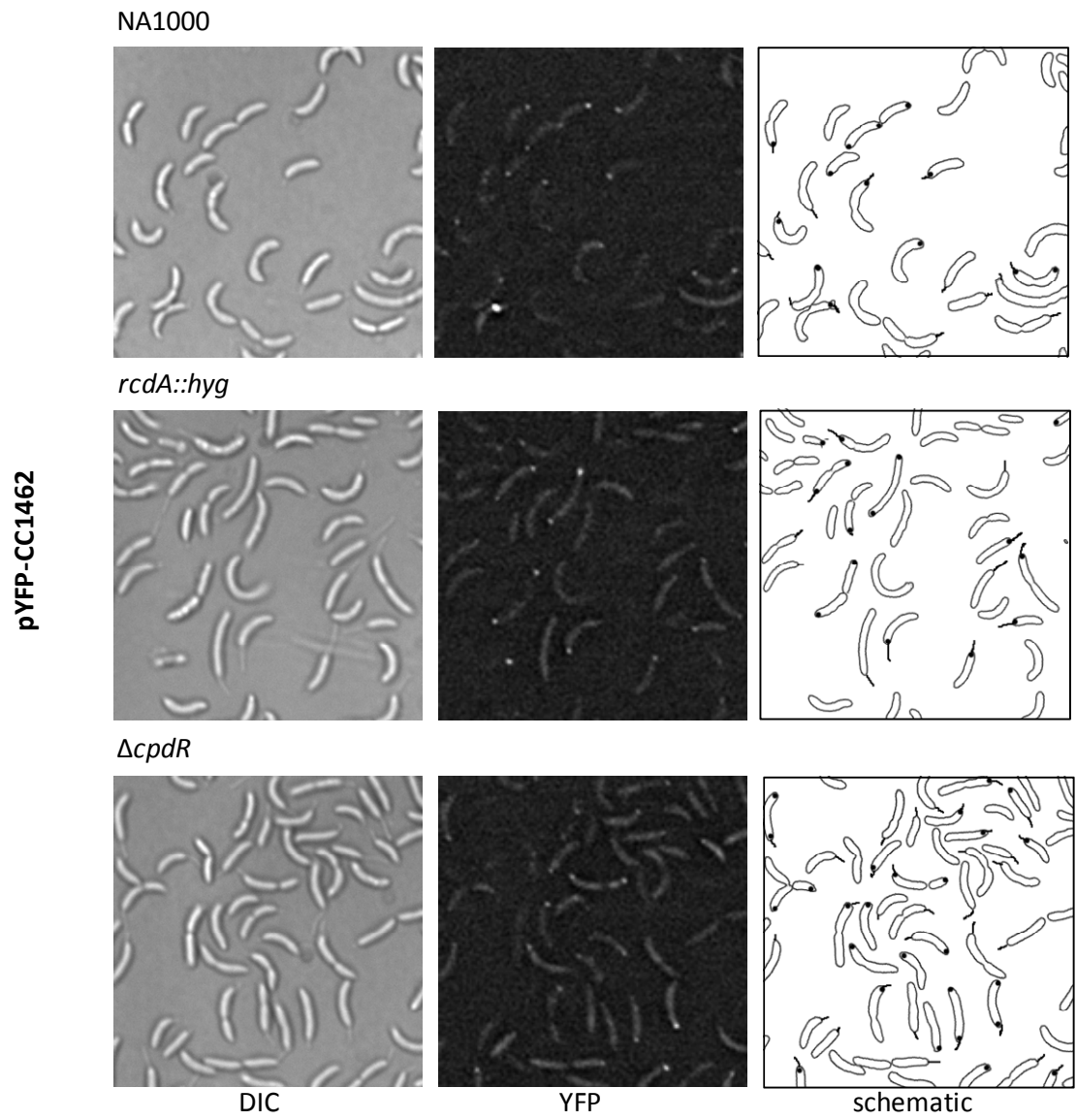
B



C

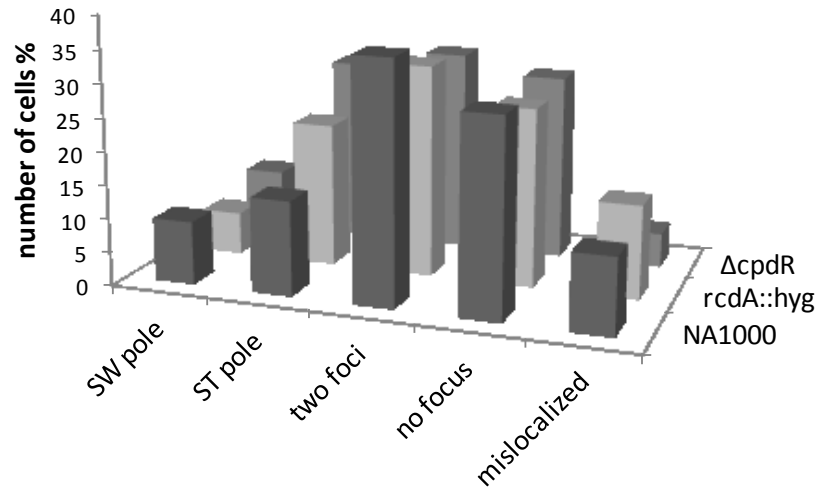


D



E

YFP-CC1462 in predivisional cells
n ≥ 79 cells/strain



YFP-CC1462 in stalked cells
n ≥ 39 cells/strain

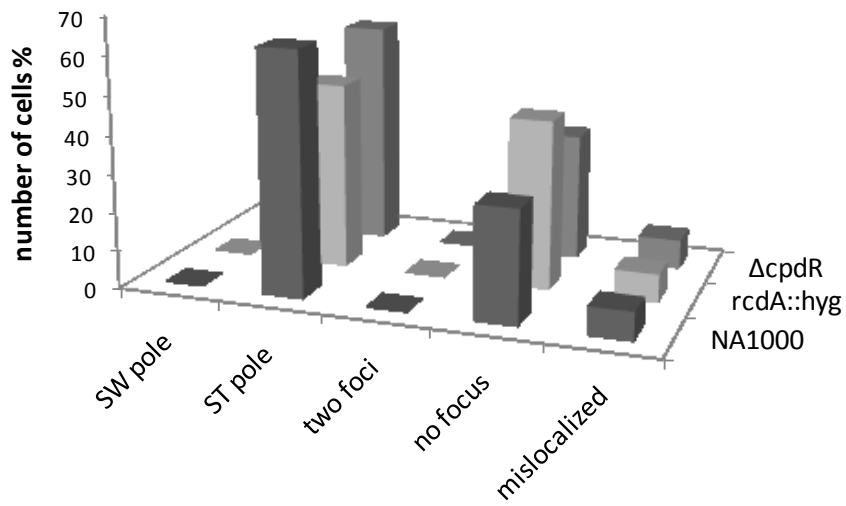
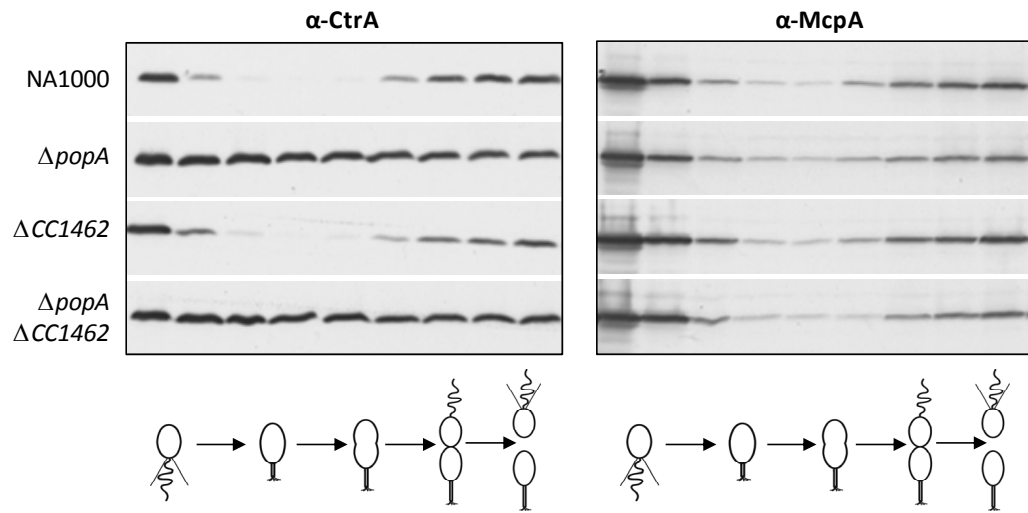


Figure 6

A



B

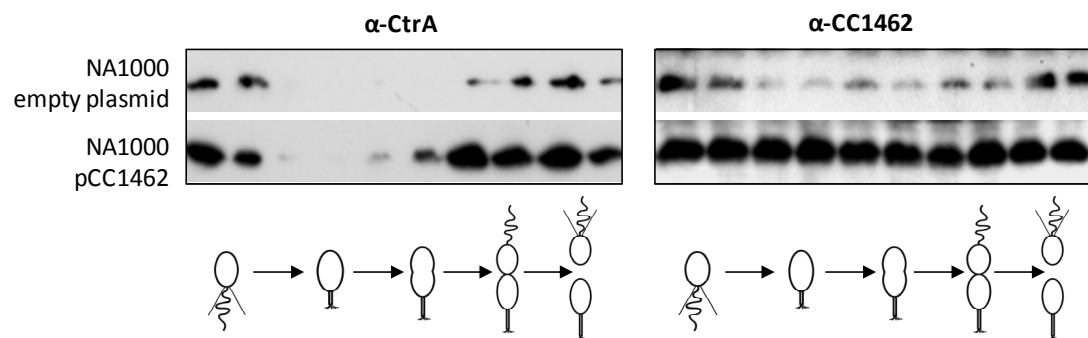
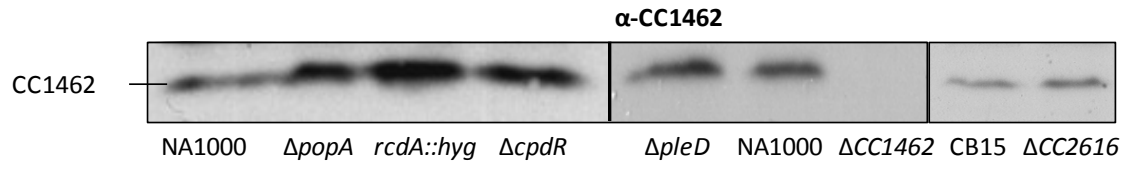
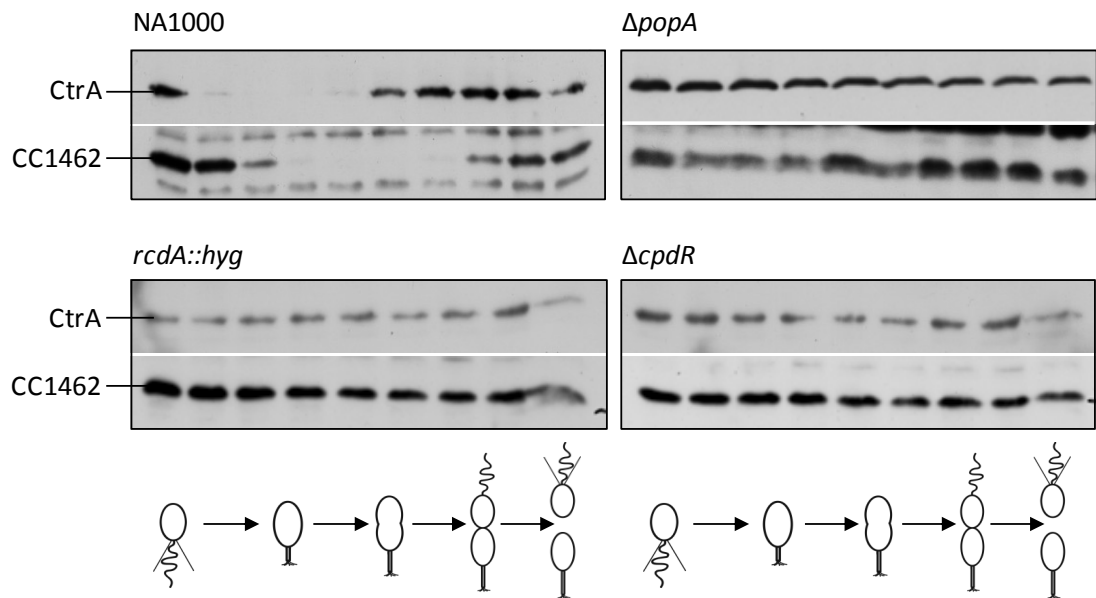


Figure 7

A



B



C

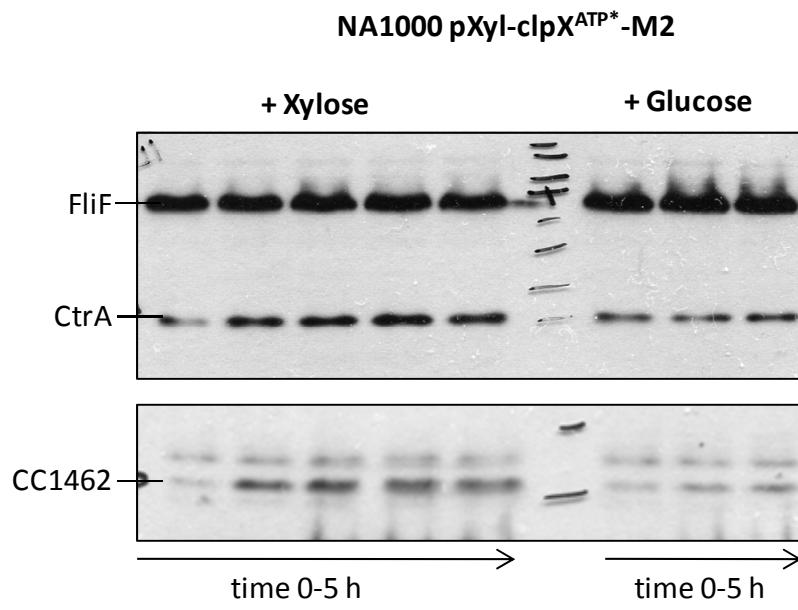
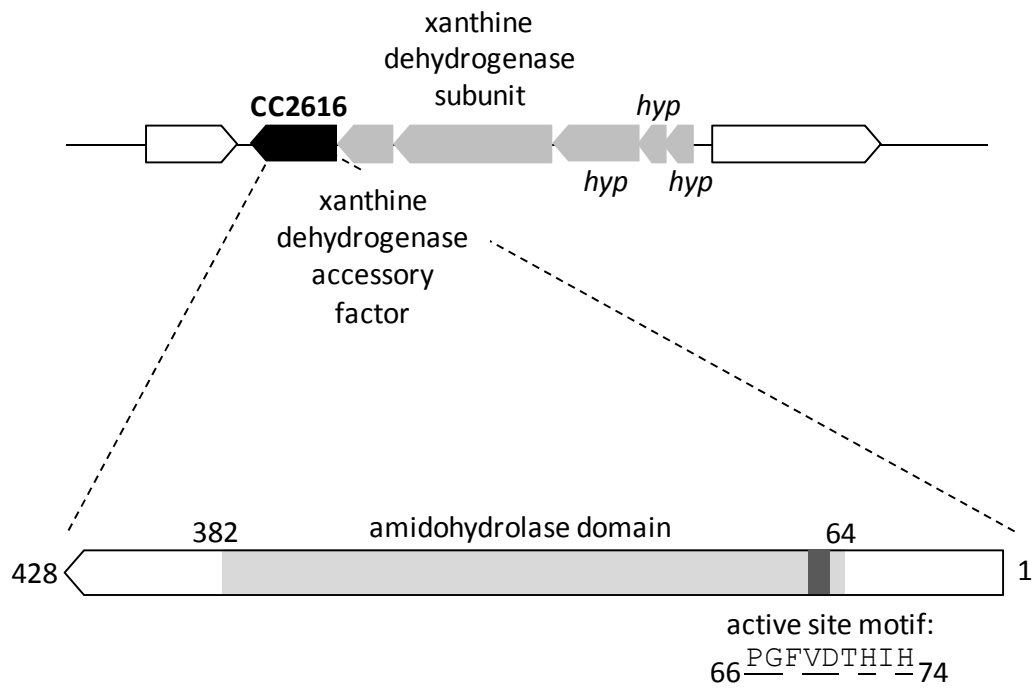
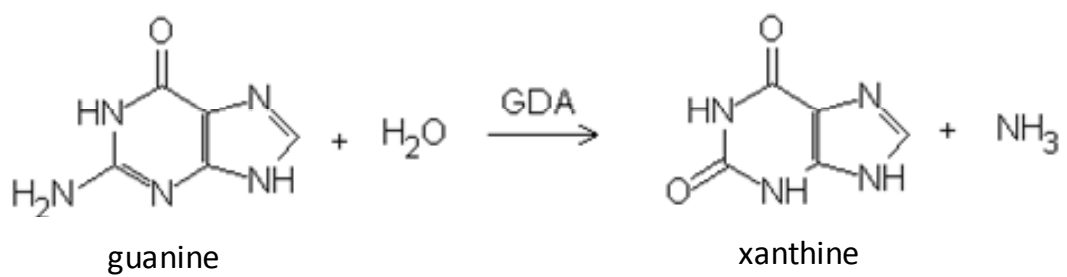


Figure 8

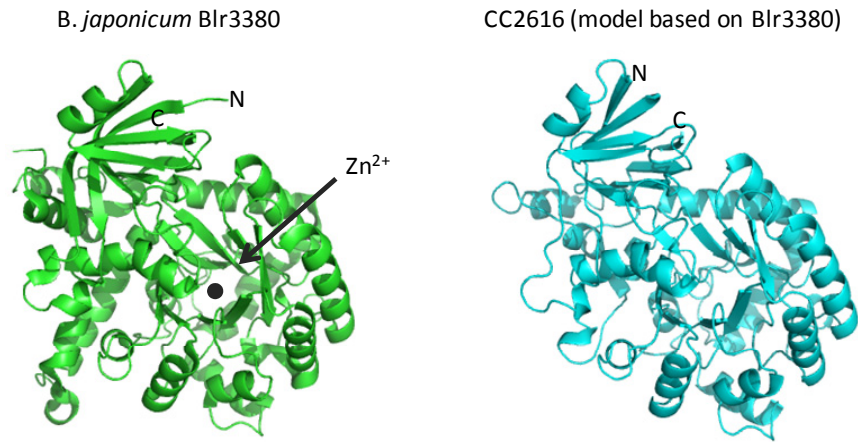
A



B



C



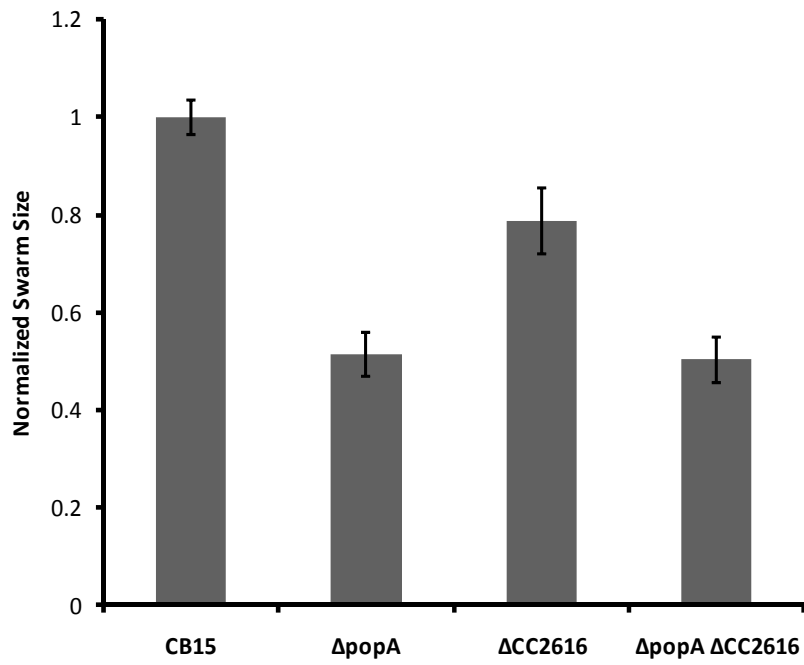
D

```

CC2616_Q9A548      -----MQAFRASILHL---LDDPAKAAEGAVAFHEDGLLLVEDGRVIGCGAYAE---- 46
GUAD_ECOLI_P76641  MMSGEHTLKAVRGSFIDVTRTIDNPEEIAS-ALRFIEDGLLLIKQKGVWFGEWEN---- 55
GUAD_HUMAN_Q9Y2T3  -----MCAAQMPPLAHIFRGTFFVHSTWTCPEVLRDHLGVSQSGKIVFLEEASQKEKL 54
                   *   .: .:   :   :   :   :   :   :   :   :   :   :   :   :
CC2616_Q9A548      LAPWLG- AELEDLTG-HLIPGFVDTHIIFPQVDVIA-AHGKQLLDWLEQHTFPAAEAF 103
GUAD_ECOLI_P76641  GKHQIPDITIRVRDYG-KLIVPGFVDTHIIFPQSEMVG-AYGEQLLEWLNKHTFFPTERRY 113
GUAD_HUMAN_Q9Y2T3  AKEWCFKPCIEIRELSHHEFFNPLGLVDTHIIFASQYSFAGSSIDLPLEWLTKYTFPAEHRF 114
                   .: .:   .: .:   .: .:   .: .:   .: .:   .: .:   .: .:   .: .:
CC2616_Q9A548      ADPKHAADTAAFFLDELLRNGTTTALVFGSVHKVSDALFAEAYARDMRLIAGKSLMDR- 162
GUAD_ECOLI_P76641  EDLEYAREMSAFFIKQLLRNGTTTALVFGTVHPQSDALFEAASHINMRMIAGKVMMDR- 172
GUAD_HUMAN_Q9Y2T3  QNIDFAEEVYTRVRRRLKNGTTTACYFATIHTDSSLLLADITDKFGQRAFGVKVCMDLN 174
                   : .: * : : : . : .: .: .: .: .: .: .: .: .: .: .: .: .: .: .: .:
CC2616_Q9A548      NAPDGLTDTVESSREDMQALIADWHGK--GRLGYAVTPRFAISCSDAQLAMAGEILAEP 220
GUAD_ECOLI_P76641  NAPDYLDTAESSYHQSKELIERWHKN--GRLLYAITPRFAPTSPEQMAMAQRLKEEYP 230
GUAD_HUMAN_Q9Y2T3  DTFPEYKETTSESIKETERFVSEMLQKNYSRVKPIVTPRFSLSCESETLMGELGNIATR- 233
                   : : .: .: .: .: .: .: .: .: .: .: .: .: .: .: .: .: .: .: .:
CC2616_Q9A548      DVWMQTHLSENLHEIKETARLFPKAKDYLDVYDRFGLLRQRSVFAHCVHLKGDARRLAA 280
GUAD_ECOLI_P76641  DTWVHTLLENKDEIAWVKSLYPDHDGYLDVYHQYGLTGKNCVFAHCVHLEEKEDWRLSE 290
GUAD_HUMAN_Q9Y2T3  DLHIQSHISENRDEVEAVKNLYPSYKNYTSVYDKNNLLTNKTYMAHGCVLSAEELNVFHE 293
                   * : .: .: .: .: .: .: .: .: .: .: .: .: .: .: .: .: .: .: .:
CC2616_Q9A548      KGGAVAFPCPTSNLFLGSGFLPLEEACSHGVKVGIGTDVAGATTF SILHTLGEAYKVG--- 337
GUAD_ECOLI_P76641  TKSSIAFCPTSNLYLGSGLFNLKKAQKVKVGMGTIDIGATTFNMLQTLNEAYKVL--- 347
GUAD_HUMAN_Q9Y2T3  RGASIAHCPNSNLSLSSGFLNVLEVLKHEVKIGLGTDVAGGYSYMLDAIRRAVMVSNIL 353
                   .: .: .: .: .: .: .: .: .: .: .: .: .: .: .: .: .: .: .: .:
CC2616_Q9A548      ---QLRGDALDPFQALYLATLGGARALDLDKIGNLAPGKEADFLVLDLAATPLIARRLA 394
GUAD_ECOLI_P76641  ---QLQGYRLSAYEAFYLATLGGAKSLGLDDLIGNFLPGKEADFVMEPTATPLQQLRYD 404
GUAD_HUMAN_Q9Y2T3  LINKVNEKSLTLKEVFRLATLGGSQALGLDGEIGNFEVKGKFDAILINPKASDSPIDLFY 413
                   : .: * : : : .: .: .: .: .: .: .: .: .: .: .: .: .: .: .: .:
CC2616_Q9A548      GGKS---LADKLFALTVLGDDRIVVARTYLAGVERWRR---- 428
GUAD_ECOLI_P76641  NSVS---LVDKLFVMMTLGDDRSIYRTYVDGRLVYERN--- 439
GUAD_HUMAN_Q9Y2T3  GDFFGDISEAVIQKFLYLGDDRIIEEVYGGKQVVPFSSSV 454
                   .: .: .: .: .: .: .: .: .: .: .: .: .: .: .: .: .: .: .:
    
```

Figure 9

A



B

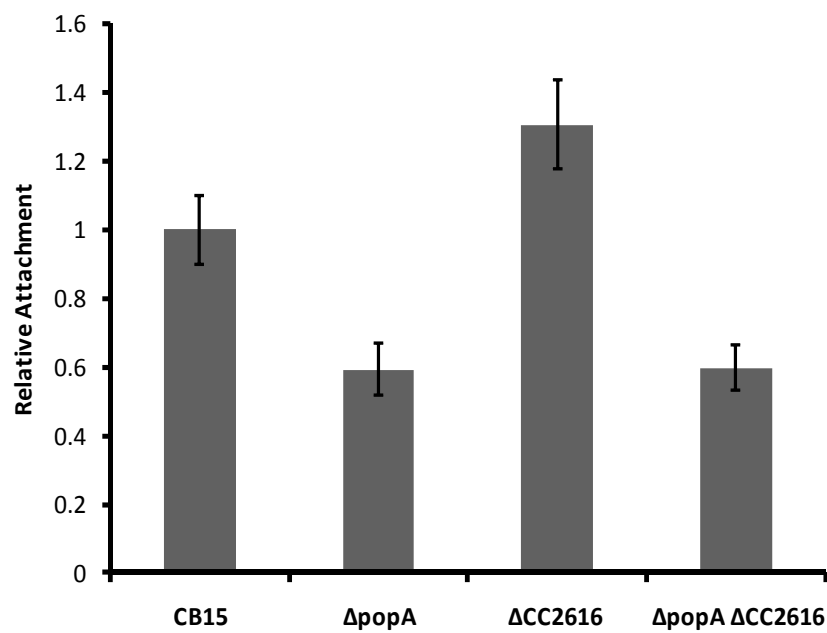
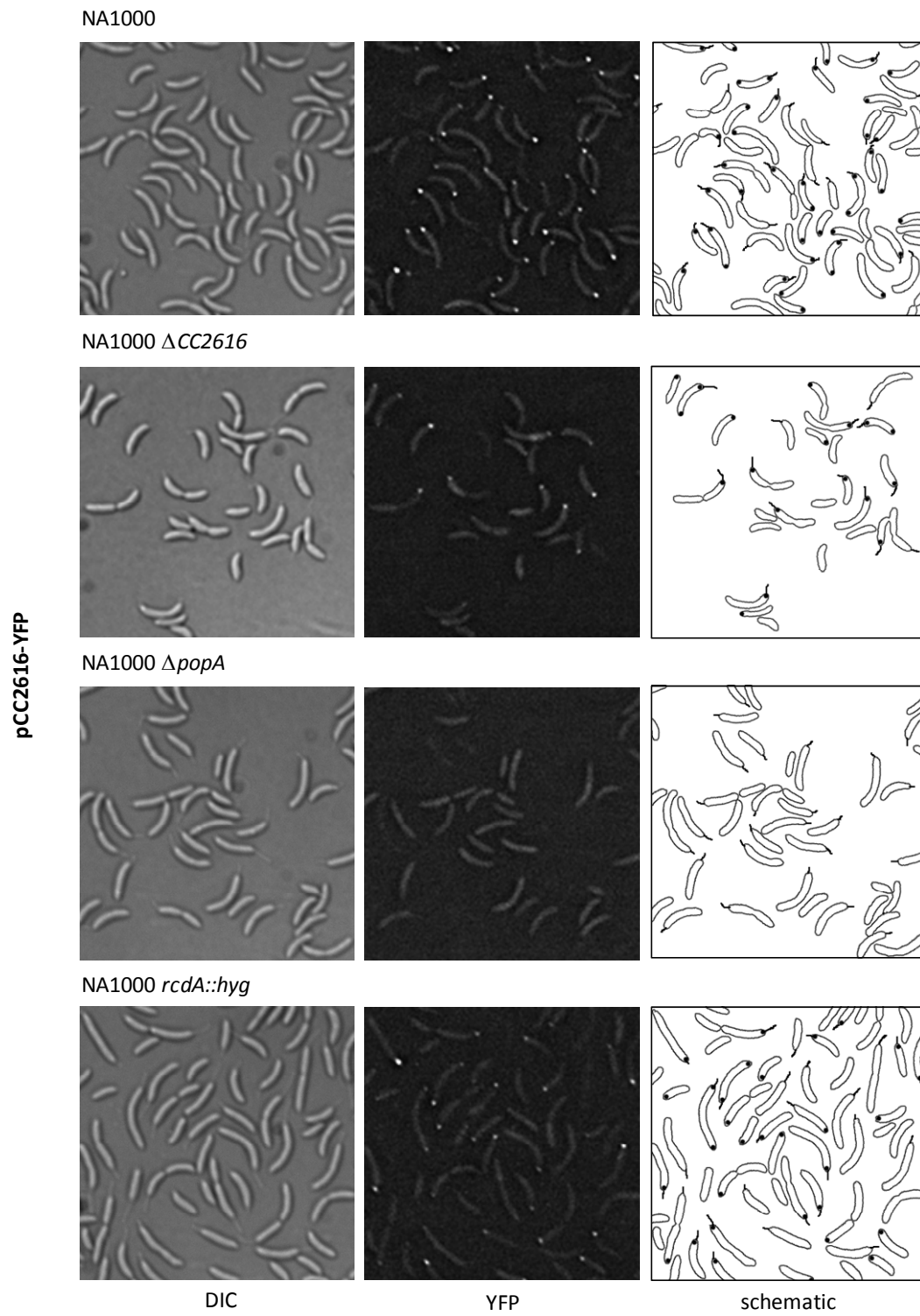
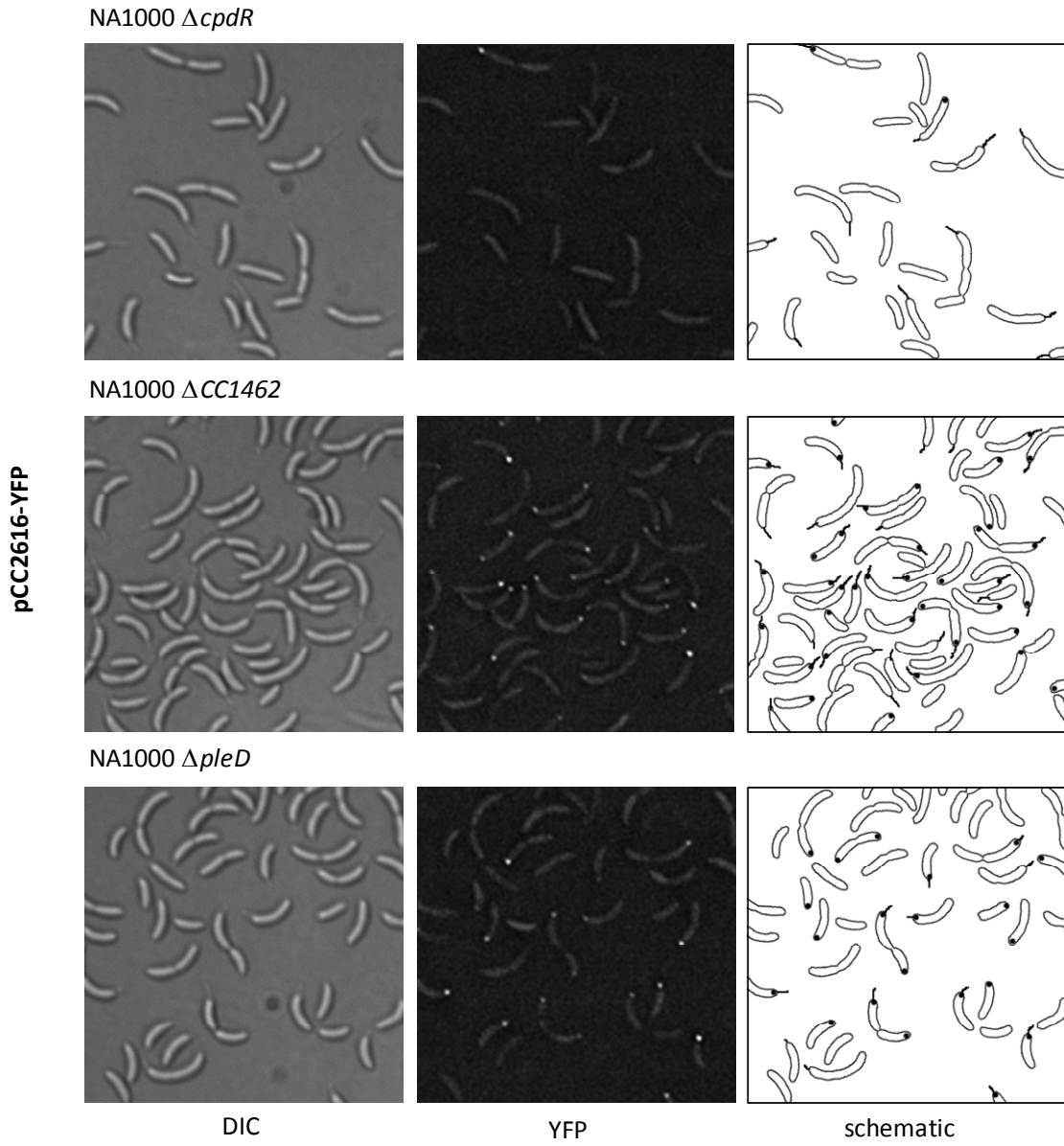


Figure 10

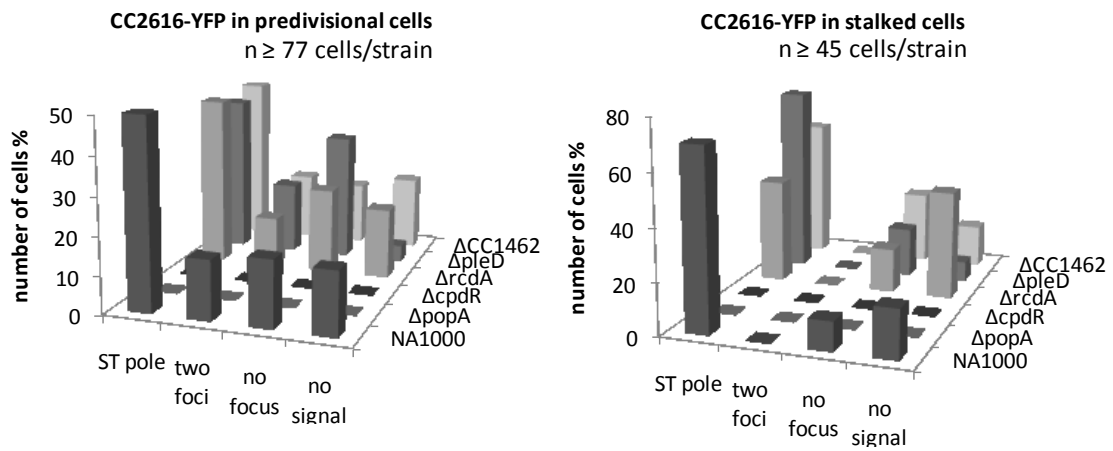
A



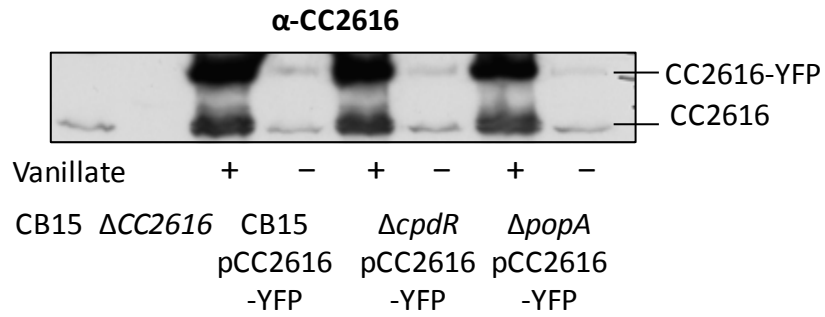
A cont.



B



C



D

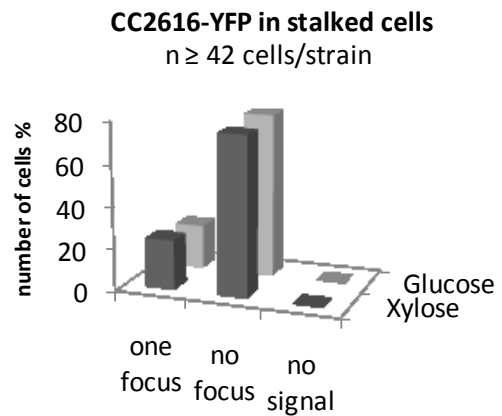
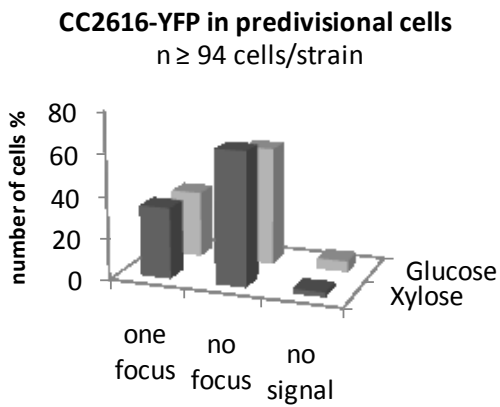
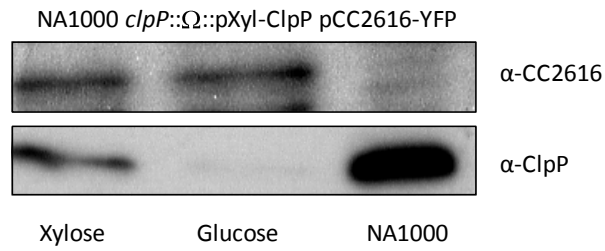
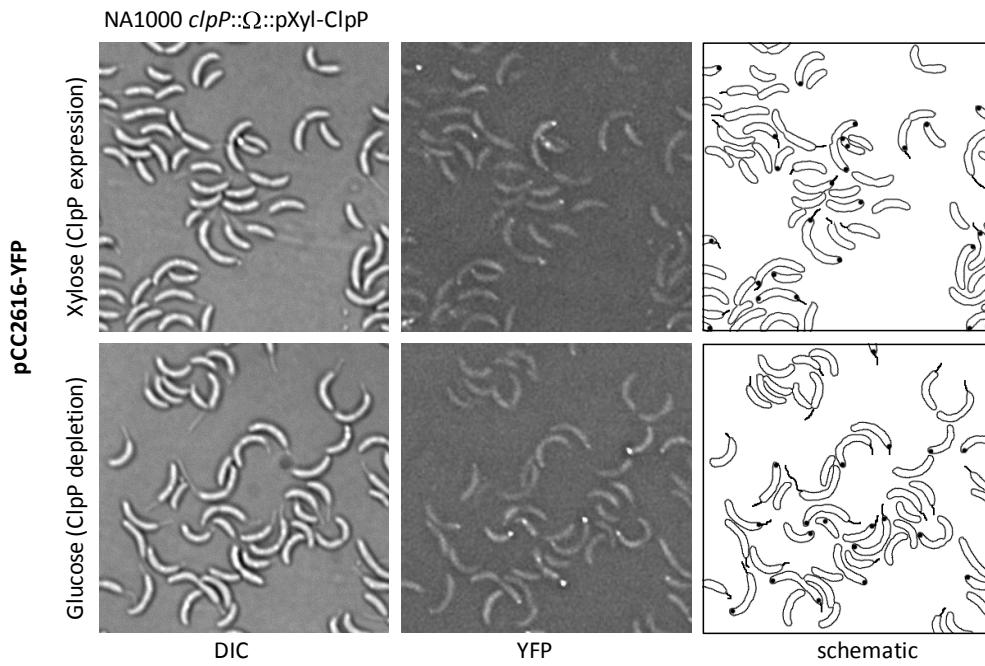


Figure 11

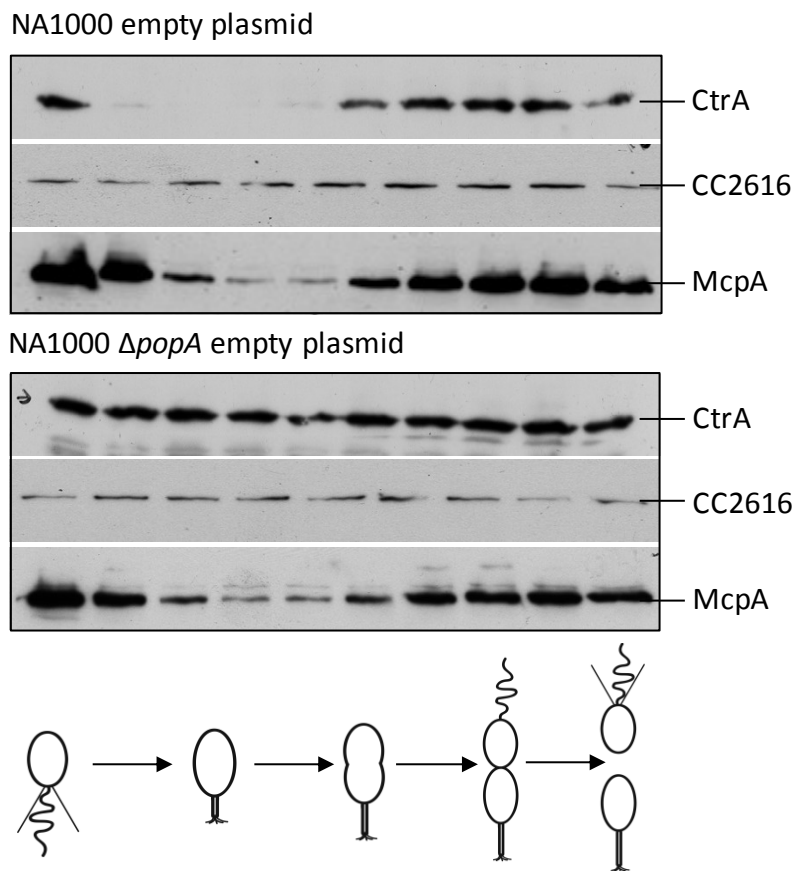
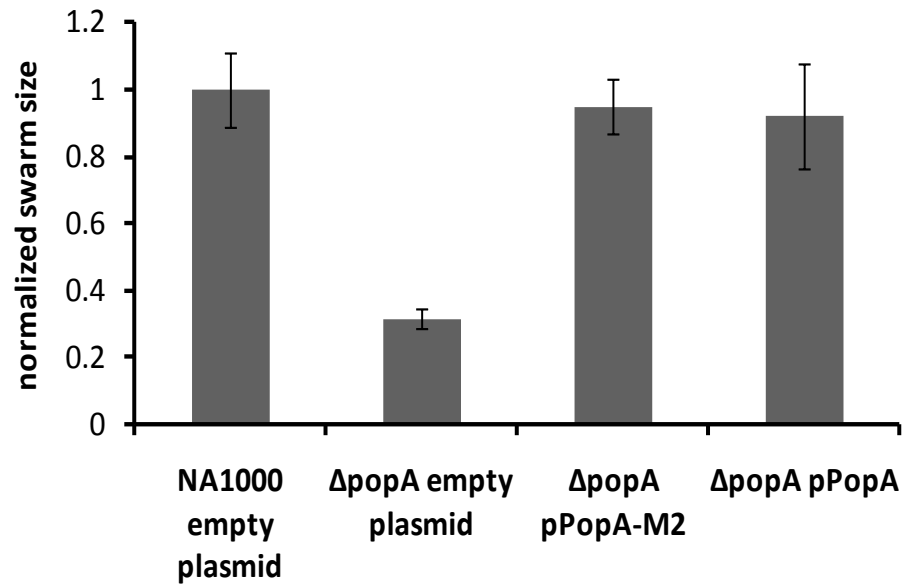


Figure 12

	C-terminal motif
CC1462	ESGDV <u>F</u> DGQA-COOH
CtrA	RDPNEQVN <u>AA</u> -COOH
KidO	<u>VA</u> LDPRRW <u>VA</u> -COOH
PdeA	DGA <u>AP</u> V <u>K</u> ARG-COOH
CpdR	<u>VAE</u> <u>VE</u> K <u>MM</u> AA-COOH

Figure S1

A



B

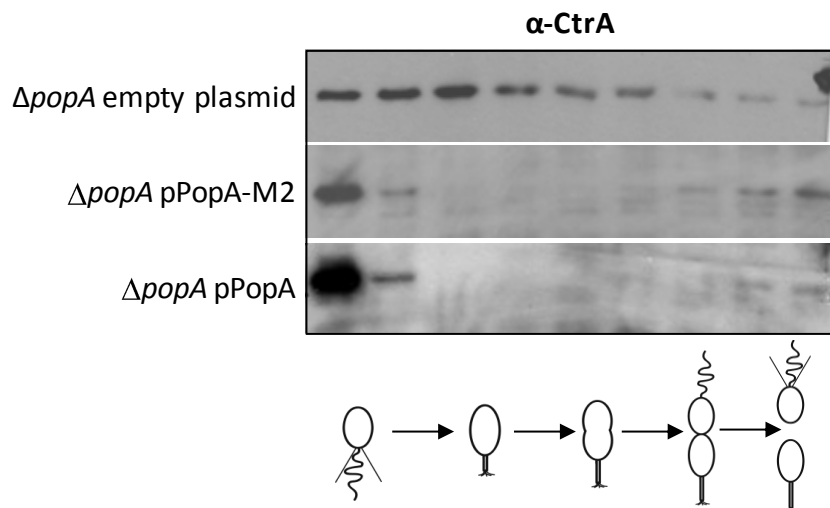
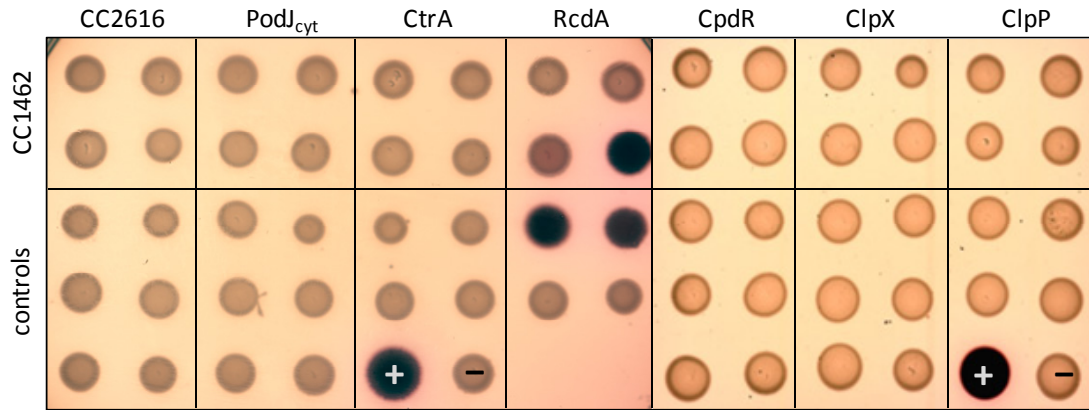
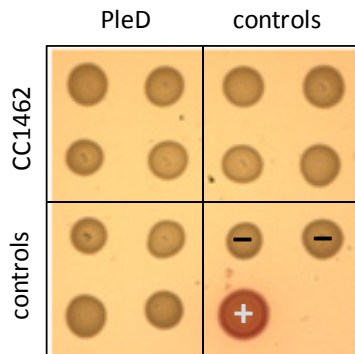


Figure S2

A

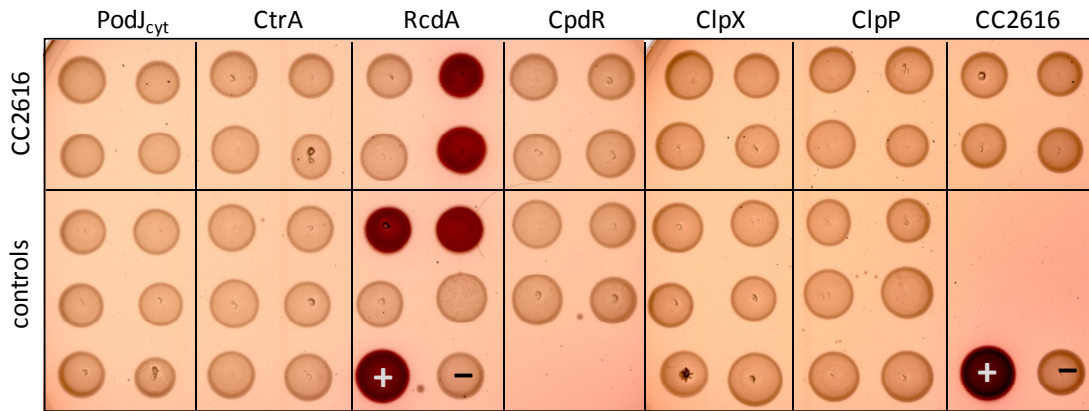


	CC2616		PodJ _{cyt}		CtrA		RcdA		CpdR		ClpX		ClpP	
CC1462	pKT25-CC1462-CC2616-pUT18	pKT25-2616-CC1462-pUT18	pKT25-CC1462-PodJ-pUT18	pKT25-CC1462-PodJ-pUT18	pKT25-CC1462-CtrA-pUT18	pKT25-CC1462-CtrA-pUT18	pKT25-CC1462-RcdA-pUT18	pKT25-CC1462-RcdA-pUT18	pKT25-CC1462-CpdR-pUT18	pKT25-CC1462-CpdR-pUT18	pKT25-CC1462-ClpX-pUT18	pKT25-CC1462-ClpX-pUT18	pKT25-CC1462-ClpP-pUT18	pKT25-CC1462-ClpP-pUT18
	pKT25-CC1462-pUT18C-CC2616	pKT25-CC2616-pUT18C-CC2616	pKT25-CC2616-pUT18C-PodJ	pKT25-CC2616-pUT18C-PodJ	pKT25-CC1462-pUT18C-CtrA	pKT25-CC1462-pUT18C-CtrA	pKT25-CC1462-pUT18C-RcdA	pKT25-CC1462-pUT18C-RcdA	pKT25-CC1462-pUT18C-CpdR	pKT25-CC1462-pUT18C-CpdR	pKT25-CC1462-pUT18C-ClpX	pKT25-CC1462-pUT18C-ClpX	pKT25-CC1462-pUT18C-ClpP	pKT25-CC1462-pUT18C-ClpP
	pKT25-CC1462-pUT18	pKT25-CC2616-pUT18C-CC2616	pKT25-pUT18C-PodJ-pUT18	pKT25-pUT18C-PodJ-pUT18	pKT25-pUT18C-CtrA-pUT18	pKT25-pUT18C-CtrA-pUT18	pKT25-pUT18C-RcdA-pUT18	pKT25-pUT18C-RcdA-pUT18	pKT25-pUT18C-CpdR-pUT18	pKT25-pUT18C-CpdR-pUT18	pKT25-pUT18C-ClpX-pUT18	pKT25-pUT18C-ClpX-pUT18	pKT25-pUT18C-ClpP-pUT18	pKT25-pUT18C-ClpP-pUT18
controls	pKT25-CC2616-pUT18	pKT25-CC2616-pUT18C-CC2616	pKT25-pUT18C-PodJ-pUT18	pKT25-pUT18C-PodJ-pUT18	pKT25-pUT18C-CtrA-pUT18	pKT25-pUT18C-CtrA-pUT18	pKT25-pUT18C-RcdA-pUT18	pKT25-pUT18C-RcdA-pUT18	pKT25-pUT18C-CpdR-pUT18	pKT25-pUT18C-CpdR-pUT18	pKT25-pUT18C-ClpX-pUT18	pKT25-pUT18C-ClpX-pUT18	pKT25-pUT18C-ClpP-pUT18	pKT25-pUT18C-ClpP-pUT18
	pKT25-CC1462-pUT18	pKT25-CC1462-pUT18C-CC1462	pKT25-pUT18C-PodJ-pUT18	pKT25-pUT18C-PodJ-pUT18	pKT25- <i>zip</i> -pUT18	pKT25-pUT18			pKT25-pUT18C-CC1462-pUT18	pKT25-pUT18C-CC1462-pUT18	pKT25-pUT18C-CC1462-pUT18	pKT25-pUT18C-CC1462-pUT18	pKT25- <i>zip</i> -pUT18	pKT25-pUT18
	pUT18	pUT18C	CC1462-pUT18	pUT18C-CC1462										

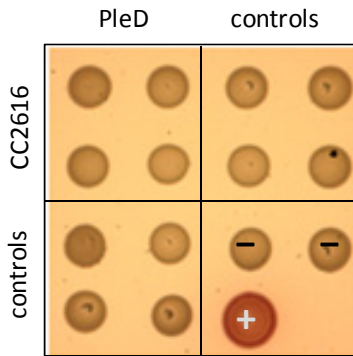


	PleD		controls	
CC1462	pKT25-CC1462-PleD-pUT18	pKT25-CC1462-pUT18C-PleD	pKT25-CC1462-pUT18	pKT25-CC1462-pUT18C
	pKT25-CC1462-pUT18C-CC1462	pKT25-pUT18C-CC1462-pUT18C	pKT25-pUT18C-CC1462-pUT18	pKT25-pUT18C-CC1462-pUT18C
	pKT25-CC1462-pUT18	pKT25-pUT18C-CC1462-pUT18C	pKT25-pUT18C-CC1462-pUT18	pKT25-pUT18C-CC1462-pUT18C
controls	pKT25-PleD-pUT18	pKT25-PleD-pUT18C	pKT25-pUT18	pKT25-pUT18C
	pKT25-PleD-pUT18	pKT25-pUT18C-PleD	pKT25- <i>zip</i> -pUT18	pKT25- <i>zip</i> -pUT18C
	pUT18	pUT18C		

B



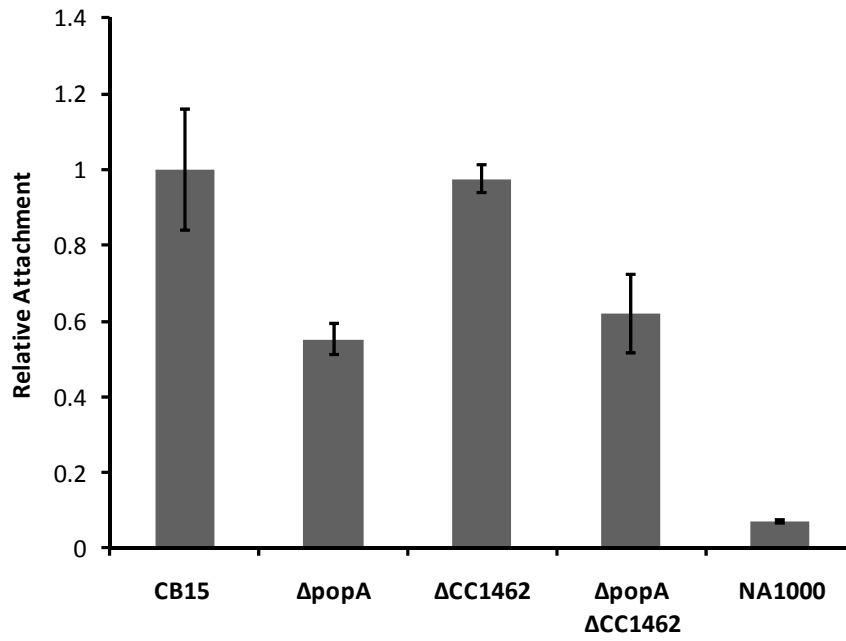
	PodJ _{cyt}		CtrA		RcdA		CpdR		ClpX		ClpP		CC2616	
CC2616	pKT25-CC2616	PodJ-CC2616	pKT25-CC2616	CtrA-CC2616	pKT25-CC2616	RcdA-CC2616	pKT25-CC2616	CpdR-CC2616	pKT25-CC2616	ClpX-CC2616	pKT25-CC2616	ClpP-CC2616	pKT25-CC2616	CC2616-CC2616
	pUT18-CC2616	PodJ-CC2616	pUT18-CC2616	CtrA-CC2616	pUT18-CC2616	RcdA-CC2616	pUT18-CC2616	CpdR-CC2616	pUT18-CC2616	ClpX-CC2616	pUT18-CC2616	ClpP-CC2616	pUT18-CC2616	CC2616-CC2616
controls	pKT25-CC2616	PodJ-CC2616	pKT25-CC2616	CtrA-CC2616	pKT25-CC2616	RcdA-CC2616	pKT25-CC2616	CpdR-CC2616	pKT25-CC2616	ClpX-CC2616	pKT25-CC2616	ClpP-CC2616	pKT25-CC2616	CC2616-CC2616
	pUT18-CC2616	PodJ-CC2616	pUT18-CC2616	CtrA-CC2616	pUT18-CC2616	RcdA-CC2616	pUT18-CC2616	CpdR-CC2616	pUT18-CC2616	ClpX-CC2616	pUT18-CC2616	ClpP-CC2616	pUT18-CC2616	CC2616-CC2616



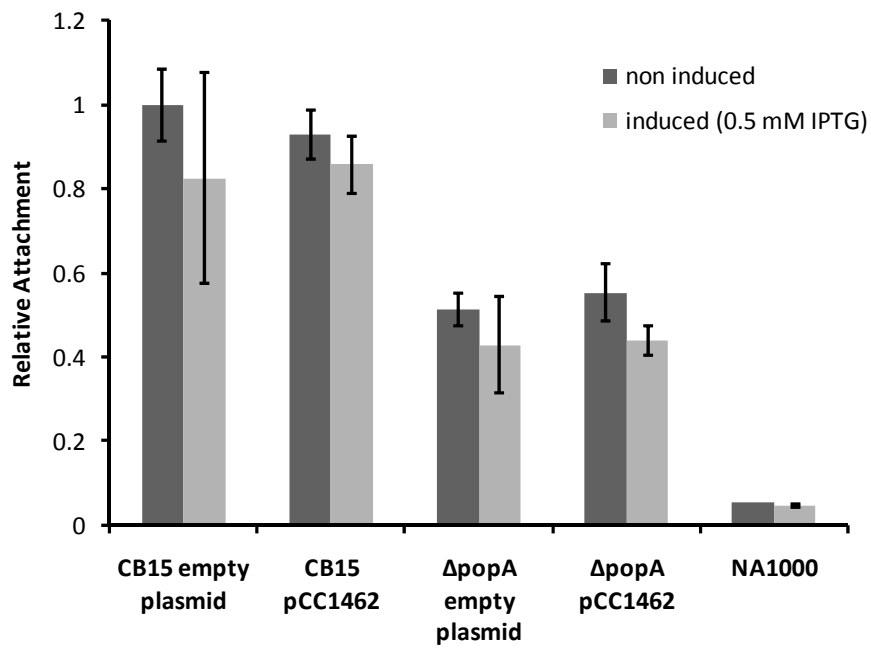
	PleD		controls	
CC2616	pKT25-CC2616	PleD-CC2616	pKT25-CC2616	CC2616-CC2616
	pUT18-CC2616	PleD-CC2616	pUT18-CC2616	CC2616-CC2616
controls	pKT25-CC2616	PleD-CC2616	pKT25-CC2616	CC2616-CC2616
	pUT18-CC2616	PleD-CC2616	pUT18-CC2616	CC2616-CC2616

Figure S3

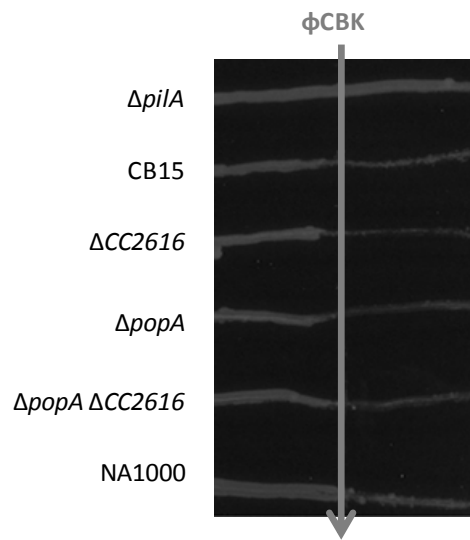
A



B



C



D

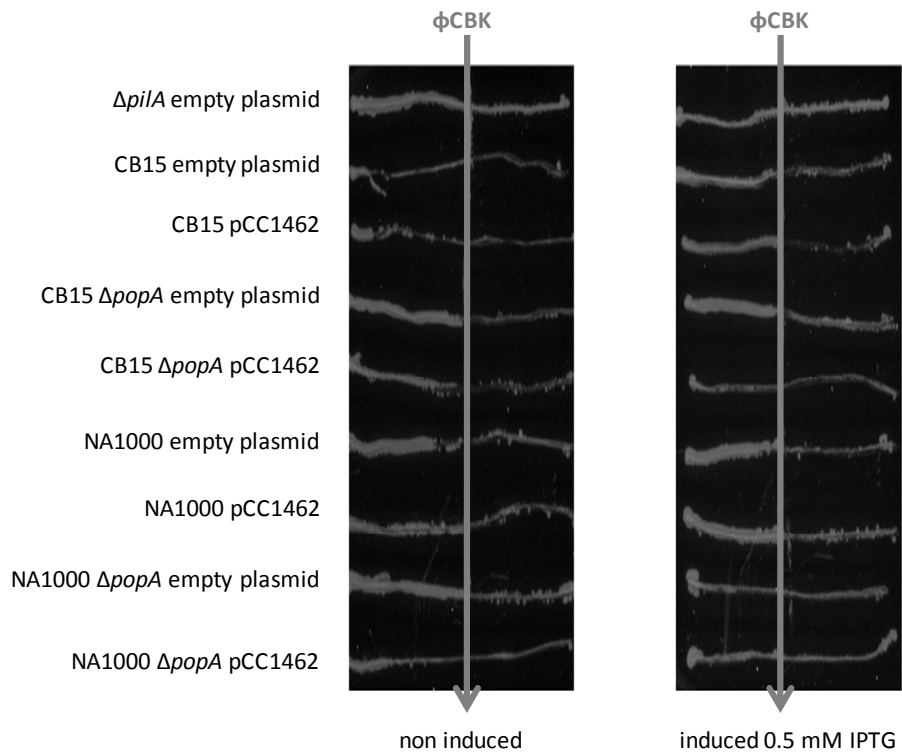
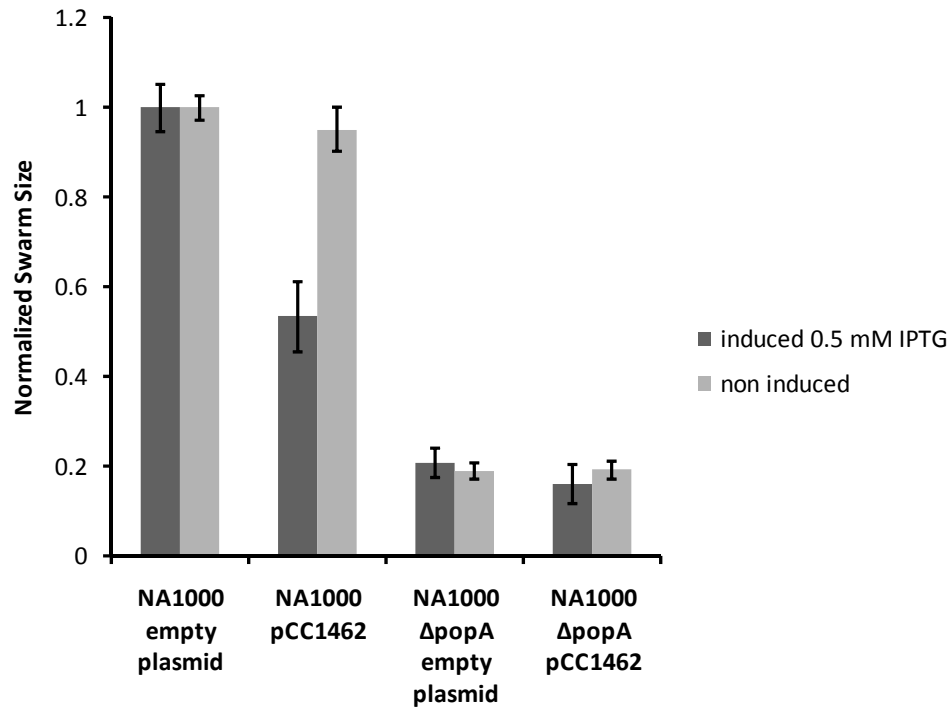


Figure S4

A



B

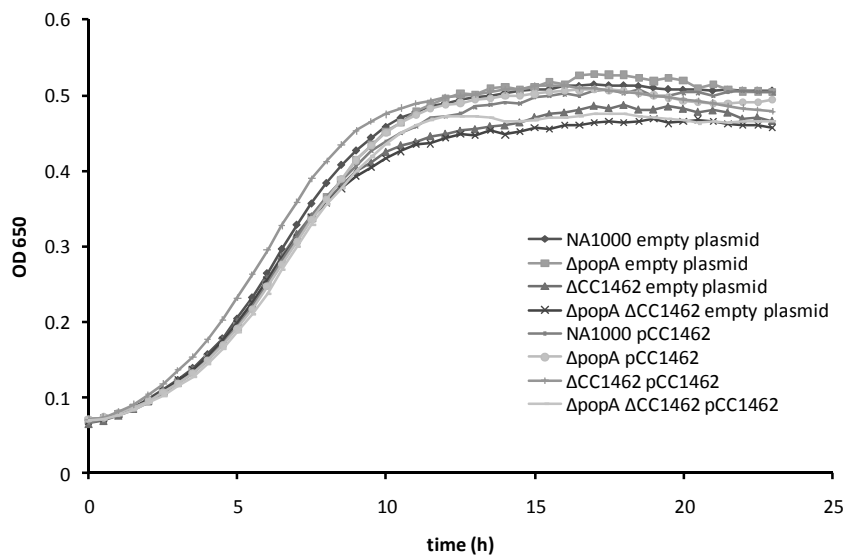
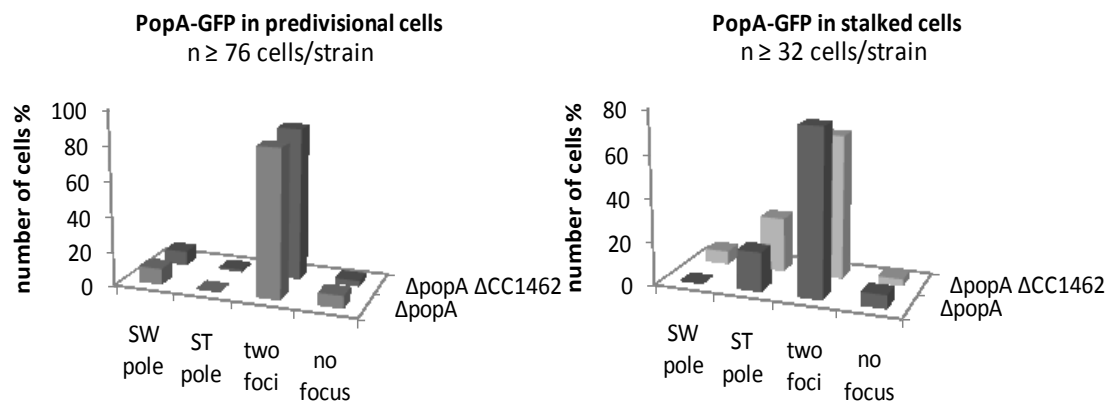
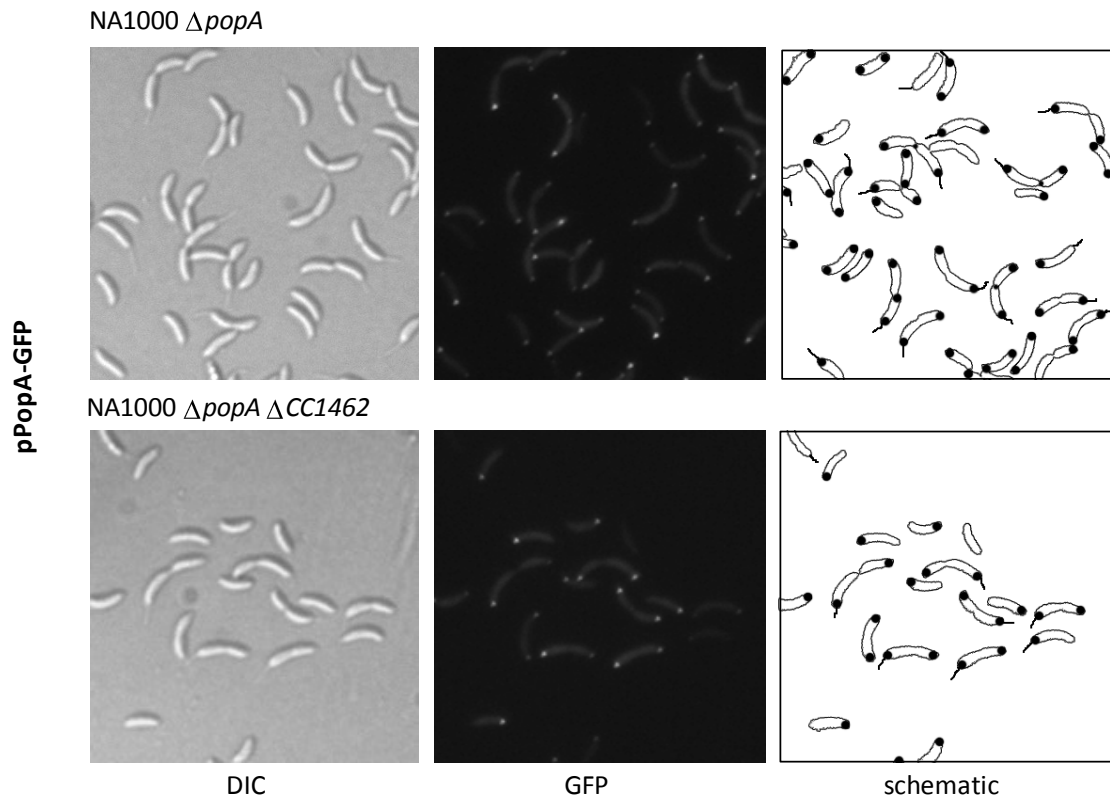
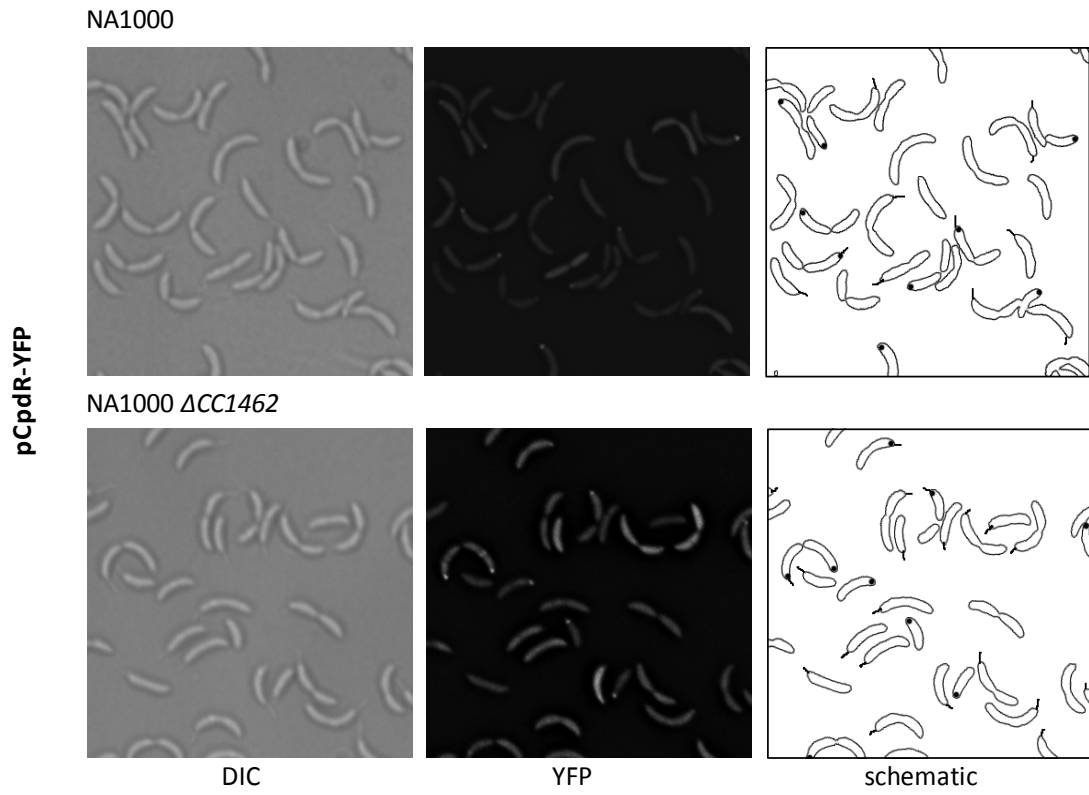


Figure S5

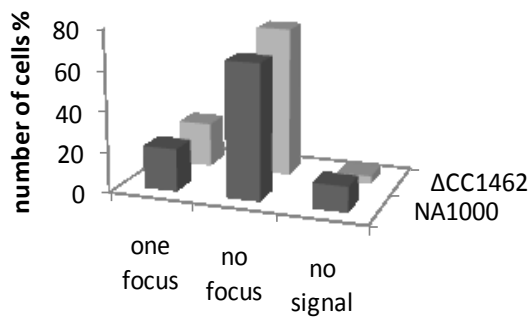
A



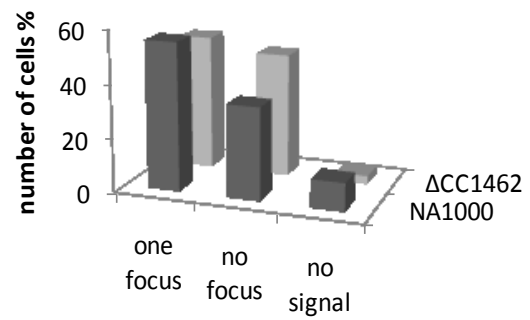
B



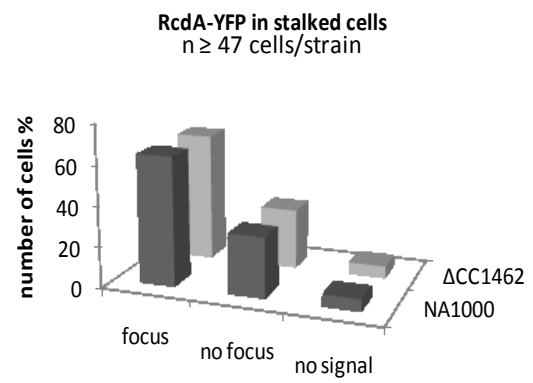
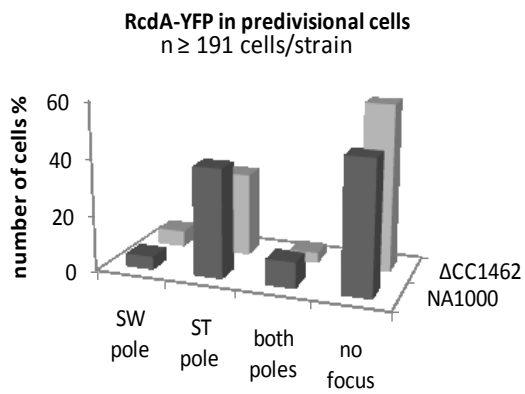
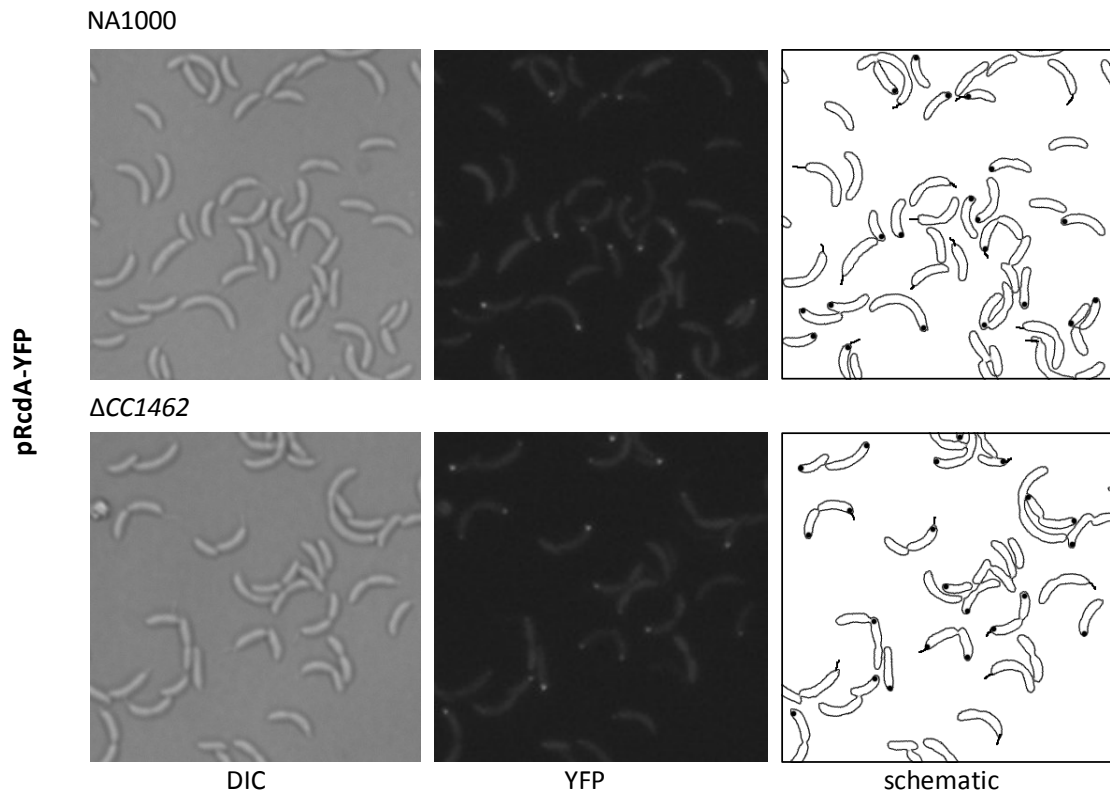
CpdR-YFP in predivisional cells
n ≥ 81 cells/strain



CpdR-YFP in stalked cells
n ≥ 67 cells/strain



C



D

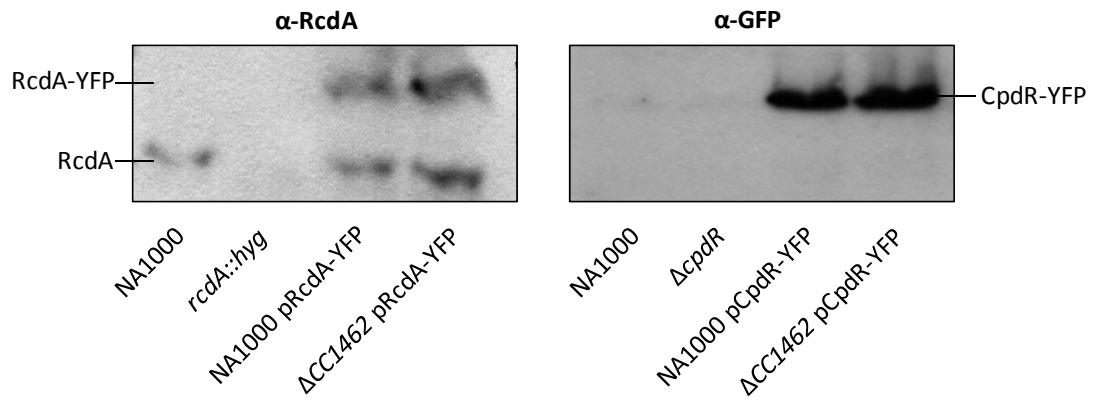
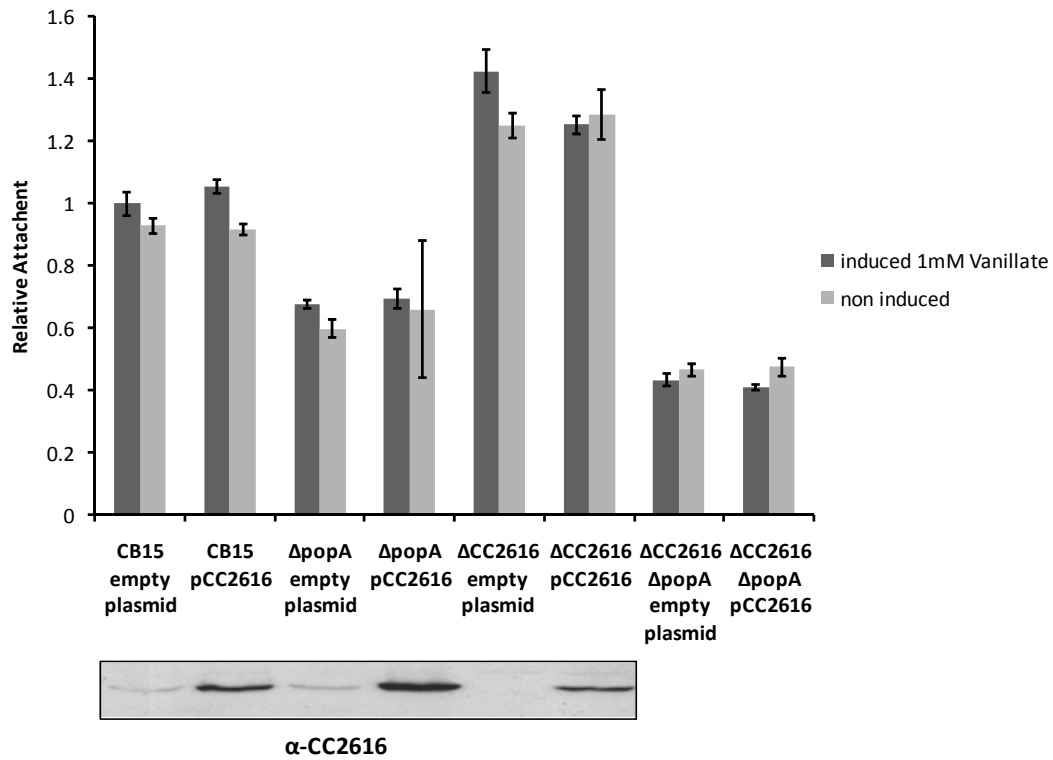
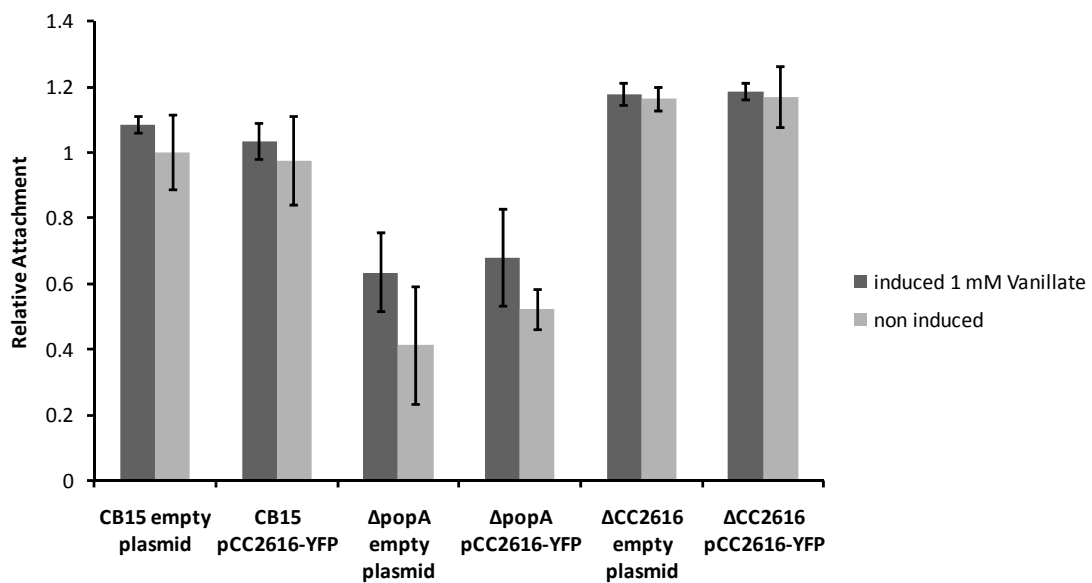


Figure S6

A



B



C

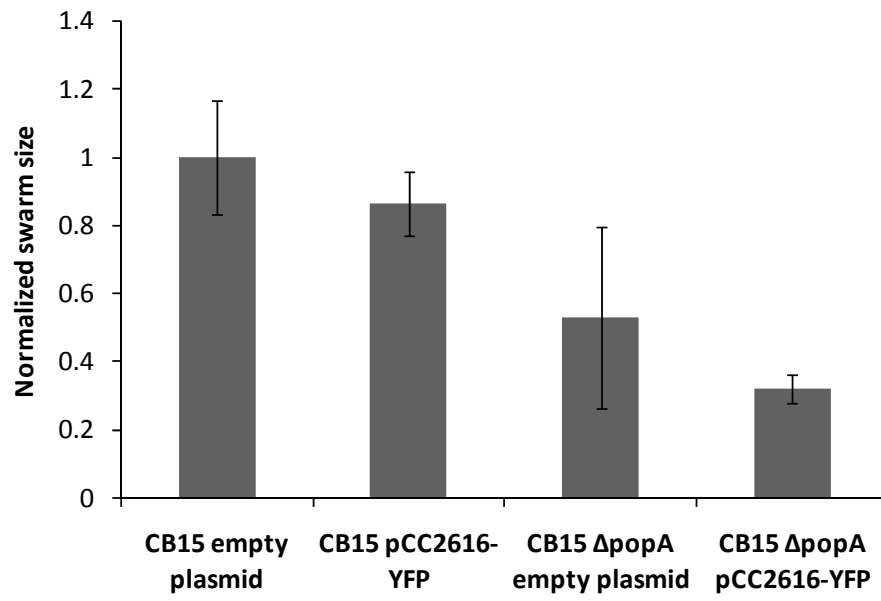
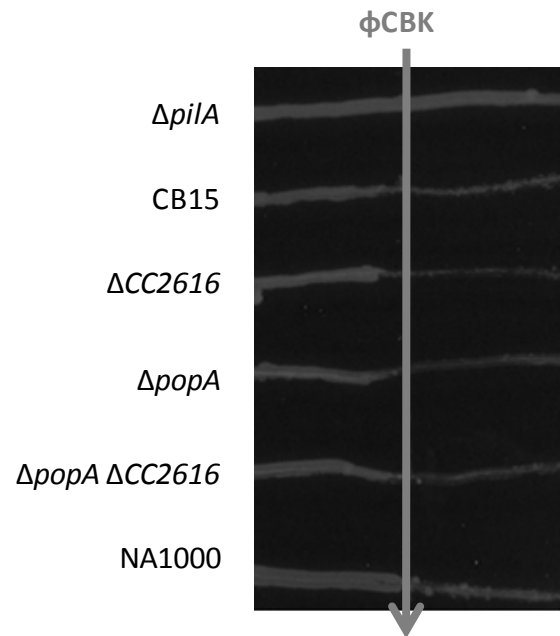


Figure S7

A



B

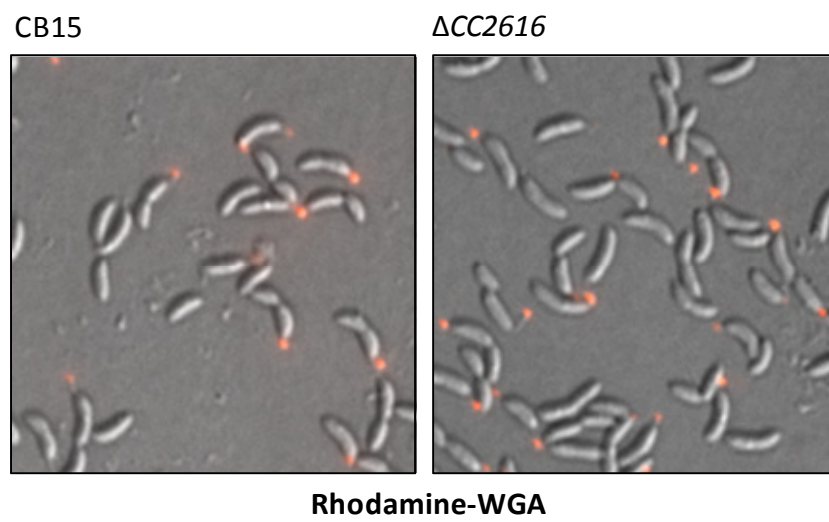
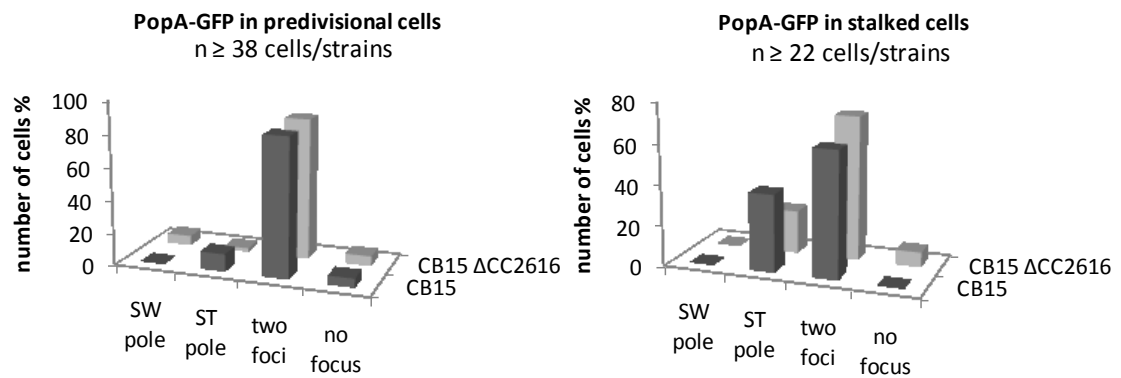
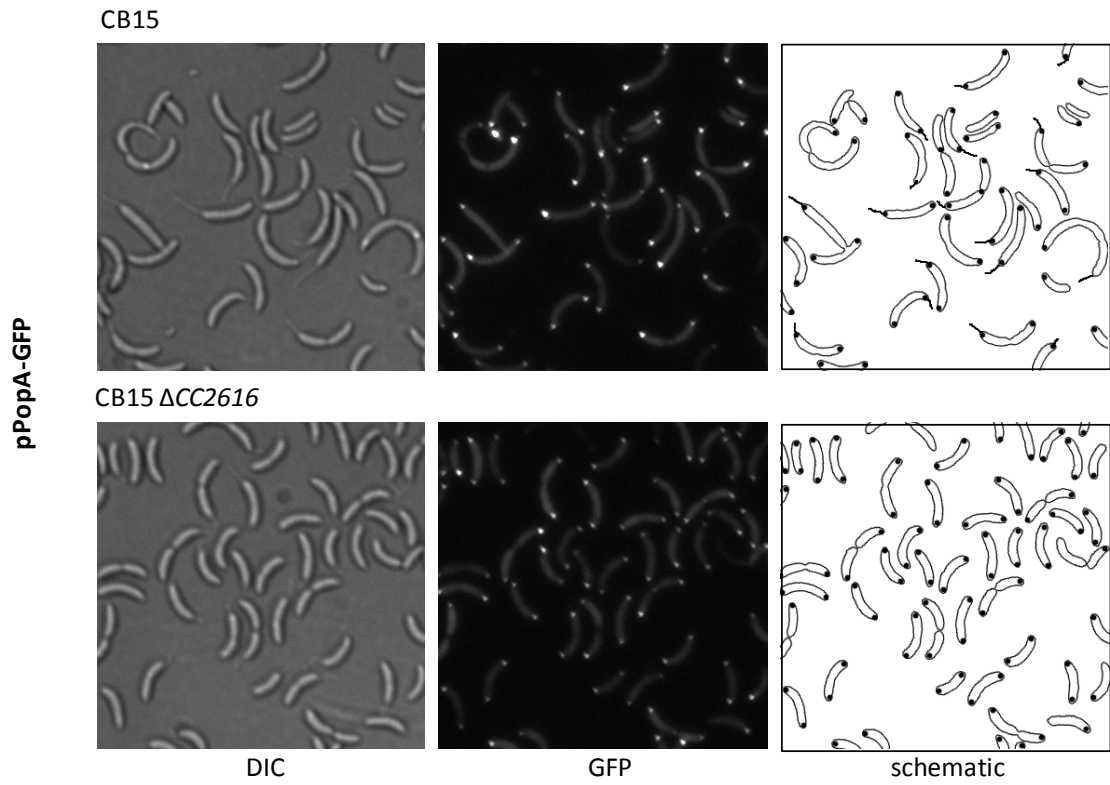
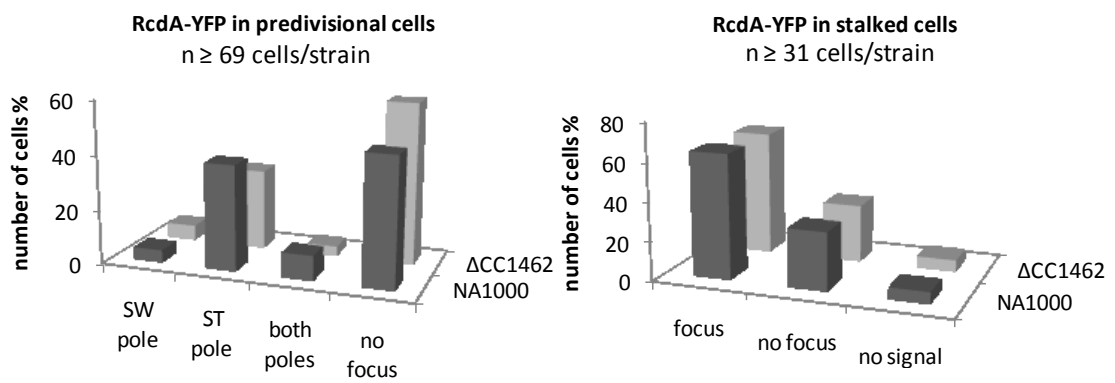
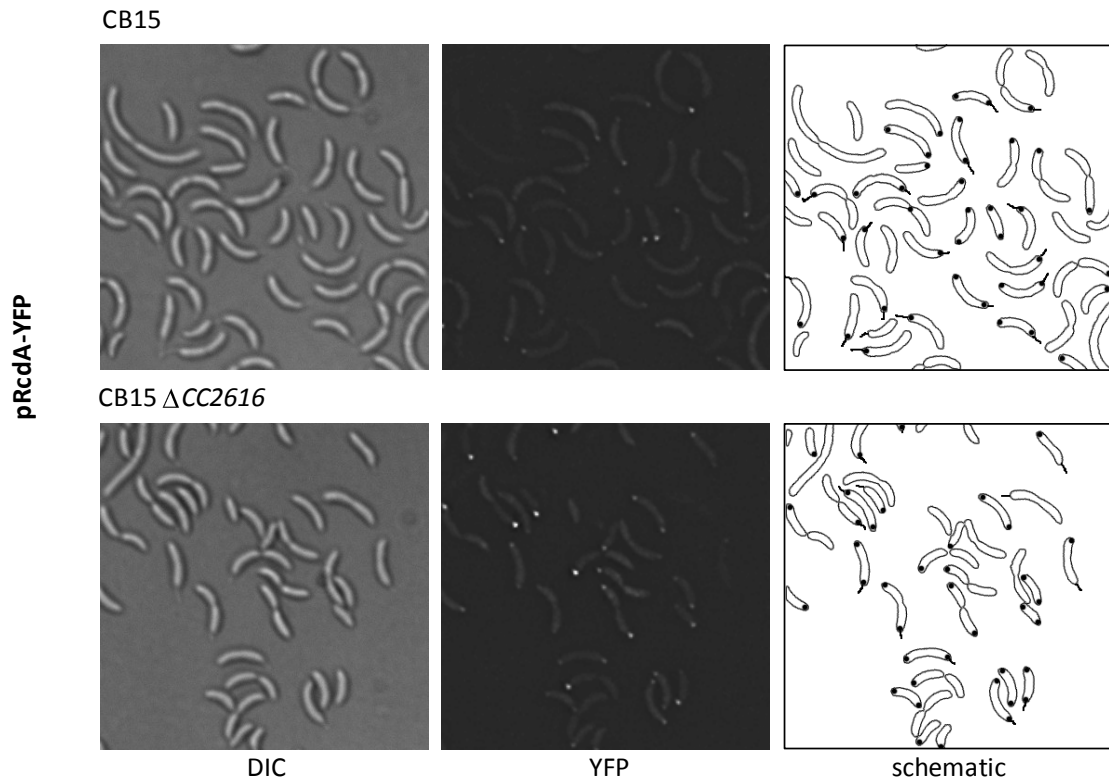


Figure S8

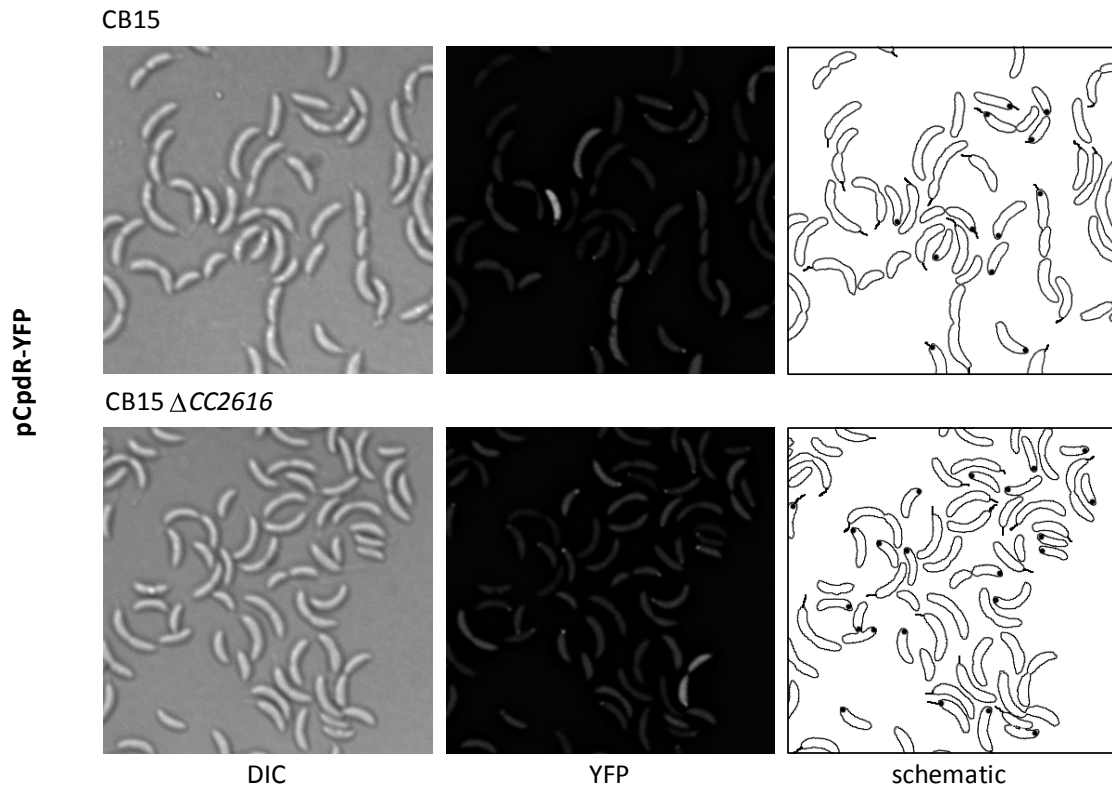
A



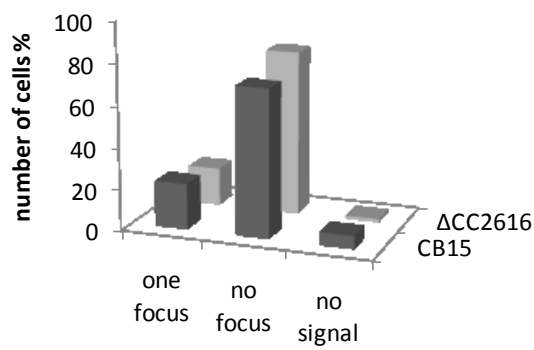
B



C



pCpdR-YFP in predivisional cells
n \geq 40 cells/strain



pCpdR-YFP in stalked cells
n \geq 47 cells/strain

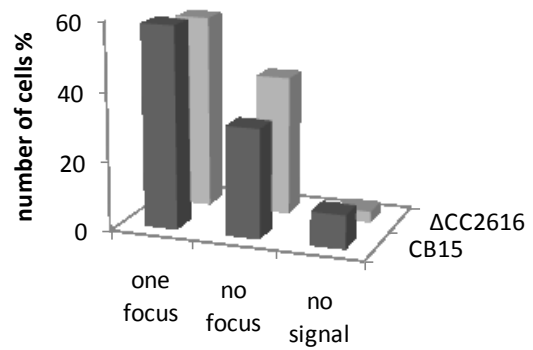
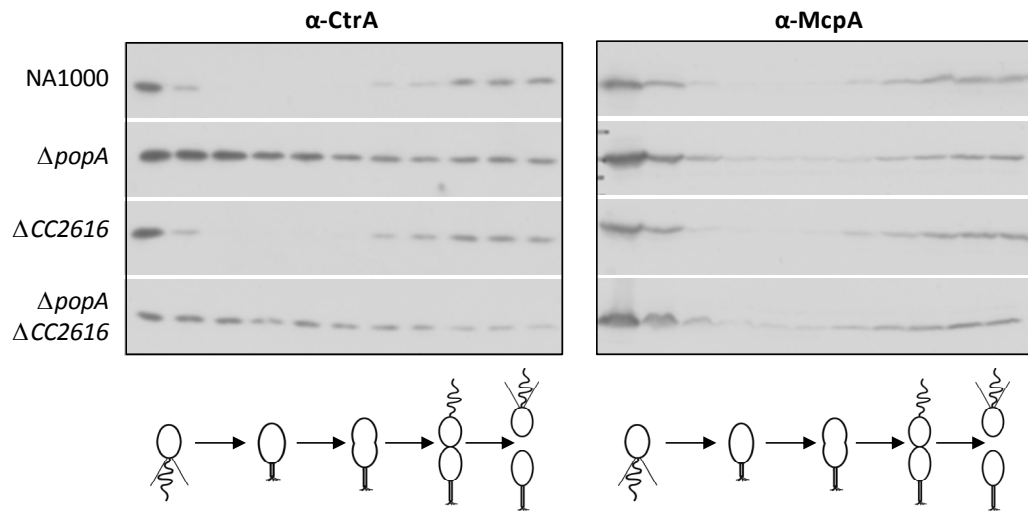


Figure S9

A



3.2.8 Table S1

***C. crescentus* Strains**

Name	Description	Source or Reference
UJ4932	CB15 and pAD5	This study
UJ5354	NA1000 Δ CC1462	This study
UJ5355	NA1000 Δ popA Δ CC1462	This study
UJ5532	NA1000 Δ CC1462 and plasmid pSRK-Km	This study
UJ5533	NA1000 Δ CC1462 Δ popA and plasmid pSRK-Km	This study
UJ5534	NA1000 and plasmid pSRK-Km	This study
UJ5537	CB15 Δ popA Δ CC2616	This study
UJ5539	CB15 Δ CC2616	This study
UJ5540	CB15 Δ popA Δ CC1462	This study
UJ5544	CB15 Δ CC1462	This study
UJ5558	CB15 and pSRK-Km	This study
UJ5559	CB15 Δ popA and pSRK-Km	This study
UJ5571	CB15 Δ pilA and plasmid pSRK-Km	This study
UJ5625	CB15 Δ CC2616 and plasmid pAD5	This study
UJ5631	CB15 and plasmid pRVMCS-2	This study
UJ5633	CB15 Δ popA and plasmid pRVMCS-2	This study
UJ5627	NA1000 and plasmid pRVMCS-2	This study
UJ5665	NA1000 Δ CC1462 and plasmid pAM76	This study
UJ5667	NA1000 Δ CC1462 and plasmid pAM75	This study
UJ5668	NA1000 Δ popA Δ CC1462 and plasmid pAM75	This study
UJ5069	NA1000 cdG ⁰ and plasmid pAD5	This study
UJ6018	NA1000 and plasmid pAM73	This study
UJ6019	NA1000 Δ cpdR and plasmid pAM73	This study
UJ6020	NA1000 <i>rcdA::hygromycin</i> and plasmid pAM73	This study
UJ6021	NA1000 Δ pleD and plasmid pAM73	This study
UJ6022	NA1000 Δ CC1462 and plasmid pAM73	This study
UJ6023	NA1000 Δ popA and plasmid pAM73	This study
UJ6024	CB15 and plasmid pAM73	This study
UJ6025	CB15 Δ CC2616 and plasmid pAM73	This study
UJ6026	CB15 Δ popA and plasmid pAM73	This study
UJ6030	NA1000 Δ CC1462 and plasmid pX-cpdR-yfp	This study
UJ6033	CB15 and plasmid pAD106	This study
UJ6035	CB15 and plasmid pX-cpdR-yfp	This study
UJ6036	CB15 Δ CC2616 and plasmid pX-cpdR-yfp	This study
UJ6057	CB15 Δ CC2616 and plasmid pRVMCS-2	This study
UJ6064	CB15 Δ CC2616 and plasmid pAD106	This study
UJ6198	NA1000 and plasmid pAM68	This study
UJ6199	NA1000 Δ popA and plasmid pAM68	This study
UJ6200	NA1000 Δ CC1462 and plasmid pAM68	This study
UJ6201	NA1000 Δ CC1462 Δ popA and plasmid pAM68	This study
UJ6202	CB15 and plasmid pAM77	This study
UJ6203	CB15 Δ popA and plasmid pAM77	This study

UJ6204	CB15 Δ CC2616 and plasmid pAM77	This study
UJ6205	CB15 Δ popA Δ CC2616 and plasmid pAM77	This study
UJ6206	NA1000 Δ CC1462 and plasmid pAD106	This study
UJ6207	NA1000 and plasmid pAM76	This study
UJ6208	NA1000 Δ podJ and plasmid pAM76	This study
UJ6209	NA1000 cdG ⁰ and plasmid pAD76	This study
UJ6210	NA1000 <i>rcdA::hygromycin</i> and plasmid pAM76	This study
UJ6211	NA1000 Δ cpdR and plasmid pAM76	This study
NA1000	Synchronizable laboratory strain of CB15	65
CB15	<i>C. crescentus</i> wild-type strain	ATCC 19089
UJ2765	NA1000 Δ podJ and pAD5	8
UJ2796	NA1000 and pAD5	30
UJ2827	NA1000 Δ popA	8
UJ3160	NA1000 Δ popA and plasmid pAD5	8
UJ3240	NA1000 and pMR20	8
UJ3565	NA1000 Δ popA and plasmid pAD30	8
UJ4324	NA1000 and plasmid pAD106	8
UJ4426	NA1000 and plasmid pX-cpdR-yfp	8
UJ284	NA1000 Δ pleD	66
UJ590	CB15 Δ pilA	67
UJ1294	NA1000 and plasmid pMO88	M. Osteras and U. Jenal
UJ1581	NA1000 Δ podJ	P. Viollier
UJ4373	NA1000 Δ cpdR	10
UJ4461	CB15 Δ popA	S. Abel and U. Jenal, unpublished
UJ5065	NA1000 cdG ⁰	S. Abel and U. Jenal, unpublished

***E. coli* Strains**

Name	Description	Source or Reference
MM337	<i>E. coli</i> K-12 <i>araD139 flbB5301 ptsF25 rbsR relA1 rpsL150-(arg-F-lac)U169-cya</i>	17
DH10B	<i>F⁻mcrA D(mrr⁻hsd RMS⁻ mcrBC) f80dlacZM15DlacX74 endA1 rec1deoR D(ara, leu)7697 araD139 galU nupG rpsL thi pro⁻hsd⁺ recA RP4-2-Tc::Mu-Tn7</i>	68
S-17	<i>F⁻, lambda (-), thi, pro, recA, restriction (-) modification (+), RP4 derivative integrated into the chromosome with Tet::Mu, Km::T7</i>	68
BL21 (DE3)	<i>E. coli</i> B <i>F⁻ dcm ompT hsdS(rB- mB-) gal lambda(DE3)</i>	Novagen

Plasmids

Name	Description	Source or Reference
pAM52	pNPTS138; suicide vector to generate a <i>CC1462</i> deletion	This study
pAM54	pKT25; <i>CC2616</i> C-terminal fused to T25 fragment	This study
pAM62	pUT18C; <i>CC2616</i> C-terminal fused to T18 fragment	This study
pAM63	pUT18; <i>CC2616</i> N-terminal fused to T18 fragment	This study
pAM60	pKT25; <i>CC1462</i> C-terminal fused to T25 fragment	This study
pAM61	pUT18C; <i>CC1462</i> C-terminal fused to T18 fragment	This study
pAM64	pUT18; <i>CC1462</i> N-terminal fused to T18 fragment	This study
pAM65	pKT25; <i>podJ</i> soluble part (aa1 – aa669) C-terminal fused to T25 fragment	This study
pAM66	pUT18; <i>podJ</i> soluble part (aa1–aa669) N-terminal fused to T18 fragment	This study
pAM67	pUT18C; <i>podJ</i> soluble part (aa1–aa669) C-terminal fused to T18 fragment	This study
pAM68	pSRK-Km; <i>CC1462</i> under the control of <i>lac</i> promoter. <i>CC1462</i> GGT is replaced by ATG start codon	This study
pAM69	pSRK-Km; <i>yfp-CC1462</i> under the control of <i>lac</i> promoter	This study
pAM72	pNPT138; suicide vector to generate a clean deletion of <i>CC2616</i>	This study
pAM73	pRVYFPC-2; <i>CC2616-yfp</i> under the control of vanillate promoter	This study
pAM74	pRVMCS-2; <i>CC1462</i> under the control of vanillate promoter	This study
pAM75	pRVYFPC-2; <i>CC1462-yfp</i> under the control of vanillate promoter	This study
pAM76	pRVYFPC-2; <i>yfp-CC1462</i> under the control of vanillate promoter	This study
pAM77	pRVMCS-2; <i>CC2616</i> under the control of vanillate promoter	This study
pAD5	pMR20; <i>popA-gfp</i> under the control of <i>popA</i> promoter	8
pAD30	pMR20; <i>popA_{R357G}-gfp</i> under the control of <i>popA</i> promoter	8
pAD35	pMR20; <i>popA-flag</i> under the control of <i>popA</i> promoter	30
pAD38	pMR20; <i>popA</i> under the control of <i>popA</i> promoter	8
pAD39	pMR20; <i>popA_{R357G}</i> under the control of <i>popA</i> promoter	8
pAD44	pUT18C; <i>clpX</i> C-terminal fused to T18 fragment	8
pAD45	pKT25; <i>clpX</i> C-terminal fused to T25 fragment	8
pAD47	pUT18C; <i>clpP</i> C-terminal fused to T18 fragment	8
pAD48	pKT25; <i>clpP</i> C-terminal fused to T25 fragment	8
pAD50	pUT18C; <i>rcdA</i> C-terminal fused to T18 fragment	8
pAD51	pKT25; <i>rcdA</i> C-terminal fused to T25 fragment	8
pAD53	pUT18C; <i>cpdR</i> C-terminal fused to T18 fragment	8
pAD54	pKT25; <i>cpdR</i> C-terminal fused to T25 fragment	8
pAD56	pUT18; <i>rcdA</i> N-terminal fused to T18 fragment	8
pAD58	pUT18; <i>clpX</i> N-terminal fused to T18 fragment	8
pAD60	pUT18; <i>clpP</i> N-terminal fused to T18 fragment	8
pAD62	pUT18; <i>cpdR</i> N-terminal fused to T18 fragment	8

pAD65	pUT18; <i>ctrA</i> N-terminal fused to T18 fragment	8
pAD67	pUT18; <i>popA</i> N-terminal fused to T18 fragment	8
pAD90	pKT25; <i>popA</i> _{R357G} C-terminal fused to T25 fragment	8
pAD106	pBBR-MCS-5; <i>rcdA-yfp</i> under control of <i>rcdA</i> promoter	8
pAD140	pKT25; <i>ctrA</i> C-terminal fused to T25 fragment	8
pAD141	pKT25; <i>popA</i> C-terminal fused to T25 fragment	8
pAD142	pUT18C; <i>ctrA</i> C-terminal fused to T18 fragment	8
pAD143	pUT18C; <i>popA</i> C-terminal fused to T18 fragment	8
pSRK-Km	Kan ^R broad host range expression vector containing <i>lac</i> promoter and <i>lacI_q</i> and <i>lacZα+</i>	69
pRVYFPC-2	pRK2 derivative; Kan ^R low copy number vector	70
pRVYFPN-2	pRK2 derivative; Kan ^R low copy number vector	70
pRVMCS-2	pRK2 derivative; Kan ^R low copy number vector	70
pNPTS138	Kan ^R , suicide vector with <i>sacB</i> gene and <i>oriT</i>	M.R.K. Alley
pX-cpdR-yfp	pMR31; <i>cpdR-yfp</i> under the control of xylose promoter	10
pMR20	Tet ^R low copy number and broad host range vector	71
pMO88	pMR20; <i>clpX</i> carrying a mutation in the ATP binding site under the control of xylose promoter	M. Osteras and U. Jenal

4 Outlook

Spatial and temporal sequestration of c-di-GMP signaling molecules provides a mechanism to prevent crosstalk between parallel operating systems^{2,15}. In this work, we presented a possible activation and sequestration mechanism for the c-di-GMP effector protein PopA, which is required for the proteolysis of key regulatory proteins at the ClpXP-occupied stalked pole during *C. crescentus* swarmer-to-stalked cell transition^{56,169}.

The analysis of a strain lacking all known diguanylate cyclases (cdG⁰ strain) confirmed that PopA polar sequestration and function are strictly dependent on c-di-GMP (S. Abel and U. Jenal, unpublished). Further analysis revealed two diguanylate cyclases, PleD and DgcB, which contribute to PopA localization⁴⁷. However, a *pleD dgcB* double mutant interferes only partially with PopA stalked pole function¹⁷¹, raising the question about additional cyclases involved in cell cycle-dependent activation of PopA. Among six possible candidates harboring a GGDEF domain two were biochemically identified as cyclases. While DgcA was reported to function as cyclase *in vitro*²⁴, the GGDEF-EAL composite protein CC0655 is bifunctional but displays predominantly cyclase activity *in vivo* (E. Friedrich and U. Jenal, unpublished). Analysis of PopA function in the respective triple or quadruple mutants will reveal if these cyclases feed into the c-di-GMP pool leading to PopA activation and localization. An alternative approach to identify additional upstream components of PopA would be to sequentially reintroduce genes coding for individual GGDEF and/or EAL proteins into the cdG⁰ background and analyze the PopA readout the resulting strains.

It is not clear why the PopA pathway leading to CtrA degradation and S-phase entry would require several converging diguanylate cyclases and possibly phosphodiesterases. One possibility is that several cell cycle and outside signals need to be integrated to commit to this important step in cell proliferation. The observation that a *pleD dgcB* double mutant fails to undergo the motile-sessile switch but only partially inactivates PopA argues that development and cell cycle progression have a different fine-tuning with respect to c-di-GMP control. It will thus

be of importance to characterize the signals sensed by PopA upstream components. Uncovering their nature will reveal if the c-di-GMP signaling cascade contributing to cell cycle progression is cross connected to other regulatory pathways such as systems monitoring DNA integrity, availability of nutrients or other environmental factors. Such cross connections have been described for other bacterial species^{39,96}.

The work presented here indicates that PopA localization is governed by its c-di-GMP binding state. We proposed a model where c-di-GMP activates PopA by imposing a conformational change through crosslinking of adjacent GGDEF domains. However, it remains unclear if c-di-GMP binding affects the PopA oligomerization state. Biochemical attempts to address this question were hampered so far by the poor solubility of this protein. However, the identified PopA interaction partners CC1462 and CC2616 might help to enhance PopA *in vitro* solubility and stability and could permit biochemical and structural analysis such as SLS (static light scattering) in the presence or absence of c-di-GMP. Likewise, crystallization of PopA in complex with c-di-GMP and its interaction partners might be possible. A possible *in vivo* approach to test the dimerization hypothesis would involve FRET analysis (fluorescence resonance energy transfer) with strains co-expressing CFP- and YFP-tagged PopA wild-type and PopA I-site mutant alleles. If the domain crosslinking hypothesis holds true, one would expect that combinations of primary and secondary I-site mutations result in a loss of the FRET signal and in addition, abolish PopA localization and CtrA degradation. In addition, the c-di-GMP-induced conformational change could lead to the exposure of a hidden polar signal. Such a structural rearrangement could be monitored using HX-MS (hydrogen exchange-coupled mass spectrometry)¹⁷² and might reveal regions that are unmasked upon c-di-GMP binding. Since these regions may contain pole specificity signals it will be interesting to analyze if they are different or identical for old and new cell poles. In a broader perspective, it will be attractive to compare activation mechanisms of other c-di-GMP effectors to deduce general regulatory concepts such as for example c-di-GMP induced oligomerization.

c-di-GMP-bound PopA is targeted to the cell pole⁵⁶. The dynamics of this process and the stability of polar PopA clusters are unclear. PopA dynamics as a function of cellular c-di-GMP levels could be addressed using FRAP (fluorescence

recovery after photobleaching) for example in a cdG^0 strain expressing an inducible heterologous cyclase (S. Abel and U. Jenal, unpublished) or in strains with different homologous cyclase combinations. It would be particularly interesting to set up a test system where cyclases are directed to distinct subcellular sites and ask if this influences PopA dynamics towards the old pole. This would allow addressing the question if upstream components like PleD or DgcB need to be at the same subcellular site to robustly target PopA to its cellular destination. We have shown that additional components that interact with PopA and are involved in cell cycle control dynamically localize to the stalked cell pole to form a macromolecular degradation platform. Colocalization studies and FRAP experiments could help to define this protein-protein interaction network and determine the dynamics and the order of assembly of its individual components. Although for some of these components dedicated localization factors have been described^{47,56,158,168}, for other proteins the mechanisms anchoring them at a specific position in the cell have not been identified yet. Considering that over 10% of all predicted *C. crescentus* proteins sequester to specific subcellular sites¹⁷³, it seems likely that general landmark proteins govern directly or indirectly the positioning of all subsequent proteins. Alternatively, certain lipid structures in the membrane could anchor specific proteins as it is observed in eukaryotic cells. Recently, PopZ, a multifunctional scaffold protein having a similar bipolar localization pattern like PopA was identified. It is not only involved in holding centromeres of replicating chromosomes apart¹⁷⁴, but also acts as localization factor for many stalked pole specific proteins such as SpmX, CckA, RcdA, CpdR and ClpX¹⁷⁵. It would be interesting to test whether targeting of PopA relies on PopZ as well. Finally, one could also screen for factors involved in the localization of PopA using an automated fluorescence microscope or alternatively search for membrane interaction partners.

Besides the known interaction partner RcdA which binds within the first PopA receiver domain we identified two novel direct PopA interaction partners. This raises the question, whether these proteins compete for overlapping binding sites or whether binding occurs independently or cooperatively. To address this question, localization of specific components should be carefully analyzed (localization, FRET, FRAP) in strains lacking or overexpressing individual partner proteins. To evaluate a

potential effect of c-di-GMP on binding affinities, these experiments should be carried out in the presence and absence of c-di-GMP. To narrow down possible binding sites on PopA, bacterial two-hybrid analysis with truncated PopA alleles could be performed.

Besides the binding properties of the newly identified interaction partners, it will be important to further characterize their cellular functions. While CC1462 was shown to be proteolytically processed by ClpXP, the physiological relevance for its cell cycle-dependent removal is not known. Although overexpression of this protein led to its stabilization during the cell cycle and to a slight decrease in swarm size, the molecular basis of this effect is not understood. To address if ectopic presence or activity of this protein during cell cycle affects cell motility, careful analysis of flagellar assembly and function should be performed. The second interaction partner, CC2616, is annotated as guanine deaminase and involved in the motile-sessile switch, however, it is not clear whether this protein has enzymatic activity or adopted a new function as guanine effector. To assess these possibilities, *C. crescentus* strains lacking CC2616 could be analyzed for their ability to metabolize guanine as sole carbon source. CC2616 active site mutants should be generated and analyzed with respect to their interaction with PopA and other components involved in cell cycle control, their polar localization and degradation pattern of key regulatory proteins. In addition, binding studies with guanine and guanine-related nucleotides could be performed. Moreover, it would be interesting to see if CC1462 or CC2616 could interfere with degradation of key regulatory proteins *in vitro*.

In addition to the prominent role of PopA in cell cycle progression at the ClpXP-occupied stalked pole, PopA contributes to cell motility and attachment¹⁷¹. It is likely, that downstream mediator proteins regulating these functions exist, however, they have not been identified yet and it is not clear if PopA localization to the PodJ dependent new pole is connected to these developmental functions. A possibility to assess components involved in the PopA pathway leading to cell motility might reside in a screen for motile suppressors in a *popA* deletion strain.

5 Bibliography

1. Camilli, A. and Bassler B.L. Bacterial small-molecule signalling pathways. *Science* **311**, 1113-1116 (2006).
2. Hengge, R. Principles of c-di-GMP signalling in bacteria. *Nature reviews. Microbiology* **7**, 263-73 (2009).
3. Gomelsky, M. cAMP, c-di-GMP, c-di-AMP and now cGMP: bacteria use them all! *Molecular Microbiology* **79**, 562-5 (2011).
4. Kim, Y.R., Kim, S.Y., Kim, C.M., Lee, S.E. and Rhee, Y.H. Essential role of an adenylate cyclase in regulation *Vibrio vulnificus* virulence. *FEMS Microbiology letters* **243**, 497-503 (2005).
5. Bai, G., Knapp, G.S. and McDonough, K.A. Cyclic AMP signalling in mycobacteria: redirecting the conversation with a common currency. *Cellular Microbiology* **13**, 349-58 (2011).
6. Ohta, N., Lane, T., Ninfa, E.G., Sommer, J.M. and Newton, A. A histidine protein kinase homologue required for regulation of bacterial cell division and differentiation. *Proceedings of the National Academy of Sciences of the United States of America* **89**, 10297-301 (1992).
7. Botsford, J.L. and Harman, J.G. Cyclic AMP in prokaryotes. *Microbiological Reviews* **56**, 100-22 (1992).
8. Potrykus, K. and Cashel, M. (p)ppGpp: still magical? *Annual Review of Microbiology* **62**, 35-51 (2008).
9. Woodward J.J., Iavarone A.T., Portnoy, D.A. C-di-AMP secreted by intracellular *Listeria monocytogenes* activates host type I interferon response. *Science* **328**, 1703-1705 (2010).
10. Witte, G., Hartung, S., Büttner, K. and Hopfner, K.-P. Structural biochemistry of a bacterial checkpoint protein reveals diadenylate cyclase activity regulated by DNA recombination intermediates. *Molecular Cell* **30**, 167-78 (2008).
11. Römling, U. Great times for small molecules: c-di-AMP, a second messenger candidate in Bacteria and Archaea. *Science Signaling* **1**, pe39 (2008).
12. Linder, J.U. cGMP production in bacteria. *Molecular and Cellular Biochemistry* **334**, 215-9 (2010).
13. Marden, J.N., Dong, Q., Roychowdhury, S., Berleman, J.E. and Bauer, C.E. Cyclic GMP controls *Rhodospirillum centenum* cyst development. *Molecular Microbiology* **79**, 600-15 (2011).
14. Galperin, M.Y., Nikolskaya, A.N. and Koonin, E.V. Novel domains of the prokaryotic two-component signal transduction systems. *FEMS Microbiology Letters* **203**, 213-214 (2001).

15. Jenal, U. and Malone, J. Mechanisms of cyclic-di-GMP signaling in bacteria. *Annual Review of Genetics* **40**, 385-407 (2006).
16. Ross, P., Weinhouse, H., Aloni, Y., Michaeli, D., Weinberger-Ohana, P., Mayer, R., Braun, S., De Vroom, E., Van der Marel, G.A. and Benziman, M. Regulation of cellulose synthesis in *Acetobacter xylinum* by cyclic diguanylic acid. *Nature* **325**, 279-281 (1987).
17. Tal, R., Wong, H.C., Calhoun, R., Gelfand, D., Fear, A.L., Volman, G., Mayer R., Ross, P., Amikan, D., Weinhouse H., Cohen A., Sapir, S., Ohana, P. and Benziman, M. Three *cdg* operons control cellular turnover of cyclic di-GMP in *Acetobacter xylinum*: genetic organization and occurrence of conserved domains in isoenzymes. *Journal of Bacteriology* **180**, 4416-25 (1998).
18. Paul, R., Weiser, S., Amiot, N.C., Chan, C., Schirmer, T., Giese, B. and Jenal, U. Cell cycle-dependent dynamic localization of a bacterial response regulator with a novel di-guanylate cyclase output domain. *Genes & Development* **18**, 715-27 (2004).
19. Ryjenkov, D.A., Tarutina, M., Moskvin, O.V. and Gomelsky, M. Cyclic Diguanylate Is a ubiquitous signaling molecule in bacteria: Insights into biochemistry of the GGDEF protein domain. *Journal of Bacteriology* **187**, 1792-1798 (2005).
20. Chan, C., Paul, R., Samoray, D., Amiot, N.C., Giese, B., Jenal, U. and Schirmer, T. Structural basis of activity and allosteric control of diguanylate cyclase. *Proceedings of the National Academy of Sciences of the United States of America* **101**, 17084-9 (2004).
21. Wassmann, P., Chan, C., Paul, R., Beck, A., Heerklotz, H., Jenal, U. and Schirmer, T. Structure of BeF₃⁻-modified response regulator PleD: implications for diguanylate cyclase activation, catalysis, and feedback inhibition. *Structure* **15**, 915-27 (2007).
22. Pei, J. and Grishin, N.V. GGDEF domain is homologous to adenylyl cyclase. *Proteins* **42**, 210-6 (2001).
23. Malone, J.G., Williams, R., Christen, M., Jenal, U., Spiers, A.J. and Rainey, P.B. The structure-function relationship of WspR, a *Pseudomonas fluorescens* response regulator with a GGDEF output domain. *Microbiology* **153**, 980-94 (2007).
24. Christen, B., Christen, M., Paul, R., Schmid, F., Folcher, M., Jenoe, P., Meuwly, M. and Jenal, U. Allosteric control of cyclic di-GMP signaling. *The Journal of Biological Chemistry* **281**, 32015-24 (2006).
25. Tamayo, R., Tischler, A.D. and Camilli, A. The EAL domain protein VieA is a cyclic diguanylate phosphodiesterase. *Journal of Biological Chemistry* **280**, 33324-33330 (2005).
26. Schmidt, A.J., Ryjenkov, D.A. and Gomelsky, M. The ubiquitous protein domain EAL is a cyclic diguanylate-specific phosphodiesterase: enzymatically active and inactive EAL domains. *Journal of Bacteriology* **187**, 4774-4781 (2005).
27. Pesavento, C. and Hengge, R. Bacterial nucleotide-based second messengers. *Current Opinion in Microbiology* **12**, 170-6 (2009).

28. Minasov, G., Pdavattan, S., Shuvalova, L., Brunzelle, J.S., Miller, D.J., Baslé, A., Massa, C., Collart, F.R., Schirmer, T., Anderson, W.F. Crystal structures of YkuL and its complex with second messenger cyclic di-GMP suggest catalytic mechanism of phosphodiester bond cleavage by EAL domains. *The Journal of Biological Chemistry* **284**, 13174-84 (2009).
29. Rao, F., Yang, Y., Qi, Y. and Liang, Z.-X. Catalytic mechanism of cyclic di-GMP-specific phosphodiesterase: a study of the EAL domain-containing RocR from *Pseudomonas aeruginosa*. *Journal of Bacteriology* **190**, 3622-31 (2008).
30. Barends, T.R.M., Hartmann, E., Griese, J.J., Beitlich, T., Kirienko, N.V., Ryjenkov, D.A., Reinstein, J., Shoeman, R.L., Gomelsky, M. and Schlichting, I. Structure and mechanism of a bacterial light-regulated cyclic nucleotide phosphodiesterase. *Nature* **459**, 1015-8 (2009).
31. Ryan, R.P., Fouhy, Y., Lucey, J.F., Crossman, L.C., Spiro, S., He, Y.-W., Zhang, L.-H., Heeb, S., Camara, M., Williams, P. and Dow, M.J. Cell-cell signaling in *Xanthomonas campestris* involves an HD-GYP domain protein that functions in cyclic di-GMP turnover. *Proceedings of the National Academy of Sciences of the United States of America* **103**, 6712-7 (2006).
32. Lovering, A.L., Capeness, M.J. and Lambert, C. Structure of an unconventional HD-GYP protein from *Bdellovibrio* reveals the roles of conserved residues in this class of cyclic-di-GMP phosphodiesterases. *Mbio* **2**, 1-8 (2011).
33. Seshasayee, A.S.N., Fraser, G.M. and Luscombe, N.M. Comparative genomics of cyclic-di-GMP signalling in bacteria: post-translational regulation and catalytic activity. *Nucleic Acids Research* **38**, 5970-81 (2010).
34. Christen, M., Christen, B., Folcher, M., Schauerte, A. and Jenal, U. Identification and characterization of a cyclic di-GMP-specific phosphodiesterase and its allosteric control by GTP. *Journal of Biological Chemistry* **280**, 30829-37 (2005).
35. Kuchma, S.L., Brothers, K.M., Merritt, J.H., Liberati, N.T., Ausubel, F.M. and O'Toole, G.A. BifA, a cyclic-Di-GMP phosphodiesterase, inversely regulates biofilm formation and swarming motility by *Pseudomonas aeruginosa* PA14. *Journal of Bacteriology* **189**, 8165-78 (2007).
36. Kazmierczak, B.I., Lebron, M.B. and Murray, T.S. Analysis of FimX, a phosphodiesterase that governs twitching motility in *Pseudomonas aeruginosa*. *Molecular Microbiology* **60**, 1026-43 (2006).
37. Huang, B., Whitchurch, C.B. & Mattick, J.S. FimX , a multidomain protein connecting environmental signals to twitching motility in *Pseudomonas aeruginosa*. *Journal of Bacteriology* **185**, 7068-7076 (2003).
38. Ferreira, R.B.R., Antunes, L.C.M., Greenberg, E.P. and McCarter, L.L. *Vibrio parahaemolyticus* ScrC modulates cyclic dimeric GMP regulation of gene expression relevant to growth on surfaces. *Journal of Bacteriology* **190**, 851-60 (2008).

39. Trimble, M.J. and McCarter, L.L. Bis-(3'-5')-cyclic dimeric GMP-linked quorum sensing controls swarming in *Vibrio parahaemolyticus*. *Proceedings of the National Academy of Sciences of the United States of America* **108**, 18079-84 (2011).
40. Kumar, M. and Chatterji, D. Cyclic di-GMP: a second messenger required for long-term survival, but not for biofilm formation, in *Mycobacterium smegmatis*. *Microbiology* **154**, 2942-55 (2008).
41. Tarutina, M., Ryjenkov, D.A. and Gomelsky, M. An unorthodox bacteriophytochrome from *Rhodobacter sphaeroides* involved in turnover of the second messenger c-di-GMP. *The Journal of Biological Chemistry* **281**, 34751-8 (2006).
42. Schirmer, T. and Jenal, U. Structural and mechanistic determinants of c-di-GMP signalling. *Nature Reviews Microbiology* **7**, 724-35 (2009).
43. Mills, E., Pultz, I.S., Kulasekara, H.D. and Miller, S.I. The bacterial second messenger c-di-GMP: mechanisms of signalling. *Cellular Microbiology* **13**, 1122-1129 (2011).
44. Sommerfeldt, N., Possling, A., Becker, G., Pesavento, C, Tschowri, N. and Hengge, R. Gene expression patterns and differential input into curli fimbriae regulation of all GGDEF/EAL domain proteins in *Escherichia coli*. *Microbiology* **155**, 1318-31 (2009).
45. Weber, H., Pesavento, C., Possling, A., Tischendorf, G. and Hengge, R. Cyclic-di-GMP-mediated signalling within the sigma network of *Escherichia coli*. *Molecular Microbiology* **62**, 1014-34 (2006).
46. Kirillina, O., Fetherston, J.D., Bobrov, A.G., Abney, J. and Perry, R.D. HmsP, a putative phosphodiesterase, and HmsT, a putative diguanylate cyclase, control Hms-dependent biofilm formation in *Yersinia pestis*. *Molecular Microbiology* **54**, 75-88 (2004).
47. Abel, S., Chien, P., Wassmann, P., Schirmer, T., Kaefer, V., Laub, M.T., Baker, T.A, and Jenal, U. Regulatory cohesion of cell cycle and cell differentiation through Interlinked phosphorylation and second messenger networks. *Molecular Cell* **43**, 550-560 (2011).
48. Hengge, R. Cyclic-di-GMP Reaches Out into the Bacterial RNA World. *Science Signalling* **3**, 2008-2011 (2010).
49. Amikam, D. and Galperin, M.Y. PilZ domain is part of the bacterial c-di-GMP binding protein. *Bioinformatics* **22**, 3-6 (2006).
50. Ryjenkov, D.A., Simm, Römling, U. and Gomelsky, M. The PilZ domain is a receptor for the second messenger c-di-GMP. *Journal of Biological Chemistry* **281**, 30310 -30314 (2006).
51. Boehm, A., Kaiser, M., Li, H., Spangler, C., Kaspar, C.A., Ackermann, M., Kaefer, V., Sourjik, V., Roth, V. and Jenal, U. Second messenger-mediated adjustment of bacterial swimming velocity. *Cell* **141**, 107-16 (2010).

52. Christen, M., Christen, B., Allan, M.G., Folcher, M., Jenoe, P., Grzesiek, S. and Jenal, U. DgrA is a member of a new family of cyclic diguanosine monophosphate receptors and controls flagellar motor function in *Caulobacter crescentus*. *Proceedings of the National Academy of Sciences of the United States of America* **104**, 4112-4117 (2007).
53. Wang, J., Zhou, J., Donaldson, G.P., Nakayama, S., Yan, L., Lam, Y., Lee, V.T. and Sintim, H.O. Conservative change to the phosphate moiety of cyclic diguanylic monophosphate remarkably affects its polymorphism and ability to bind DGC, PDE, and PilZ proteins. *Journal of the American Chemical Society* **133**, 9320-30 (2011).
54. Benach, J., Swaminathan, S.S., Tamayo, R., Handelman, S.K., Folta-Stogniew, E., Ramos, J.E., Forouhar, F., Neely, H., Seetharaman, J., Camilli, A., Hunt, J.F. The structural basis of cyclic diguanylate signal transduction by PilZ domains. *The EMBO Journal* **26**, 5153-66 (2007).
55. Habazettl, J., Allan, M.G., Jenal, U. and Grzesiek, S. Solution structure of the PilZ domain protein PA4608 complex with cyclic di-GMP identifies charge clustering as molecular readout. *The Journal of Biological Chemistry* **286**, 14304-14 (2011).
56. Duerig, A., Abel, S., Folcher, M., Nicollier, M., Schwede, T., Amiot, N.C., Giese, B. and Jenal, U. Second messenger-mediated spatiotemporal control of protein degradation regulates bacterial cell cycle progression. *Genes & Development* **23**, 93-104 (2009).
57. Lee, V.T., Kessler, J.L., Hayakawa, Y., Matewish, J.M., Hyodo, M. and Lory, S. A cyclic-di-GMP receptor required for bacterial exopolysaccharide production. *Molecular Microbiology* **65**, 1474-84 (2007).
58. Navarro, M.V.A.S., De, N., Bae, N., Wang, Q. and Sondermann, H. Structural analysis of the GGDEF-EAL domain-containing c-di-GMP receptor FimX. *Structure* **17**, 1104-16 (2009).
59. Newell, P.D., Monds, R.D. and O'Toole, G.A.. LapD is a bis-(3', 5')-cyclic dimeric GMP binding protein that regulates surface attachment by *Pseudomonas fluorescens* Pf0-1. *Proceedings of the National Academy of Sciences of the United States of America* **106**, 3461-3466 (2009).
60. Navarro, M.V.A.S., Newell, P.D., Krasteva, P.V., Chatterjee, D., Madden, D.R., O'Toole, G.A. and Sondermann, H. Structural basis for c-di-GMP-mediated inside-out signaling controlling periplasmic proteolysis. *PLoS Biology* **9**, (2011).
61. Hickman, J.W. and Harwood, C.S. Identification of FleQ from *Pseudomonas aeruginosa* as a c-di-GMP-responsive transcription factor. *Molecular Microbiology* **69**, 376-89 (2008).
62. Leduc, J.L. and Roberts, G.P. Cyclic di-GMP allosterically inhibits the CRP-like protein (Clp) of *Xanthomonas axonopodis* pv. *citri*. *Journal of Bacteriology* **191**, 7121-2 (2009).
63. Chin, K.-H., Lee, Y.-C., Tu, Z.-L., Tseng, Y.-H., Yang, J.-M., Ryan, R.P., McCarthy, Y., Dow, M.J., Wang, A.H. and Chou, S.-H. The cAMP receptor-like protein CLP is a novel c-di-GMP receptor linking cell-cell signaling to virulence gene expression in *Xanthomonas campestris*. *Journal of Molecular Biology* **396**, 646-62 (2010).

64. Krasteva, P.V., Fong, J.C.N., Shikuma, N.J., Beyhan, S., Navarro, M.V.A.A., Yildiz, F.H. and Sondermann, H. *Vibrio cholerae* VpsT regulates matrix production and motility by directly sensing cyclic di-GMP. *Science* **327**, 866-8 (2010).
65. Beyhan, S., Tischler, A.D., Camilli, A. and Yildiz, F.H. Transcriptome and Phenotypic Responses of *Vibrio cholerae* to Increased Cyclic di-GMP Level. *Journal of Bacteriology* **188**, 3600-3613 (2006).
66. Lee, E.R., Baker, J.L., Weinberg, Z., Sudarsan, N. and Breaker, R.R. An allosteric self-splicing ribozyme triggered by a bacterial second messenger. *Science* **329**, 845-8 (2010).
67. Sudarsan, N., Lee, E.R., Weinberg, Z., Moy, R.H., Kim, J.N., Link, K.H. and Breaker, R.R. Riboswitches in eubacteria sense the second messenger cyclic di-GMP. *Science* **321**, 411-3 (2008).
68. Smith, K.D. and Strobel, S.A. Interactions of the c-di-GMP riboswitch with its second messenger ligand. *Biochemical Society Transactions* **39**, 647-51 (2011).
69. Chen, A.G.Y., Sudarsan, N. and Breaker, R.R. Mechanism for gene control by a natural allosteric group I ribozyme. *RNA* 1967-1972 (2011).
70. Römling, U. and Simm, R. Prevailing concepts of c-di-GMP signaling. *Contributions to Microbiology* **16**, 161-81 (2009).
71. Goodman, A.L., Kulasekara B., Rietsch, A., Boyd, D., Smith, R.S. and Lory, S. A signaling network reciprocally regulates genes associated with acute infection and chronic persistence in *Pseudomonas aeruginosa*. *Developmental Cell* **7**, 745-754 (2004).
72. Cotter, P.A. and Stibitz, S. c-di-GMP-mediated regulation of virulence and biofilm formation. *Current Opinion in Microbiology* **10**, 17-23 (2007).
73. Jarrell, K.F. and McBride, M.J. The surprisingly diverse ways that prokaryotes move. *Nature Reviews Microbiology* **6**, 466-76 (2008).
74. Harshey, R.M. Bacterial motility on a surface: many ways to a common goal. *Annual Review of Microbiology* **57**, 249-73 (2003).
75. McCarter, L. The multiple identities of *Vibrio parahaemolyticus*. *Journal of Molecular Microbiology and Biotechnology* **1**, 51-57 (1999).
76. Jenal, U. The role of proteolysis in the *Caulobacter crescentus* cell cycle and development. *Research in Microbiology* **160**, 687-95 (2009).
77. Huitema, E., Pritchard, S., Matteson, D., Radhakrishnan, S.K. and Viollier, P.H. Bacterial birth scar proteins mark future flagellum assembly site. *Cell* **124**, 1025-37 (2006).
78. Macnab, R.M. How bacteria assemble flagella. *Annual Review of Microbiology* **57**, 77-100 (2003).

79. Paul, K., Nieto, V., Carlquist, W.C., Blair, D.F. and Rasika, M. The c-di-GMP binding protein YcgR controls flagellar motor direction and speed to affect chemotaxis by a “backstop brake” mechanism. *Molecular Cell* **38**, 128-139 (2010).
80. Merz, A.J., So, M. and Sheetz, M.P. Pilus retraction powers bacterial twitching motility. *Nature* **407**, 683-687 (2000).
81. Yang, L., Liu, Y., Wu, H. and Hø, N. Current understanding of multi-species biofilms. *International Journal of Oral Science* **3**, 74-81 (2011).
82. Flemming, H.C. and Wingender, J. The biofilm matrix. *Nature Reviews Microbiology* **8**, 623-633 (2010).
83. Karunakaran, E. and Mukherjee, J. “ Biofilmology ”: a multidisciplinary review of the study of microbial biofilms. *Applied Microbiology* 1869-1881 (2011).
84. Newell, P.D., Yoshioko, S., Hvorecny, K.L., Monds, R.D., O'Toole, G.A. Systematic analysis of diguanylate cyclases that promote biofilm formation by *Pseudomonas fluorescens* Pf0-1. *Journal of Bacteriology* **193**, 4685-4698 (2011).
85. Mikkelsen, H., Sivaneson, M. and Filloux, A. Key two-component regulatory systems that control biofilm formation in *Pseudomonas aeruginosa*. *Environmental Microbiology* **13**, 1666-81 (2011).
86. Malone, J.G., Jaeger, T., Spangler, C., Ritz, D., Spang, A., Kaefer, V., Landmann, R. and Jenal, U. YfiBNR mediates cyclic di-GMP dependent small colony variant formation and persistence in *Pseudomonas aeruginosa*. *PLoS Pathogens* **6** (2010).
87. Bassis, C.M. and Visick, K.L. The cyclic-di-GMP phosphodiesterase BinA negatively regulates cellulose-containing biofilms in *Vibrio fischeri*. *Journal of Bacteriology* **192**, 1269-78 (2010).
88. Yildiz, F.H. and Visick, K.L. *Vibrio* biofilms: so much the same yet so different. *Trends in Microbiology* **17**, 109-118 (2010).
89. Boehm, A., Steiner, S., Zaehring, F., Casanova, A., Hamburger F., Ritz, D., Keck, W., Ackermann, M., Schirmer, T. and Jenal, U. Second messenger signalling governs *Escherichia coli* biofilm induction upon ribosomal stress. *Molecular Microbiology* **72**, 1500-16 (2009).
90. Bobrov, A.G., Kirillina, O., Forman, S., Mack, D. and Perry, R.D. Insights into *Yersinia pestis* biofilm development: topology and co-interaction of Hms inner membrane proteins involved in exopolysaccharide production. *Environmental Microbiology* **10**, 1419-32 (2008).
91. Sun, Y.-C., Koumoutsis, A., Jarrett, C., Lawrence, K., Gherardini, F.C., Darby, C. and Hinnebusch, J. Differential control of *Yersinia pestis* biofilm formation *in vitro* and in the flea vector by two c-di-GMP diguanylate cyclases. *PLoS One* **6**, e19267 (2011).

92. Simm, R., Lusch, A., Kader, A., Andersson, M. and Römling, U. Role of EAL-containing proteins in multicellular behavior of *Salmonella enterica* serovar *Typhimurium*. *Journal of Bacteriology* **189**, 3613-23 (2007).
93. Solano, C., Garcia, B., Latasa, C., Toledo-Arana, A., Zorraquinoa, V., Vallea, J., Casals, J., Pedroso, E. and Lasa, I. Genetic reductionist approach for dissecting individual roles of GGDEF proteins within the c-di-GMP signaling network in *Salmonella*. *Proceedings of the National Academy of Sciences of the United States of America* **106**, 7997-8002 (2009).
94. García, B., Latasa, C., Solano, C., Garica-del Portillo, F., Gamazo, C. and Lasa, I. Role of the GGDEF protein family in *Salmonella* cellulose biosynthesis and biofilm formation. *Molecular Microbiology* **54**, 264-277 (2004).
95. Wilksch, J.J., Clements, A., Gabbe, J.L., Short, K.R., Cao, H., Cavaliere, R., James, C.E., Whitchurch, C.B., Schembri, M.A., Chuah, M.L.C.m Liang, Z., Wijburg, O.L., Jenney, A.W., Lithgow, T. and Strugnell, R.A. MrkH, a Novel c-di-GMP-Dependent Transcriptional Activator, Controls *Klebsiella pneumoniae* Biofilm Formation by Regulating Type 3 Fimbriae Expression. *PLoS Pathogens* **7** (2011).
96. Newell, P.D., Boyd, C.D., Sondermann, H. and O'Toole, G.A. A c-di-GMP effector system controls cell adhesion by inside-out signaling and surface protein cleavage. *PLoS Biology* **9**, (2011).
97. Tamayo, R., Pratt, J.T. and Camilli, A. Roles of cyclic diguanylate in the regulation of bacterial pathogenesis. *Molecular Biology* 131-148 (2009).
98. Tischler, A.D., Lee, S.H. and Camilli, A. The *Vibrio cholerae* vieSAB Locus Encodes a Pathway Contributing to Cholera Toxin Production. *Journal of Bacteriology* **184**, 4104-4113 (2002).
99. Higgins, D.E., Nazareno, E. and Dirital, V.J. The Virulence Gene Activator ToxT from *Vibrio cholerae* Is a Member of the AraC Family of Transcriptional Activators. *Journal of Bacteriology* **174**, 6974-6980 (1992).
100. Tischler, A.D. and Camilli, A. Cyclic diguanylate (c-di-GMP) regulates *Vibrio cholerae* biofilm formation. *Molecular Microbiology* **53**, 857-869 (2004).
101. Tischler, A.D. and Camilli, A. Cyclic diguanylate regulates *Vibrio cholerae* virulence gene expression. *Infection and Immunity* **73**, 5873-5882 (2005).
102. Römling, U. Characterization of the *rdar* morphotype, a multicellular behaviour in *Enterobacteriaceae*. *Cellular and Molecular Life Sciences* **62**, 1234-1246 (2005).
103. Lamprokostopoulou, A., Monteiro, C., Rhen, M. and Römling, U. Cyclic di-GMP signalling controls virulence properties of *Salmonella enterica* serovar *Typhimurium* at the mucosal lining. *Environmental Microbiology* **12**, 40-53 (2010).

104. Wang, L.-H., He, Y., Gao, Y., Dong, Y.H., He, C., Wang, S.X., Weng, L.-X., Xu, J.-L., Tay, L., Fang, R.X. and Zhang, L.H. A bacterial cell-cell communication signal with cross-kingdom structural analogues. *Molecular Microbiology* **51**, 903-912 (2004).
105. Ryan, R.P., McCarthy, Y., Andrade, M., Farahb, C.S., Armitage, J.P. and Dow, M. Cell – cell signal-dependent dynamic interactions between HD-GYP and GGDEF domain proteins mediate virulence in *Xanthomonas campestris*. *Proceedings of the National Academy of Sciences of the United States of America* **107**, 5989-5994 (2010).
106. Thomas, C., Andersson, C.R., Canales, S.R. and Golden, S.S. PsfR, a factor that stimulates psbAI expression in the cyanobacterium *Synechococcus elongatus* PCC 7942. *Microbiology* **150**, 1031-1040 (2004).
107. Neunuebel, M.R. and Golden, J.W. The *Anabaena* sp. strain PCC 7120 gene all2874 encodes a diguanylate cyclase and is required for normal heterocyst development under high-light growth conditions. *Journal of Bacteriology* **190**, 6829-36 (2008).
108. Paul, R., Abel, S., Wassmann, P., Beck, A., Heerklotz, H. and Jenal, U. Activation of the diguanylate cyclase PleD by phosphorylation-mediated dimerization. *The Journal of Biological Chemistry* **282**, 29170-7 (2007).
109. Paul, R. Jaeger, T., Abel, S., Wiederkehr, I., Folcher, M., Biondi, G., Laub, M.T. and Jenal, U. Allosteric regulation of histidine kinases by their cognate response regulator determines cell fate. *Cell* **133**, 452-61 (2008).
110. Poindexter, J.S. The *Caulobacters*: Ubiquitous unusual bacteria. *Microbiological Reviews* **45**, 123-179 (1981).
111. Merker, R.I. and Smit, J. Characterization of the adhesive holdfast of marine and freshwater *Caulobacters*. *Applied and Environmental Microbiology* **54**, 2078-2085 (1988).
112. Degnen S.T., Newton, A. Chromosome replication during development in *Caulobacter crescentus*. *Journal of Molecular Biology* **64**, 671-680 (1972).
113. Marczyński, G.T. and Shapiro, L. Cell-cycle control of a cloned chromosomal origin of replication from *Caulobacter crescentus*. *Journal of Molecular Biology* **226**, 959-77 (1992).
114. McAdams, H.H. and Shapiro, L. System-level design of bacterial cell cycle control. *FEBS Letters* **583**, 3984-91 (2009).
115. Marczyński, G.T. Chromosome methylation and measurement of faithful, once and only once per cell cycle chromosome replication in *Caulobacter crescentus*. *Journal of Bacteriology* **181**, 1984-93 (1999).
116. Bodenmiller, D., Toh, E. and Brun, Y.V. Development of surface adhesion in *Caulobacter crescentus*. *Journal of Bacteriology* **186**, 1438-1447 (2004).

117. Levi, A. and Jenal, U. Holdfast formation in motile swarmer cells optimizes surface attachment during *Caulobacter crescentus* development. *Journal of Bacteriology* **188**, 5315-8 (2006).
118. Jacobs-Wagner, C. Regulatory proteins with a sense of direction: cell cycle signalling network in *Caulobacter*. *Molecular Microbiology* **51**, 7-13 (2004).
119. Christen, M., Kulasekara, H.D., Christen, B., Kulasekara, B.R., Hoffman, L.R. and Miller, S.I. Asymmetrical distribution of the second messenger c-di-GMP upon bacterial cell division. *Science* **328**, 1295-7 (2010).
120. Aldridge, P., Paul, R., Goymer, P., Rainey, P. and Jenal, U. Role of the GGDEF regulator PleD in polar development of *Caulobacter crescentus*. *Molecular Microbiology* **47**, 1695-708 (2003).
121. Aldridge, P. and Jenal, U. Cell cycle-dependent degradation of a flagellar motor component requires a novel-type response regulator. *Molecular Microbiology* **32**, 379-391 (1999).
122. Sommer, J.M. and Newton, A. Turning off flagellum rotation requires the pleiotropic gene *pleD*: *pleA*, *pleC*, and *pleD* define two morphogenic pathways in *Caulobacter crescentus*. *Journal of Bacteriology* **171**, 392-401 (1989).
123. Burton, G.J., Hecht, G.B., Newton, A. Roles of the histidine protein kinase PleC in *Caulobacter crescentus* motility and chemotaxis. *Microbiology* **179**, 5849-5853 (1997).
124. Dyer, C.M. and Dahlquist, F.W. Switched or not?: the structure of unphosphorylated CheY bound to the N-terminus of FliM. *Journal of Bacteriology* **188**, 7354-7363 (2006).
125. Jenal, U. and Galperin, M.Y. Single domain response regulators: molecular switches with emerging roles in cell organization and dynamics. *Current Opinion in Microbiology* **12**, 152-60 (2009).
126. Laub, M.T., Chen, S.L., Shapiro, L. and McAdams, H.H. Genes directly controlled by CtrA, a master regulator of the *Caulobacter* cell cycle. *Proceedings of the National Academy of Sciences of the United States of America* **99**, 4632-7 (2002).
127. Holtzendorff, J., Hung, D., Brende, P., Reisenauer, A., Viollier, P.H., McAdams, H.H. and Shapiro, L. Oscillating global regulators control the genetic circuit driving a bacterial cell cycle. *Science* **304**, 983-7 (2004).
128. Hottes, A.K., Shapiro, L. and McAdams, H.H. DnaA coordinates replication initiation and cell cycle transcription in *Caulobacter crescentus*. *Molecular Microbiology* **58**, 1340-53 (2005).
129. Collier, J., Murray, S.R. and Shapiro, L. DnaA couples DNA replication and the expression of two cell cycle master regulators. *The EMBO Journal* **25**, 346-56 (2006).
130. Lenz, P. and Sogaard-Andersen, L. Temporal and spatial oscillations in bacteria. *Nature Reviews Microbiology* **9**, 565-577 (2011).

131. Goley, E.D., Toro, E., McAdams, H.H. and Shapiro, L. Dynamic chromosome organization and protein localization coordinate the regulatory circuitry that drives the bacterial cell cycle. *Cold Spring Harbor Symposia on Quantitative Biology* **74**, 55-64 (2009).
132. Goley, E.D., Iniesta, A.A. and Shapiro, L. Cell cycle regulation in *Caulobacter*: location, location, location. *Journal of Cell Science* **120**, 3501-7 (2007).
133. Quon, K.C., Marczyński, G.T. and Shapiro, L. Cell cycle control by an essential bacterial two-component signal transduction protein. *Cell* **84**, 83-93 (1996).
134. Quon, K.C., Yang, B., Domian, I.J., Shapiro, L. and Marczyński, G.T. Negative control of bacterial DNA replication by a cell cycle regulatory protein that binds at the chromosome origin. *Proceedings of the National Academy of Sciences of the United States of America* **95**, 120-5 (1998).
135. Kelly, A.J., Sackett, M.J., Din, N., Quardokus, E. and Brun, Y.V. Cell cycle-dependent transcriptional and proteolytic regulation of FtsZ in *Caulobacter*. *Genes & Development* **12**, 880-93 (1998).
136. Crymes, W.B., Zhang, D. and Ely, B. Regulation of podJ expression during the *Caulobacter crescentus* cell cycle. *Journal of Bacteriology* **181**, 3967-73 (1999).
137. Hinz, A.J., Larson, D.E., Smith, C.S. & Brun, Y.V. The *Caulobacter crescentus* polar organelle development protein PodJ is differentially localized and is required for polar targeting of the PleC development regulator. *Molecular Microbiology* **47**, 929-41 (2003).
138. Viollier, P.H., Sternheim, N. and Shapiro, L. Identification of a localization factor for the polar positioning of bacterial structural and regulatory proteins. *Proceedings of the National Academy of Science* **99**, 13831-13836 (2002).
139. Crosson, S., McAdams, H. and Shapiro, L. A genetic oscillator and the regulation of cell cycle progression in *Caulobacter crescentus*. *Cell Cycle* 55-57 (2004).
140. Gorbatyuk, B. and Marczyński, G.T. Regulated degradation of chromosome replication proteins DnaA and CtrA in *Caulobacter crescentus*. *Molecular Microbiology* **55**, 1233-45 (2005).
141. Domian, I.J., Reisenauer, A. and Shapiro, L. Feedback control of a master bacterial cell-cycle regulator. *Proceedings of the National Academy of Sciences of the United States of America* **96**, 6648-53 (1999).
142. Reisenauer, A., Quon, K. and Shapiro, L. The CtrA response regulator mediates temporal control of gene expression during the *Caulobacter* cell cycle. *Journal of Bacteriology* **181**, 2430-9 (1999).
143. Reisenauer, A. and Shapiro, L. DNA methylation affects the cell cycle transcription of the CtrA global regulator in *Caulobacter*. *The EMBO Journal* **21**, 4969-77 (2002).

144. Zweiger, G., Marczynski, G.T. and Shapiro, L. A *Caulobacter* DNA methyltransferase that functions only in the predivisional cell. *Journal of Molecular Biology* **235**, 472-485 (1994).
145. Collier, J., McAdams, H.H. and Shapiro, L. A DNA methylation ratchet governs progression through a bacterial cell cycle. *Proceedings of the National Academy of Sciences of the United States of America* **104**, 17111-6 (2007).
146. Stephens, C.M., Zweiger, G. and Shapiro, L. Coordinate cell cycle control of a *Caulobacter* DNA methyltransferase and the flagellar genetic hierarchy. *Journal of Bacteriology* **177**, 1662-1669 (1995).
147. Wright, R., Stephens, C., Zweiger, G., Shapiro, L. and Alley, M.R. *Caulobacter* Lon protease has a critical role in cell-cycle control of DNA methylation. *Genes & Development* **10**, 1532-1542 (1996).
148. Quimet, M.C. and Marczynski, G.T. Analysis of a cell-cycle promoter bound by a response regulator. *Journal of Molecular Biology* **302**, 761-75 (2000).
149. Brown, P.J.B., Hardy, G.G., Trimble, M.J. and Brun, Y.V. Complex regulatory pathways coordinate cell cycle progression and development in *Caulobacter crescentus*. *Advances in Microbial Physiology* **54**, 1-101 (2009).
150. Domian, I.J., Quon, K.C. and Shapiro, L. Cell type-specific phosphorylation and proteolysis of a transcriptional regulator controls the G1-to-S transition in a bacterial cell cycle. *Cell* **90**, 415-24 (1997).
151. Siam, R. and Marczynski, G.T. Cell cycle regulator phosphorylation stimulates two distinct modes of binding at a chromosome replication origin. *The EMBO Journal* **19**, 1138-47 (2000).
152. Iniesta, A.A., McGrath, P.T., Reisenauer, A., McAdams, H.H. and Shapiro, L. A phospho-signaling pathway controls the localization and activity of a protease complex critical for bacterial cell cycle progression. *Proceedings of the National Academy of Sciences of the United States of America* **103**, 10935-40 (2006).
153. Biondi, E.G., Reisinger, S.J., Skerker, J.M., Arif, M., Perchuk, B.S., Ryan, K.R. and Laub, M.T. Regulation of the bacterial cell cycle by an integrated genetic circuit. *Nature* **444**, 899-904 (2006).
154. Jenal, U. and Fuchs, T. An essential protease involved in bacterial cell-cycle control. *The EMBO Journal* **17**, 5658-69 (1998).
155. Gora, K.G., Tsokos, C.G., Chen, E.Y., Srinivasan, B.S., Perchuk, B.S. and Laub, M.T. A cell-type-specific protein-protein interaction modulates transcriptional activity of a master regulator in *Caulobacter crescentus*. *Molecular cell* **39**, 455-67 (2010).
156. How, M., Kozdon, J.B., Shen, X., Shapiro, L. and McAdams, H.H. An essential transcription factor, SciP, enhances robustness of *Caulobacter* cell cycle regulation. *Proceedings of the National Academy of Sciences of the United States of America* **107**, (2010).

157. Jacobs, C., Domian, I.J., Maddock, J.R. and Shapiro, L. Cell cycle-dependent polar localization of an essential bacterial histidine kinase that controls DNA replication and cell division. *Cell* **97**, 111-20 (1999).
158. Iniesta, A.A. and Shapiro, L. A bacterial control circuit integrates polar localization and proteolysis of key regulatory proteins with a phospho-signaling cascade. *Proceedings of the National Academy of Sciences of the United States of America* **105**, 16602-7 (2008).
159. Wu, J., Ohta, N., Zhao, J.L. and Newton, A. A novel bacterial tyrosine kinase essential for cell division and differentiation. *Proceedings of the National Academy of Sciences of the United States of America* **96**, 13068-73 (1999).
160. Hecht, G.B., Lane, T., Ohta, N., Sommer, J.M. and Newton, A. An essential single domain response regulator required for normal cell division and differentiation in *Caulobacter crescentus*. *The EMBO Journal* **14**, 3915-24 (1995).
161. Iniesta, A.A., Hillson, N.J. and Shapiro, L. Cell pole-specific activation of a critical bacterial cell cycle kinase. *Proceedings of the National Academy of Sciences of the United States of America* **107**, 7012-7 (2010).
162. Tsokos, C.G., Perchuk, B.S. and Laub, M.T. A dynamic complex of signaling proteins uses polar localization to regulate cell-fate asymmetry in *Caulobacter crescentus*. *Developmental Cell* **20**, 329-41 (2011).
163. Chien, P., Perchuk, B.S., Laub, M.T., Sauer, R.T. and Baker, T.A. Direct and adaptor-mediated substrate recognition by an essential AAA+ protease. *Proceedings of the National Academy of Sciences of the United States of America* **104**, 6590-5 (2007).
164. Ortega, J., Singh, S.K., Ishikawa, T., Maurizi, M.R. and Steven, A.C. Visualization of substrate binding and translocation by the ATP-dependent protease, ClpXP. *Molecular Cell* **6**, 1515-21 (2000).
165. Wang, J., Hartling, J.A. and Flanagan, J.M. The structure of ClpP at 2.3 Å resolution suggests a model for ATP-dependent proteolysis. *Cell* **91**, 447-456 (1997).
166. Flynn, J.M., Neher, S.B., Kim, Y.I., Sauer, R.T. and Baker, T. a Proteomic discovery of cellular substrates of the ClpXP protease reveals five classes of ClpX-recognition signals. *Molecular Cell* **11**, 671-83 (2003).
167. Ryan, K.R., Huntwork, S. and Shapiro, L. Recruitment of a cytoplasmic response regulator to the cell pole is linked to its cell cycle-regulated proteolysis. *Proceedings of the National Academy of Sciences of the United States of America* **101**, 7415-20 (2004).
168. McGrath, P.T., Iniesta, A.A. Ryan, K.R., Shapiro, L. and McAdams, H.H. A dynamically localized protease complex and a polar specificity factor control a cell cycle master regulator. *Cell* **124**, 535-47 (2006).

-
169. Radhakrishnan, S.K., Pritchard, S. and Viollier, P.H. Coupling prokaryotic cell fate and division control with a bifunctional and oscillating oxidoreductase homolog. *Developmental Cell* **18**, 90-101 (2010).
 170. Lawler, M.L., Larson, D.E., Hinz, A.J., Klein, D. and Brun, Y.V. Dissection of functional domains of the polar localization factor PodJ in *Caulobacter crescentus*. *Molecular Microbiology* **59**, 301-316 (2006).
 171. Duerig, A. Second messenger mediated spatiotemporal control of cell cycle and development. *PhD thesis* (2008).
 172. Wales, A. Hydrogen exchange mass spectrometry for the analysis of protein dynamics. *Mass Spectrometry Reviews* **25**, 158-170 (2006).
 173. Werner, J.N., Chen, E.Y., Gubermann, J.M., Zippilli, A.R., Irgon, J.J. and Gitai, Z. Quantitative genome-scale analysis of protein localization in an asymmetric bacterium. *Proceedings of the National Academy of Sciences of the United States of America* **106**, 7858-63 (2009).
 174. Bowman, G.R., Comolli, L.R., Zhu, J., Eckart, M., Koenig, M., Downing, K.H., Moerner, W.E., Earnest, T. and Shapiro, L. A polymeric protein anchors the chromosomal origin/ParB complex at a bacterial cell pole. *Cell* **134**, 945-955 (2008).
 175. Bowman, G.R., Comolli, L.R., Gaietta, G.M., Fero, M., Hong, S.-H., Jones, Y., Lee, J.H., Downing, K.H., Ellisman, M.H., McAdams, H.H. and Shapiro, L. *Caulobacter* PopZ forms a polar subdomain dictating sequential changes in pole composition and function. *Molecular Microbiology* **1**, 173-189 (2010).

6 Acknowledgements

It is a pleasure to thank those who made this thesis possible: In first place my supervisor Prof. Urs Jenal for giving me the opportunity to work on this interesting research project and for many fruitful scientific discussions and advices. I am especially grateful to him for encouraging me to finish this PhD after birth of my son. I also want to thank my PhD committee, Prof. Hans-Martin Fischer and Prof. Tilman Schirmer for their interest in my work and for scientific advices in the annual PhD meetings. Special thanks go to Dr. Jutta Nesper and Dr. Sören Abel who read parts of this manuscript and considerably contributed to the successful completion of this thesis.

I would also like to give thanks to my collaborators Dr. Paul Wassmann and Ludwig Zumthor, who invested a lot of time trying to crystallize PopA, Suzette Moes and Dr. Paul Jenö for MS-MS analysis and Vesna Olivieri and Ursula Sauder for preparing electron micrograph pictures of *Caulobacter crescentus* mutants.

I am obliged to many people in the lab for their great help and support: I thank Yaniv and Svetlana for their deep friendship and for all lively discussions about this world, Elvira for inoculating strains for me on almost every Sunday evening since I moved away from Basel, Jutta for many scientific advice and funny conversations about Gottfried Stutz, Sören for his incredible patience explaining me the microscope and the world of *Caulobacter crescentus*, Fabienne for her golden cloning hands and for the evenings painting Hungarian Easter eggs. Furthermore, I would like to thank all the present and former lab members for their companionship: Alberto, Christian, Isa, Kathrin, Lucie, Marco, Raphael, Samuel, Alex, Anna, Jake, Jennifer, Marc, Matthias, Michael, Ralf, Régis, Regula and Tabitha.

Last but not at least, I am indebted and thankful to my family, my husband Marco and my son Moritz who supported me with love and faith, sharing all my up and downs and never complained when I did not have enough time for them. I am also especially grateful to my parents and my parents-in-law who took care of Moritz when I was working.

Name Annina Larissa Schalch-Moser
Contact Mattenhofweg 1c
 CH - 5610 Wohlen

Date of Birth 02.07.1982

Nationality Swiss

EDUCATION

- **PhD in Molecular Microbiology:** „Insights into the Activation mechanism of PopA, a cyclic di-GMP Effector Protein Involved in Cell Cycle and Development of *Caulobacter crescentus*“
Supervisor Prof. U. Jenal, Biozentrum, University of Basel, Switzerland 4/2007 – 12/2011
- **Diploma studies in Integrative Biology** with focus on microbiology, cell biology, genetics, biochemistry, and immunology
ETH Zurich, Switzerland 10/2002 – 10/2006
- **“Matura” with focus on languages (English, French, Italian, and Latin)**
Kantonsschule Wohlen, Switzerland 5/2002

PROFESSIONAL EXPERIENCE

- **Scientific assistant** 11/2006-2/2007
Prof. H. Hennecke, Institute of Microbiology, ETH Zurich
- **Diploma thesis:** „Charakterisierung des ORF bll2109 in *Bradyrhizobium japonicum*“
Supervisor Prof. H. Hennecke, Institute of Microbiology, ETH Zurich 7/2005-7/2006
- **Practical course in x-ray crystallography** 10/2002
Max-Planck-Institute of Biophysics, Frankfurt, Germany
- **Practical course in Molecular Biology** 10/2001
Biozentrum, University of Basel, Switzerland
 organized by the foundation “Schweizer Jugend forscht”

SPECIAL EFFORTS AND AWARDS

- **Poster prize at the Society for General Microbiology (SGM)** 6/2008
Meeting: „Polar sequestration mechanism of a c-di-GMP effector protein involved in *Caulobacter crescentus* cell cycle control“
Interlaken, Switzerland
- **Special award for the matura thesis** in the national 4/2002
competition of the foundation “Schweizer Jugend forscht”
- **Board member in the association of biology students** 2/2005 – 2/2006
VEBIS (Verein der Biologiestudierenden)
ETH Zurich

LANGUAGES

German	mother tongue
English	fluent (C1 European language scale)
French	advanced (B2 European language scale)
Italian	advanced (B2 European language scale)

COMPUTER SKILLS

MS Office
Adobe Illustrator and Photoshop

PUBLICATIONS

- **Lindemann A., Moser A., Pessi G., Hauser F., Friberg M., Hennecke H., Fischer HM., 2007.**
„New target genes controlled by the *Bradyrhizobium japonicum* two-component regulatory system RegSR“. *J Bacteriol.* 189(24):8928-43.

INTERESTS

Cooking, hiking, singing in the choir